School of Pharmacy

Thesis submitted to the University of Nottingham for the degree of
Doctor of Philosophy

Ph.D. Thesis

The synthesis and testing of novel analogues of (+)-ambuic acid as inhibitors of staphylococcal virulence

James Reekes, BSc.

Academic supervisors: Prof. Weng Chan and Prof. Paul Williams

Declaration

I declare that the work outlined in this thesis is the result of my own investigation and any work carried out by other investigators is fully acknowledged in the text. I also declare that this thesis has not been submitted, nor is currently being submitted for any other degree at this, or another institution.

James Reekes

Abstract

Staphylococcus aureus is a Gram-positive human pathogen of significant clinical importance. The development of resistance to numerous classes of clinically important antibiotics has exacerbated the need for the development of novel therapeutic modalities for the treatment of serious, drug-resistant *S. aureus* infections.

One approach for developing new therapies is the discovery of anti-virulence compounds. Virulence in *S. aureus* is mainly regulated by the *agr* quorum sensing system. The *agr* system is a master regulator of staphylococcal virulence and utilises the thiolactone macrocyclic peptide, auto-inducing peptide (AIP) as the signal molecule. The *agr* system is based around two divergent promoters, *agrP2* and *agrP3*. The *agrP2* promoter drives expression of the *agr* operon, which consists of 4 genes, *agrB*, *agrD*, *agrC* and *agrA*. AgrB and AgrD are responsible for the synthesis of AIP. AgrD is the pre-pro-peptide of AIP and is processed in part by the membrane bound cysteine protease AgrB, a process which ultimately forms the thiolactone macrocycle within the AIP molecule. Inhibitors of AgrC and AgrA have been studied extensively, however at present, there remains limited study of inhibitors of AgrB
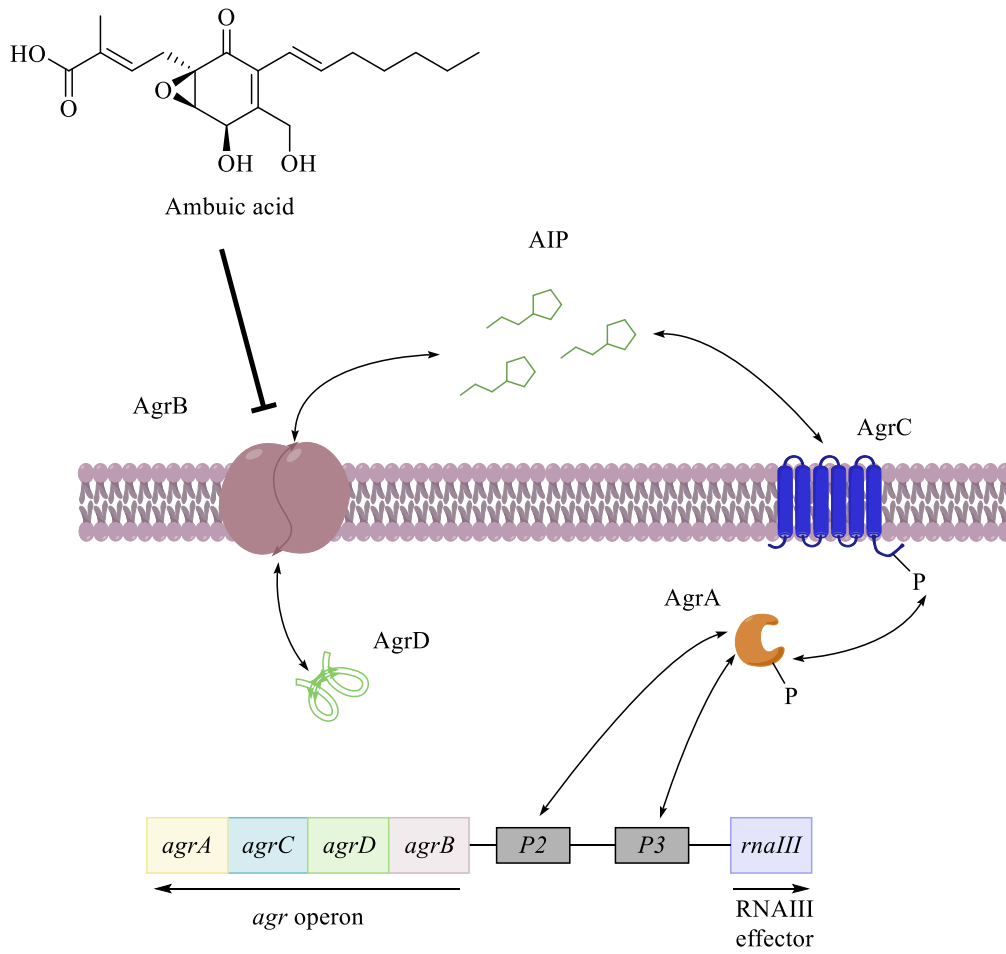
This thesis describes research towards the development of inhibitors of AgrB through the production of analogues of the natural product ambuic acid. This represents the first study of analogues of ambuic acid as inhibitors of staphylococcal virulence. These analogues include the synthesis of a (-)-enantiomer of a truncated ambuic acid analogue and the production of a range of ketal analogues. In addition, the attempted synthesis of a range of silyl ether analogues was also carried out, unfortunately, it was only possible to synthesise one analogue.

In addition, the full chemical synthesis of a cyclopropyl isostere of the epoxide within a truncated ambuic acid analogue was established. This isostere was produced to determine whether the epoxide is required for inhibition of the putative target AgrB in an effort to advance the knowledge of how these compounds function.

The anti-*agr* activity of ambuic acid has been fully characterised *in vitro*. Ambuic acid was found to be a potent inhibitor of staphylococcal *agr* activity utilising a bioluminescent *S. aureus* reporter. In addition, ambuic acid was found to cause a reduction in the level of expression of the staphylococcal exotoxin α-haemolysin. Furthermore, utilising a bioluminescent *S. aureus* reporter strain which is incapable of synthesising AIP, but capable of sensing exogenous AIP (designed for the characterisation of inhibitors of AIP sensing), ambuic acid was found to have no effect. This suggests that ambuic acid inhibits the synthesis of AIP rather than the sensing of AIP.

The testing of the synthesised analogues has been carried out *in vitro* using the bioluminescent *S. aureus agr*-activity reporter and pharmacological paramaters such as IC_{50} were determined. The majority of compounds were found to be potent inhibitors of *agr* activity, with the majority of compounds found to have IC_{50} values of < 10 µM. Surprisingly, the cyclopropyl isosteric analogue was found to be a potent inhibitor of *agr* activity, suggesting that the epoxide is not required for *agr*-inhibitory activity.

These data, taken together represent the first study of analogues of the natural fungal product ambuic acid as inhibitors of staphylococcal virulence. In addition, these data show that these analogues are promising inhibitors of *agr*-activity and the production of further analogues could be used for developing a structure-activity understanding of how this class of compounds function.

Ambuic acid

AIP

AgrB

AgrC

AgrD

AgrA

P

P

| *agrA* | *agrC* | *agrD* | *agrB* | | P2 | | P3 | | *rnaIII* |

agr operon

RNAIII
effector

iv

Acknowledgments

Finally I'd like to thank my family for their constant support and encouragement throughout my PhD and all aspects of my life. Thank you for always being there for me.

For Dad

Like the dust that settles all around me

I must find a new home

The ways and holes that used to give me shelter

Are all as one to me now

But I, I would search everywhere

Just to hear your call

And walk upon stranger roads than this one

In a world I used to know before.

I miss you more

- Genesis

Table of Abbreviations

agr	Accessory gene regulator
AIDS	Acquired immunodeficiency syndrome
AIP	Auto-inducing peptide
BHI	Brain-heart infusion
Bn	Benzyl
CA-MRSA	Community-acquired methicillin-resistant *S. aureus*
cLogP	Calculated LogP
COSY	Correlation spectroscopy
DBU	1,8-diazabicyclo(5.4.0)undec-7-ene
DCM	Dichloromethane
DIBAL-H	Diisobutylaluminium hydride
DMF	Dimethylformamide
DMSO	Dimethylsulfoxide
DNA	Deoxyribonucleic acid
EC_{50}	Effective concentration of agonist for 50% activation
EMSA	Electrophoretic mobility shift assay
Eq.	Equivalents
Et_2O	Diethyl ether
EtOAc	Ethyl acetate
$\times$ G	Multiple of force of gravity
g	Grams
GBAP	Gelatinase biosynthesis activating pheromone
GFP	Green fluorescent protein
h	Hours
HA-MRSA	Hospital-acquired methicillin-resistant *S. aureus*
HPLC	High-performance liquid chromatography
HRMS	High-resolution mass spectometry
HSQC	Heteronuclear single quantum correlation
IC_{50}	Concentration of inhibitor required for 50% inhibition
IE	Infective endocarditis
LC-MS	Liquid chromatography-mass spectrometry
M	Molar

MeCN	Acetonitrile
MeOH	Methanol
MIC	Minimum inhibitory concentration
min	Minutes
mL	Millilitres
MOA	Mode of action
mRNA	Messenger-ribonucleic acid
MRSA	Methicillin-resistant *S. aureus*
MSSA	Methicillin-sensitive *S. aureus*
NAG	*N*-acetylglucosamine
NAM	*N*-acetylmuramic acid
NMR	Nuclear magnetic resonance
NOESY	Nuclear-Overhauser effect spectroscopy
NOS	Nitric oxide synthase
OD	Optical density
PBP	Penicillin-binding protein
Ph_2O	Diphenyl ether
ppm	Parts per million
pTLC	Preparative thin-layer chromatography
QS	Quorum sensing
RLU	Relative luminescence units
RNA	Ribonuclei acid
r.t.	Room temperature
SAR	Structure-activity relationship
SDS-PAGE	Sodium dodecyl sulfate-polyacrylamide gel electrophoresis
SSTI	Skin and soft-tissue infection
TBAF	Tetra *n*-butyl ammonium fluoride
TBAI	Tetra *n*-butyl ammonium iodide
TBDMS	*t*-butyldimethyl silyl
TBDPS	*t*-butyldiphenyl silyl
TEA	Triethylamine
TFA	Trifluoroacetic acid
THF	Tetrahydrofuran

TLC	Thin-layer chromatography
TSS	Toxic shock syndrome
TSST-1	Toxic shock syndrome toxin-1
WHO	World health Organisation
XDR	Extensively drug resistant
VRSA	Vancomycin-resistant *S. aureus*

Table of contents

Chapter 1. Introduction

1.1 Chapter outline

.

This chapter describes the organism *Staphylococcus aureus*, its pathogenicity, mechanisms of antibiotic resistance, incidence of infection, human impact and its worldwide burden on healthcare. With the establishment of *S. aureus* as a pathogen of significant clinical importance and the great need for new therapeutic strategies for treating staphylococcal infections, the virulence of *S. aureus* and its potential as a target for the development of novel therapeutic modalities is outlined. This includes discussion of the staphylococcal *agr* quorum sensing system and the potential for its disruption using small molecules such as ambuic acid (**1.1**) (Figure 1.1).
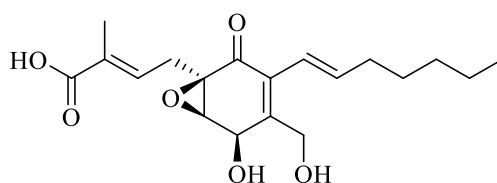
1.1

Figure 1.1 Ambuic acid (**1.1**)

1.2 *Staphylococcus aureus*

Staphylococcus aureus is a Gram-positive bacterium that is both a human commensal and a pathogen.[1] *S. aureus* colonisation is common (about 30 % of the global population) and most often asymptomatic, typically localised to the skin, anterior nares and gastrointestinal tract.[1-5] Despite the frequent occurrence of *S. aureus* in the normal human microbial flora, the bacterium is an opportunistic pathogen and is a common cause of nosocomial infection.[6-7] The major route of transmission of infection is direct contact, mediated by skin-to-skin contact and contact with contaminated objects.[6, 8-9]

S. aureus infection is typically associated with individuals whom through a number of factors are at a higher risk. These risks include loss of the normal skin barrier (from recent surgery or injury) and underlying health conditions such as acquired immune deficiency syndrome and diabetes.[6, 8] Persistent host colonisation by *S. aureus* is also an increased risk factor, notably nasal carriage.[2, 10-11]

The exquisite ability of *S. aureus* to be both part of the commensal microbial flora and an opportunistic pathogen is due to the tight regulation of a broad array of virulence factors (such as exo-toxins) that are dependent on local bacteria population density and environment.[12]

In recent times, strains of methicillin-resistant *S. aureus* (MRSA, as discussed in greater detail in section 1.3) have received significant media attention, notably as a nosocomial pathogenic agent.[7, 13]

1.3 The pathology and epidemiology of *S. aureus*

The *S. aureus* infection can clinically present with a broad range of severity. Infection can take the form of mild skin infections, such as boils, impetigo and cellulitis to more invasive and severe infections, such as endocarditis, bacteraemia, pneumonia, osteomyelitis and sepsis.[2, 14-20] Furthermore, diseases mediated by staphylococcal toxins are also known, which include food poisoning, scalded skin syndrome and toxic shock syndrome (TSS).[21-23] The most severe of these diseases are often fatal.

S. aureus infections are often caused by inoculation of an injury such as a surgical incision by the host's own commensal bacteria. Wertheim *et al.* found that the risk of *S. aureus* bacteraemia

in hospital is 3-fold more likely in *S. aureus* carriers than non-carriers.[24] Further studies by von Eiff *et al.* found the blood and anterior nares bacterial isolates are identical in 82 % of the study group, thus indicating that endogenous colonisation is a significant risk.[25] Healthcare workers, whose hands have been contaminated with staphylococci from their own reservoir or that of an infected patient is another source of *S. aureus* infection.[8]

Initial infection usually causes localised minor pathology, such as the formation of an abscess, the most severe of which may require drainage.[8] This can complicate the recovery from surgery.[26] Further complications can arise if the infection is caused by a strain of MRSA. Systemic dissemination of the bacteria, away from the site of initial infection can lead to endocarditis, bacteraemia and sepsis.[17, 27]

Numerous other factors can predispose an individual to an increased risk of developing more severe *S. aureus* infections. These include acquired immunodeficiency syndrome (AIDS), diabetes, disorders of neutrophils, intravenous drug use, chronic hepatitis C and cancers.[6, 28-29] This can lead to severe soft-tissue infections such as necrotising fasciitis, causing extensive necrosis of the fascia and subcutaneous tissue, often requiring amputation, if it has not already proved fatal.[30]

Although typically associated with infections arising from within healthcare settings, *S. aureus* is also known to cause disease in otherwise healthy individuals. A well-documented example is toxic shock syndrome (TSS). The introduction of super-absorbent tampons containing cross-linked carboxymethylcellulose, manufactured by Rely Ltd was linked to a spike in cases of TSS in otherwise healthy women.[31] Numerous studies failed to attribute this to a direct increase in the production of toxic shock syndrome toxin-I (TSST-I), the super-antigen causative agent of TSS.[23, 31] However, it was suggested the composition of the tampon was the cause, and that it may act as a reservoir for TSST-I, allowing it to cross the vaginal mucosa, causing TSS.[31] TSS is a severe acute disease and is characterised by hypotension and fever, which can also lead to multisystem organ failure.[32]

At present, the vast majority of MRSA cases are hospital-acquired (HA-MRSA) and since the 1960s, it has been considered a healthcare related pathogen, with a high incidence.[33] However, there has been a recent emergence of strains of community-acquired MRSA (CA-MRSA), which can spread rapidly among otherwise healthy individuals.[6] One of the strains, known as

S. aureus USA300, postulated to have emerged during the early 1990s is an increasingly common cause of CA-MRSA infections.[34] Many cases have emerged in different demographics, including military trainees, prison inmates and American football teams.[6, 35] A study of the St. Louis Rams during the 2003 American football season found 5 of the 58 players had MRSA infections, typically at abrasion sites from falling.[35] Further to soft tissue infections, CA-MRSA infections have also been found to cause sepsis and necrotising pneumonia.[33] These more severe cases account for up to 4 % of CA-MRSA infections.[36]

Although the most pronounced CA-MRSA epidemic has been in the U.S, it is a global issue.[6, 36] There has been a rapid spread of CA-MRSA across the globe, with cases reported throughout North America, South America, Europe and Australia.[6] Furthermore, CA-MRSA is also an issue in Scandinavian countries where MRSA cases have typically been low.[6]

In the industrialised world, the approximate incidence of *S. aureus* bacteraemia is 10-30 per 100,000 person years.[1, 37] For example, in Denmark, there has been a gradual increase (from 3 to 20 per 100,000 person years) in observed cases from the 1950s to the 1990s, which is concurrent with an exponential increase in hospital admissions and invasive surgeries in Denmark.[1, 38] There has also been an increase in the contribution of MRSA to the incidence of *S. aureus* bacteraemia.[1] A study in Quebec, Canada found an increase from 0 to 7.4 cases per 100,000 person years between 1991 and 2005.[1, 39] During the same study period, cases of methicillin sensitive *S. aureus* (MSSA) bacteraemia remained relatively stable.[39] These findings have also been replicated in studies from the United Kingdom and North America.[1, 40-41] Furthermore, in the United States of America, the observed increase in MRSA bacteraemia has been largely linked to CA-MRSA, with strains such as *S. aureus* USA300 being particularly prevalent.[1, 42]

Infective endocarditis (IE) also presents a strain on global healthcare, with estimates suggesting that incidence ranges between 1.5 to 6 per 100,000 person years (in the USA and Europe between 1970-2000).[1, 43] Of these cases, *S. aureus* was found to cause 16-34 % of IE.[1, 43] During the period of study, no relative change in the prevalence of an individual bacterial species was noted. More current studies have shown that there has been an increase in the incidence of IE, the driving force of which has been an increase in *S. aureus* causing IE.[1] Furthermore, *S. aureus* IE was found to have an increased mortality rate, relative to other pathogens.[1, 44] *S. aureus* is also a substantial risk in prosthetic valve endocarditis.[1] The total annual incidence of prosthetic

valve IE is 0.8-3.6 %; of these, *S. aureus* is the causative agent of 23-33 % of cases.[1] The greatest risk of developing prosthetic valve IE is during the first 12 months after heart valve replacement surgery (greater for mechanical in the first 3 months, greater risk over the whole 12 months for porcine).[1, 45] Various studies have estimated the mortality rate of *S. aureus* IE to be between 22-66 %, higher than other causative agents of IE.[1]

As previously discussed, *S. aureus* can cause skin and soft tissue infections (SSTIs) ranging in severity from abscesses, impetigo and cellulitis to life-threatening conditions, such as necrotising fasciitis. In recent years, the importance of *S. aureus* as a causative agent of SSTIs has grown, exacerbated by a global epidemic of CA-MRSA SSTIs.[1, 36, 46] Studies have shown that CA-MRSA is not merely causing cases of SSTIs, but increasing the incidence.[1] A study between 1993-2005 found an increase in presentation of SSTIs in emergency departments in the USA from 1.2 million to 3.4 million annually.[47] Pallin *et al*. noted that this rise was 'contemporaneous' with the emergence of CA-MRSA. Although they cannot determine a causality between the two factors, they are concerned that CA-MRSA may be causing more disease, instead of replacing other causative agents.[1, 47] At the start of the study, treatment of SSTIs with drugs specific for CA-MRSA (such as trimethoprim **1.2**/sulphamethoxazole **1.3**, [Figure 1.2]) was rare, but by the end of the study (2005), treatment of clinical presentation of SSTIs with such drugs was commonplace.[47]

1.2   1.3
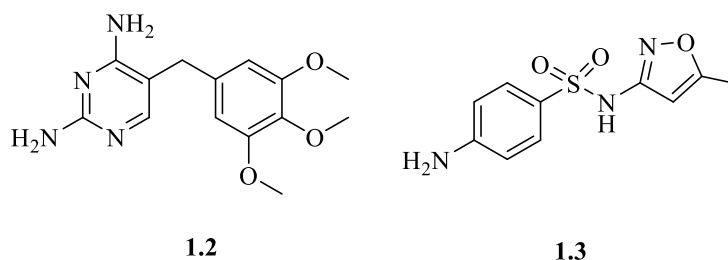
Figure 1.2. Trimethoprim (**1.2**)/ sulphamethoxazole (**1.3**) (co-trimoxazole), administered together

With the growing incidence of CA-MRSA, several studies have shown that there are distinct differences between CA-MRSA and both HA-MRSA and MSSA.[48] These distinct differences are believed to have enabled CA-MRSA to spread within the wider community, not just localised to the heathcare setting. One of the major differences between HA-MRSA and CA-MRSA is the possession of different antibiotic resistance profiles.[48] Notably, differences in the SCC*mec* cassette, which causes resistance to β-lactams (described in greater detail later in this chapter), can distinguish CA-MRSA and HA-MRSA. HA-MRSA strains typically belong to

SCC*mec* groups I, II and II, whereas CA-MRSA isolates typically carry SCC*mec* IV or V.[48] Type IV is known to not carry any resistance genes with the exception of those required for the resistance to β-lactams.[49] It is believed that this means SCC*mec* IV within strains of CA-MRSA confers a lower fitness burden. This is particualry important in an environment where antibiotic challenge is less common, i.e. outside of a healthcare environment where resistance genes are not always required.[50] In addition, CA-MRSA strains are typically resistant to a narrower spectrum of antibiotics when compared to strains of HA-MRSA.[36] The level of resistance to antibiotics in CA-MRSA has also been shown to be lower than in HA-MRSA, for example, Cheung *et al*. found the MIC of oxacillin to be 50 fold lower for the CA-MRSA strain USA300 than the HA-MRSA strain MRSA252.[51] This lower level of resistance could also be due to the lower level of exposure to antibiotic outside of the hospital environment.

In addition to their difference in antibiotic expression profiles, CA-MRSA strains have been shown to have increased virulence relative to HA-MRSA strains. The CA-MRSA strain LAC has been shown to be more virulent in a mouse infection model than HA-MRSA strains such as MRSA252.[52] Furthermore, the increased level of virulence of CA-MRSA strains relative to HA-MRSA may be explained by an increase in expression of virulence factors, such as toxins. Studies have also shown that there is increased level of expression of *agr* (a master regulator of staphylococcal virulence, described in more detail later in this chapter), which may lead to an increase in the observed levels of virulence factor production.[51]

Thus, it is clear that for *S. aureus*, both MSSA and MRSA strains present a clear burden on global healthcare systems. The development of antibiotic-resistant *S. aureus* species such as strains of MRSA and vancomycin-resistant *S. aureus* (VRSA) are a further complicating factors.[6] MRSA is a leading cause of death by an infectious agent within the USA and, as highlighted above, the recent emergence of CA-MRSA has further compounded this issue.[46] The data presented here provide a compelling case for the need of new therapies for the treatment of *S. aureus* infections.

1.4 *S. aureus* and antibiotic resistance

Prior to Alexander Fleming's discovery of penicillin, bacterial infection often proved fatal meaning that even a simple injury, if it became infected could be imminently life-threatening.[6]

Indeed, the first patient to be treated with penicillin, a police constable called Albert Alexander had developed sepsis after pricking his hand on roses whilst gardening. Antibiotics are one of the few drugs within pharmaceutical sciences which can be described as Paul Ehrlich's famous 'magic bullet' (Zauberkugel) due to their ability to kill a microbial infective agent, whilst having minimal effect on the host.

Antibiotics are crucial to modern medicine, critical to invasive surgery and chemotherapies. However, poor stewardship of antibiotics has led to the development of widespread antibiotic resistance in a range of species. These include; MRSA, VRSA, extensively drug-resistant (XDR) *Mycobacterium tuberculosis* and clindamycin-resistant *Clostridium difficile*.[6, 53-54] These present a significant global burden on health services. Indeed, the World Health Organisation (WHO) global report on anti-microbial resistance presents MRSA as an antibiotic resistant pathogen of international concern.[55]

In addition to the development of bacterial resistance to antibiotics, there has been a reduction in the research and development of novel antimicrobial therapies. Between the 1940 and 1990, there was a huge surge in the discovery and the development of antibiotics.[56] Companies were striving for scientific breakthrough, identifying new chemical entities and novel modes of action (MOA) in an aim to secure patents, a great financial incentive.[56] As resistance was encountered, replacement of drugs with a subsequent new generation of antibiotics was possible.[56] However in more recent years, the pharmaceutical industry has moved away from the production of new antibiotics towards more profitable therapeutics, primarily due to the huge financial investment required to bring a new drug to market.[56-57] The current situation has been described as 'the perfect storm', with a dramatic increase in untreatable antibiotic-resistant infections and a limited pipeline of novel antibiotics coming to market.[57]

1.4.1 Antibiotics used for treatment of *S. aureus* infections

Fleming's discovery (1928) and the exploitation of penicillin by Florey and Chain (1939) ushered in the antibiotic era, whereby previously fatal infections could be easily treated.[6, 58] With the exception of Salvarsan (**1.4**, Figure 1.3), discovered by Ehrlich in 1910, which was used for the treatment of syphilis, penicillin was the first class of antibiotic.[59]
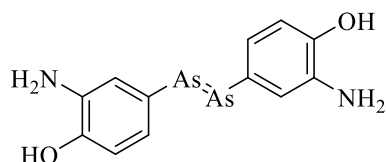
1.4

Figure 1.3. Salvarsan (**1.4**)

Penicillin describes a number of antibiotics which are produced by the moulds of *Penicillium spp.* and fall into a family of antibiotics called β-lactams. These compounds are based around a core structure, consisting of a fused thiazolidine and β-lactam bi-cyclic ring system and a variant side chain **1.5** (Figure 1.4).[60] The penicillins include penicillin G **1.6** (for intravenous use), penicillin V (oral) **1.7**, and benzathine penicillin **1.8** (intramuscular) (Figure 1.4).[61-63] Penicillin G **1.6** was the original molecule extracted from Fleming's *Penicillium notatam*.[61]
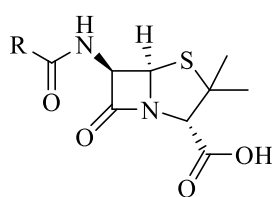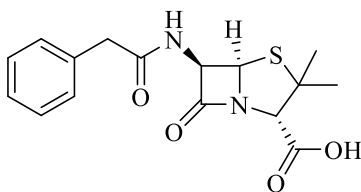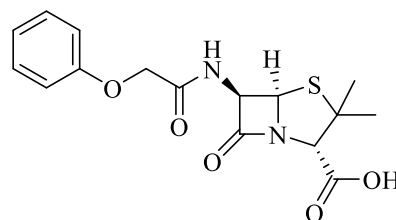
1.5   **1.6**   **1.7**
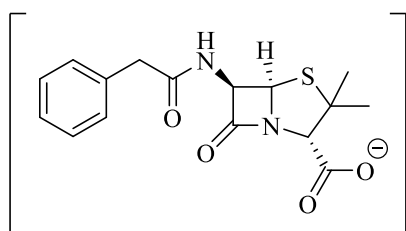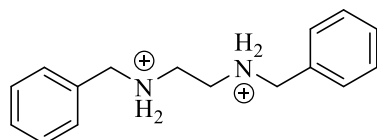
1.8

Figure 1.4. Structures of numerous penicillins. **1.5** General structure of penicillin, **1.6** penicillin G, **1.7** penicillin V and benzathine penicillin **1.8**

Penicillins are bactericidal, meaning they kill actively growing and dividing bacteria. They inhibit the synthesis of the bacterial cell wall, specifically the biosynthetic step involved in the cross-linking of peptidoglycan, resulting in structural weakness.[60] The target enzymes are

18

transpeptidases, also known as penicillin binding proteins (PBPs). [60, 64] *S. aureus* synthesises cell wall during normal growth and division. The cell wall is a polymer made up of repeating *N*-acetylglucosamine (NAG) **1.9** and *N*-acetylmuramic acid (NAM) **1.10** subunits, which forms the 'backbone' of the peptidoglycan (Figure 1.5, **1.11**).[64] Peptide side chains branch off NAM within the backbone (Figure 1.5).[64] In *S. aureus*, these peptide chains are branched penta-peptide chains consisting of L-Ala-γ-D-Glu-L-Lys(Gly)$_5$-D-Ala-D-Ala (Figure 1.5).[64] Elongation of the NAM-NAG glycan chain is carried out by PBPs which have transglycosylase activity, which involves the transfer of the disaccharide-pentapeptide (as described above) from membrane-bound lipid-II, adding it to the polysaccharide chain (Figure 1.5).[64-65] Cross-linking of the 'strands' is achieved through a transpeptidation reaction, wherein the terminal D-Ala is displaced by the terminal glycine of the pentaglyl side-chain on the L-Lys (Figure 1.5).[64] PBPs are crucial to the survival of *S. aureus* as unproductive formation of peptidoglycan cell wall leads to cell death.

A

B
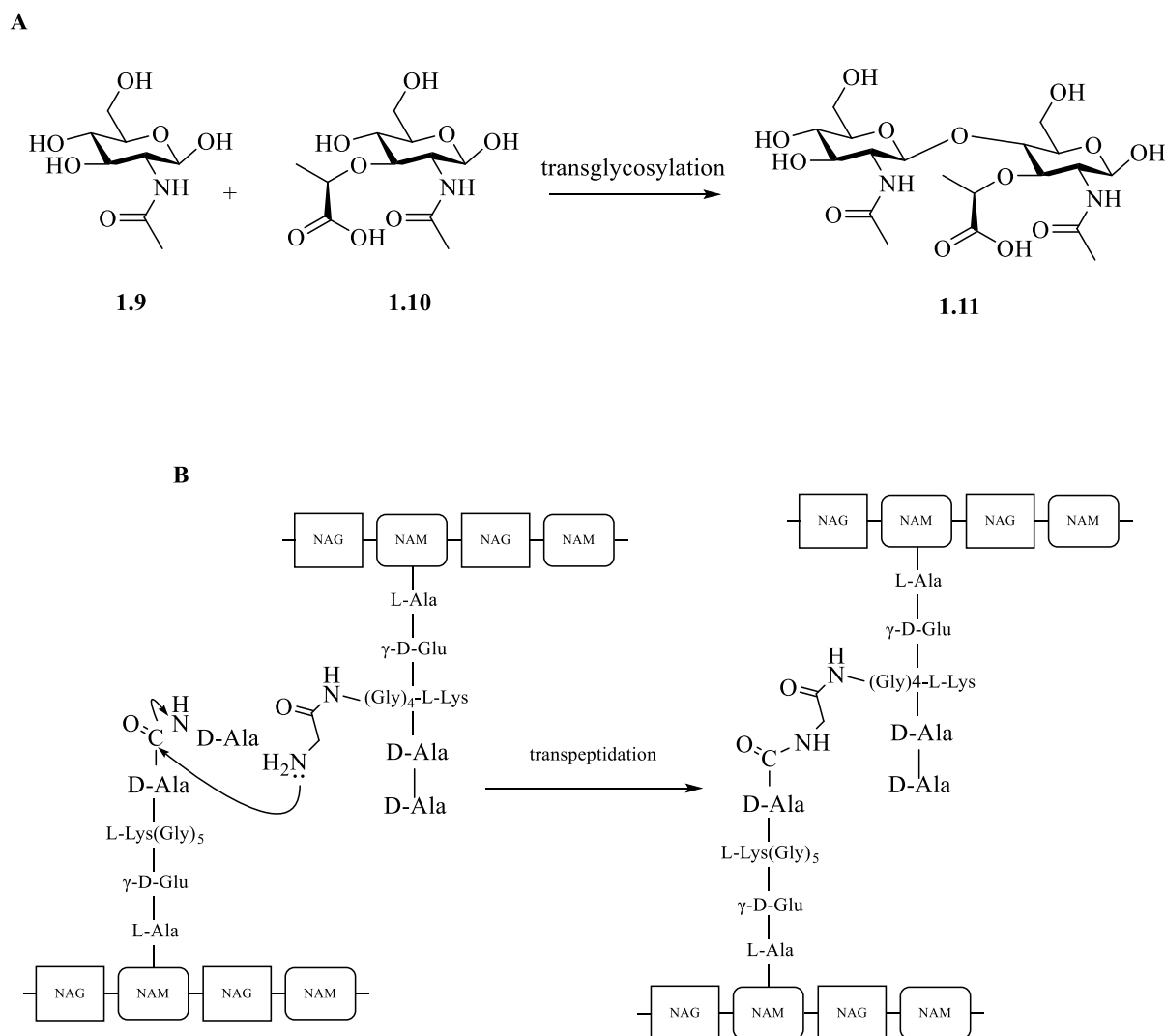
Figure 1.5. A. Transglycosylation between individual NAG **1.9** and NAM **1.10** subunits, forming the NAG-NAM dimer **1.11**, a polymer of which forms the glycan backbone of peptidoglycan. **B.** Transpeptidation, allowing for cross-linking between two peptidoglycan strands giving the polymer the strength required to function as the cell wall. Cross-linking occurs with the displacement of the terminal D-Ala by the terminal amino of the pentaglyl side chain.

β-lactam antibiotics inhibit the synthesis of the cell wall of *S. aureus* through inhibition of the transglycolase-transpeptidase PBP2.[65] Indeed transglycolase-transpeptidase enzymes are called PBPs because of their known binding of penicillins.[66] It is thought that β-lactam antibiotics mimic the natural substrate of the transpeptidase domain, the terminal portion of the peptidyl chain (D-Ala-D-Ala) (Figure 1.5).[66-67] Both the natural peptidoglycan substrate and β-lactam acylate a catalytic serine within the active site of the transpeptidase active site of the PBP.[66] The natural peptidoglycan-enzyme acyl species can react with a second peptidoglycan chain (terminal glylyl) forming the desired peptidoglycan cross-link (Figure 1.5).[66] The acyl

20

intermediate formed with the β-lactam, cannot undergo this second step, thus inhibiting the PBP, disrupting the synthesis of the cell wall of *S. aureus*, leading to cell death.[66]

1.11 Vancomycin

1.12 Teicoplanin

1.13 Telavancin

1.14 Dalbavancin
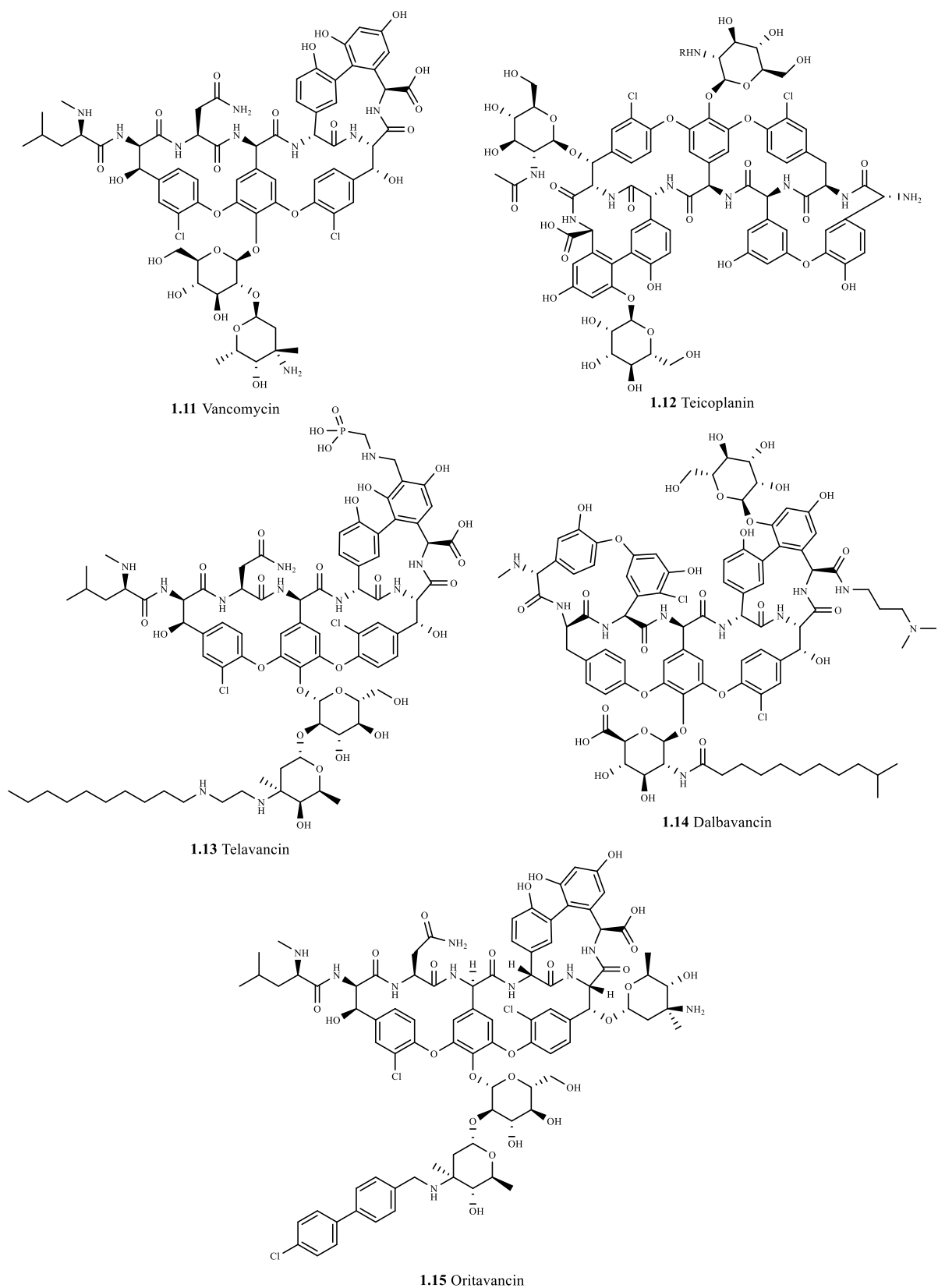
1.15 Oritavancin

Figure 1.6. The structures of glycopeptides. vancomycin **1.12**, general structure of teicoplanin **1.13**, telavancin **1.14**, dalbavancin **1.15** and oritavancin **1.16**

22

There are other classes of antibiotics that target the cell wall. For example, the glycopeptides, including vancomycin **1.12** (Figure 1.6), disrupt the synthesis of the cell wall of *S. aureus*.[65] Vancomycin is widely used to treat serious infections, caused by *S. aureus*.[65] The most widely used members of the glycopeptides are vancomycin **1.12** and the lipoglycopeptide analogue teicoplanin **1.13** (Figure 1.6).[68] Semi-synthetic lipoglycopeptide analogues telavancin **1.14**, dalbavancin **1.15** and oritavancin **1.16** are also in clinical use (Figure 1.6).[68] These compounds are known to bind to D-Ala[4]-D-Ala[5] of lipid-II monomer, acting as a 'substrate binder', preventing the key transglycosylation step catalysed by PBP2, and consequently disrupting peptidoglycan synthesis (Figure 1.6).[65, 68] Although the lipid-II monomer is expressed in the vast majority of bacterial species, the activity of glycopeptides is limited to Gram-positive species.[68] This is due to the physiochemical properties of glyopeptides preventing them from crossing the outer membrane of Gram-negative bacteria.[68]

1.17
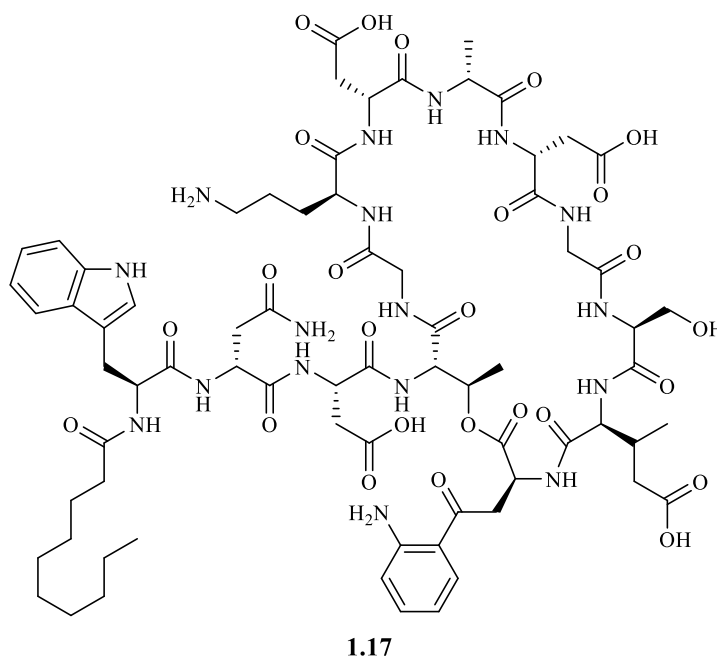
Figure 1.7. The peptidic antibiotic daptomycin **1.17**.

Daptomycin **1.17** (Figure 1.7) is a cyclic peptide antibiotic, used for the treatment of *S. aureus* bacteraemia and IE.[65] It is also commonly used to treat MRSA infections, and bacteria that are resistant to vancomycin.[65, 69] Daptomycin **1.17** is known to target the *S. aureus* cell membrane.[65, 70]

Daptomycin requires calcium for bactericidal activity, forming an active Ca^{2+}-daptomycin complex, with coordination of the Ca^{2+} ion by an aspartate and several carbonyls within the

peptidic backbone.[65, 70-71] The Ca^{2+}-daptomycin complex behaves as a cationic peptide upon interaction with the cell, it undergoes oligomerisation forming cell-wall permeable micelles, which then interact with the negatively charged phosphate head groups of phosphatidyl glycerol.[65] This leads to disruption of the phospholipid bilayer resulting in membrane permeabilization, leakage of ions, membrane depolarisation and ultimately death of the bacterial cell.[65]

In addition to targeting the synthesis of bacterial cell wall components, antibiotics interfere with key bacterial life processes. This includes the inhibition of protein synthesis, through the inhibition of both the 30S and 50S ribosomal subunits. Inhibitors of the 30 S subunit include tetracyclines, such as tetracycline **1.18** and tigecycline **1.19** (Figure 1.8).[65] The aminoglycosides, such as neomycin **1.20** and gentamicin **1.21** (Figure 1.9) are also known inhibitors of the 30S subunit.[65] Inhibitors of the 50S subunit include linezolid **1.22** and chloramphenicol **1.23** (Figure 1.10).[65]
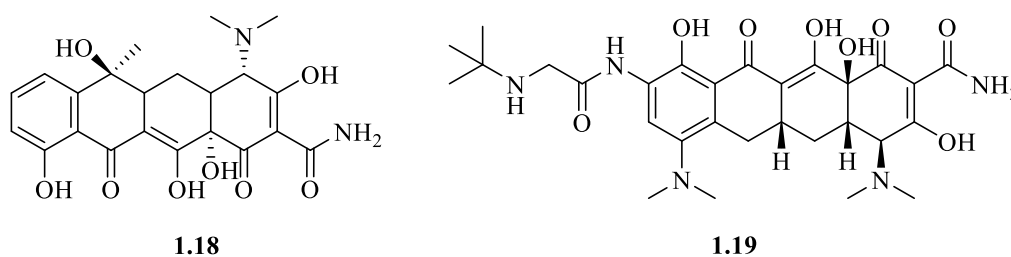
Figure 1.8. Tetracyclines, tetracycline **1.18** and tigecycline **1.19**.

Tetracyclines are bacteriostatic antibiotics.[72] They function through binding near to the mRNA codon recognition site of the amino acyl-tRNA (aa-tRNA).[65, 73-74] In fact, Mg^{2+} within the ribosome forms a complex with tetracycline and is stabilised by a further six intramolecular contacts with residues within the 16S rRNA, which effectively disrupts binding of the aa-tRNA, leading to dissociation and cessation of protein synthesis.[65, 72, 74]

Aminoglycosides are the only known bactericidal ribosome binding antibiotic.[65] They function by blocking initiation of translation at ribosomes and causing a 10-fold increase in mistranslation of RNA, from < 1 per 1,000 amino acids to ~1 in 100.[65, 75] Davis *et al*. suggest that the bactericidal effect comes from the production of defective membrane proteins, leading to disruption of the cell membrane and subsequent cell death.[65, 75]
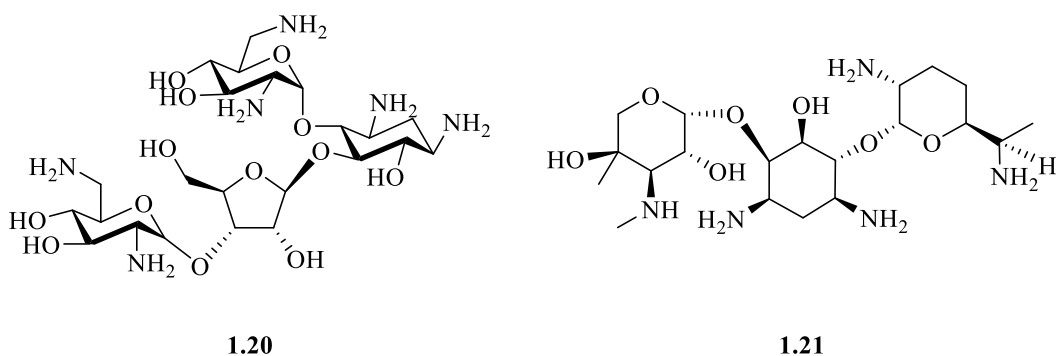
Figure 1.9. Examples of aminoglycosides, neomycin B **1.20** and gentamicin C2 **1.21**.

Inhibitors of the 50S subunit include linezolid **1.22**, an oxazolidinone, which binds at the peptidyl transfer centre of the ribosome, which results in disruption of peptide backbone formation.[65] Like linezolid **1.22**, chloramphenicol **1.23** also disrupts peptidyltransferase through interference with the amino acyl terminal of aa-tRNA.[65]
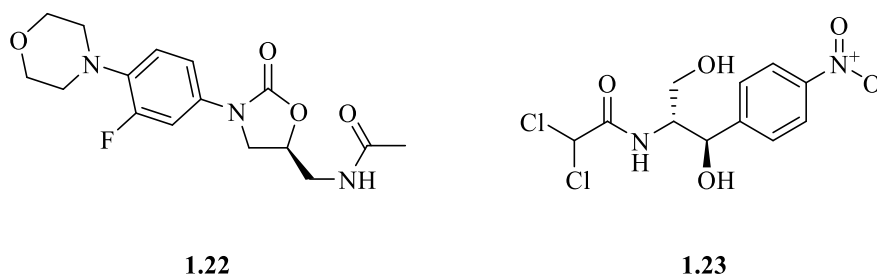
Figure 1.10. Inhibitors of the ribosomal 50S subunit linezolid **1.22** and chloramphenicol **1.23**.

Protein synthesis can also be interrupted through the disruption of the transcription machinery. Rifampicin **1.24** (Figure 1.11) targets the β-subunit RNA polymerase (encoded by the *rpoβ* gene).[65, 76] Rifampicin is known to sterically block transcriptional elongation.[77] Rifampicin is bactericidal due to its high affinity binding and RNA polymerase inhibitory activity, arresting transcription, a key life process.[77]

The replication of bacterial DNA is another essential process that is targeted by antibiotics. Fluoroquinolones, such as ciprofloxacin **1.25** (Figure 1.12) have been used previously for the treatment of *S. aureus* infections.[78] Fluoroquinolones have two main targets within the bacterial cell, these are DNA gyrase and topoisomerase IV.[65, 79] DNA gyrase is a type-II topoisomerase, consisting of four individual subunits (2 GyrA and 2 GyrB) and induces negative supercoils into the double stranded circular genomic DNA during DNA replication.[79-80] This prevents the

accumulation of positive supercoils ahead of the advancing replication fork.[79-80] The accumulation of positive super coils exerts considerable stress on the DNA and can lead to double-strand breakage, fatal for the bacteria.[79-81] Topoisomerase IV is the second target of fluoroquinolones.[79] It is a tetramer (2 ParC and 2 ParE subunits) and shares homology with DNA gyrase.[79] Like DNA gyrase, topoisomerase IV carries out relaxation of the circular genomic bacterial DNA during replication and when disrupted, contributes further to bacterial cell death.[79]

1.24

Figure 1.11. The RNA polymerase inhibitor rifampicin **1.24**

For both gyrase and topoisomerase IV, the production of double-stranded DNA is cruicial to the activity of the enzyme. If too many unregulated double-stranded breaks breaks occur this can lead to cell death. Aldred states that quinolones capitalise on this and convert both gyrase and topoisomerase into cellular toxins, through inhibition, leading to an increase in the number of enzyme-DNA cleavage complexes, this increases the risk of double stranded DNA breaks.[81]

1.25

Figure 1.12. The fluoroquinolone ciprofloxacin **1.25**

1.4.2 Mechanisms of *S. aureus* antibiotic resistance

Naturally, *S. aureus* is susceptible to almost all antibiotics.[6] Poor stewardship of antibiotics has led to the development of widespread antibiotic resistance. Antibiotics impose a significant selection pressure on *S. aureus* and hence an evolutionary driving force. Evolution drives resistance as those bacteria adapted to survive (resistant to antibiotics) are selected for.

The resistance to antibiotics occurs through a number of mechanisms. These include, but are not limited to, mutation leading to alteration of the antibiotic target binding site, an increase in the level of expression of efflux pumps and reduced cell envelope permeability.[65]

Within a few years of the introduction of the penicillin β-lactam (early 1940s) antibiotics, resistant strains were being observed clinically. This highlights the ease by which *S. aureus* can develop resistance to antibiotics. These resistant strains of *S. aureus* were found to be expressing a β-lactamse enzyme which can specifically hydrolyse the β-lactam moiety, critical to its bactericidal activity.[65] The β-lactamase which causes resistance to penicillins in *S. aureus* is BlaZ, (encoded by *blaZ*) which contains a key catalytic serine residue (Figure 1.13).[65] This serine residue is utilised for hydrolysis of the β-lactam moiety, rendering the penicillin molecule inactive (Figure 1.13).[65, 82]
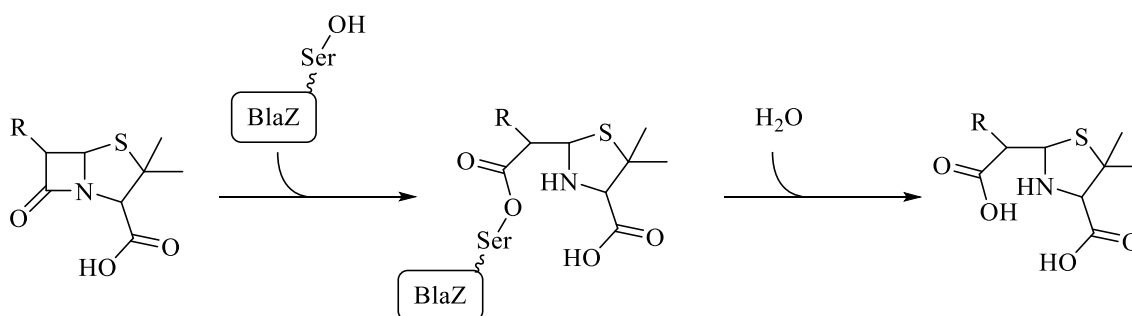
Figure 1.13. BlaZ catalysed opening of the β-lactam ring of penicillin antibiotics.

BlaZ is an extracellular enzyme and is produced when the cell is exposed to a β-lactam antibiotic.[82] Its expression is controlled by two regulatory genes, the *blaI* repressor and the *blaR1* anti-repressor.[82] Studies suggested that upon exposure to β-lactams and binding of a β-lactam to the known transmembrane receptor/signal transducer BlaR1, BlaR1 undergoes rapid autolytic cleavage.[83] Zhang *et al*. indicated that the un-cleaved BlaR1 is a prometalloprotease, which upon autolytic activation can then cleave the BlaI repressor (Figure 1.14). This removes BlaI from its intergenic operator between *blaZ* and *blaR1* (Figure 1.14).[82-84] This allows for

transcription of *blaZ* and expression of the BlaZ β-lactamase, allowing for resistance.[83] De-repression of *blaR1* is necessary, as once cleaved, it can no longer transmit a signal, thus to ensure longevity of the signal, the continual production of BlaR1 is required.[83]

blaZ is carried on the transposon Tn552, which is often on a large β-lactamase/heavy-metal resistance plasmid.[65, 85] This is a mobile genetic element, which allows for the transmission of resistance genes.
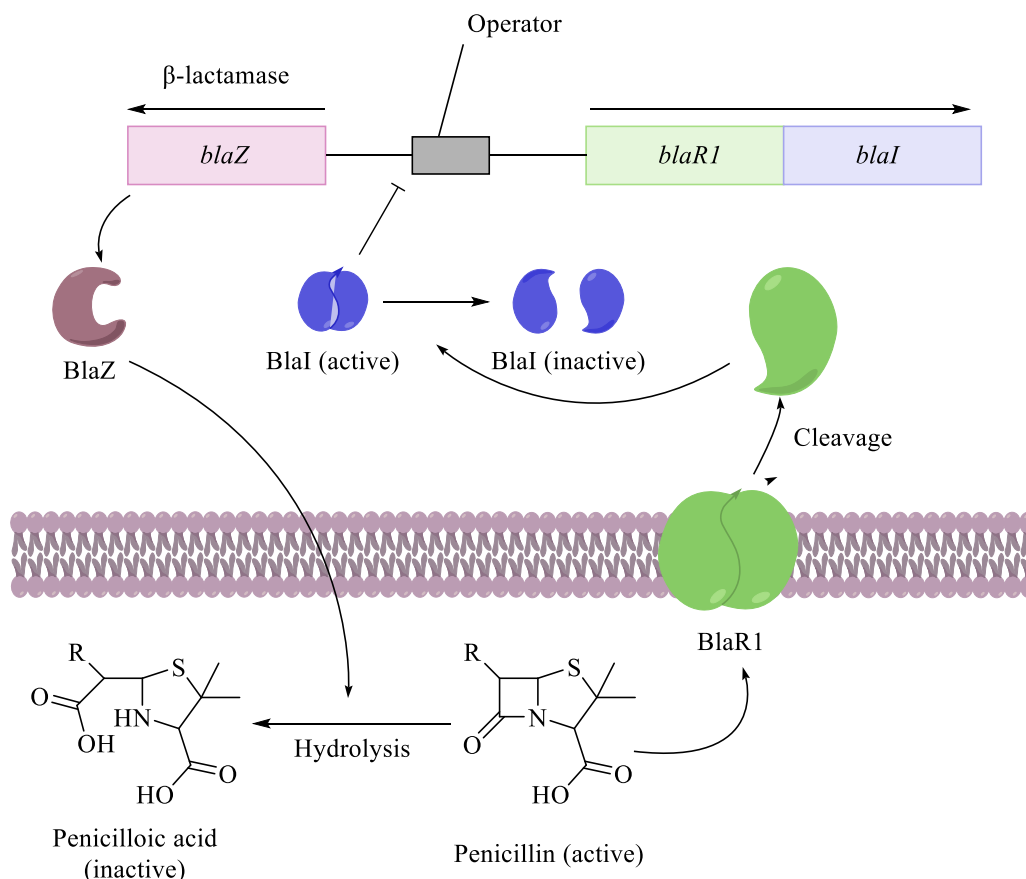
Figure 1.14. The regulation of the synthesis of the BlaZ β-lactamase in *S. aureus*. Briefly, a penicillin antibiotic binds the membrane bound BlaR1 receptor/signal transducer, which then undergoes rapid autolytic cleavage. After autolytic activation, active BlaR1 can cleave the BlaI repressor, preventing binding to it's intergenic operator region. This allows for expression of *blaR1*, *blaI* and *blaZ*. *blaZ* encodes the BlaZ β-lactamase, which can then hydrolyse the β-lactam heterocycle within penicillin molecules.

As previously outlined, within a few years of the introduction of penicillins for clinical use, resistance was observed. To counter this, second generation semi-synthetic penicillins were introduced in 1959.[64] This second generation include oxacillin **1.26** and methicillin **1.27** (Figure 1.15).[64] However, within two years, cases of MRSA were being observed clinically.[86] This sudden emergence of resistance was due to the acquisition of the *mecA* gene, which encodes a PBP, called PBP2a, the transpeptidase domain of which is not potently inhibited by

β-lactams.[64] This allows for the synthesis of peptidoglycan even in the presence of methicillin. Studies have shown that the active site of the PBP2a transpeptidase has a more closed conformation than the normal PBP2, occluding access by active β-lactams.[64] PBP2a is still able to efficiently catalyse the crosslinking of peptidoglycan, despite the closed conformation of the active site and the ~ 1000 Å^3 size of the two peptidoglycan subunits.[64] It is suggested that the protein undergoes a significant conformational change during catalysis.[64]
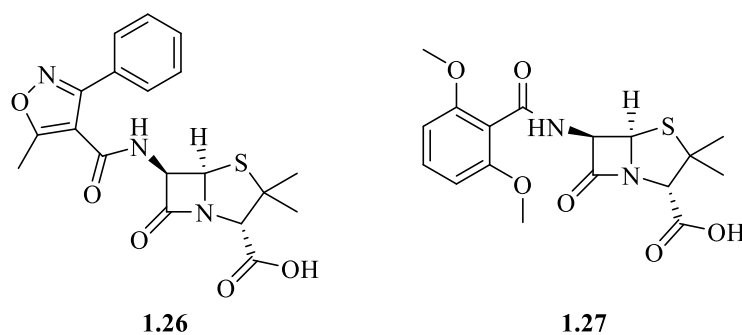
Figure 1.15. Second generation semi-synthetic penicillins oxacillin **1.26** and methicillin **1.27**.

The *mecA* is within the chromosome of all MRSA strains and is part of a mobile genetic element called *SCCmec*, a genomic island, transferred between cells due to the action of cassette chromosome recombinases A and B (*ccrA* and *ccrB*), both encoded within *SCCmec*.[82, 85, 87] These are site specific recombinases and can excise the cassette and integrate it at a specific site within the chromosome.[87] Integration of *SCCmec* into the genome of *S. aureus* at the *attBscc* locus (near the *S. aureus* origin of replication) is sufficient to convert drug sensitive MSSA into the drug-reistant nosocomial pathogen MRSA, which is resistant to the majority of β-lactam antibiotics.[49] *SCCmec* elements are diverse in nature and have been characterised into 13 types.[88] These are based on different combinations of five *mec* complexes (A, B, C1, C2 and E) and nine distinct *ccr* complexes (1-9).[88] *SCCmec* also contain *mecR1* and *mecI*, both of which regulate the expression of *mecA*.[85] MecR1, in the presence of a β-lactam antibiotics cleaves the MecI repressor, which is bound to the operator of the *mecA* promoter, this allows for the expression of PBP2a.[85]

1.28   **1.29**
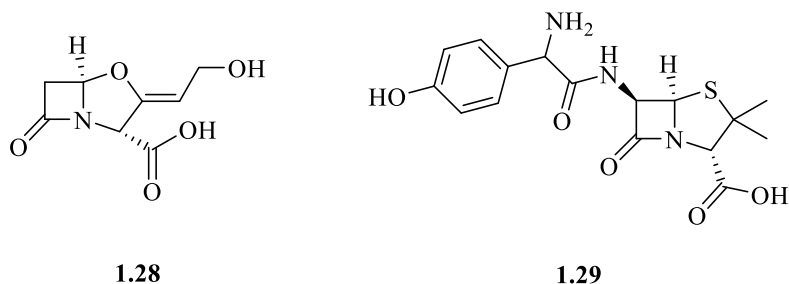
Figure 1.16. The β-lactamase suicide inhibitor clavulanic acid **1.28** which is used in conjunction with amoxicillin **1.29** as a means to extend its spectrum.

With the development of resistance to β-lactams by *S. aureus*, attempts have been made to circumvent this. These include the development of so-called suicide inhibitors of β-lactamases including clavulanic acid **1.28**, which has been used in conjunction with amoxicillin **1.29** to extend its spectrum of activity in the era of antibiotic resistance (Figure 1.16).[89] Furthermore, the development of further β-lactam antibiotics which are chemically more resistant to β-lactamases, these include carbapenems **1.30** and cephalosporins **1.31** (Figure 1.17).[90-91]

1.30   **1.31**
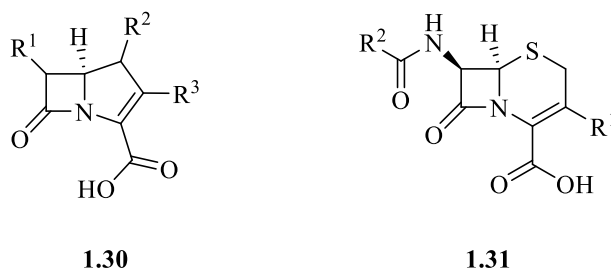
Figure 1.17. General structure of carbapenems **1.30** and cephalosporins **1.31**.

Resistance to glycopeptides including vancomycin has also been observed.[65] By the end of the 1990s, MRSA strains had become the most common cause of *S. aureus* infections and the most common therapy for these infections were glycopeptide antibiotics, predominantly vancomycin.[92] The development of vancomycin resistance in *S. aureus* is thought to be polygenic and requires the development of mutations in a number of genes in cell wall biosynthesis.[93] This resulted in the development of vancomycin intermediate-resistant *S. aureus* (MIC= 4-8 µg/mL) and vancomycin-resistant *S. aureus* (MIC= >16 µg/mL).[93] Vancomycin resistance is caused by the *vanA* operon, part of the transposon Tn1546, originally part of a vancomycin resistant enterococci conjugative plasmid.[93] The *vanA* operon consists of seven genes (*vanA*, *vanH*, *vanX*, *vanS*, *vanR*, *vanY* and *vanZ*) and is regulated by a two component sensory (VanS) and regulatory (VanR) system.[93]

As described earlier, vancomycin binds to the D-Ala4-D-Ala5 of newly synthesised peptide pre-cursors, required for the synthesis of peptidoglycan. In contrast, the *vanA* operon allows for the synthesis of a D-Ala4-D-lactate peptidoglycan precursor, which cannot be bound by vancomycin.[93] This yields a peptidoglycan that is not susceptible to glycopeptide interference.[93] The production of the D-Ala4-D-lactate precursor is carried out by VanA (catalyses the D-Ala4-D-lactate ester bond formation) and VanH (forms D-lactate).[93] VanX hydrolyses the D-Ala-D-Ala bond and VanY is capable of removing D-Ala-D-Ala which has already been attached to the larger pentapeptide peptidoglycan precursor (Figure 1.18).[93] Together, the *vanA* operon produces a cell wall resistant to glycopeptide antibiotics.
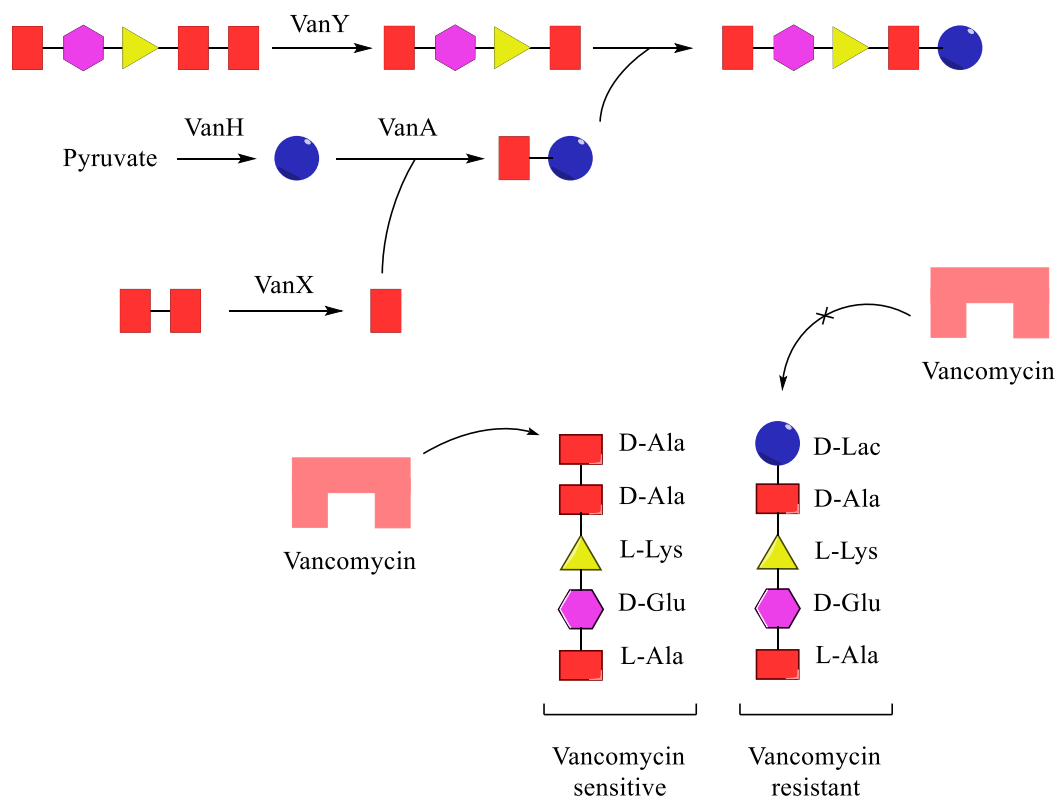
Figure 1.18. Schematic of how resistance to vancomycin develops in *S. aureus*, adapted from Mcguinness et al.[93]

Resistance to antibiotics that target the 30S ribosomal subunit has also been observed. Resistance to tetracyclines has been observed through two main mechanisms. Firstly, through efflux which is mediated by two tetracycline efflux pumps TetA(K) and TetA(L).[65] The efflux pumps use a proton gradient as the driving force for tetracycline efflux. The TetA(K) pump is encoded on the plasmid pT181 and is integrated into the *SCCmecIII* cassette of numerous MRSA strains.[65] In addition to efflux pumps, mechanisms of ribosomal protection have also been observed.[65] These include TetO/M, which resemble elongation factor-G, it does not

function as an elongation factor, but instead helps displace tetracyclines from the ribosomal active site.[65]

Resistance to aminoglycosides, such as neomycin and gentamicin, which also inhibit the 30S ribosomal subunit has also been recorded. This typically occurs through the expression of enzymes, again encoded by mobile genetic elements, which chemically modify aminoglycosides.[65] Modification prevents binding of the drug to the ribosome, rendering it useless. The gene *aaC-aphD* encodes an acetyltransferase-phosphotransferase (carried on transposon TN4001) can lead to resistance against both neomycin and gentimycin.[65]

Resistance to linezolid **1.22** and chloramphenicol **1.23**, antibiotics which target the 50S ribosomal subunit has also been seen.[65, 85] Chloramphenicol resistance occurs through the inducible expression of the chloramphenicol acetyltransferase enzyme, which is carried on the pC221 plasmid.[85] The acetylation of chloramphenicol to produce acetyl-chloramphenicol **1.32** prevents binding to the 50S subunit of the ribosome (Figure 1.19). In addition to chloramphenicol acetyltransferase, 23S rRNA methyltransferase, which methylates A2503 of 23S rRNA, causing resistance to chloramphenicol.[94] The methyltransferase can also confer resistance to linezolid.[85]
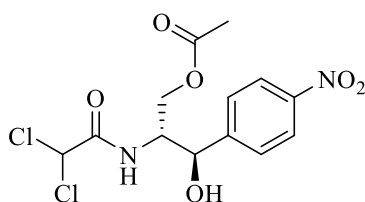
1.32

Figure 1.19. Acetyl-chloramphenicol **1.32**, produced by the chloramphenicol acetyltransferase enzyme.

As described above, *S. aureus* has also developed resistance to a broad spectrum of antibiotics. It is hardly surprising that resistance should arise, given the stringent selection pressure conferred on *S. aureus* by antibiotics. Those organisms which are not adapted die and those which survive can pass on their genes to the subsequent generation. One could argue that resistance is merely a product of evolution and could be deemed to be inevitable. In addition, mobile genetic elements further compound the issue and aid in the development of resistance. This, taken with the evidence above provides a compelling case for the development of new therapeutic strategies for the treatment of antibiotic resistant *S. aureus* infection. These

strategies would need to disrupt the organism sufficiently to ease infection, whilst applying minimal selective pressure. This could be carried out by the targeting of non-critical bacterial life processes. One such avenue of therapy could be the development of anti-virulence compounds, with the goal of 'disarming' the bacteria, aiding the perturbation of infection.

1.5 The virulence of *S. aureus*

As described previously, *S. aureus* can exist as both a commensal bacterium and an opportunistic pathogen. The ability of *S. aureus* to fulfil both roles is due to its exquisite regulation of expression of an arsenal of virulence factors. These virulence factors and their regulatory elements are known as accessory genes and are not essential for normal bacterial growth.[12] The accessory genes fulfil numerous roles, including tissue adhesion, evasion of the immune system and injury to the host tissues and cells.[95] The pathogenesis of *S. aureus* is a complex process, requiring the coordination of both extracellular and integral cell wall proteins, each of which is key for different stages of infection, such as cell wall adhesins, e.g. protein A and the fibronectin binding proteins required for early stage infection and the production of toxins in later infection.[96] The majority of these accessory genes encode bacterial cell wall surface and secreted proteins.[97] Together, these allow the bacteria to fulfil the functions described above and are collectively known as the virulon.[97]

In the late 1980s, a number of studies described the global regulator, the accessory gene regulator (*agr*) as an overarching regulator of the *S. aureus* virulon that regulates the expression of numerous staphylococcal exoproteins.[97-100] In addition to the *agr* system, *S. aureus* has numerous other virulence regulatory systems such as the Sae (*S. aureus* exoprotein expression) two-component response system, which in conjunction with *agr* drives the expression of numerous exoproteins such as alpha-toxin, coagulase (activates prothrombin), Panton-Valentine leucocidin (cytotoxin that destroys leukocytes) and TSST-1.[12, 101-102] Another major regulator of staphyclococcal virulence is SarA, a cytoplasmic DNA binding protein that can enhance expression of α, β and δ toxins, through direct effect and/ or up-regulation of *agr* activity.[96]

1.5.1 The staphylococcal *agr* system

Recsei *et al*. identified the *agr* system through insertion of an erythromycin resistance cassette between the *purB* and *ilv* loci.[98] They noted a 50 fold decrease in the expression of α, β and δ

haemolysins and TSST-1.[98] Furthermore, the staphylococcal *agr* system has been shown to regulate the expression of numerous exoproteins, a list of which is surmised in (Table 1.1).[97] It acts as a 'molecular switch', driving expression of a range of toxins and repressing the expression of integral cell wall proteins during the *post*-exponential growth phase of *S. aureus*.[96] This aids in the dissemination of biofilms and the propagation of infection.

The staphylococcal *agr* system is a quorum sensing (QS) system.[103] QS is a phenomenon where bacteria can produce, sense and respond to small extracellular signal molecules in a cell density dependent manner.[104] This allows the bacteria to employ community-wide behaviours, such as virulence, bioluminescence and swarming through co-ordination of gene expression.[104-106] QS systems utilise a range of chemical signal molecules. Despite these differences in signal molecule chemistry and overall mechanism of each system, they all function based on similar principles.[104] At low bacterial population densities, the signal molecules diffuse away and are therefore present at very low concentrations, thus are not detected.[104] At a higher bacterial cell population densities, the signal molecule reaches a sufficient concentration due to the cumulative production (autoinduction), which in turn allows for the detection and subsequent response to the signal molecule.[104] The signal molecules are all recognised by either membrane bound or cytoplasmic receptors and upon recognition of signal molecule, its production is upregulated.[104]

Table 1.1. Some of the genes regulated by the *agr* system

Gene	Product	Reference
Directly regulated by *agr*		
agrBDCA	Agr B, D, C and A	[107]
rna-III	RNA-III and δ-toxin	[108]
Indirect Regulation		
Toxins		
tst	TSST-1	[98]
hla	α-haemolysin	[98]
hlb	β-haemolysin	[98]
hlgBC	γ-haemolysin	[109]
hld	δ-haemolysin	[98]
seb	Enterotoxin B	[110]

sec	Enterotoxin C	[111]
sed	Enterotoxin D	[110]
pvl	Panton-Valentine Leukocidin	[109]
Enzymes		
sak	Staphylokinase	[98]
lip	Lipase	
splA-F	Spl proteases	[112]
aur	Aureolysin	[113]
ssp	Staphylococcal serine proteases	[113]
scp	Staphylococcal cysteine proteases	[113]
Immunomodulation		
psmα1-4	Phenol soluble modulin-α 1-4	[114]
psmβ1-2	Phenol soluble modulin-β1-2	[114]
scn	Staphylococcal complement inhibitor	[115]
Down-regulated		
Surface proteins		
spa	Protein A	[98]
fnbA/B	Fibronectin-binding protein A/B	[116]
coa	Coagulase	[117]
Regulators		
rot	Rot transcription factor	[118]

Both Gram-negative and Gram-positive bacteria utilise QS systems.[104] Gram-negative bacteria use small molecules such as acyl-homoserine lactones **1.33**, which can diffuse across both the outer and inner membranes and bind to cytoplasmic receptors which can regulate gene expression (Figure 1.20).[104]

In contrast, Gram-positive bacteria generally use peptide signal molecules called auto-inducing peptides (AIPs).[104] These are produced and secreted by bacteria and bind to a membrane bound histidine kinase which, as part of a two-component signal transduction cascade can regulate gene expression.[104]
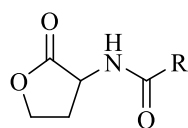
1.33

Figure 1.20. General structure of an *N*-acyl-homoserine lactone **1.33**.

Thus, in *S. aureus*, the *agr* system is based around two promoters, *P2* and *P3* which drive two divergent transcripts (Figure 1.21).[103] *P3* drives expression of RNAIII, a master regulator of staphylococcal virulence.[119] *P2* drives expression of the *agr* operon, which consists of four genes, *agrB*, *agrD*, *agrC* and *agrA* which encode the components of the *agr* system.

AgrB and AgrD are responsible for the synthesis of the signal molecule AIP, a thiolactone macrocyclic (macrocycle of 5 amino acids) peptide **1.34** (AIP-I)(Figure 1.21). AgrD is the precursor to AIP and is synthesised as a pre-pro-peptide consisting of a core AIP sequence flanked N-terminally by an amphipathic helical region and C-terminally by an hydrophilic region.[120] In *S. aureus*, the core AIP sequence is 7-9 amino acids in length (Table 1.2) and can be divided into four distinct groups, each with their own corresponding *agr* system, differentiated by primary amino acid sequence.[121] AIPs have strong cognate *agr* agonistic properties and potent cross-group antagonism.[103]

A

AIP

AgrB

AgrC

AgrD

AgrA

P

P

| *agrA* | *agrC* | *agrD* | *agrB* | | P2 | | P3 | | *rnaIII* |

agr operon

RNAIII effector

B
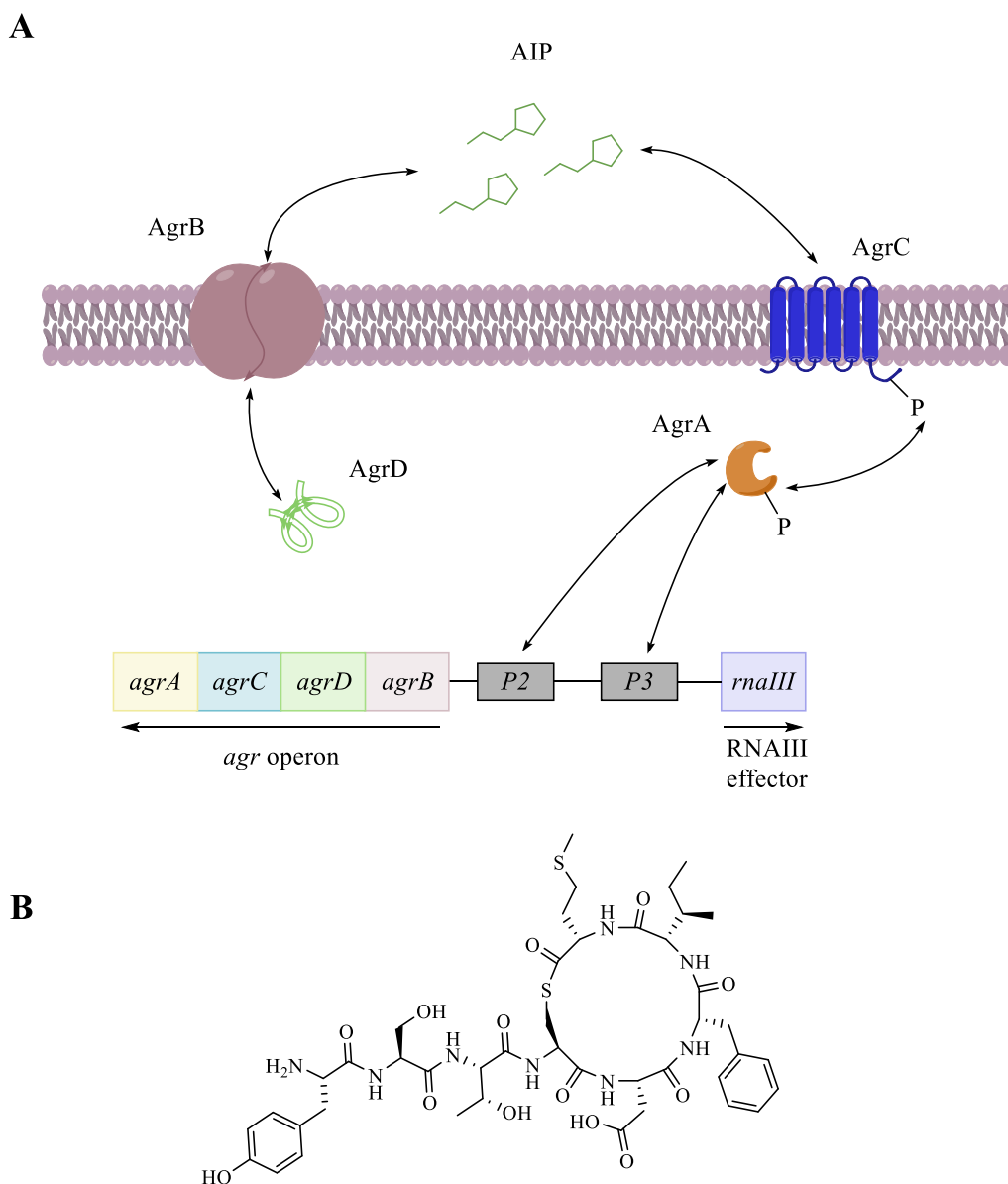
1.34

Figure 1.21. (A) The staphylococcal *agr* system: AgrD, the precursor to AIP is processed by the membrane bound cysteine protease AgrB and MroQ, a putative signal endopeptidase, releasing mature AIP. AIP can subsequently bind to AgrC, a canonical histidine kinase receptor, allowing auto-phosphorylation, recruitment of AgrA and subsequent phosphotransfer. Once phosphorylated, AgrA, can drive expression of both the P2 and P3 transcripts. **(B)** Structure of AIP-I **1.34** containing the key 5-membered thiolactone macrocycle.

The N-terminal region of AgrD is required for localisation to the inner leaflet of the membrane, to bring AgrD proximal to AgrB, a membrane bound cysteine protease, recognition of which is carried out by the C-terminal region of AgrD.[120] AgrB (Figure 1.22) catalytically excises the C-terminal region of AgrD, forming a thioacyl-enzyme intermediate between a key catalytic cysteine (Cys77) within AgrB and the terminal methionine of the processed AIP sequence (Figure 1.22 and Figure 1.23).[120] The thio-acyl intermediate then undergoes an intramolecular

trans thio-esterification reaction with the thiol of an absolutely conserved cysteine internal to the pre-AIP molecule (Figure 1.22). This process forms the 5-membered thiolactone macrocycle and releases the macrocyclic pre-AIP molecule from AgrB, restoring the active site.[122-123] All staphyclococcal AIP molecules contain this thiolactone macrocycle, with the exception of the sub-species of *Staphylococcus intermedius, Staphylococcus pseudointermidius*, which has a lactone macrocycle **1.35**, formed between the terminal carboxyl and an internal serine residue (Figure 1.24).[120]

The thiolactone pre-AIP molecule is then translocated to the outer leaflet of the membrane where the N-terminal amphipathic helix is removed by the putative CAAX metalloprotease MroQ (Figure 1.23).[124] The result of these processes is the secretion of the mature AIP signal molecule into the extracellular milieu (Figure 1.21).

Table 1.2. The primary amino acid sequences of AIP *S. aureus* AIPs. AIP I-IV where AIP-I and AIP-IV only differ by one amino acid. Highlighted the absolutely conserved cysteine residue, critical for the formation of the thiolactone macrocycle.

S. aureus AIP	Primary Amino Acid Sequence							
AIP-I		Y	S	T	C	D	F	I	M
AIP-II	G	V	N	A	C	S	S	L	F
AIP-III			I	N	C	D	F	L	L
AIP-IV		Y	S	T	C	Y	F	I	M

The mature AIP molecule from each *agr* group has its own distinct structure (Figure 1.25). AIPs are between 7-9 amino acids in length and contain a thiolactone macrocycle comprising of 5 amino acids and an N-terminal tail region of either 2 or 4 residues. The thiolactone connection is made between a conserved cysteine residue, 5 residues from the C-terminus of the AIP sequence and the terminal carboxylic acid (Figure 1.25).

Mature, extracellular, mature AIP can bind to AgrC, a canonical histidine kinase receptor, consisting of 5-6 transmembrane regions with a C-terminal histidine kinase domain, which exists as a homodimer within the membrane of *S. aureus*.[103, 121, 125] Upon the binding of cognate AIP, that is, AIP of the same *agr* group, the AgrC receptor undergoes auto-phosphorylation *in-trans*, allowing for recruitment and subsequent transfer of phosphate to AgrA (Figure 1.21).[125]

The phosphorylated AgrA subsequently binds to promoters *P2* and *P3* in order to drive the expression of the *agr* operon and an upregulation of toxin production, mediated by RNA-III.[119] This leads to up-regulation of *agr* activity, through the 'self-synthesis' of components, one of the conserved mechanisms of QS systems described earlier.
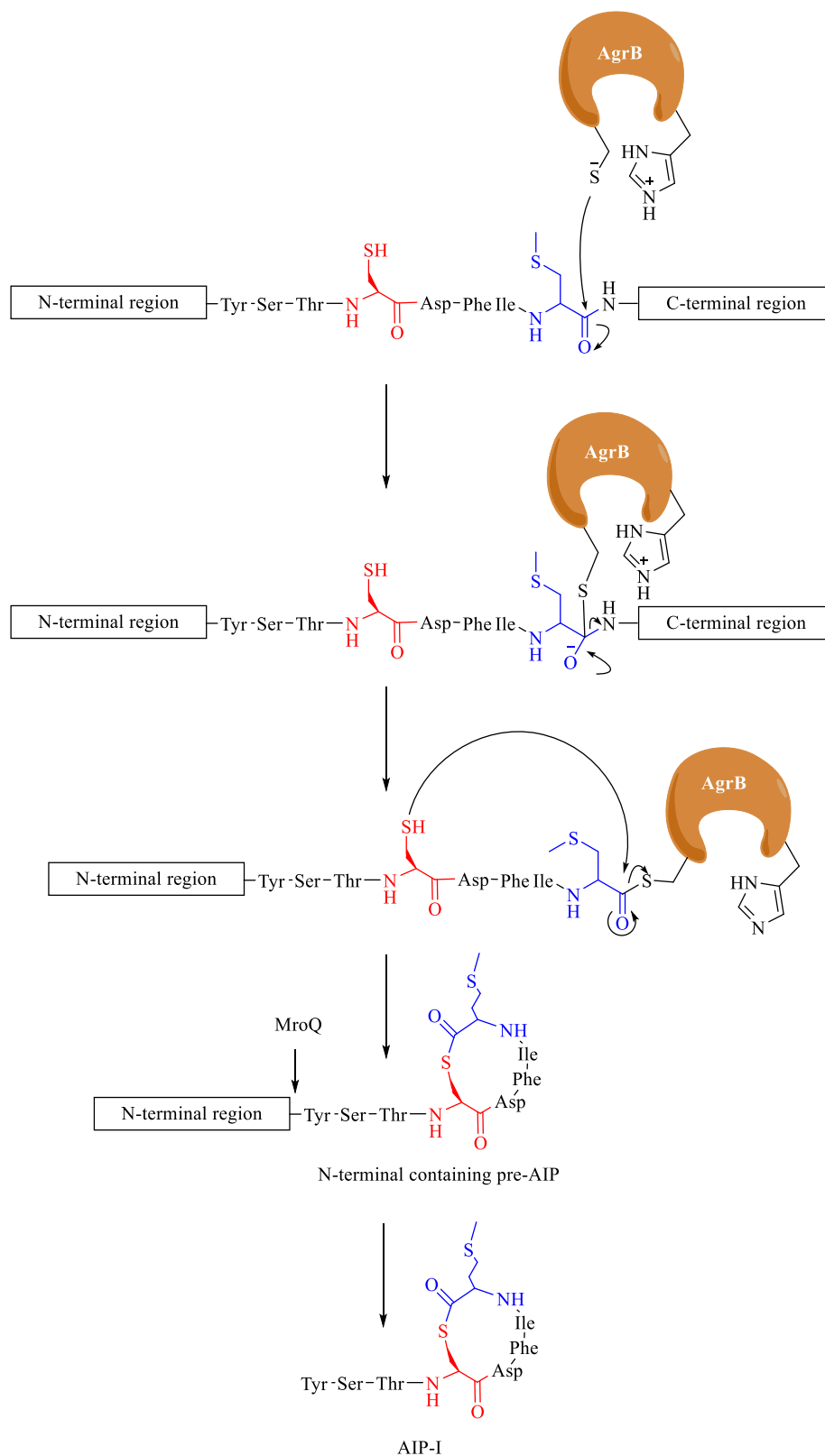
Figure 1.22. The proposed mechanism for the formation of AIP-I by AgrB. Nucleophilic attack at the methionyl carbonyl by the absolutely conserved Cys84 (part of an ion pair with His77) within AgrB leads to lysis of the amide bond, liberating the C-terminal AgrB recognition region. Attack at the thiolacyl intermediate as part of an intra-molecular thiolesterification , carried out by an absolutely conserved cysteine, 5-residues internal to the AIP sequence (summised as a concerted mechanism above) leads to the formation of the thiolactone macrocycle and restoring the active site of AgrB.

Both the *P2* and *P3* promoters exhibit basal transcriptional activity, at a higher level for the *P2* transcript.[126] This allows for low level production of AIP. At low population densities, this is insufficient for *agr* activation, however, when the population density reaches the threshold level, activation of the *agr* system occurs.[126]
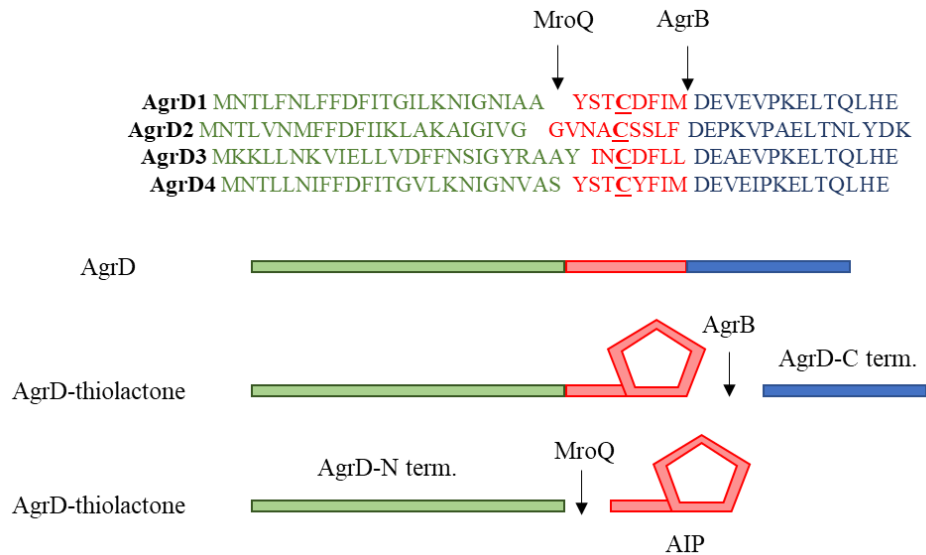
Figure 1.23. The full primary amino acid sequences of AgrD from each of the staphylococcal *agr* groups highlighting the cleavage sites.and the product of each cleavage.

The final major component of the *agr* system is the main effector molecule, RNA-III, a master regulator of staphylococcal virulence.[119, 127] RNA-III is 514 nucleotides in length and is one of the largest known small regulatory RNA that functions through an anti-sense mechanism, by complementary base pairing with target mRNAs.[127] These leads to downstream effects on the expression of accessory genes such as superantigens and cytotoxins (Table 1.1).[97] Moreover, the *hld* gene is encoded within *rna-III*, therefore δ-toxin is directly expressed as a function of *agr* activity.
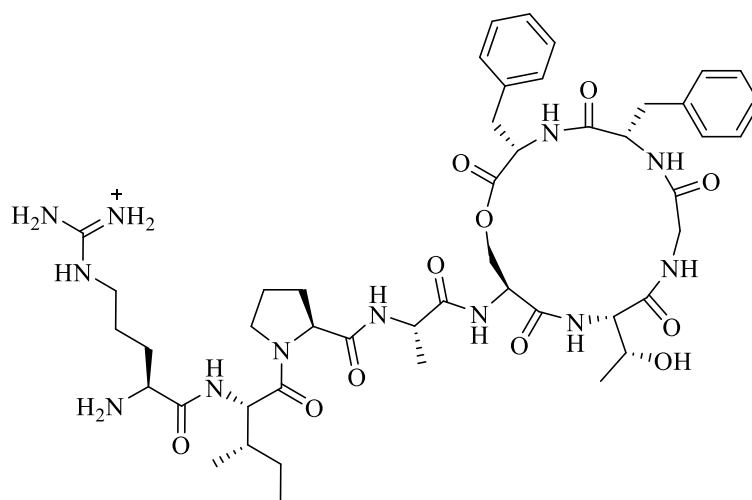
1.35

Figure 1.24. The AIP signal molecule of the *S. intermedius* sub-species *S. pseudointermedius* **1.35**, with an atypical lactone macrocycle.

The result of *agr* activation leads to an overall increase in virulence factor expression, the arsenal of weapons by which *S. aureus* can propagate infection and a decrease in surface proteins (Table 1.1), which leads to the breakdown of biofilms allowing the bacteria to spread infection to distal sites within the host.

1.5.2 The different *agr* groups of *S. aureus*

As previously discussed, *S. aureus* has four distinct *agr* groups, I-IV, each with their own distinctive AIP molecule (**1.34, 1.36, 1.37, 1.38**, Figure 1.25). The cognate AIP is a potent agonist at the corresponding AgrC receptor whereas non-cognate AIPs act as potent competitive antagonists. Notably, AIP-II acts as an inverse agonist at the AgrC1 receptor.[128] Studies have shown that a single dose of non-cognate AIP can block murine abscess formation in an experimental model.[121, 129]
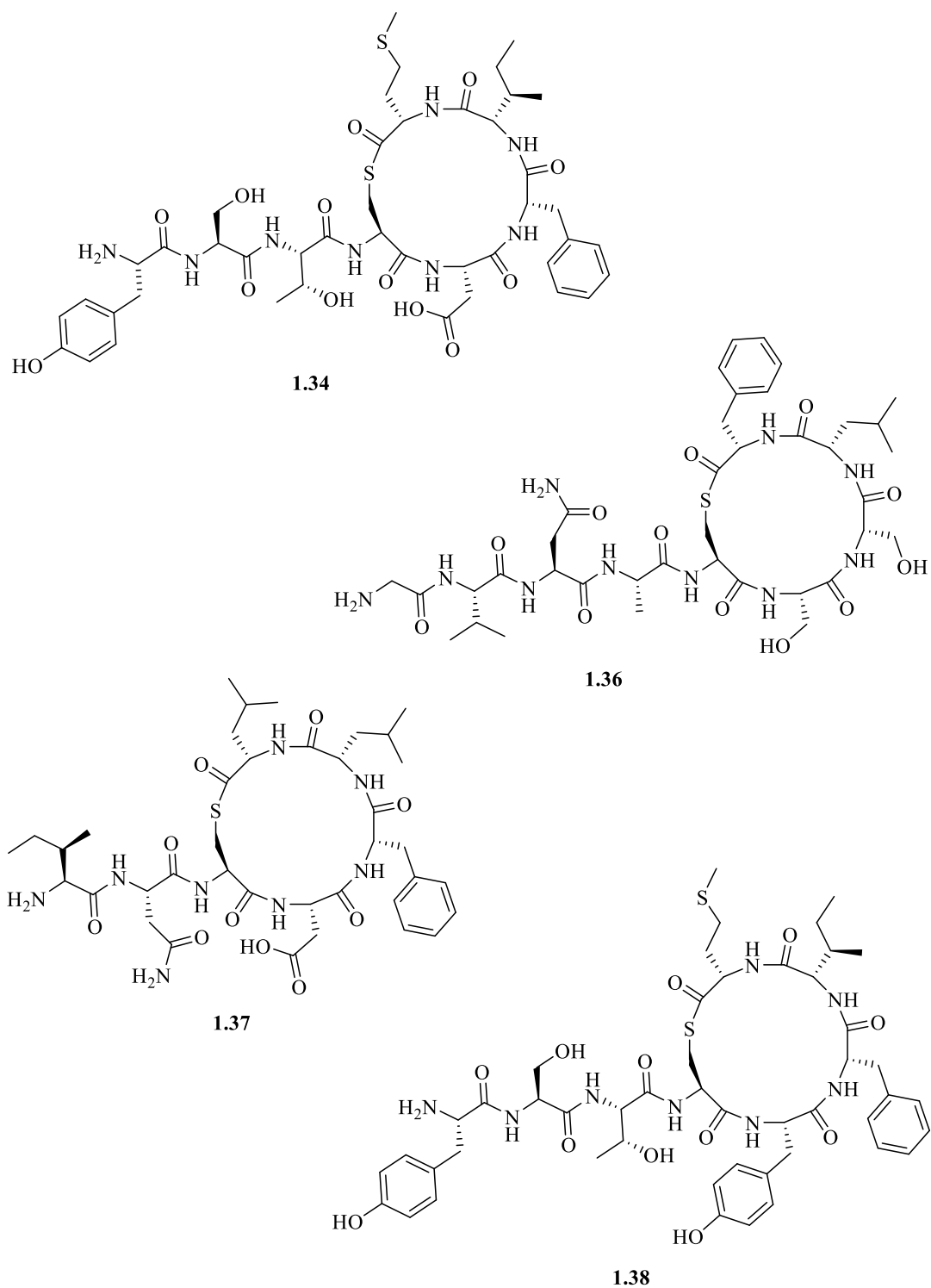
Figure 1.25. The thiolactone AIP molecules endogenous to *S. aureus*. AIP-I **1.34**, AIP-II **1.36**, AIP-III **1.37** and AIP-IV **1.38**.

The *agr* operon, *agrBDCA* contains a variable region including the 3' end of both *agrB* and *agrD*, as well as the 5' end of *agrC*.[121, 130] This suggests that variation in AIP structure (*agrD*) requires concurrent changes in AgrB and AgrC to retain auto-inducing activity.[121] Variation in

the nucleotide sequence between groups is most notable within *agrD*, the precursor to AIP, which is unsurprising given different *agr* groups produce different signal molecules (Figure 1.25)[130] Further variance is seen within the C-terminal two thirds of AgrB, potentially involved in the processing of AgrD, which again enables recognition of cognate AgrD.[130] AgrC also exhibits N-terminal divergence, with variation in the receptor domain, notably within extracellular loops I and II, which have been found by Jensen *et al*. to be necessary for the exquisite differentiation between AIP-I and IV, which differ by only a single amino acid.[121]

1.6 The *agr* systems of other species

Analogous *agr* systems are present within other Gram-positive species, including coagulase negative staphylococci, clostridia, listeria, lactococci and enterococci.

1.6.1 Staphylococci

Apart from *S. aureus*, the most clinically relevant staphylococcal species is *Staphylococcus epidermidis*, which like *S. aureus* is an opportunistic pathogen but also a commensal of skin microbial flora.[131] *S. epidermidis* is a leading cause of medical implant/device infections.[131] The fundamentals of the *agr* system are conserved between *S. aureus* and *S. epidermidis*.[131] However, unlike *S. aureus*, which is an invasive pathogen, *S. epidermidis* infection is typically associated with chronic biofilm associated infections, which are the primary mechanism of pathogenesis.[131] In *S. epidermidis*, *agr* activity differs to *S. aureus* in relation to the genes regulated. For example, in *S. epidermidis*, *agr* upregulates adhesins including polysaccharide intercellular adhesion (encoded by the *icaADBC* locus) that facilitate biofilm formation.[132]

S. intermedius is another staphylococcal species that utilises an *agr* system. In fact, *S. intermedius* which is part of the normal commensal flora of dogs, is often associated in causing SSTIs in humans who have been exposed to dogs, for example after surgery.[133] *S. intermedius* infection can be invasive, leading to systemic infection.[134] As mentioned previously, *S. pseudointermedius* utilises a unique AIP **1.35** containing a 5-amino acid lactone macrocycle between an internal serine residue and the terminal carboxyl. Ji *et al*. have shown that the lactone macrocycle is important for the activity of the AIP.[135] Replacement of the serine with a cysteine, to produce a thiolactone analogue of **1.35**, **1.39** afforded an AIP molecule with weak self-activation properties (Figure 1.26).[135]
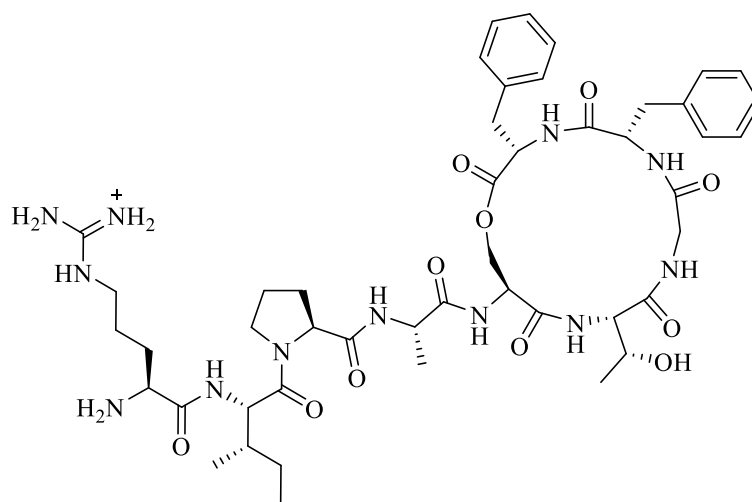
1.35
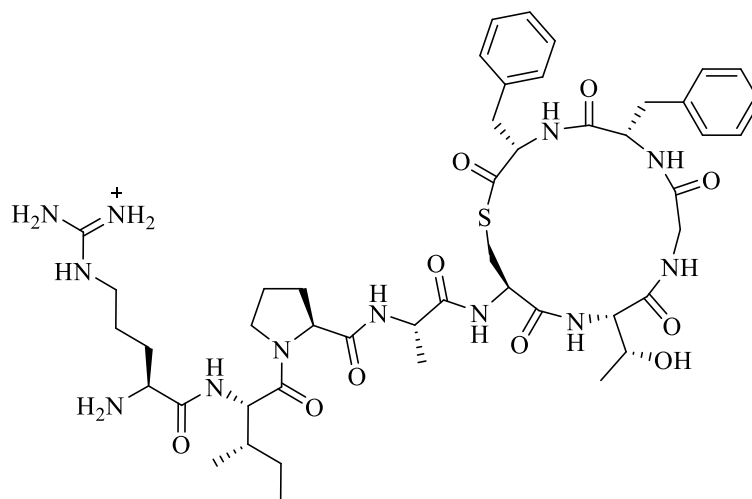
1.39

Figure 1.26. The lactone AIP of *S. pseudointermedius* **1.35** and the thiolactone analogue **1.39**.

1.6.2 Enterococci

The enterococci, such as *Enterococcus faecalis* also use *agr*-like QS systems to facilitate their pathogenesis. *E. faecalis* is a commensal bacteria found in the gastro-intestinal tract and is also an opportunistic pathogen.[136] Pathogenesis in *E. faecalis* involves colonisation of host tissues and the formation of biofilms, which requires the expression of numerous surface proteins.[136]

E. faecalis uses the *fsr* system to regulate virulence.[137] Encoded within the *fsr* locus, it consists of four genes, *fsrA*, *fsrB, fsrD* and *fsrC*.[138] The signal molecule of the *fsr* system is gelatinase biosynthesis activating pheromone (GBAP) **1.40** (Figure 1.27), consisting of 11 amino acids and is synthesised as a precursor, encoded within the *fsrD* gene in a manner similar to AIP within *S. aureus*.[138] GBAP, when produced, binds to FsrC, which is then phosphorylated

enabling activation of FsrA, the response regulator, which through activity as a transcription regulator, drives expression of the *fsr* cassette and numerous other loci, including *gelE-sprE*.[139] *gelE* and *sprE* encode gelatinase and serine protease and are both positively regulated by Fsr activity.[139] Gelatinase is a type II metalloprotease that targets, fibrin, collagen, fibrinogen, haemoglobin and a number of complement proteins.[139] Furthermore, gelatinase activates an autolysin which is important in biofilm formation.[139] Gelatinase is also known to activate protease-activated receptor 2 (PAR2), causing chronic inflammation within the intestines of a mouse model.[139] Serine protease, encoded by *sprE* is a glutamyl endopeptidase and also contributes to the pathogenesis of *E. faecalis*.[139]
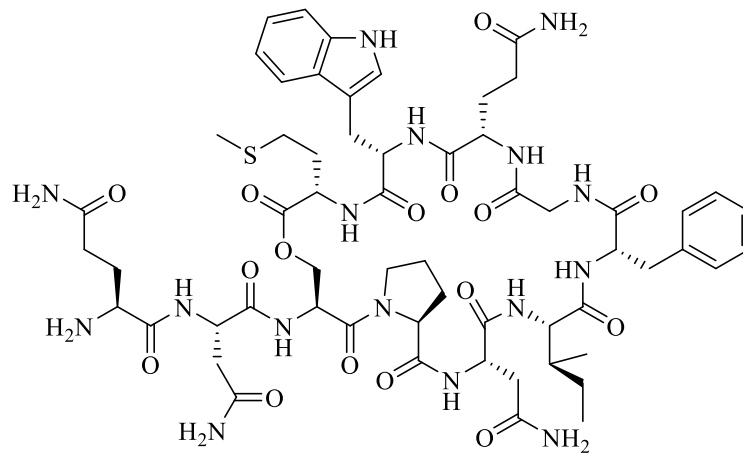
1.40

Figure 1.27. The signal molecule of the *E. faecalis* Fsr system, GBAP **1.40**

1.6.3 *Clostridia*

Clostridia are Gram-positive bacteria that cause a wide range of diseases, such as botulism and gas gangrene. In order to cause these diseases, *Clostridia* produce an array of toxins such as the botulinum toxin. *Clostridia* use an *agr*-like system, which is known to play a crucial role in the pathogenesis of several clostridial species including *Clostridium botulinum* and *Clostridium perfringens*.[140] However, less is known about the *agr*-like system of *Clostridia* than the staphylococcal *agr* system. Some species of *clostridia*, such as *C. botulinum* have two copies of the *agrBD* genes, required for the synthesis of the signal molecule.[140]

Three clinically relevant species of *Clostridia* are *C. perfringens*, *C. botulinum* and *Clostridium difficile*. *C. perfringens* is a causative agent of food poisoning and gas gangrene, mediated through the production of an arsenal of toxins, including proteases which digest host tissue, to provide a pool of amino acids for the bacteria.[140] Knock-out/targeted mutagenesis on *agr* genes

within *C. perfringens* have been shown to have effects on toxin production and thus implicated in regulation of toxin production.[140]

C. botulinum produces an array of toxins, including some neurotoxins which are amongst the most harmful known.[140] In their 2015 review, Darkoh *et al*. state that all recently studied genomes of *C. botulinum* contained 'putative homologues' of the *agr* system, and within ten of these genomes, analysis found two copies of *agrB* and *agrD*.[140] *AgrD* mutants have been found to have disrupted neurotoxin production.[140]

Lastly, *C. difficile*, is a nosocomial pathogen and one of the leading causes of hospital-associated diarrhoea worldwide.[141] Multi-drug resistant *C. difficile* can cause infection in the gut after the local microbiota have been disrupted by broad-spectrum antibiotics, due to the loss of competition for nutrients.[141] This bacterium relies on two toxins, named toxin A and B for pathogenesis.[140-141] A 2015 study found that *C. difficile* utilises a QS system for the regulation of toxin production, mediated through a small thiolactone that can be detected in stools of *C. difficile* patients.[141] The authors noted that *C. difficile* QS system offers novel therapeutic targets for non-antibiotic modalities for the treatment of infection.[141]

1.7 The *agr* system as a pharmacological target

The clinically important organisms discussed above depend on *agr*-like systems for the production of their virulence weaponry. There has been some success in the disruption of individual virulence factors. Human antibodies against *S. aureus* α-haemolysin have been previously shown to have therapeutic potential for the treatment of infection.[142] Furthermore, a reduction in virulence factor production has also been attributed to improved prognosis for *S. aureus* infection.[143] This makes the development of a broad range inhibitor of virulence a promising new avenue for the production of new therapies. With a focus on *S. aureus*, inhibition of one of the major global regulators of virulence, the *agr* system presents the opportunity to develop unique classes of potential therapeutic agents.

Inhibitors of the *agr* system have been previously studied and will be discussed herein. The *agr* system presents several viable targets for novel inhibitors. Inhibitors of AgrC and AgrA have been studied previously and will be discussed herein. Furthermore, the potential of AgrB to be utilised as a drugable target will also be discussed.

1.7.1 Inhibitors of AgrC

AgrC, as discussed earlier, is the sensor of the *agr* system, recognising the AIP signal molecule. Numerous inhibitory strategies have been studied, which will be discussed here.

One such inhibitor-discovery strategy is the production of pan-group AIP analogues as direct, competitive inhibitors of the AgrC histidine kinase receptor. An example being when a mouse challenged with an *agr* group I murine infection model was dosed with AIP-II there was a reduction in abscess formation.[123] This reduction was comparable to that of an *agr* knock-out control.[123] Numerous studies have shown that small changes to the structure of cognate AIP led to conversion of the molecule to an antagonist of the AgrC receptor.[144-145] This further highlights the exquisite selectivity of AgrC for the cognate AIP ligand. The AIP-I analogue (Ala^5)-AIP-I **1.41** (Figure 1.28), has been identified as a potent global inhibitor of AgrC, with nM potency against all four *agr* groups.[143]

An additional family of inhibitors of AgrC are the solonamides. These compounds were first identified by Mansson *et al.* from over 500 samples of marine bacteria collected as part of a global research expedition.[146] These bacteria were investigated to determine whether they were

a potential source of compounds with the ability to disrupt *agr* QS.[146] They recorded *agr* interference in a number of ways, such as enhanced expression of *spa*, the gene encoding protein A, with reduced expression of *hla* (α-haemolysin) and *rna-III*.[146] A marine *Photobacerium* was found to produce compounds which interfered with *agr* activity, and bioactivity guided fractionation resulted in the isolation of two novel cyclic depsipeptides called solonamide A **1.42** and solonamide B **1.43** (Figure 1.29).[146]

The solonamides were found to be active against *S. aureus* 8325-4 and the CA-MRSA strain USA300.[146] Specifically, solonamide B was found to reduce the expression of *hla* and *rna-III* whilst causing a concurrent increase in *spa* expression, whereas solonamide A caused an increase in *spa* expression, with only marginal depression of expression of *hla* and *rna-III*.[146] Importantly, neither of the compounds inhibited bacterial growth.[146] Further studies suggested that the target of the solonamides is AgrC, since no effect on *rna-III* expression was observed with bacteria expressing a constitutively active (R238H) AgrC receptor.[147] Nielsen *et al.* note that there was a 'tendency towards dose-dependency' when cells were treated with cognate AIP and solonamide B, which suggested competitive inhibition.[147]

1.41
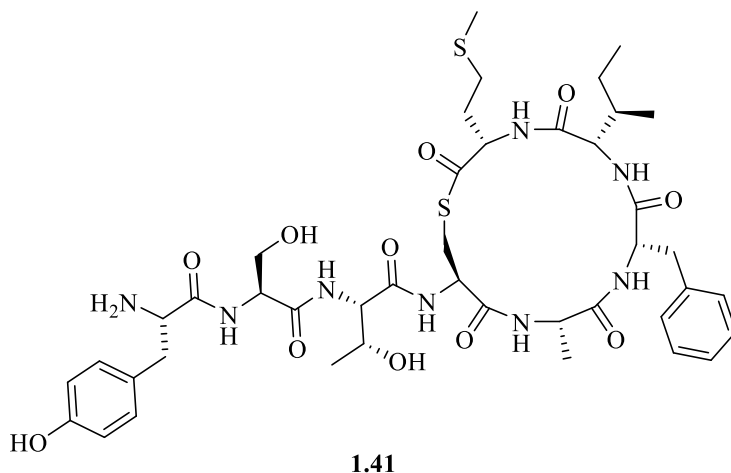
Figure 1.28. (Ala^5) AIP-I **1.41**, a potent inhibitor of AgrC

The finding that solonamide B may be a competitive antagonist is hardly surprising, given the structural similarity between solonamides (Figure 1.29) and AIPs (Figure 1.25). This was first noted by Mansson *et al.* in their manuscript first identifying the solonamides.[146] The solonamides are cyclized by a 3-hydroxy fatty acid forming a lactone with the terminal carboxyl of the amino acid chain (Figure 1.29). The difference in anti-*agr* activity between solonamide A and B is postulated to be due to the change in length of the fatty acyl chain, with the increased hydrophobicity of solonamide B being correlated to its improved potency.[146]

Non-competitive inhibitors of the AgrC receptor have also been reported. Murray *et al.* described the synthesis and testing of a range of analogues of 3-oxo-C_{12}-HSL (*N*-(3-oxododecanoyl)-L-homoserine lactone) **1.44** analogues (Figure 1.30).[148] 3-oxo-C_{12}-HSL is a known signal molecule utilised for QS by the Gram-negative bacteria *Pseudomonas aeruginosa*.[148] Gram-negative bacteria utilise small, non-peptidic signal molecules such as HSLs that can freely diffuse across the bacterial membrane and bind to either cytoplasmic or inner membrane bound receptors, the downstream effects of which can alter the expression of numerous genes.[149] In *P. aeruginosa*, 3-oxo-C_{12}-HSL activates the transcriptional regulator LasR, which drives expression of numerous genes implicated in exotoxin production and exoenzyme production.[148] 3-oxo-C_{12}-HSL is also known to inhibit the growth of some Gram-positive bacteria and at sub-lethal concentrations, it has been shown to disrupt the production of *S. aureus* exotoxins.[148, 150]

1.42 **1.43**
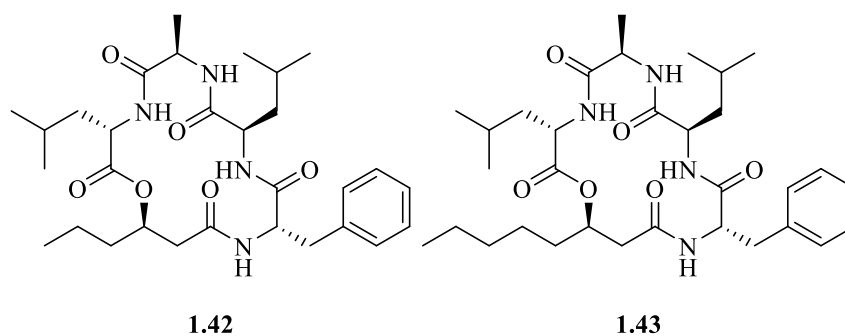
Figure 1.29. The Solonamides, (A **1.42** and B **1.43**) known inhibitors of AgrC

Murray *et al.* synthesised a range of 3-oxo-C_{12}-HSL (**1.44**), tetramic acid (**1.45**) and tetronic acid (**1.46**) analogues and tested their anti-bacterial and anti-virulence activities (Figure 1.30).[148] The most potent of these, 3-tetradecanoyltetronic acid **1.47** (Figure 1.30) showed promising *in vivo* activity, reducing nasal colonisation and bacterial arthritis in a mouse urine infection model.[148] It was found that these compounds act as non-competitive inhibitors, as negative allosteric modulators of the AgrC receptor.[148] Unfortunately, the scope for the use of these compounds for their anti-virulence properties is limited, due to the small therapeutic window between anti-virulence activity and undesired growth inhibitory activity. For example, 3-tetradecanoyltetronic acid has an MIC of 25 µM and an *agr* IC_{50} 3µM.[148]
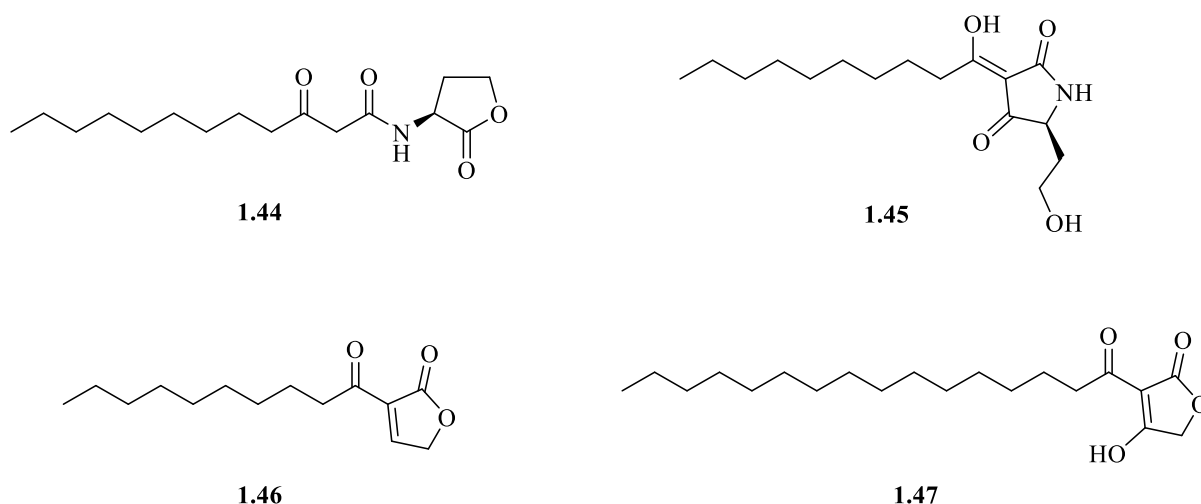
Figure 1.30. Compounds from the Murray *et al.* study. 3-oxo-C$_{12}$-HSL **1.44**, tetranoic acid derivatives **1.45**, a tetronic acid analogue **1.46** and the compound found to be an highly potent inhibitor of AgrC, 3-tetradecanoyltetronic acid **1.47**.

1.7.2 Inhibitors of AgrA

AgrA has also been investigated as a target for novel anti-virulence compounds. Sully *et al.* identified the synthetic small molecule *Staphylococcus aureus* virulence inhibitor (savirin) **1.48** as a potent inhibitor of AgrA through a high-throughput screen (Figure 1.31).[151] Molecular docking identified a binding pocket for savirin on AgrA.[151] Docking studies, carried out by Sully *et al.* suggested that savirin occupies a binding pocket adjacent to the DNA binding motif of AgrA which allows it to inhibit funciton.[151] Specific inhibition of AgrA by savirin was elucidated through the production of a reporter strain, where plasmid encoded AgrA is produced constitutively, which drives activation of *agr*::P3 *lux* in the absence of any other *agr* components.[151] Savirin was found to inhibit constitutive bioluminescence without any adverse effects on bacterial growth.[151] Furthermore, electrophoretic mobility shift assay (EMSA) confirmed inhibition of AgrA by savirin.[151]
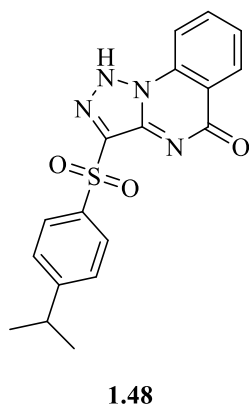
Figure 1.31. The synthetic AgrA inhibitor savirin **1.48**.

Although savirin proved to be an effective inhibitor of AgrA in *S. aureus*, when it was tested in *S. epidermidis*, it proved ineffective *in vitro* and *in silico*.[151] Thus variation in the amino acid sequence of AgrA between *S. aureus* and *S. epidermidis* (*agr* group II) is suggested as the reason for this.[151] Indeed, it was noted that one of the key intermolecular contacts, Tyr229 in AgrA of *S. aureus* is replaced by Phe in AgrA of *S. epidermidis*.[151] The ineffectiveness of savirin to act in *S. epidermidis* suggests that inter-group variation in the structure of AgrA could prove problematic in the development of a broad spectrum inhibitor of AgrA.

1.7.3 The potential of AgrB as an anti-virulence target

As discussed above, promising inhibitors of both AgrC and AgrA have been previously studied. AgrB remains the least studied component of the *agr* system as a potential pharmacological target. Like AgrC and AgrA, AgrB has considerable cross-group amino acid sequence variation. However it is predicted that all AgrB variants share both structural and mechanistic features.[120] This is enforced by studies which found high levels of homology of hydropathy profiling amongst AgrB homologs as well as absolute conservation of Cys84 and His77 residues, which together form the putative active site.[120, 152] Thus, the conservation of structure and function of AgrB and its homologues in different species makes AgrB an attractive target for a broad-spectrum inhibitor of virulence.
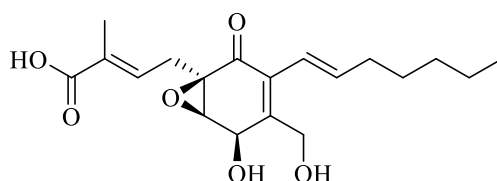
1.1

Figure 1.32. The highly functionalised epoxycyclohexenone ambuic acid **1.1**, produced by species of the Pestalotiopsis fungi.

In their 2009 paper, Nakayama *et al.* carried out a screen of fungal extracts for the modulation of the GBAP-mediated QS system.[153] Through this screen, they found that ambuic acid **1.1** (Figure 1.32), an epoxy cyclohexenone with known anti-fungal properties, as an inhibitor of *fsr* QS.[153-154] Nakayama *et al.* demonstrated that ambuic acid **1.1** inhibited the biosynthesis of GBAP, as well as the biosynthesis of AIP-I in *S. aureus* and cyclic peptide QS signal molecules in *Listeria innocua*.[153] Furthermore, a database search based on the amino acid sequence of AgrB found several molecules comparable to AgrB in a range of Gram-positive bacteria.[153] In addition, studies have confirmed inhibition of AIP biosynthesis in the clinically relevant MRSA

strain *S. aureus* USA300, as well as reducing ulcer formation in a mouse murine model of MRSA infection.[155] In addition, Todd *et al.* utilised mass-spectrometric methods to measure the effects of ambuic acid **1.1** on the production of AIP-I in *S. aureus* USA300 and a strain wherein AIP-I synthesis was deregulated.[155] They observed inhibition of AIP-I production in both the constitutively active strain and USA300 (IC$_{50}$ 2.5 ± 0.1 μM).[155] They also screened ambuic acid against a further 11 strains/ species, eight of which showed IC$_{50}$ values of < 25 μM.[155] Two-thirds of the strains with an IC$_{50}$ of > 25 μM were *S. epidermidis* strains which were of the *agr* groups II and III.[155]

These findings make ambuic acid **1.1** a promising broad-spectrum-inhibitor of Gram-positive virulence. The finding of further AgrB homologues in a number of Gram-positive species further increases the potential scope of ambuic acid **1.1**.

1.8 Ambuic acid

1.8.1 Known bioactivities of ambuic acid

Ambuic acid **1.1**, a highly functionalised epoxy cyclohexenone, is produced as a secondary metabolite by species of tropical endophytic fungi of the *Pestalotiopsis* and *Monochaetia*.[154] *Pestalotiopsis microspore* is one of the most common of these organisms and is one of several related organisms which have been isolated from the stems and leaves of economically important tropical crops such as mangos and guavas.[154] These fungi are weak, plant pathogens.[154] The fungal-produced ambuic acid has been shown to have biological activity against several phytopathogenic *Fusarium* sp., including *Diplodia natelensis* and *Cephalosporium gramineum*.[154] The biological function of ambuic acid may be as a protectant against other species of fungi or may play a role in fungus-plant relationships.[154]

1.49
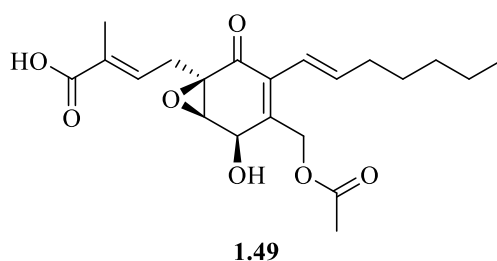
Figure 1.33. Acyl ambuic acid derivative **1.49**.

The acyl ambuic acid derivative **1.49** (Figure 1.33) has been shown to inhibit the inter-cellular signal molecule nitric oxide (NO).[156] NO is produced by the oxidation of L-arginine by a group

of enzymes called nitric oxide synthases (NOS). Overproduction of NO is attributed to several diseases including cancers and chronic inflammation, thus, NOS inhibitors or scavengers of the NO radical could potentially become new therapeutics.[156]

Furthermore, ambuic acid **1.1** has shown anti-proliferative activity against the human ovarian cancer cell line A2780 and the cisplatin resistant line A2780CisR with IC_{50} values of 10.1 μM and 17 μM respectively.[157]

Studies have also reported that ambuic acid **1.1** and acyl derivative **1.49** have mild growth inhibitory activity against *S. aureus*, with IC_{50} values of 43.9 μM and 27.8 μM respectively.[158] However, at present, work undertaken within the Chan and Williams laboratory (discussed in Chapter 4), no growth inhibition was observed with ambuic acid, even at concentrations far in excess of those reported by Ding *et al.*.[158]

1.8.2 The potential mode of action of AgrB inhibition by ambuic acid

AgrB is a putative cysteine protease, with Cys 84 and His77 forming the proposed active site of the enzyme.[120] Broadly, cysteine proteases are a distinct family of proteases that hydrolyse peptide bonds utilising the thiolate of a deprotonated cysteine residue as the nucleophile for attack at the carbonyl of a peptide bond (Figure 1.34).[159] The catalytic mechanism of the clan CA family of cysteine proteases is one of the most extensively studied.[160] Briefly, cleavage of the peptide bond depends on the thiolate-imidazolium ion pair, formed between a cysteine and histidine residue within the active site of the protease (Figure 1.34).[160] Thiolate attack at the carboxyl of the target peptide bond within the substrate leads to the formation of a tetrahedral oxyanion intermediate, the amine of which can receive the proton from the imidazolium ion, forming a thioacyl enzyme-substrate intermediate, releasing the amino fragment (Figure 1.34).[160] Subsequent hydrolysis of this thioester intermediate releases the remaining portion of the substrate and re-generates the active site, ready for further catalysis.[160] The improved nucleophilicity of the sulphur atom in cysteine compared to that of oxygen in serine (within serine proteases) negates the requirement for a full triad of catalytic residues Within serine proteases, the triad is typically formed by the Ser, His and Asp residues, where the aspartate is negatively charged and the serine and histidine are ionized intermittently during the catalytic cycle.[161]
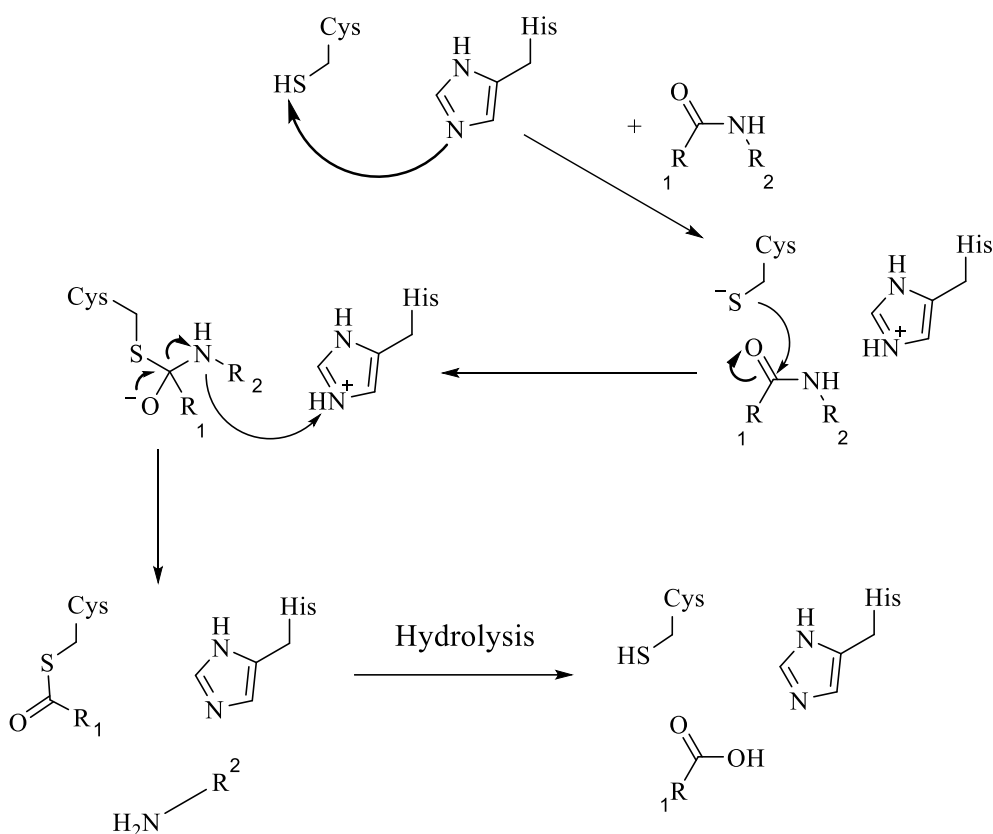
Figure 1.34. The general mechanism of cysteine proteases. Attack at the carbonyl of the peptide bond by the thiol within cysteine, this leads to release of the amino portion of the peptide substrate, forming a thiolacyl substrate-enzyme intermediate. This can then undergo subsequent hydrolysis, releasing the carboxylic acid segment and restoring the active site of the enzyme.

Thus, in *S.* aureus Group I the Cys84 and His77, which form the putative active site of AgrB are able to catalyse the processing of AgrD, eventually forming the key thiolactone macrocycle of AIP.[120]

The cysteine proteases are common in nature and are required for a diverse array of functions. They are known to play important roles in a number of pathologies and as such, inhibitors have been widely studied.[159] Disorders involving cysteine proteases and several classes of inhibitor are discussed at greater depth in chapter 3.

One class of cysteine protease inhibitors is the epoxysuccinates **1.50** and **1.51** which are able to irreversibly alkylate the key active cysteine within the active site, via the epoxydione electrophilic warhead (Figure 1.35). They form a thioether, thus irreversibly alkylating the enzyme.[162] Alkylation occurs through nucleophilic attack at either carbon of the epoxide heterocycle, resulting in opening of the strained ring (Figure 1.35).[162] This results in inhibition of the enzyme, surmountable only by *de novo* protein synthesis.[162]
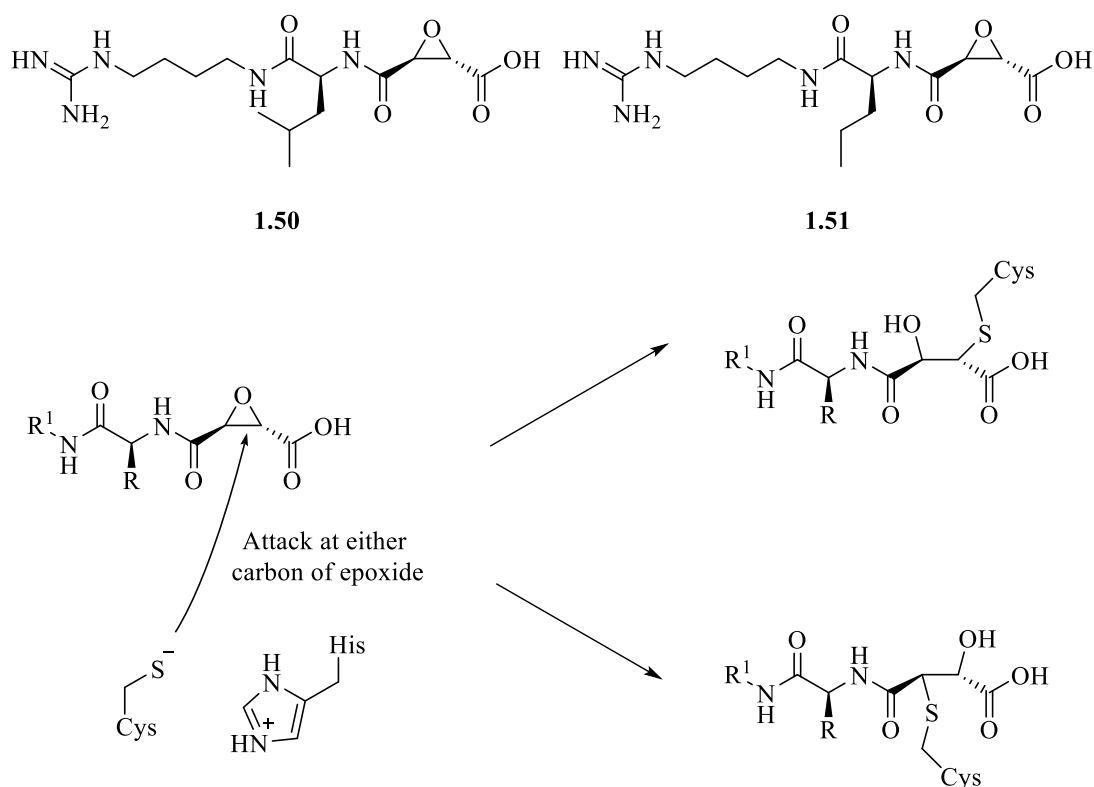
Figure 1.35. Examples of epoxysuccinates (**1.50** and **1.51**) and their mode of inhibition of cysteine proteases.

At present, the mechanism by which ambuic acid **1.1** attenuates staphylococcal *agr*-mediated virulence remains unknown. However, the presence of the epoxide may be a clue for how ambuic acid functions as an AgrB inhibitor. It is postulated that ambuic acid covalently modifies the key Cys84 within AgrB, forming a thioether drug-enzyme covalent complex (Figure 1.36), leading to inhibition. This will be discussed in more detail in Chapter 3.
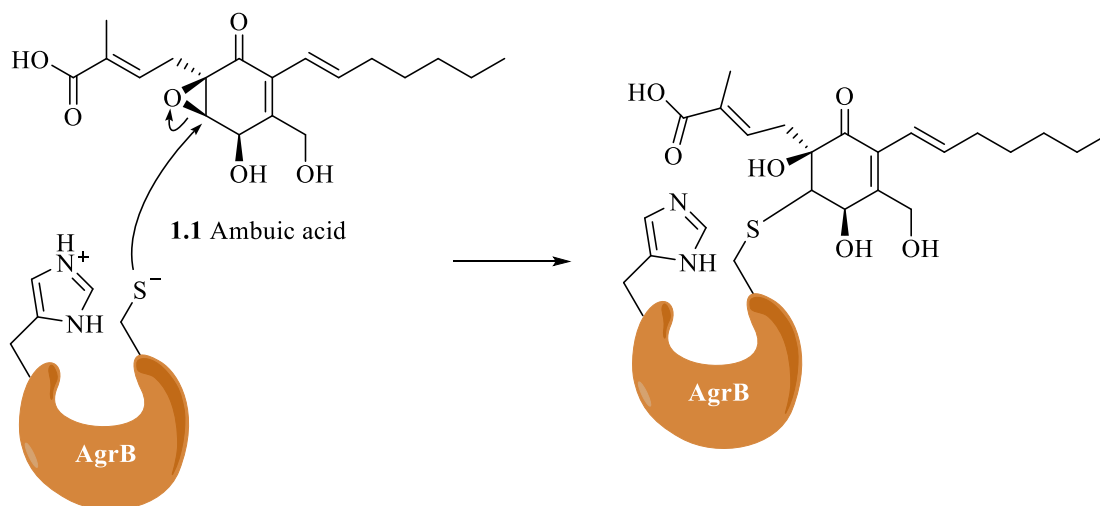
Figure 1.36. The proposed mechanism of inhibition of AgrB by ambuic acid.

1.9 Aims and objectives

The work outlined in this thesis focuses on the synthesis and biological characterisation of novel anti-virulence compounds for the treatment of serious multi-drug resistant *S. aureus* infection. To this end, the aims of this thesis are outlined below.

- The synthesis of a range of analogues of the natural product ambuic acid in order to investigate their inhibitory activity towards the *agr*-mediated quorum sensing system.

- The synthesis of a cyclopropyl isostere of the epoxide electrophilic centre within ambuic acid to determine how modification alters the anti-virulence activity.

- The *in vitro* biological characterisation of the synthesised analogues *in vitro*.

The approach for the completion of these research aims will be outlined briefly here.

1.9.1 The synthesis of analogues of ambuic acid

The synthesis of analogues of the natural fungal product ambuic acid **1.1** has been carried out. These analogues were based on the truncated, racemic ambuic acid analogue **1.52** which was found to show promising anti-virulence activity at the onset of this work (Figure 1.37).
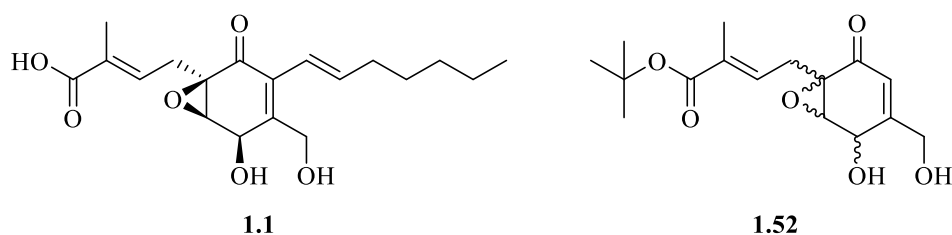
Figure 1.37. Ambuic acid **1.1** and the truncated racemic analogue **1.52** of which enantioselective syntheses have been carried out.

The synthesis of analogues broadly followed the synthetic strategy utilised by Jung *et al*. in their total synthesis of ambuic acid, which has been strategically modified by Dr Leonardo Baldessarre, formerly of the Williams/Chan group.[163] This synthesis involves the production of a key, chiral Diels-Alder adduct intermediate **1.53** produced from reaction of ketal **1.54** with cyclopentadiene **1.55** in the presence of chiral (*R*)-(+)-*o*-tolyl-CBS-oxazaborolidene catalyst

1.56 (Scheme 1.1). The Diels-Alder adduct is capable of imparting stereoselectivity on subsequent chemical transformations through steric hindrance of formation of the undesired enantiomer.
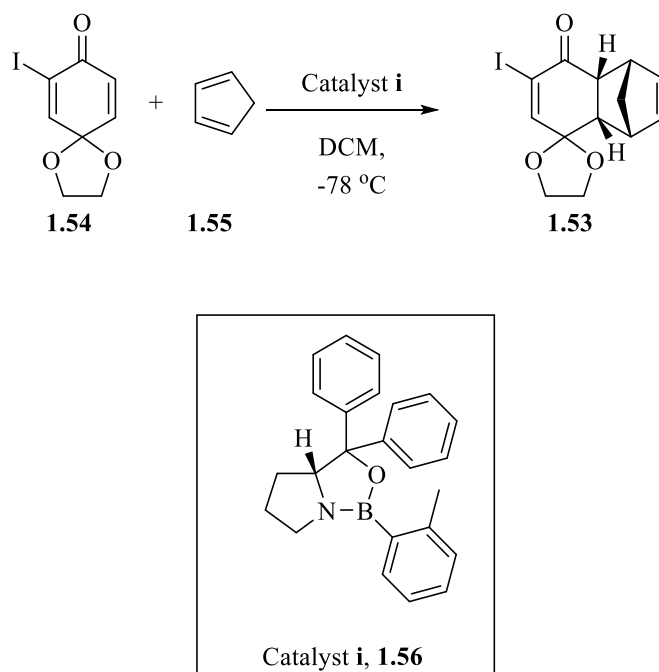
Scheme 1.1. Proposed conditions for the Diels-Alder reaction between ketal **1.54** and cyclopentadiene **1.55** in the presence of chiral catalyst **1.56** to generate the key, chiral Diels-Alder adduct **1.53**.

Subsequent transformations involved the installation of an allyl group through Stille cross-coupling to give **1.57**. The epoxide was installed using hydrogen peroxide in the presence of Na_2CO_3 to afford the epoxide **1.58** (Scheme 1.2). The epoxide was taken into a hydroxymethylation procedure, first pioneered by Mehta *et al.* giving alcohol **1.59**.[164] The lower ketone was enantioselectivly reduced to the corresponding alcohol utilising DIBAL-H, using a procedure adapted from Jung *et al* affording diol **1.60** (Scheme 1.2).[163] A retro Diels-Alder reaction was utilised to dismantle the adduct to give the quinolone derivative **1.61** which was then followed by an ozonolysis and a Wittig reaction to yield the final compound **1.62** (Scheme 1.2). This synthesis will be outlined in greater detail in Chapter 2.
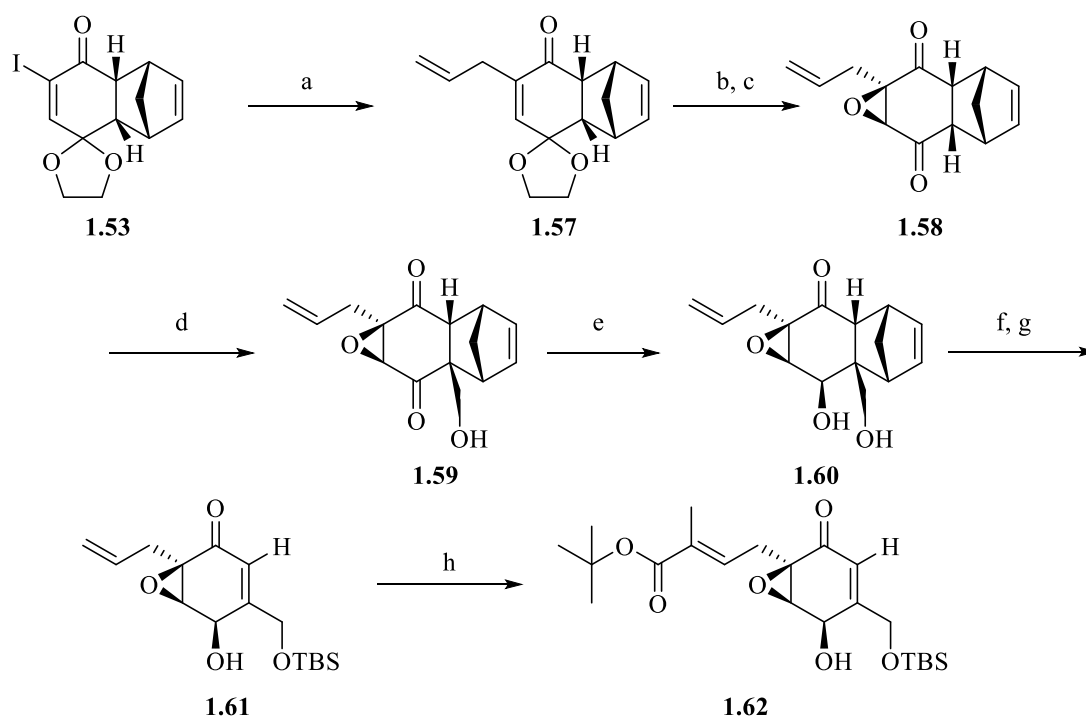
Scheme 1.2. Proposed route to the truncated ambuic acid analogue **1.62**. (a) Pd(PPh₃)₄, allyltributyl stannane, μW radiation; (b) 1 N H₂SO₄; (c) H₂O₂, NaHCO₃ (aq.); (d) formaldehyde, DBU; (e) DIBAL-H; (f) TBSCl, imidazole; (g) Ph₂O, heat; (h) O₃, dimethylsulphide then Ph₃P=C(Me)CO₂*t*-Bu.

Analogues of **1.62** were also synthesised. These included **1.63**, the corresponding (-)-enantiomer of **1.62.** The synthesis of ether analogues of the primary alcohol, shown as general structure **1.64** was also attempted. In addition, a range of silyl ether analogues based on the general structure **1.65** and a range of ketal analogues based on the general structure **1.66** was also carried out (Figure 1.38).
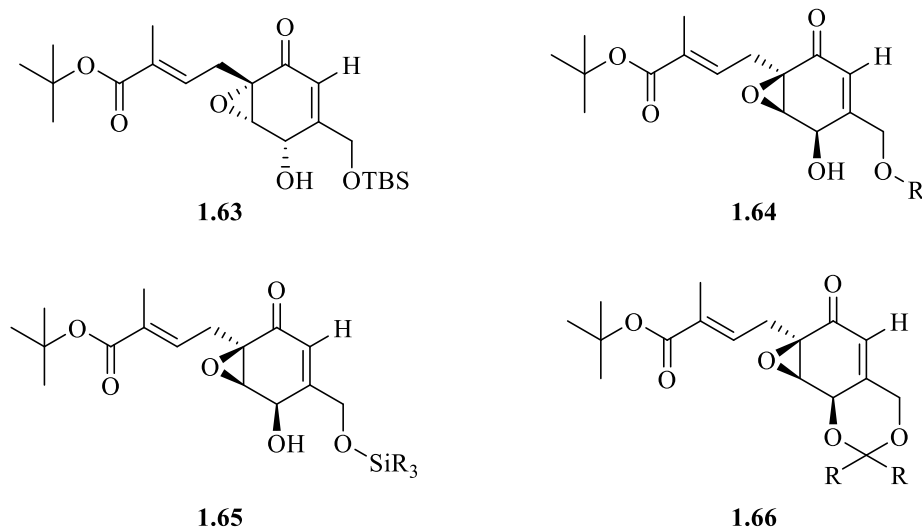
Figure 1.38. The target compounds to be synthesised. **1.63**, the corresponding (-)-enantiomer of **1.62**, the general structure of ether analogues **1.64**, the general structure of the silyl ether analogues **1.65** and the ketal analogues general structure **1.66**.

The route to (-)-enantiomer **1.63** was established. This required the enantioselective production of the Diels-Alder adduct **1.67**, produced from ketal **1.54** in a reaction with cyclopentadiene **1.55** in the presence of (*S*)-(-)-*o*-tolyl-CBS-oxazaborolidene catalyst **1.68**. The adduct **1.67** confers stereoselectivity on subsequent chemical transformations through steric occlusion of the undesired enantiomer (Scheme 1.3).

The final, (-)-compound **1.63** was to be produced in a similar fashion to the (+)-enantiomer **1.62**. A Stille coupling was to be utilised to install the allyl chain to afford **1.69** (Scheme 1.4). Following the installation of the epoxide moiety, giving **1.70** a hydroxymethylation procedure adapted from Mehta *et al.* will be utilised to provide alcohol **1.71**.[164] The lower ketone was then reduced using a procedure adapted from Jung *et al.*, to the corresponding secondary alcohol **1.72**.[163] The Diels-Alder adduct was to be dismantled to yield **1.73** which was followed by an ozonolysis and Wittig olefination procedure to give target compound **1.63** (Scheme 1.4).
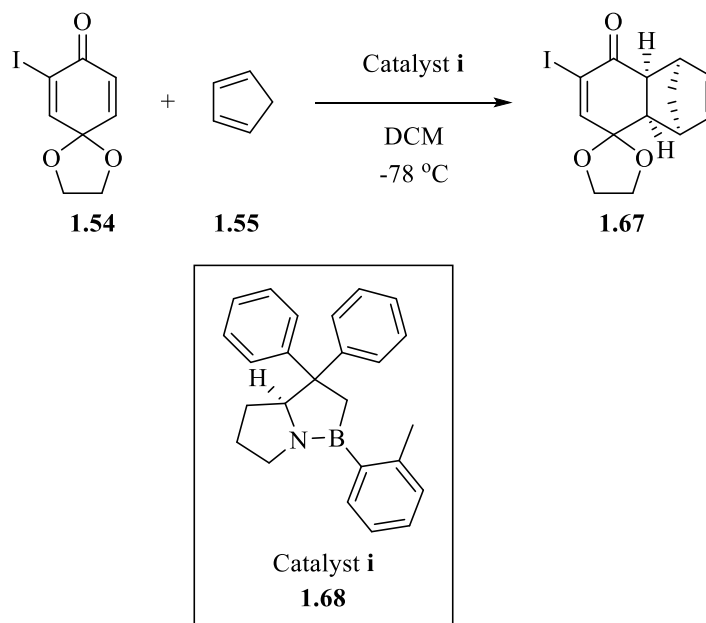
Scheme 1.3. Conditions to be used to produce (-)-adduct **1.67**, a key intermediate in the synthesis of target molecule **1.63**. The adduct **1.67** is formed in Diels-Alder reaction between ketal **1.54** and cyclopentadiene **1.55** in the presence of (*S*)-(-)-*o*-tolyl-CBS-oxazaborolidene catalyst **1.68**.

Ether analogues of the primary alcohol **1.64** were to be synthesised through a modified Williamson ether synthesis to install the desired functionality. Diol **1.60** (Scheme 1.2) was to be used as the starting material for the production of a range of ether analogues.
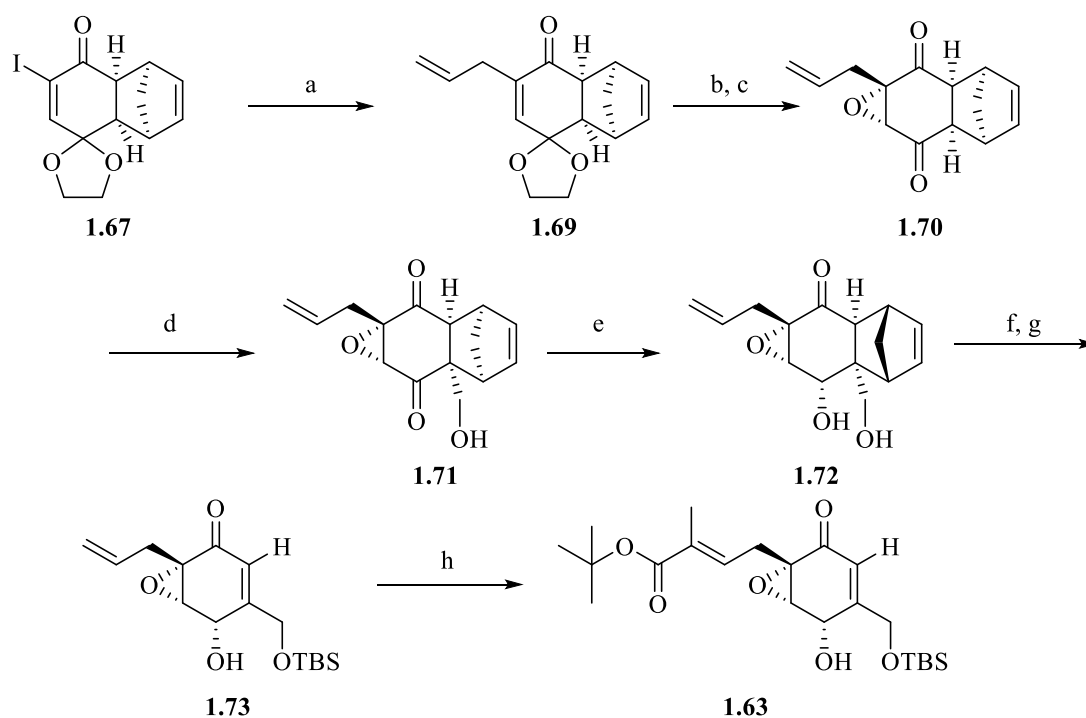
Scheme 1.4. Proposed route to the (-)- enantiomer of truncated ambuic acid analogue **1.63**. a) Pd(PPh$_3$)$_4$, allyltributyl stannane, µW radiation; b) 1 N H$_2$SO$_4$; c) H$_2$O$_2$, NaHCO$_3$ (aq.); d) formaldehyde, DBU; e) DIBAL-H; f) TBSCl, imidazole; g) Ph$_2$O, heat; h) O$_3$, dimethylsulphide then Ph$_3$P=C(Me)CO$_2$t-Bu.

Silyl ether analogues **1.65** were to be produced from a key diol intermediate **1.74** which is produced through dismantling of the *t*-butyl dimethyl silyl ether within **1.62**. Diol **1.74** was subsequently taken into a number of reactions with a range of silyl chlorides to generate a range of silyl ethers based on general structure **1.65** (Scheme 1.5).
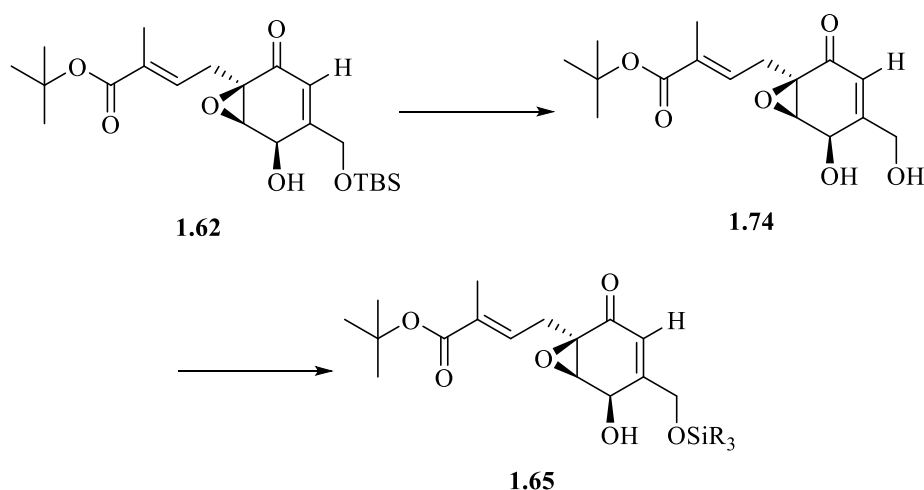
Scheme 1.5. Proposed route to silyl ether analogues based on structure **1.65**.

The diol **1.74** was to be utilised for the synthesis of numerous ketal analogues based on the general structure **1.66**. The synthesis of ketals was undertaken through the reaction of the key diol intermediate **1.74** with desired symmetric ketone in the presence of catalytic *p*-toluene sulfonic acid (Scheme 1.6).
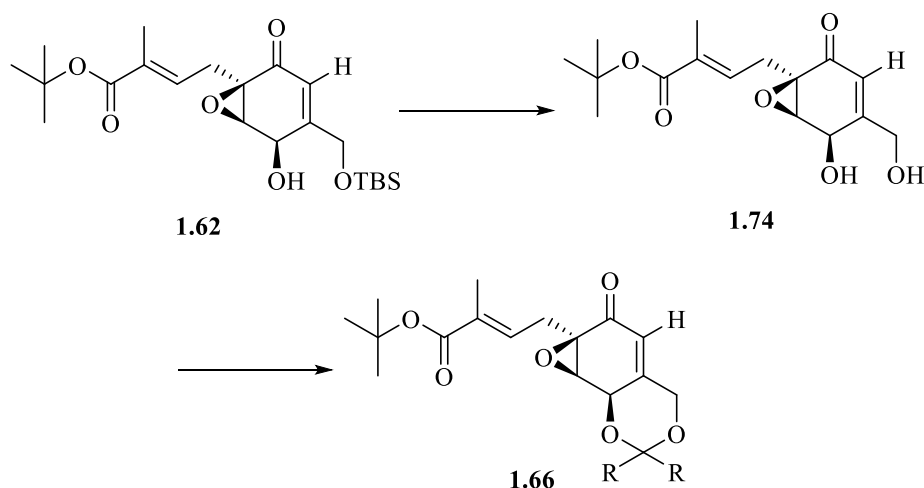
Scheme 1.6. Proposed route to ketal analogues **1.66**

1.9.2 The synthesis of a cyclopropyl isostere of ambuic acid

The synthesis of a cyclopropyl isostere **1.75** (Figure 1.39) of the epoxide within a truncated ambuic acid analogue was to be carried out. This was done to determine whether the epoxide is required for inhibition, potentially as an electrophilic warhead, irreversibly alkylating the key catalytic cysteine within AgrB.
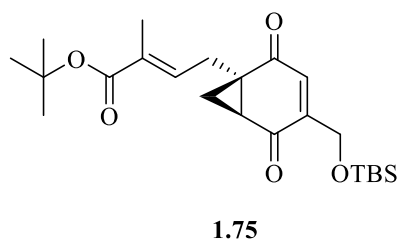
Figure 1.39. The target cyclopropyl compound **1.75**.

The key step in this synthesis of cyclopropyl target **1.75** is the enantioselective installation of the cyclopropyl ring through conjugate addition of methylene at the α,β-unsaturated system of key dione intermediate **1.76**. The approach used for this was a modified Corey-Chaycovsky cyclopropylation reaction, in which activated sulphur ylide trimethyl sulphoxonium iodide **1.77**

is used to add methylene across the α,β-double bond of **1.76** generating cyclopropane **1.78** (Scheme 1.7).[165-166]
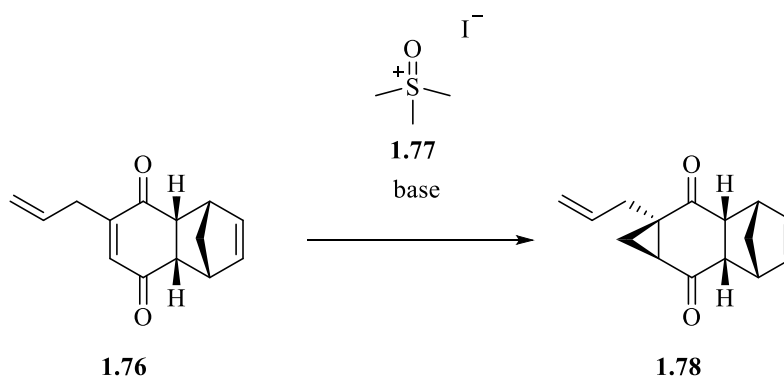
Scheme 1.7. Proposed reaction to install the cyclopropyl ring in a reaction of **1.76** with trimethylsulphoxonium iodide **1.77** in the presence of base giving cyclopropane **1.78**.

Upon the optimisation of this key synthetic step, the synthesis of the final analogue **1.75** was to be carried out. The production of the compound **1.75** broadly follows the synthesis of analogues **1.62**, outlined above. The proposed route to the final compound is outlined in (Scheme 1.8). Briefly, after the successful installation of the cyclopropyl ring and the verification that it has the desired stereochemistry, by Nuclear-Overhauser effect spectroscopy (NOESY), the primary alcohol was installed using a procedure adapted from Mehta *et al.* and Jung *et al.* to yield alcohol **1.79** (Scheme 1.8).[163-164] Following this, the alcohol was subsequently protected as the corresponding *t*-butyldimethyl silyl ether **1.80**, before a retro Diels-Alder reaction was carried out to dismantle the Diels-Alder adduct to afford the quinone derivative **1.81**. Quinone **1.81** was then to be taken into an ozonolysis and Wittig olefination to produce final compound **1.75** (Scheme 1.8).
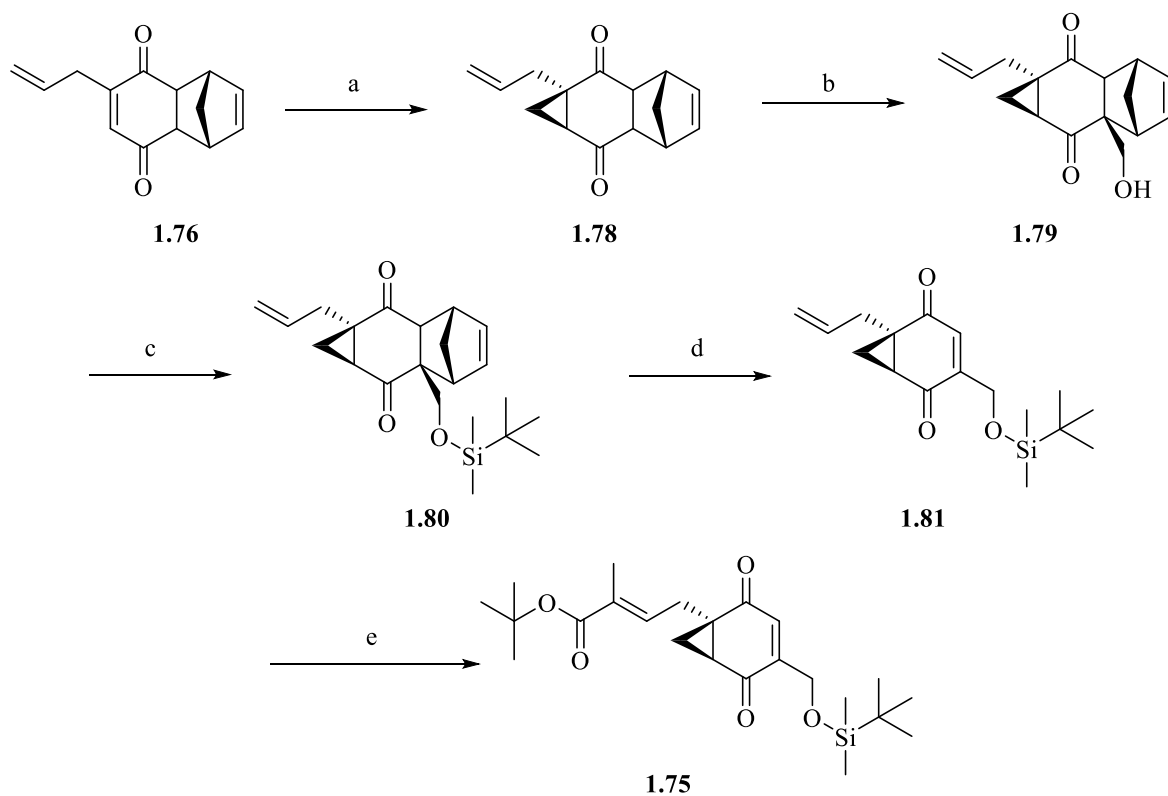
Scheme 1.8. Proposed route to the desired cyclopropyl compound **1.75**. a) trimethylsulphoxonium iodide, base; b) aqueous formaldehyde, DBU; c) TBSCl, imidazole; d) Ph$_2$O, heat; e) O$_3$, dimethylsulphide then Ph$_3$P=C(Me)CO$_2$t-Bu.

1.9.3 The microbiological evaluation of the synthesised analogues

After the synthesis of the analogues outlined briefly above, their *in vitro agr*-inhibitory activity was to be assessed. The anti-virulence properties of ambuic acid **1.1** were to also be fully determined.

The *agr*-inhibitory properties of the test compounds was to be assessed through the use of a bioluminescent reporter, EJM82, produced by Dr Ewan Murray of the Williams/Chan group. This reporter will be described in greater detail in Chapter 4. Briefly, a methicillin-sensitive *S. aureus* SH1000 strain with a native *agr* system has been modified at the *attB* ectopic locus with insertion of *agrP3::luxABCDE*. This allows for a real-time, bioluminescent readout of *agr* activity. If a high level of bioluminescence is observed, this is indicative of a high level of activity. A reduction in bioluminescence correlates to a reduction in *agr* activity, indicative of inhibition. Ambuic acid **1.1** and the synthesised analogues were to be assessed for anti-virulence activity using this reporter to establish pharmacological parameters, such as IC_{50}.

In addition to the use of the bioluminescent reporter strain described above, the phenotypic effect of compounds on toxin (α-haemolysin) and AIP-I production was to be assessed. The effect on toxin production was determined through Western blot analysis, wherein *S. aureus* is grown ± treatment with test compounds. The spent growth media was then collected and the secreted α-haemolysin levels were assessed.

To investigate whether the test compounds have an effect on AIP-I production, a reporter strain, ROJ143 was utilised. This strain has a Δ*agr* background with *agrP3::luxABCDE* and *agrP2agrC1agrA* and has previously been utilised by Jensen *et al.*.[121] The bacterium is incapable of producing AIP-I, but is capable of sensing AIP-I and like the EJM82 strain (described above), the sensing of AIP-I produces a bioluminescent signal. As these cells cannot produce AIP-I, exogenous AIP-I is therefore required to elicit a response from these cells. Thus, filtered, cell-free media from *S. aureus* strains with an intact *agr* system exposed to the desired test compound was used to treat the ROJ143 cells. If the compound inhibits the production of AIP-I, a lower level of bioluminescence will be expected.

The methods outlined here were utilised to determine if ambuic acid and the synthetic analogues proposed above are potent inhibitors of *agr* mediated virulence, particularly if they are acting through the inhibition of the biosynthetic enzyme AgrB.

Chapter 2. Total synthesis of ambuic acid analogues

2.1 Chapter outline

The synthetic route to a number of unique ambuic acid analogues is outlined in this chapter. The synthetic route for the production of the silyl ether **1.62** is discussed. The development of a route for the enantioselective production of **1.63**, the corresponding (-)-enantiomer of **1.62** is also discussed. The attempted production of ether analogues of the primary alcohol, as well as the successful assembly of other silyl ethers, illustrated by the general structures **1.64** and **1.65**, respectively is also described. Finally, the synthesis of a number of unique ketal-based analogues of the general structure **1.66** is outlined.
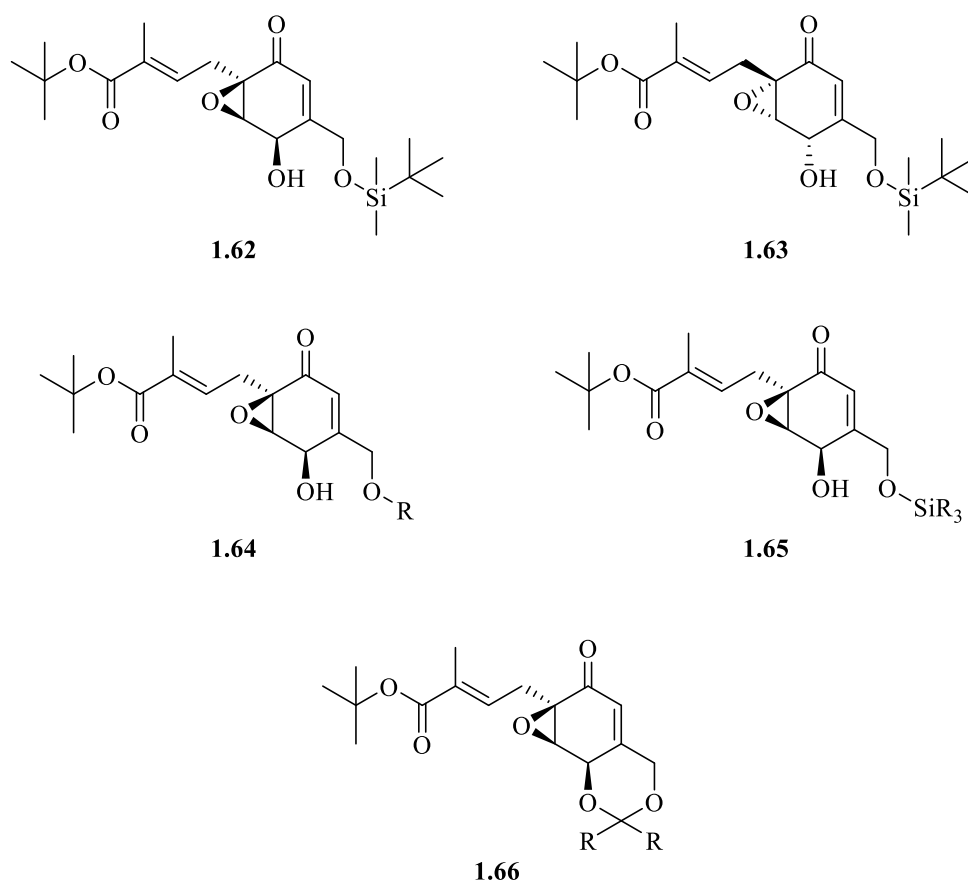
Figure 2.1. The synthetic targets.

2.2 Introduction

2.2.1 Ambuic acid

As outlined in Chapter 1, ambuic acid **1.1** is a highly functionalised epoxy cyclohexenone produced by a number of species of endophytic fungi with several documented bioactivities.[154] As such, several total chemical syntheses of ambuic acid have previously been published by Li *et al.*, Mehta *et al.* and Jung *et al.*, and these will be discussed herein.[163, 167-168]
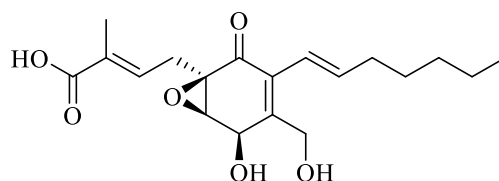
1.1

Figure 2.2. Ambuic acid

2.2.2 Li synthesis of (±)-ambuic acid

The total synthesis of (±)-ambuic acid has previously been carried out by Li *et al.* as part of their published synthesis of the quinone epoxide dimer torreyanic acid **2.1**.[167] Since both ambuic acid **1.1** and the related compound jesterone **2.2** were isolated from the same fungal species, they suggested a biosynthetic route to **2.1** is likely to involve oxidative dimerization of these intermediates **1.1** and **2.2**.[167]
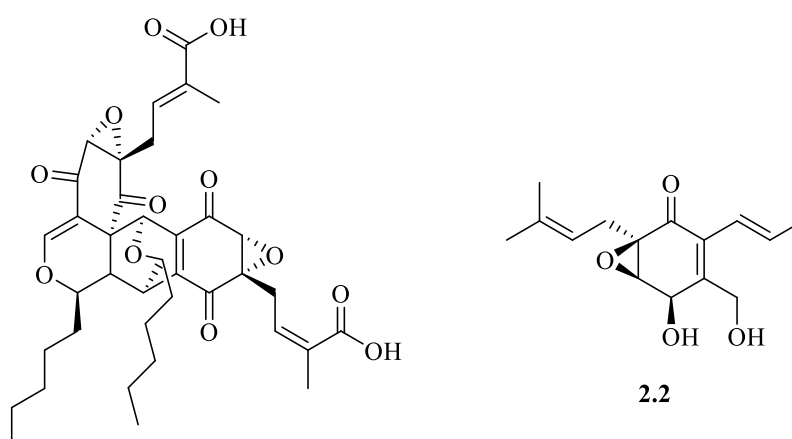
2.1

2.2

Figure 2.3. The quinone epoxide dimer torreyanic acid **2.1** and the related compound jesterone **2.2**

The Li synthesis of ambuic acid focuses on the enantioselective formation of epoxide **2.3** from the quinone monoketal **2.4**.[167] Initially, Li *et al.* found poor formation of epoxide **2.3** directly from **2.4** with an observed yield of < 40% after 20 h.[167] In addition, to a poor yield, they found the direct epoxidation of **2.4** afforded poor enantioselectivity.[167] To alleviate this they, generated alcohol **2.5** through a 2-step procedure, i.e. oxidative cleavage of the terminal alkene within **2.4** by a Lemieux-Johnson oxidation, followed by a subsequent reduction reaction.[167] The authors generate alcohol **2.5** to facilitate the enantioselective epoxidation through directing group effects.[167] They found an improved outcome of the epoxidation when alcohol **2.5** was used as the substrate, with a good yield and enantioselectivity observed.[167]
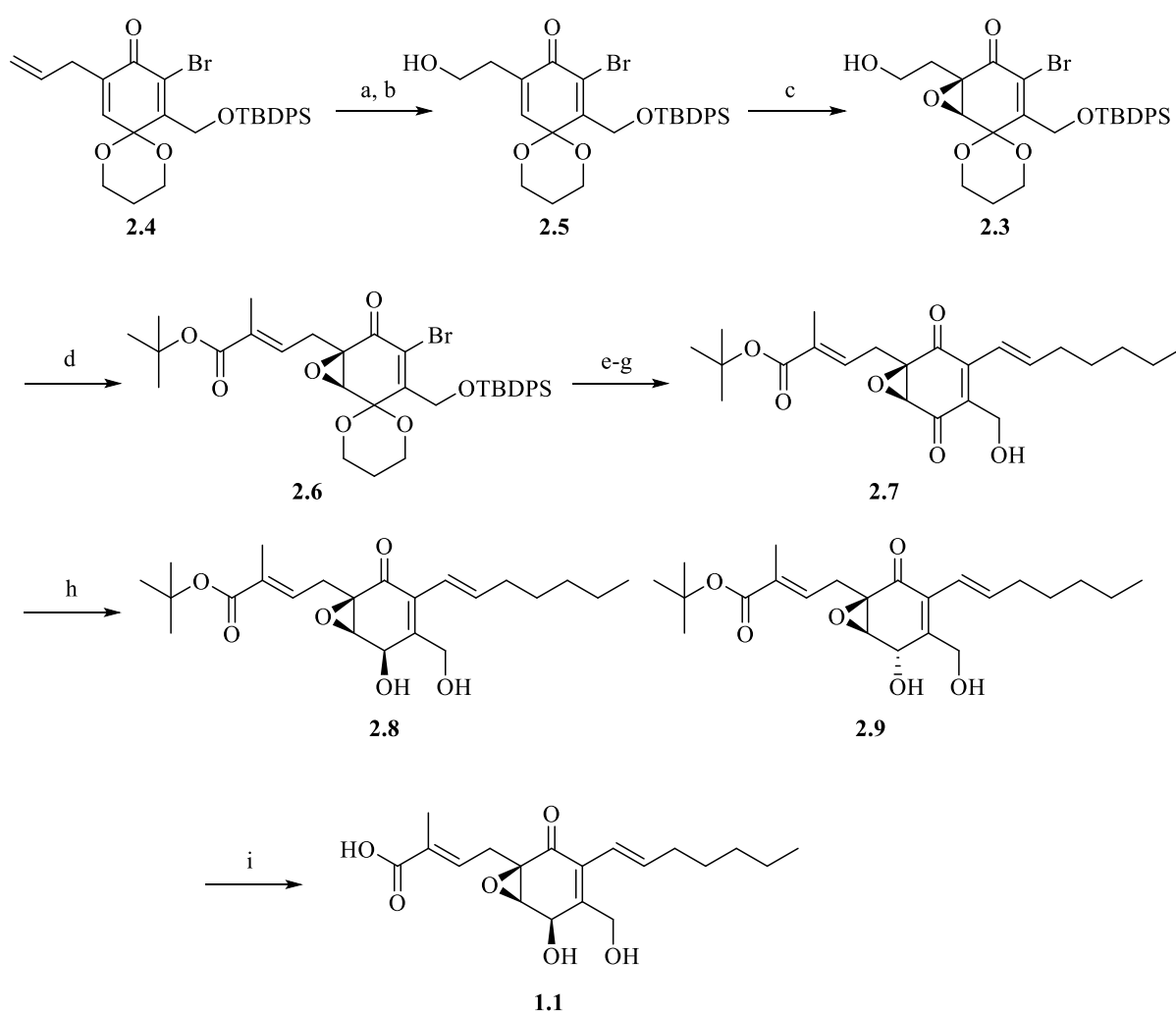
Scheme 2.1. Li synthesis of ambuic acid. (a) NaIO$_4$, OsO$_4$, THF/H$_2$O, 1.5 h, 62%; (b) BH$_3$· *t*BuNH$_2$, MeOH/H$_2$O, 0 °C, 20 min, 76%; (c) Ph$_3$COOH, NaHMDS, *L*-DIPT, 4 Å MS, toluene, -40 °C, 50 h, 91%; (d) (i) Dess-Martin periodinane, DCM, 35 min, (ii) Ph$_3$P=C(Me)CO$_2$*t*-Bu, DCM, -78 - -5 °C, 4 h, 94 %; (e) (*E*)-tributyl-1-heptenylstannane, Pd(PPh$_3$)$_4$, toluene, 110 °C, 2 h, 94%; (f) TBAF/ acetic acid (1:1), THF, 20 h, 76%; (g) 48% aq. HF, MeCN, 15 min, 93%; (h) MeOBEt$_2$, NaBH$_4$, -78 °C, 30 min, **2.8** 48%, **2.9** 39%; (i) 48% HF, MeCN, 1 h, 70%.

Dess-Martin oxidation of the alcohol within **2.3** and subsequent Wittig olefination generated the *t*-butyl ester **2.6**.[167] Stille cross-coupling allowed for installation of the heptene chain which was followed by deprotection of both the ketal and the TBDPS silyl ether yielded **2.7**.[167]

With the production of **2.7**, the authors proceed with the production of ambuic acid. Reduction of ketone **2.7** afforded a mixture of enantiomers **2.8** and **2.9** in a 1.2:1 ratio.[167] Li *et al*. attempted to alleviate this through the use of a range of borohydride reagents but did not find an improvement in the reaction outcome in terms of selectivity.[167] Final hydrolysis of the *t*-butyl ester yielded (+)-ambuic acid **1.1**.[167]

2.2.3 Mehta synthesis of ambuic acid

Mehta *et al*. presented a simplified method relative to the Li method for the production of racemic (±)-ambuic acid **1.1**.[168] The key intermediate in the Mehta synthesis is the epoxy cyclohexenone **2.10** produced from the readily available *endo*-Diels-Alder adduct **2.11** (Scheme 2.2).[168]
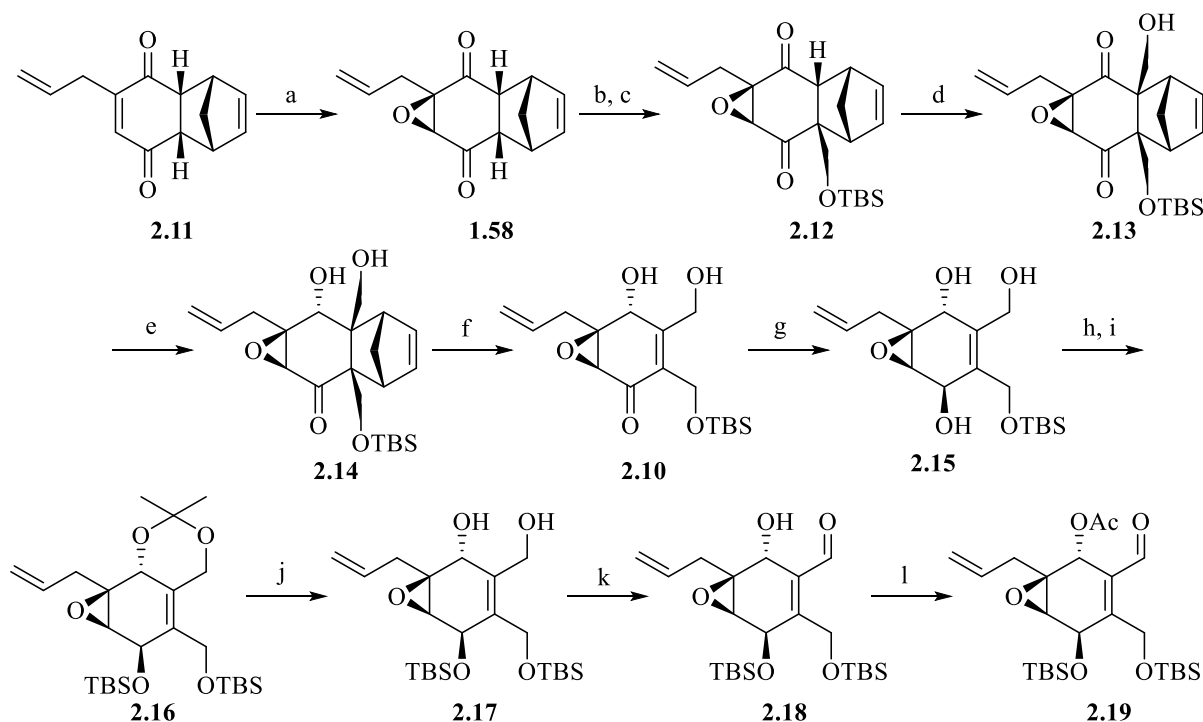
Scheme 2.2. (a) 10% (w/v) Na$_2$CO$_3$, 30% H$_2$O$_2$, acetone, 0 °C, 92%; (b) 35% formaldehyde, DBU, THF, rt., 0 °C, 30 min, 95%; (c) TBSCl, imidazole, DMAP, DMF, 0 °C, 90%; (d) 35% formaldehyde, DBU, THF, rt., 36 h, 80%; (e) NaBH$_4$, MeOH, -5 °C, 84%; (f) Ph$_2$O, 220 °C, 96%; (g) NaBH$_4$, MeOH, -5 °C, 10 min, 75%; (h) PPTS (2 eq.), 2,2-dimethoxypropane, rt., 5 h, 92%; (i) TBSOTf, 2,6-lutidene, DCM, 0 °C, 15 min, 95%; (j) PPTS (0.4 eq.), MeOH, rt., 2 h, 78%; (k) TEMPO, O$_2$, CuCl, DMF, rt., 3 h, 90%; (l) acetic anhydride, pyridine, DMAP, DCM, 0 °C, 2.5 h, 98%.

In their 2004 paper, Mehta *et al*. describe the transformation of Diels-Alder adduct **2.11** to epoxy cyclohexenone **2.10** (Scheme 2.2).[164] They observed that the epoxide **1.58** is formed in a stereo- and chemo-selective manner through the use of hydrogen peroxide.[164] Hydroxymethylation with formaldehyde and DBU and subsequent silyl protection gave **2.12** in a regio and stereo-selective manner.[164] A second hydroxymethyl group was then installed under the same conditions giving **2.13**.[164] Mehta *et al*. suggested that the adduct, as well as the newly installed primary alcohol allows for stereoselective reduction of the ketone using NaBH$_4$ to give desired *endo*-alcohol **2.14**.[164] With the successful production of **2.14**, the Diels-Alder adduct was then dismantled through heating to produce the desired epoxy cyclohexenone **2.10**.[164]

With the successful production of epoxy cyclohexenone **2.10**, the subsequent step was the reduction of the ketone to the corresponding alcohol **2.15** (Scheme 2.2).[168] Mehta *et al*. found that the hydride addition occurred on the opposite face of the ring to the epoxide, generating the desired *syn* alcohol **2.15** as the major product in a ratio of 7:1 of **2.15** to undesired *anti*-alcohol.[168] The diol was then protected as a cyclic dimethyl ketal and the free secondary alcohol as a TBDMS silyl ether giving **2.16**.[168]

The cyclic ketal **2.16** was then dismantled to give the diol **2.17**, and the newly deprotected primary alcohol was selectively oxidised through the use of TEMPO to give the corresponding aldehyde **2.18**.[168] The secondary alcohol was then protected in the form of an acetate **2.19**.[168] The aldehyde functionality was then utilised for Wittig olefination for the installation of the heptenyl side chain to afford **2.20** as a mix of *E:Z* isomers in a 1:2.2 ratio (Scheme 2.3).[168]

With the successful installation of the heptene chain, Mehta *et al*. turned their attention to the modification of the allyl functionality to allow for the installation of the *t*-butyl ester moiety. Thus, the intermediate **2.20** was treated with OsO$_4$ in a dihydroxylation procedure to give a vicinal diol intermediate which was subsequently cleaved with Pb(OAc)$_4$ to give the aldehyde **2.21** which in turn was taken into a Wittig olefination with the ylide Ph$_3$P=C(Me)CO$_2$*t*-Bu to finally afford the *t*-butyl ester **2.22** (Scheme 2.3).[168]

The acetyl group was then hydrolysed to yield a secondary alcohol which was then oxidised to the ketone **2.23** with tetra-*n*-propylammoniumperruthenate (TPAP).[168] At this point in the

synthesis, Mehta *et al.* decided that it was appropriate to resolve the issue of the stereochemistry of the heptene chain. Mehta *et al.* postulated that due to the proximal position of the dienone chromphore to the double bond within the heptene chain, photochemical mediated *E:Z* equilibration should be possible, and indeed they achieve complete conversion affording the desired *E* isomer **2.24**.[168] Final deprotection of the ester and silyl ether was achieved through the use of 40% HF giving ambuic acid **1.1**.[168]
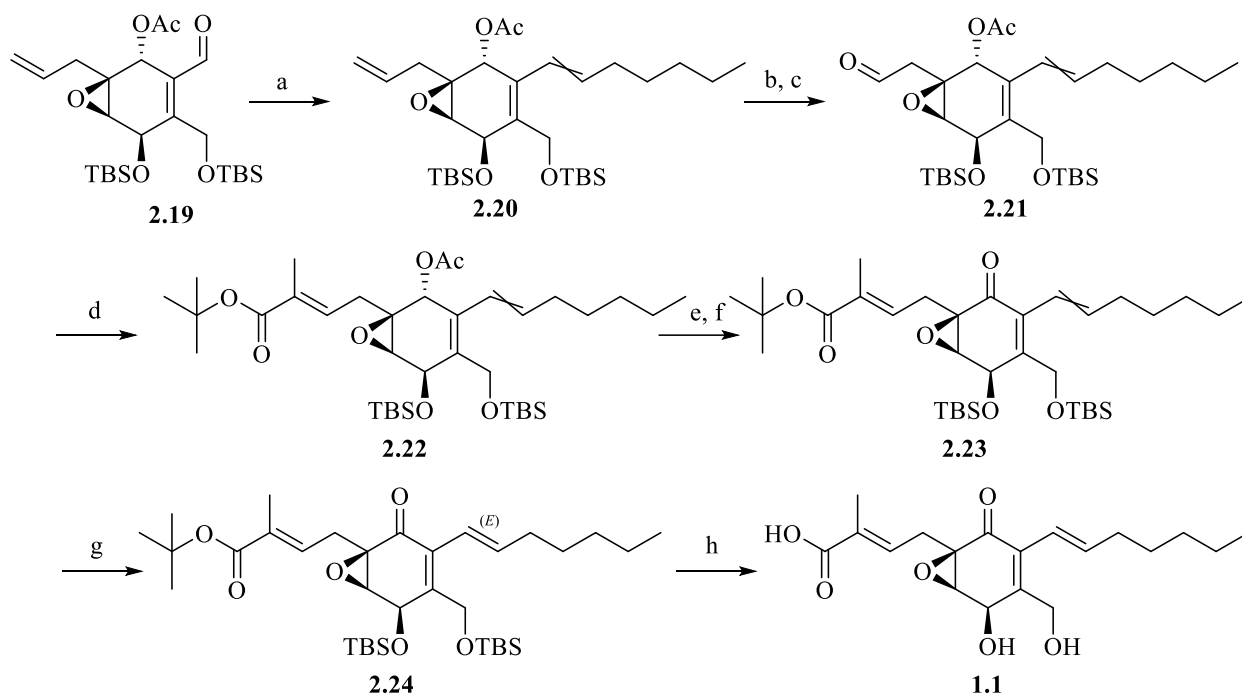
Scheme 2.3. (a) *n*-C$_6$H$_{13}$PPh$_3$Br, *t*-BuOK, diethyl ether, 0 °C, 75%; (b) OsO$_4$, NMMO, acetone and water, -25 °C, 3 h, 40%; (c) Pb(OAc)$_4$, THF, 0 °C, 1.5 h, 95%; (d) Ph$_3$P=C(Me)CO$_2$*t*-Bu, DCM, -78 °C - -5 °C, 9 h, 65%; (e) LiOH, MeOH, 0 °C, 4 h, 65%; (f) TPAP, NMMO, 4 Å MS, 3 h, 85%; (g) *hv*, 450 W, I$_2$, chloroform-d, 10 h, 80%; (h) 40% HF, MeCN, 3 h, 75%.

2.2.4 Jung synthesis of ambuic acid

Jung *et al*. presented a simplified total synthesis of (+)-ambuic acid, when compared to the Li and Mehta syntheses outlined above.[167-168] Jung *et al.* utilise a key, chiral Diels-Alder adduct intermediate **1.53** prepared through a reaction of cyclopentadiene with 2-iodo-1,4-quinone monoketal **1.54** in the presence of a chiral (*R*)-(+)-*o*-tolyl-CBS-oxazaborolidene catalyst **1.56** (Scheme 2.4, Figure 2.4).[163]

Chiral oxaborolidenes, such as **1.56** have significant utility in organic synthesis. They are traditionally used as chiral auxiliary agents to confer enantioselectivity in the reduction of ketones with borohydride reagents.[169]

In a 2002 paper, Corey *et al.* described a new enantioselective Diels-Alder procedure by employing an oxazaborolidene catalyst **1.56** (Figure 2.4).[169] Treatment of catalyst **1.56** with the strong protic acid, triflic acid generated the strongly Lewis acidic species **2.25** which exists at equilibrium with **2.26**.[169] Through an optimisation study, Corey *et al*. find that the test Diels-Alder reaction with cyclopentadiene in the presence of catalyst **1.56** provides excellent enantioselectivity (99% of desired *exo* product).[169]

Hence, it is anticipated that **2.25** can coordinate with the reaction substrate **1.54** (Figure 2.4). Corey *et al*. suggested hydrogen bonding between the α-proton of the substrate with the oxygen within the oxazaborolidene ring of **2.25** (Figure 2.4).[169] In this conformation, the aromatic group on the oxazaborolidene can undergo a π-π interaction with the α,β unsaturated region of the substrate, shielding one face of the substrate and preventing formation of the undesired enantiomer.[169]
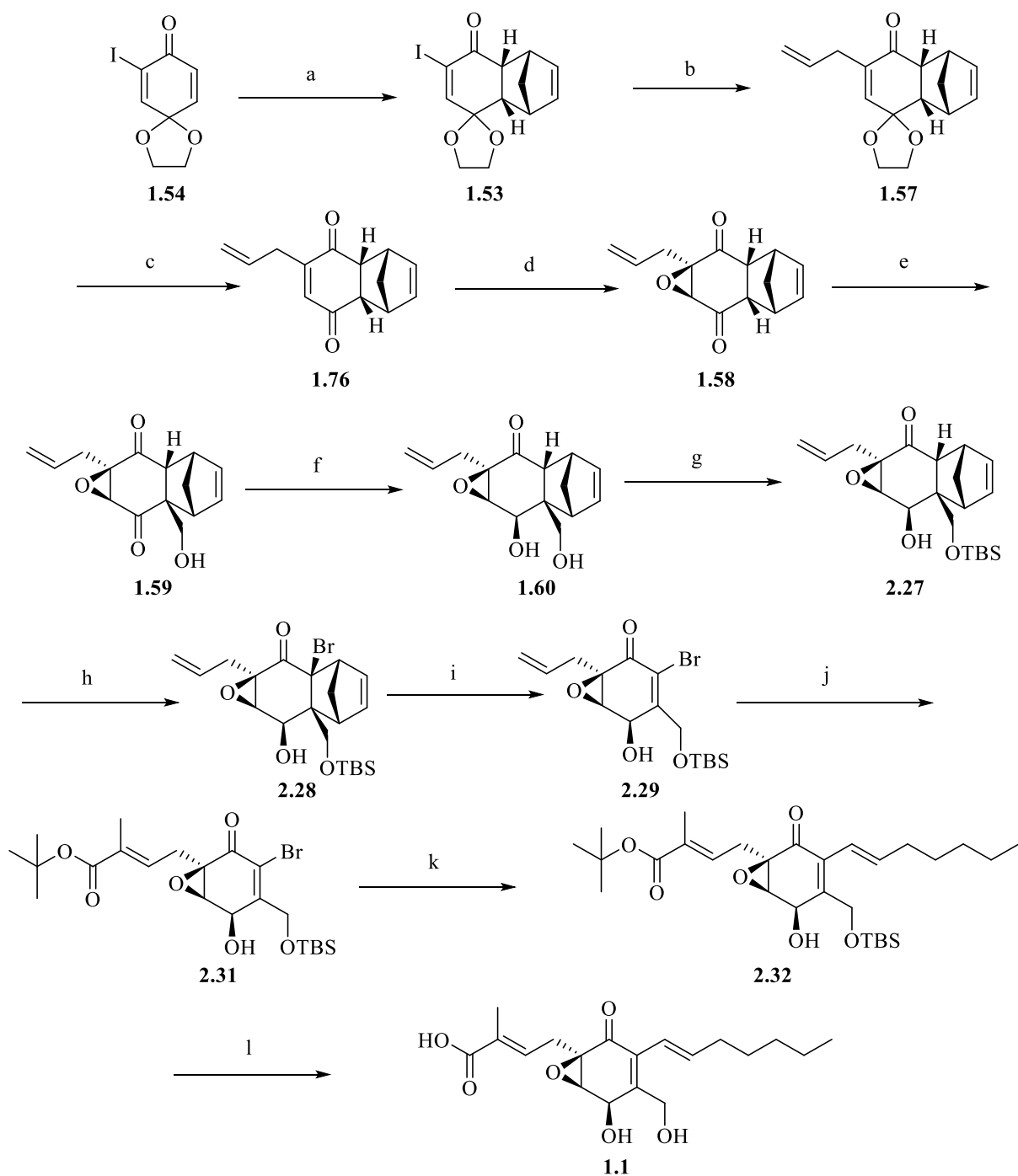
Scheme 2.4. The Jung synthesis of ambuic acid. (a) cyclopentadiene, catalyst **1.56** (20 mol%), DCM, -78 °C, 1 h, 94%; (b) Pd(PPh₃)₄, allyltributyl stannane, THF, 100 °C, 92%; (c) 1 N H₂SO₄, acetone, THF, 0 °C, 94%, (d) H₂O₂, 10% (w/v) Na₂CO₃, 0 °C, 93%; (e) formaldehyde, DBU, THF, 0 °C, 90%; (f) DIBAL-H, THF, -78 °C, 87%; (g) TBSCl, imidazole, DMF, 0 °C, 95%; (h) 1,2-dibromotetrachloroetane, DBU, DCM, 98%; (i) Ph₂O, 230 °C, 81%; (j) O₃, dimethylsulfide then Ph₃P=C(Me)CO₂t-Bu, DCM, -40 to -10 °C, 74%; (k) Pd(PPh₃)₄, (*E*)—tributyl-1-heptenyl-stanane, toluene, 110 °C, 86%; (l) HF, MeCN, 0 °C to rt., 70%.

1.56

2.25 **2.26**
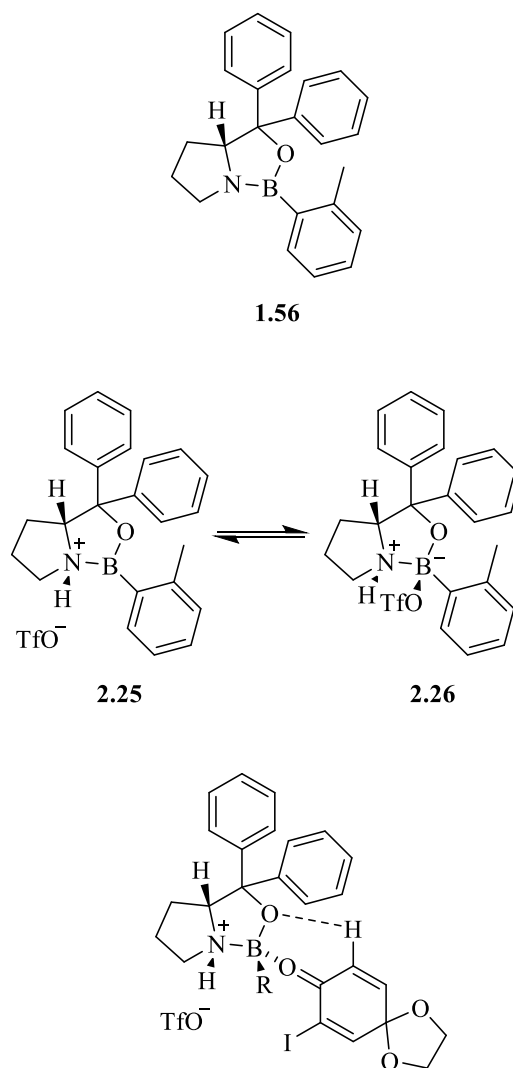
Figure 2.4. (*R*)-(+)-o-tolyl-CBS-oxazaborolidene **1.56**, the equilibrium states when catalyst **1.56** is treated with triflic acid and the proposed complex formed between **2.25** and **2.26**, adapted from Corey *et al.*.[169]

Jung *et al.* found that in their application, (*R*)-(+)-*o*-tolyl-CBS-oxazaborolidene **1.56** catalysis provided the desired *exo*-product **1.53** in good enantiomeric excess (95%, Scheme 2.4).[163] With the successful production of the Diels-Alder adduct **1.53**, the subsequent step was to install the allyl group through a Stille cross-coupling reaction to give **1.57**.[163] Treatment with acid gave the de-protected ketone **1.76**.[163] Epoxidation, mediated by hydrogen peroxide and base smoothly gave only the *exo*-epoxide **1.58** (Scheme 2.4).[163] Monohydroxymethylation was carried out using a protocol previously developed by Mehta *et al.* to give the alcohol **1.59**.[163-164] Jung *et al.* evaluated a number of reducing agents to selectively give *exo*-alcohol **1.60** and found that DIBAL-H gave the desired product with good regio- and stereoselectivity.[163] The primary alcohol was then protected as the TBDMS ether **2.27** (Scheme 2.4).[163]

A key synthetic step in the Jung synthesis was the α-bromination generating bromide **2.28** (Scheme 2.4).[163] They evaluated a range of brominating reagents including *N*-bromosuccinimide and elemental bromine. However, they found 1,2-dibromotetrachloroethane to be an excellent brominating agent for this application.[163] The silyl ether **2.27** was stirred with DBU to extract the α-proton allowing for reaction with 1,2-dibromotetrachloroethane to afford **2.28** in a good yield (98%).[163] With the production of **2.28** the Diels-Alder adduct was dismantled through heating giving quinone derivative **2.29** (Scheme 2.4).[163]

Another part of the Jung synthesis which differs significantly from the Li and Mehta approaches is the manner in which the *t*-butyl ester moiety is installed (Figure 2.5). In the Jung approach, the *t*-butyl ester was installed via ozonolysis and subsequent Wittig olefination.[163] In contrast, both the Li and Mehta approaches utilised a dihydroxylation approach to cleave the terminal alkene within the allylic side chain, through the use of OsO_4 (Figure 2.5).[167-168] Subsequent cleavage of the vicinal diol by $Pb(OAc)_4$ in the Mehta study and $NaIO_4$ in the Li study gave the corresponding aldehyde.[167-168] In the Li study, this aldehyde is reduced to the primary alcohol for the subsequent synthetic transformations, before Dess-martin oxidation, giving hte aldehyde for the Wittig reaction.[167] The Li and Mehta syntheses both require more synthetic steps to install the *t*-butyl ester in addition, OsO_4, used for the dihydroxylation is highly toxic which makes its use undesirable. Both of these are disadvantageous when compared to the Jung approach.
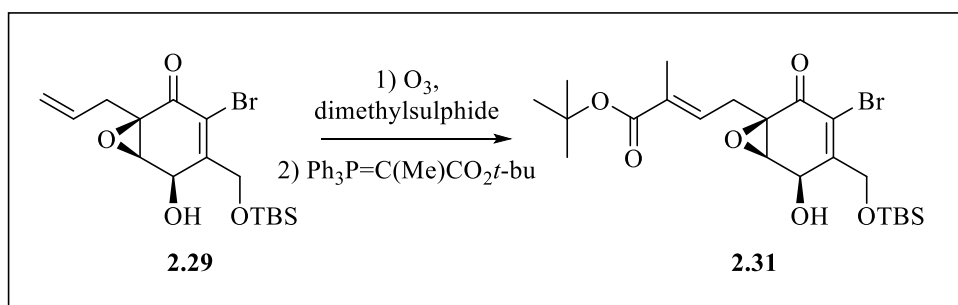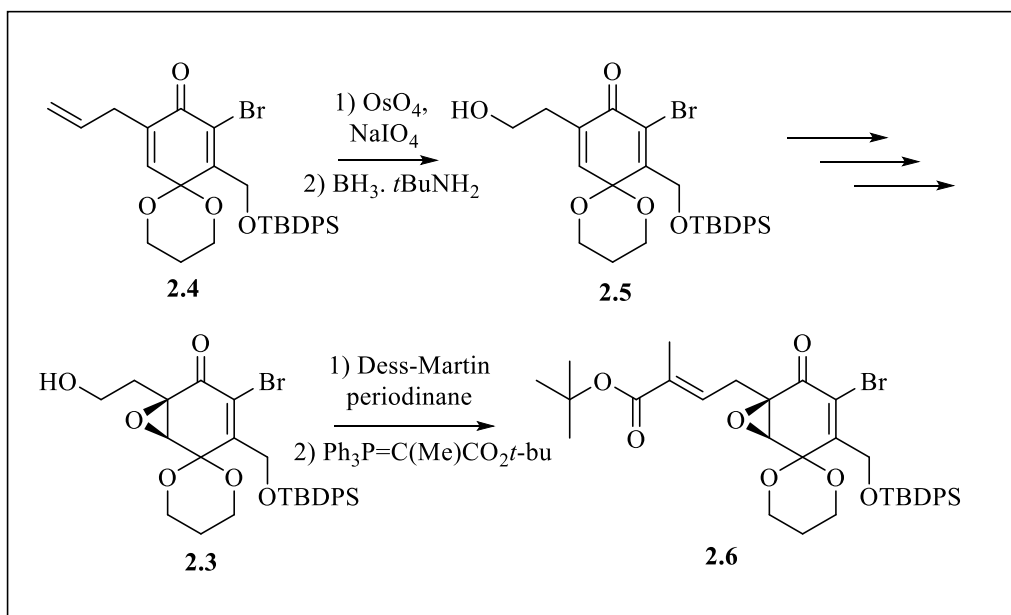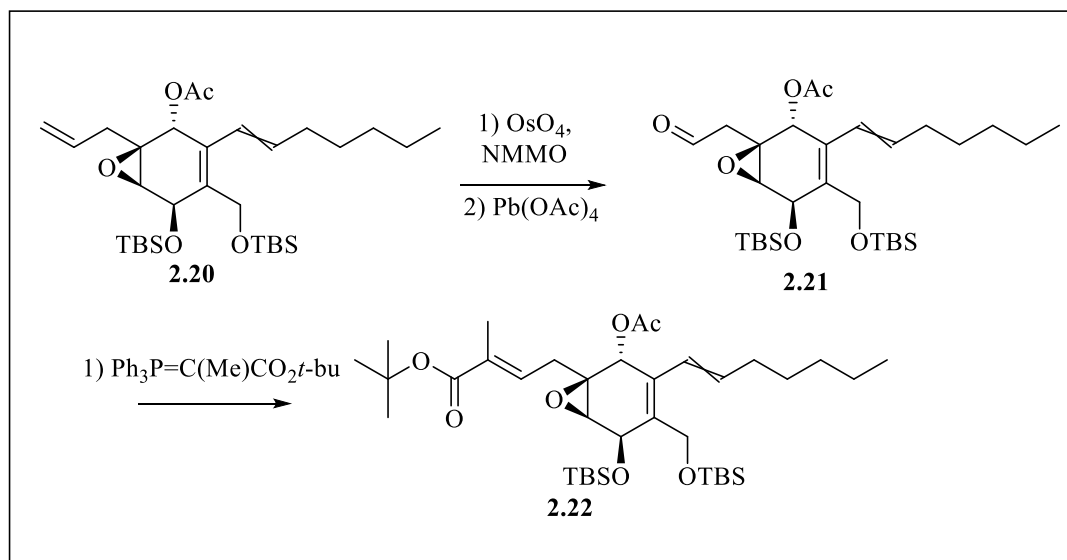
Figure 2.5. The synthetic approaches employed by **(A)** Jung et al., **(B)** Li et al. and **(C)** Mehta et al. for the installation of the t-butyl ester.

Jung *et al*. produce the aldehyde **2.30** (Figure 2.6) precursor for the Wittig-mediated installation of the *t*-butyl ester protected acid moiety in a one-pot ozonolysis procedure (this procedure is expanded upon later in this chapter).[163] Quinone **2.29** is treated with ozone gas followed by dimethyl sulfide giving aldehyde **2.30**.[163] The aldehyde **2.30** was taken directly into a Wittig olefination with $Ph_3P=C(Me)CO_2t$-Bu to install the *t*-butyl ester, thus giving **2.31** (Scheme 2.4).[163] This procedure is an improvement upon those outlined previously in this chapter due to its relative simplicity as well as not requiring toxic OsO_4.

2.30
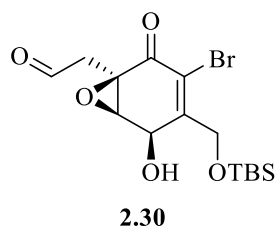
Figure 2.6. Aldehyde intermediate **2.30** produced by Jung et al. in the ozonolysis procedure.

Next, a Stille cross-coupling with (*E*)-tributyl-1-heptenyl-stannane allowed for installation of heptene right-hand chain giving **2.32**.[163] This is an improvement when compared to the Mehta synthesis which gave a mixture of (*E*) and (*Z*) isomers in a ratio of 1:2.2.[168] With the successful installation of the (*E*)-heptene chain, subsequent deprotection through the use of dilute HF gave the final ambuic acid **1.1** (Scheme 2.4).[163]

2.3 General Synthetic Route

2.3.1 The synthetic target

With the exception of ambuic acid **1.1**, within the literature there are no documented inhibitors of AgrB. Thus, the production of analogues of ambuic acid may provide an interesting avenue of research for the investigation into inhibitors of AgrB.

At the outset of this study, the racemate LB75 **1.52** (produced by Dr Leonardo Baldassarre) was found to be active against *agr* activity at a comparable level to that of ambuic acid **1.1** (Figure 2.7)
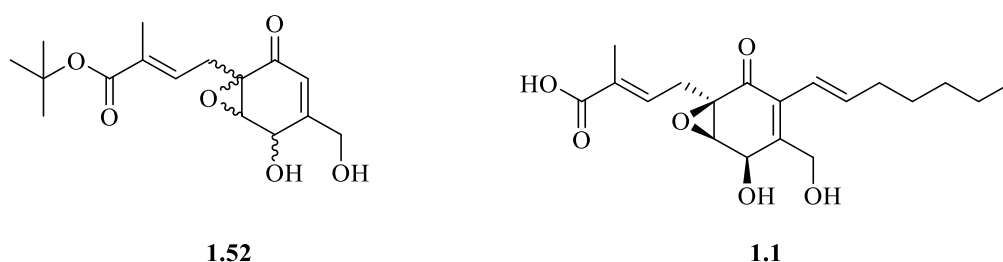
Figure 2.7. Racemate **1.52** found to be as active as Ambuic acid **1.1** against *agr*-mediated quorum sensing in *S. aureus*.

As such, it was decided to use enantiomerically pure versions of **1.52** as the scaffold for the production of a range of unique ambuic acid analogues. This was done because of the more facile nature of the synthetic route, relative to that of ambuic acid. The attempted synthesis and synthesis of novel analogues will be discussed herein.

2.2.2 Synthesis target 1.62

The synthesis of enantiomerically pure **1.62** (Figure 2.8) is based on a modified procedure from the total synthesis of (+)-ambuic acid previously carried out by Jung *et al*. outlined previously.[163] Dr Leonardo Baldesarre, carried out modification of the Jung *et al*. procedure to produce the (+)-enantiomer **1.62** (LB151) of racemate **1.52**. An efficient workflow was established by Baldassarre which allows for the production of numerous unique analogues. This synthetic approach was utilised in this study as it provided the opportunity to produce numerous unique analogues.
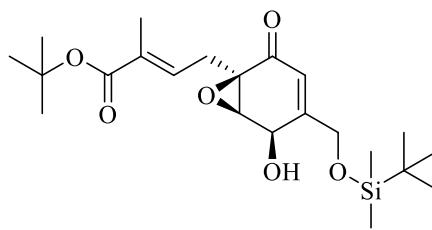
1.62

Figure 2.8. Enantiomerically pure (+)-enantiomer of LB151 **1.62**

Commercially available 2-iodo phenol **2.33** was treated in an oxidative dearomatization reaction with (diacetoxyiodo)benzene in MeOH to yield the quinone derivative **2.34** (Scheme 2.5). This reaction generally proceeded with reasonable yields, typically with 40-60% conversion to the desired product **2.35**. This was followed by the formation of the cyclic ketal **1.54**, which was achieved by treatment with ethylene glycol in the presence of BF_3Et_2O (yields typically 70-80%) (Scheme 2.5). However, difficulty was encountered with the stability of product **2.34**, as well as the quality of commercially available 2-iodo phenol **2.33**.

It was noted that there was an apparent batch-to-batch variation in 2-iodo phenol **2.33**. Differences in the physical appearance of 2-iodo phenol were observed, with variation in colour and texture found. The colour variation ranged from being light purple/ pink in some batches to white in others. Indeed, this variation in colour is described in technical information provided by the supplier.

Texture variation included the compound having an almost free-running crystalline appearance to a mildly viscid, fine, powdery appearance. Typically, the light pink/ purple crystals were of this viscid nature and were associated with poor reaction outcome.

In addition to apparent batch-to-batch variation in starting material, it was also found that quinone derivative **2.34** was unstable. When left at ambient temperature, not in solution, the dark red/brown oil was observed to spontaneously sublimate iodine vapour in an exothermic manner. This yielded an intractable dark green/black tar. This should be noted for future applications using related compounds as a matter of safety and to avoid the wasting of reagents.
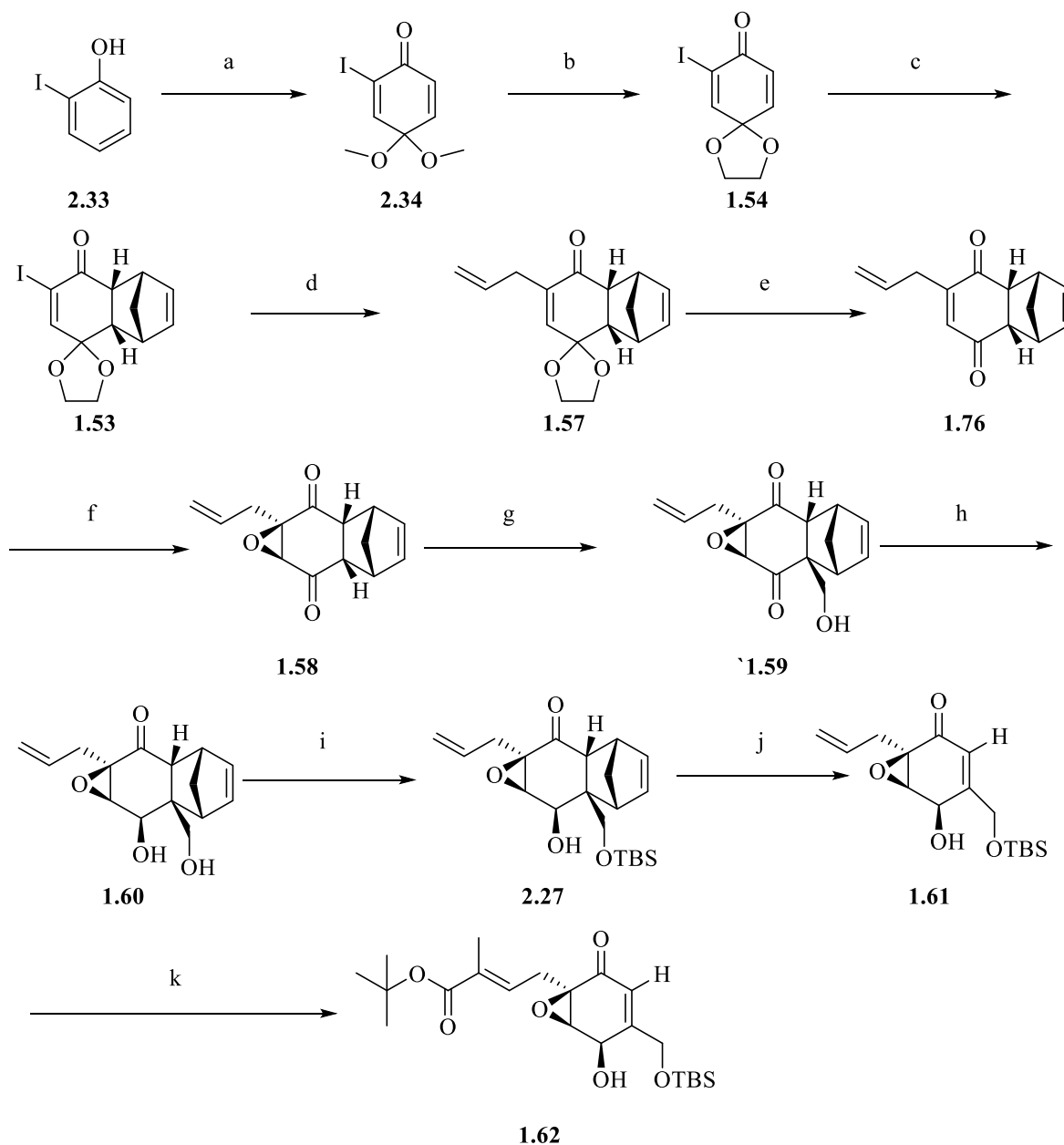
Scheme 2.5. Scheme showing the general synthesis scheme of target **1.62**. (a) (diacetoxyiodo)benzene, MeOH, 2 h, 0 °C, 55%; (b) BF₃Et₂O, ethylene glycol, dimethoxyethane, 2 h, -78 °C, 81%; (c) catalyst **1.56**, cyclopentadiene, DCM, 15 min, -78 °C, 88%; (d) Pd(PPh₃)₄, allyltributyl stannane, THF, 10 min, 110 °C, 150 W MW radiation, 68%; (e) 1 N H₂SO₄, acetone, THF, 30 min, rt., 96%; (f) 10% (w/v) Na₂CO₃, 30% (v/v non-stab.) H₂O₂, acetone, 30 min, 0 °C, 83%; (g) 37% (w/v) aqueous formaldehyde, DBU, THF, 30 min, 0 °C, 79%; (h) DIBAL-H, THF, 30 min, -78 °C, 43%; (i) TBSCl, imidazole, DMF, 4 h, 0 °C, 83%; (j) Ph₂O, 4 h, 230 °C, 73%; (k) O₃, dimethylsulfide, MeOH, -78 °C, 30 min then Ph₃P=C(Me)CO₂t-Bu, DCM, 2 h, -40 °C, 25%.

Attempts were made to circumvent these issues. Firstly, to overcome the issue of the batch-to-batch variability of 2-iodo phenol, an alternative starting material was considered. Thus, 2-bromo phenol **2.35** was chosen as a substitute for 2-iodophenol **2.33** as it possesses the required functionality for subsequent transformations. In addition, the replacement of iodine with bromine, a poorer leaving group may impart stability to **2.36** relative to **2.34**. Given that iodine

was seen to sublimate when **2.34** decomposed, it was anticipated that this would help alleviate the issue.

A
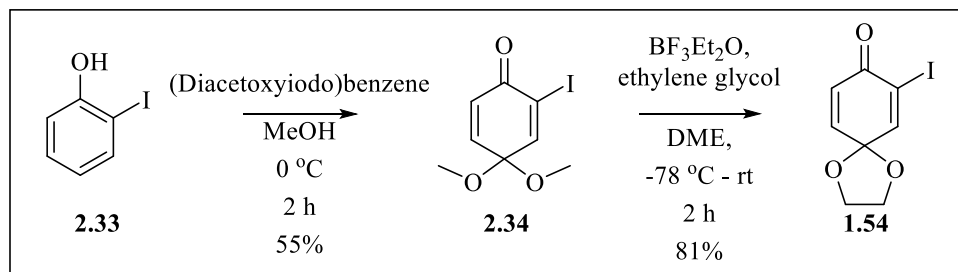
B
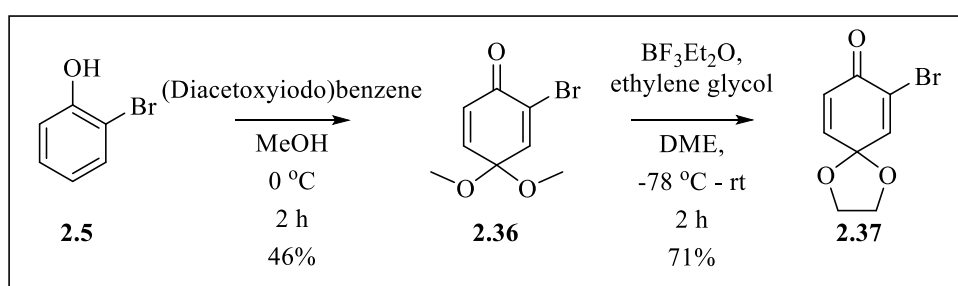
Scheme 2.6. Reaction schemes showing dearomatization of 2-iodophenol **2.33** (**A**) and 2-bromo phenol **2.35** (**B**) to quinone derivatives **2.34** and **2.36**, respectively, followed by the formation of the cyclic ketals **1.54** and **2.37.**

Oxidative dearomatization of 2-bromophenol **2.35** proceeded with reasonable yield of the product **2.36** (46%) which is comparable to formation of the iodo variant (Scheme 2.6). Furthermore, transformation to the cyclic ketal **2.37** proceeded with a good yield of 71% (Scheme 2.6). Thus, it appeared that 2-bromophenol is a suitable substitute for 2-iodophenol as overall yields of **1.54** and **2.37** in the two-step synthetic procedure are comparable with yields of 45% and 33% observed respectively. Furthermore, the costs of 2-iodo phenol and 2-bromophenol are comparable. In future applications, if issues with 2-iodophenol are encountered, 2-bromophenol is a suitable substitute for the synthesis.

Further to the above attempts to improve the stability of **2.34**, it should be noted that for future work involving this compound, once purified, it should be used directly in the subsequent step. Additionally, keeping **2.34** either in solution or cold (keeping the compound in an acetone/dry ice bath (-78 °C)) until it was required was found to be beneficial, with fewer incidences of degradation if these factors were employed.
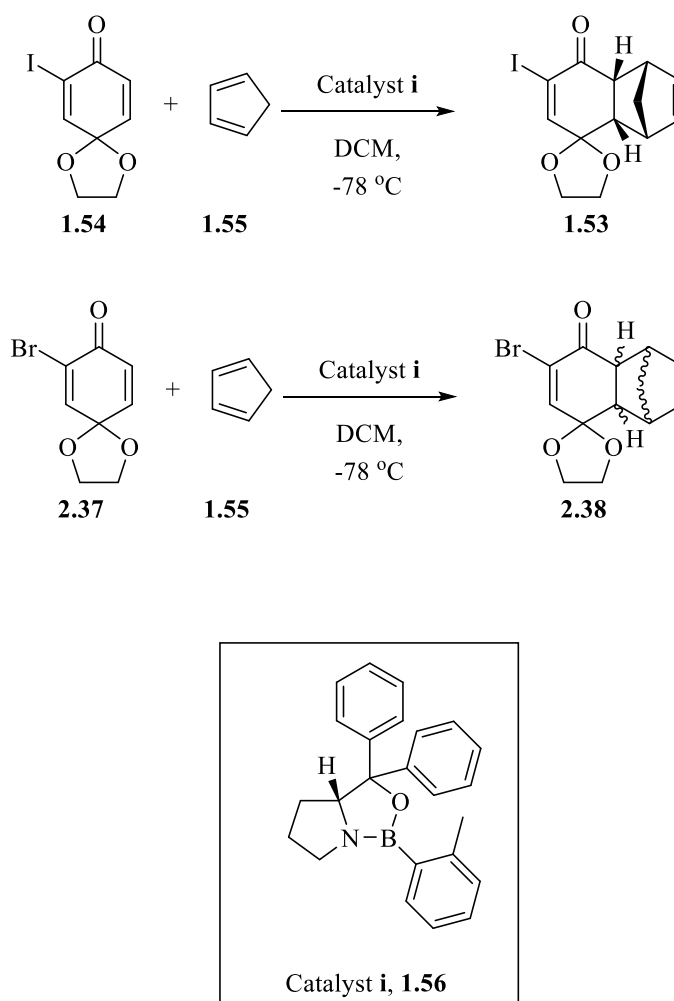
Scheme 2.7. The Diels alder reaction forming the desired adduct **1.53** and the racemic adduct **2.38** as well as the (*R*)-(+)-*o*-tolyl-CBS-oxazaborolidene catalyst **1.56**

With the successful production of both the iodo- and bromo- cyclic ketal compounds, **1.54** and **2.37**, both were both taken forward to the chiral Diels-Alder reaction to produce the adducts **1.53** and **2.38**, respectively (Scheme 2.7). The adducts, **1.53** and **2.38** are produced to impart stereoselectivity on subsequent chemical transformations through steric hindrance of formation of the undesired enantiomer. The production of the Diels-Alder adduct is a key step in the production of ambuic acid by Jung *et al.*.[163]

2.39
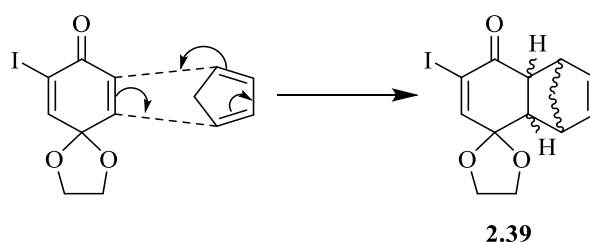
Figure 2.9. The Diels-Alder reaction in the absence of CBS chiral catalyst, generating racemate **2.39**

The Diels-Alder reaction between **1.54** (and **2.37** for the bromo analogue) and freshly distilled cyclopentadiene **1.55** is the key step in this synthetic route and utilises (*R*)-(+)-o-tolyl-CBS-oxazaborolidine **1.56** to selectively generate the desired (+)- adduct **1.53** (Scheme 2.7).[163, 170-171] Due to the achiral nature of starting materials **1.54/2.37** and cyclopentadiene **1.55**, the reaction in the absence of chiral catalyst would generate a racemate **2.39** (Figure 2.9), which is undesirable.

2.25   **2.26**
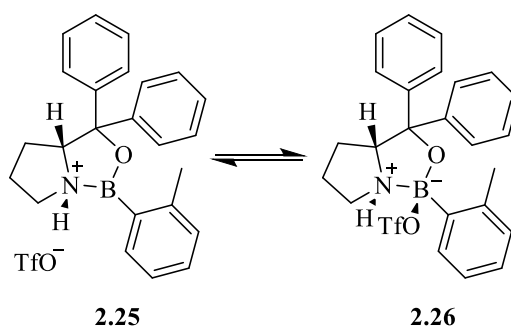
Figure 2.10. The facile equilibrium between species of (*R*)-(+)-o-tolyl-CBS-oxazaborolidene upon treatment with trifluoromethanesulfonic acid

The CBS catalyst **1.56** was activated through the addition of trifluoromethanesulfonic acid, producing the chiral and strongly Lewis acidic species **2.25**, which exists at facile equilibrium with **2.26** (Figure 2.10).[170] Acting as a Lewis acid, the Boron within **2.25** can coordinate to the carbonyl within either **1.54** or **2.37.** This allows for steric occlusion of the superfacial π-orbitals of **1.54/2.37**, mediated by the bulky tolyl group within **2.25**.[170] This occlusion prevents alignment of the superfacial π-orbitals of the dienophile starting material (either **1.54**/**2.37**) and the π-orbitals within cyclopentadiene, preventing formation of the undesired (-)-adduct. This procedure produced the desired adduct **1.53** in good yields (60-80%) and good enantioselectivity, $[\alpha]_D^{25} = -70.3$, which is comparable to the literature value reported by Jung *et al.* ($[\alpha]_D^{25}$ -84.7).[163] The bromo variant **2.38** was produced in comparable yield 73%. Unfortunately, upon optical rotation analysis, it was found that the bromo adduct **2.38** was a racemic mixture. The observed value of $[\alpha]_D^{25} = 0.0$, indicated racemisation. However, due to

the poor reaction outcome when forming iodo-cyclic ketal **1.54**, it was necessary to use racemate **2.38** for subsequent steps for the production of the diethyl and cyclohexyl ketal final compounds, thus producing racemic diethyl and cyclohexyl ketals. The synthesis of these two ketal analogues is outlined later in this chapter. Racemic synthesis followed the same general synthetic route as outlined herein.

With the production of adducts **1.53** and **2.38**, the subsequent step was to install the allyl chain α to the ketone (Scheme 2.8). Stille cross-coupling was utilised for this purpose. Alternatives routes such as Suzuki coupling could also have been considered, however Stille coupling was employed due to the milder nature of reaction conditions, the diversity of permitted R-groups and the successful previous application by Jung *et al.*[163] However, an issue with the Stille coupling is the toxicity of the stannane (tin) reagents required.
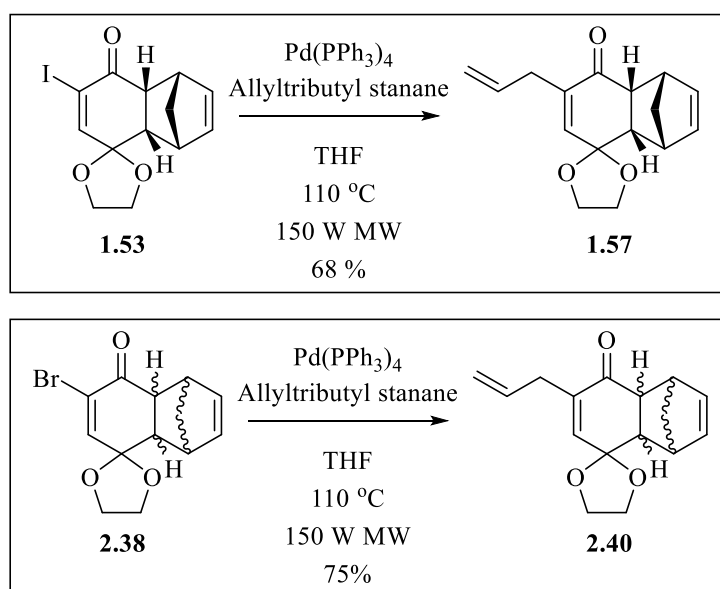
Scheme 2.8. The installation of the allyl group by Stille coupling with iodo **1.53** and racemic bromo **2.38** adduct starting materials which afforded **1.57** and racemate **2.40**.

Stille coupling utilises palladium(0) to catalyse the coupling of conjugated stannanes to electrophilic carbon centres such as an alkyl halide.[172-173] Stille coupling proceeds in a three-step pathway, summarised as follows; oxidative addition, transmetallation and reductive elimination (Scheme 2.9).[172-174] Briefly, using the iodo compound **1.53** as an example, oxidative addition of the alkyl halide (Diels-Alder adduct **1.53**) to triphenylphosphine palladium(0) catalyst **2.41** generates a palladium(II) species which can undergo transmetallation with allyl tributyl stannane **2.42** (Scheme 2.9). The allyl group displaces the

halide through action as a nucleophile (Scheme 2.9). Preceding reductive elimination, *trans /
cis* isomerisation occurs to bring to the allyl and starting material within proximity of one
another for the final reductive elimination step, which releases the desired product **1.57** and
regenerates the triphenylphosphine palladium(0) catalyst **2.41** (Scheme 2.9). Thus, the Stille
coupling successfully produced the desired allyl compound **1.57** in a good yield of 68 %. The
yield observed experimentally in this study is lower than that observed in the Jung *et al.*
synthesis, which was found to be 91 %.[163]
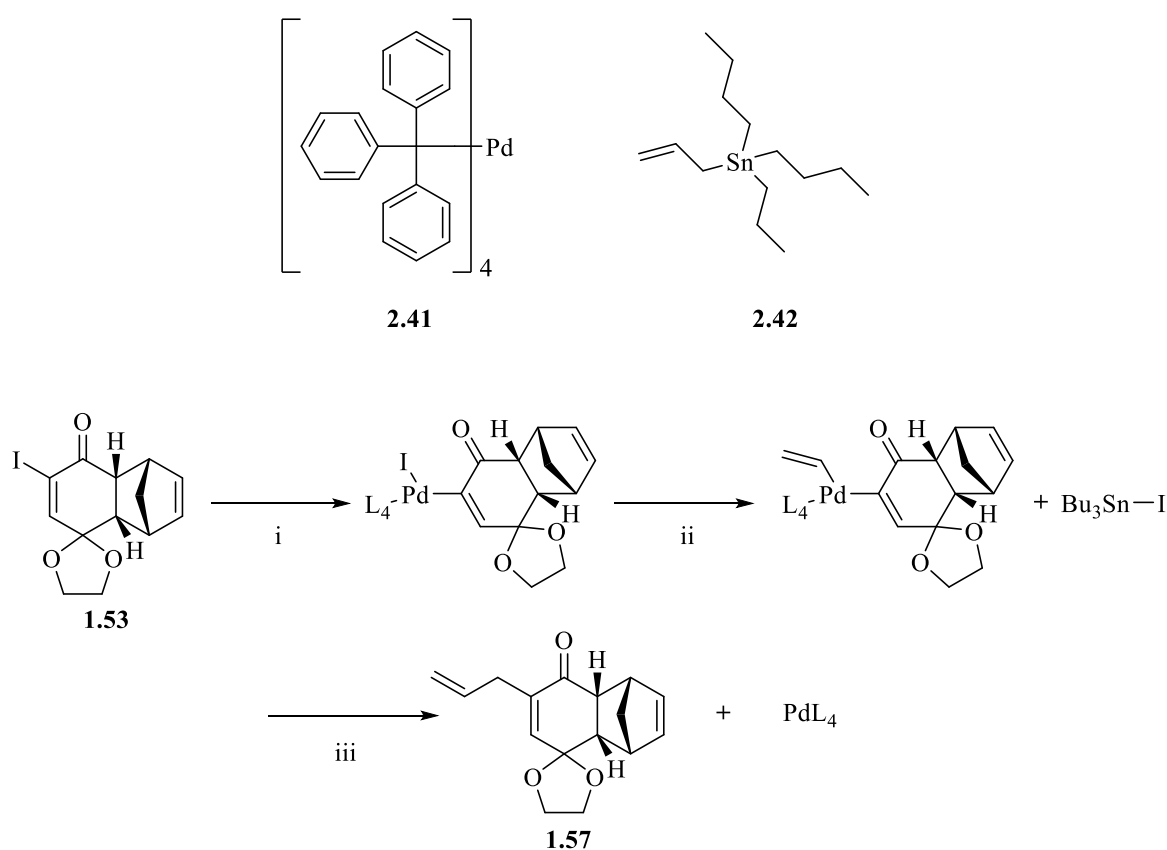
Scheme 2.9. The catalytic pathway of Stille coupling; (i) Oxidative addition, (ii) transmetallation and (iii)
reductive elimination.

The racemic bromo adduct **2.38** was also taken into the Stille reaction with allyl tributyl
stannane. The reaction also proceeded in a facile nature, however the reaction mixture required
additional heating with microwave radiation (20 minutes, compared to 10 minutes for iodo
variant) (Scheme 2.8). The lower efficiency of bromine as a leaving group, relative to iodine
could be a reason for this. Despite this, the reaction yield of **2.40** proved to be good at 75%,
compared to 68% in the corresponding iodo route (Scheme 2.8). This shows that the bromo-
route is a viable alternative to the iodo-route. As described above, the allyl compound **2.40**,

produced from the bromo Stille coupling substrate **2.38** is racemic. This racemate was only used for the production of the diethyl and cyclohexyl ketal compounds, the synthesis of which is outlined in section 2.6. The synthesis of the racemic ketal analogues follows the synthetic route outlined herein.

With the successful production of allyl compound 1.**57**, the cyclic ketal was cleaved by the addition of dilute H_2SO_4 to afford the de-protected ketone **1.76** in near quantitative yield (96 %) (Scheme 2.10).
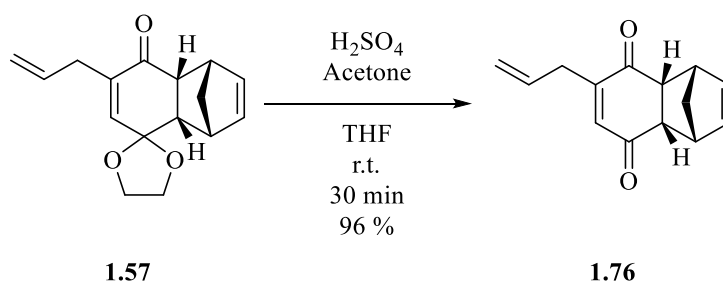
Scheme 2.10. Deprotection of the lower ketone by H_2SO_4 yielding dione **1.76**.

The intermediate **1.76** was taken forward into a modified Juliá-Colonna epoxidation which had previously been employed by Jung *et al.*[163] The Juliá-Colonna epoxidation is the oxidation of an electrophilic α, β-unsaturated enone by hydrogen peroxide (as the hydroperoxide anion) in the presence of a poly-amino acid chains with high α-helical content (typically poly-leucine or alanine).[175-176] The poly-amino acid chain is thought to act as a catalyst in the Weitz-Sheffer (Figure 2.11) epoxidation to produce the desired epoxide in an highly enantioselective manner.[175-178] However, it is well known that endocyclic enones are not suitable substrates for Juliá-Colonna epoxidation with poly-amino acid catalysts.[178] Nonetheless, in this case, enantioselectivity is ensured through the steric hindrance of formation of the *endo*-epoxide, caused by the Diels-Alder adduct (Scheme 2.11). This yielded the desired epoxide **1.58** in good yield (83%) (Scheme 2.11). This yield is comparable to that observed by Jung *et al*. in their total synthesis of ambuic acid (93%).[163]
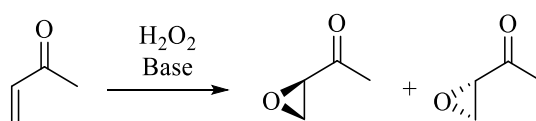
Figure 2.11. The Weitz-Scheffer epoxidation
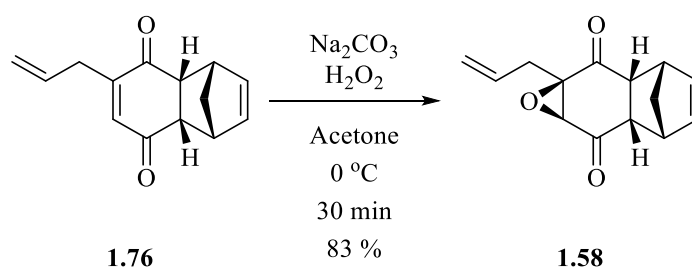
Scheme 2.11. Installation of the epoxide forming **1.58**.

With the successful production of the epoxide **1.58**, a mono-hydroxymethylation procedure was utilised to install the primary alcohol affording **1.59**. A monohydroxymethyation procedure, previously used by Jung *et al.* and Mehta *et al.* in their synthesis of the epoxyquinone (±)-jesterone **2.2**, also produced by *Pestalotiopsis sp.* was used for this application. [163, 179] In addition, Mehta *et al.* had further success with this procedure in their total synthesis of the epoxyquinone dimer (±)-torreyanic acid **2.1**.[164] DBU was used to extract the α-proton of **1.58** allowing for reaction with aqueous formaldehyde to furnish **1.59** in a good yield (79%, Scheme 2.12). The yield observed experimentally in this study was unfortunately lower than those within the literature, Jung *et al.* and Mehta *et al.* found yields of 90% and 92%, respectively.[163, 168]
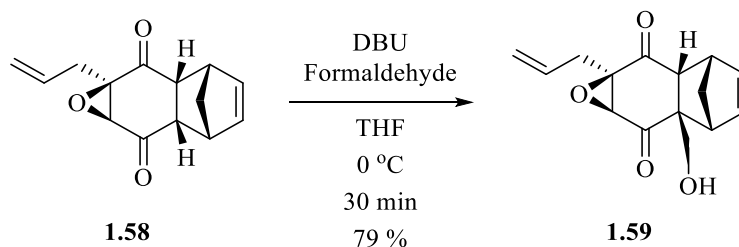
Scheme 2.12. Installation of the primary alcohol forming **1.59**.

The newly installed primary alcohol within **1.59** was utilised for the stereoselective reduction of the adjacent ketone to the secondary alcohol **1.60** (Scheme 2.13). Mehta *et al.* (2005) postulate that regioselectivity of the reaction can be explained through initial coordination of aluminium to the carbonyl and hydroxyl group blocking the preferred *exo*-face (Scheme 2.13) thus, favouring hydride delivery to the hindered *endo*-face, to yield the desired *exo*-secondary alcohol (Scheme 2.13).[180] DIBAL-H reduction yielded the desired diol, **1.60** in reasonable yield (43%), albeit lower than those previously reported in the literature, Jung *et al.* reported a yield of 87%.[163] Diol **1.60** was produced with good enantioselectivity, $[\alpha]_D^{25} = -44.4$, which is comparable to the value reported by Jung *et al.* ($[\alpha]_D^{25} = -59.9$).[163]

Stubborn aluminium salts formed upon the quenching of the reaction with MeOH proved problematic during the aqueous workup, due to their poor solubility in the aqueous phase, they may be a cause of the lower than expected yield. Notably, they form a viscous paste when anhydrous MgSO$_4$ was added as a drying agent. This caused blockage of filters, potentially causing the loss of compound. Therefore, dilute HCl was employed to try and aid solvation of the aluminium salts. Despite this, yields remained lower than those previously observed in the literature.[163]
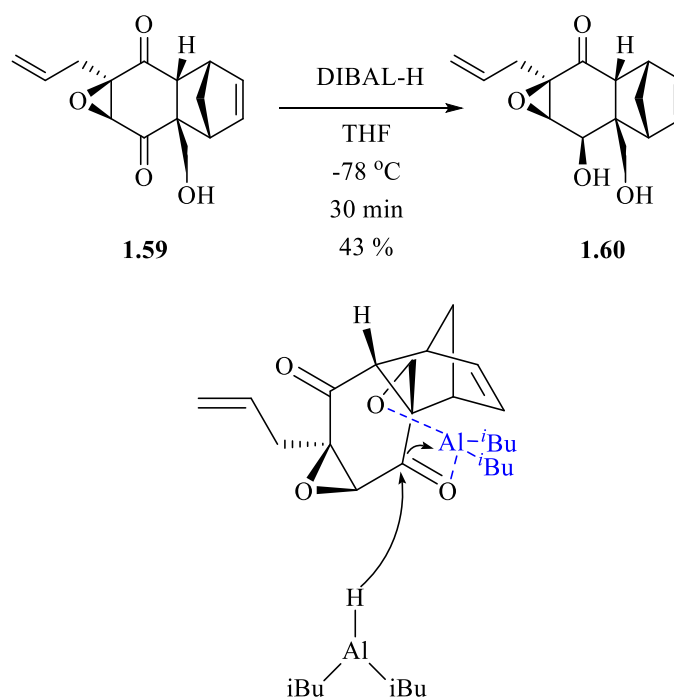
Scheme 2.13. Reduction of the lower ketone to the corresponding secondary alcohol. Potential transition state of the reduction, adapted from Mehta et al..[180]

Following the reduction, the primary alcohol of diol **1.60** was protected as a *t*-butyl dimethyl silyl (TBDMS) ether **2.27** (Scheme 2.14). Silylation is a widespread approach for the protection of alcohols and has been used broadly in other synthetic applications, including the Jung and Mehta syntheses outlined previously in this chapter.[163, 168, 181-182] A solution of diol **1.60** in DMF was treated with imidazole and TBDMSCl to yield the desired silyl ether **2.28** in an excellent yield (83%, Scheme 2.14).

Corey initially postulated that this reaction was catalysed by the formation of a reactive imidazole-silicone species (Scheme 2.15). However, in more recent studies, such as Patschinski *et al.* postulated that DMF, acting as a Lewis basic solvent may also play a role in the reaction mechanism.[181-182]
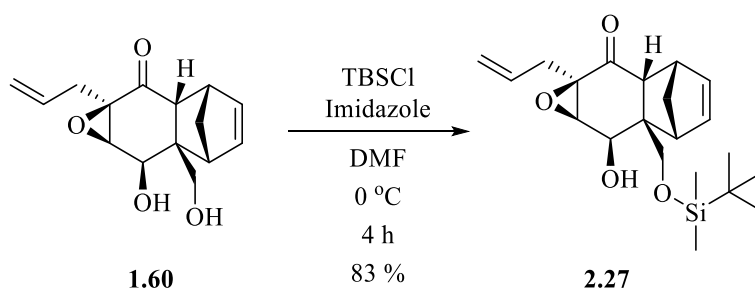
Scheme 2.14. TBDMS protection of primary alcohol as the *t*-butyl dimethyl silyl ether

In addition to high yields, the removal of silyl ether protecting groups is often facile, typically using tetra-*n*-butylammonium fluoride (TBAF).[181] Efficiency of protection and deprotection are both highly desirable properties of a protection step. Silyl ether **2.27** was taken forward.

The Diels-Alder adduct was dismantled using a procedure modified from Jung *et al.* by heating **2.27** to 230 °C in Ph$_2$O for 2 h liberating cyclopentadiene and forming **1.61** in good yield (73 %, Scheme 2.16).[163] The yield observed in this study is comparable to the yield observed by Jung *et al.* in their total synthesis of ambuic acid (81 %).[163]
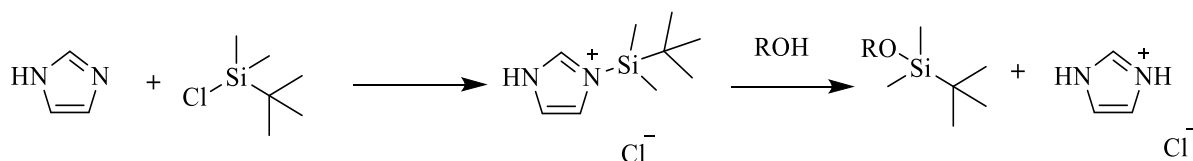
Scheme 2.15. TBDMSCl protection of a primary alcohol showing the reactive imidazole-silyl species as postulated by Corey (1972) to be the catalyst of the reaction.[182]

The compound **1.61** was treated in an ozonolysis procedure, modified from Jung *et al.* with a reductive workup with dimethylsulfide to convert the terminal allylic alkene into aldehyde **2.43**. The aldehyde **2.43** was then taken into a Wittig reaction with ylide **2.44** to install the *t*-butyl ester moiety yielding the final compound **1.62**.
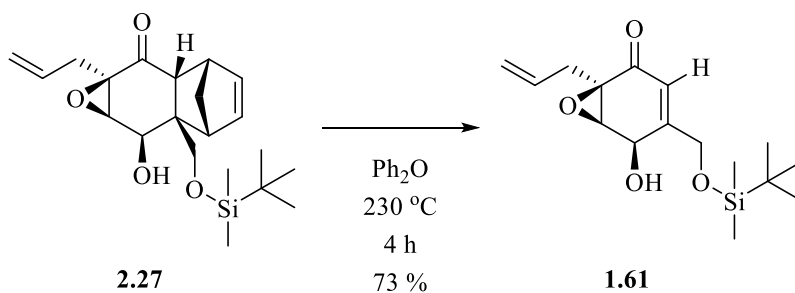
Scheme 2.16. Retro Diels-Alder reaction, dismantling of the adduct **2.27** yielding **1.61**.

Ozonolysis is the oxidative cleavage of olefins utilising O_3 (Scheme 2.17) and was first investigated by Harries *et al.*.[183] Initial addition of ozone across the olefin generates an unstable, 5-membered 'primary' ozonide, a melozonide (Scheme 2.18).[184-185] Subsequent decomposition of the melozonide yields a carbonyl and 'carbonyl oxide' (Scheme 2.18).[184, 186] Addition of the 'carbonyl oxide' to the carbonyl yields the secondary ozonide, a 1,2,4-trioxolane, first observed by Rieche *et al.*, an interesting heterocycle with both an ether and peroxide linkage (Scheme 2.19).[184-185, 187] After ozonolysis, the reaction mix was treated with dimethylsulfide, and stirred for 30 minutes, causing lysis of the 1,2,4-trioxolane, forming formaldehyde, dimethylsulfide and the desired aldehyde **2.43** (Scheme 2.19).
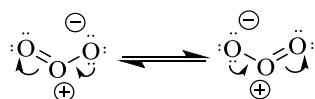
Scheme 2.17. Ozone and its resonance structures

The crude aldehyde **2.43** was then taken into a Wittig olefination with ylide **2.44**. The Wittig reaction initially proceeds through a [2+2] cycloaddition between the aldehyde and ylide forming an oxaphosphetane ring (Scheme 2.20). The ring then degrades via reverse [2 + 2] cycloaddition to give the desired alkene and triphenylphosphine oxide (Scheme 2.20).[188] Formation of the P=O bond provides an enthalpic driving force for this reaction. This reaction proceeds as a stabilised Wittig as the electron withdrawing ester within ylide **2.44** delocalises the charge of the carbanion. This stabilises the intermediate, allowing for formation of the thermodynamically favourable (*E*)-alkene instead of the kinetic (*Z*)-alkene.
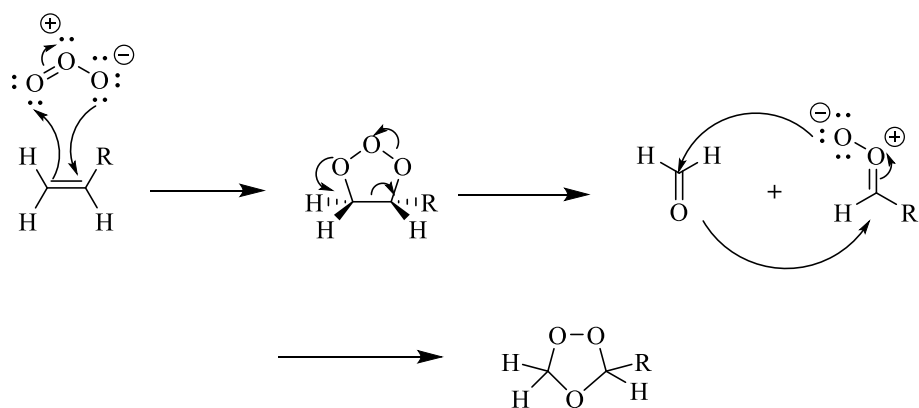
Scheme 2.18. Ozonolysis, showing formation of the unstable primary melozonide, subsequent degradation and formation of the 1,2,3-trioxolane.

The multi-step ozonolysis and Wittig reaction produced the desired *t*-butyl ester, albeit in poor yield (25 %) (Scheme 2.21). Unfortunately, the yield observed in this study is substantially worse than those previously observed in the literature. Jung *et al.* found a good yield of 74 %.[163] The poor yield could be explained by the difficulty in the monitoring of the ozonolysis reaction and the formation of the 1,2,4-trioxolane. The only way of monitoring the ozonolysis reaction is the observation of a colour change of the solution from colourless to a light blue. This may be a cause of the poor yields of the aldehyde **2.43**.

2.43
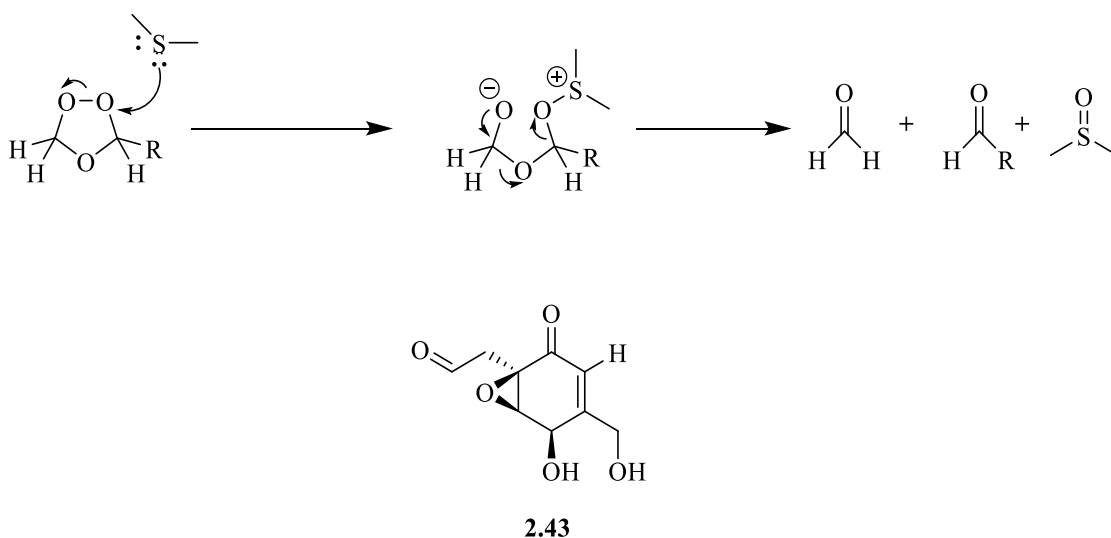
Scheme 2.19. Reductive workup of ozonolysis with dimethylsulfide, forming formaldehyde, the desired aldehyde and DMSO. Desired aldehyde in this application **2.43**
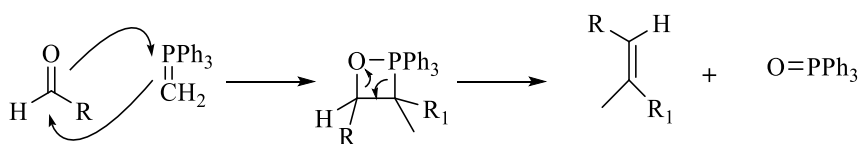
Scheme 2.20. Mechanism for a Wittig olefination showing [2 + 2] addition, and subsequent degradation of the oxaphosphetane forming the olefin and triphenylphosphine oxide

The above synthetic transformations yielded the target compound **1.62** and provided a scaffold for the production of a range of unique analogues. Furthermore, this synthetic route provides several starting materials for the production of a variety of analogues.
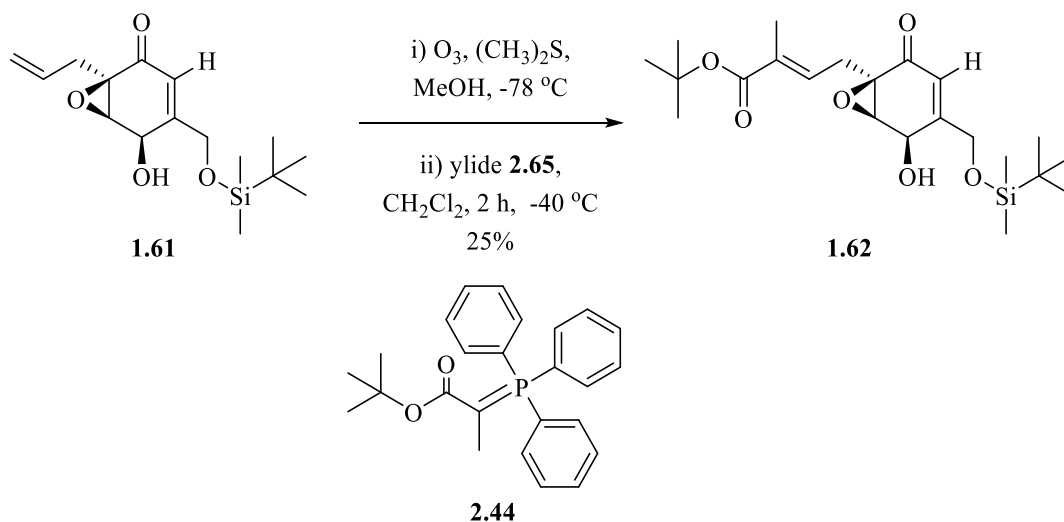
Scheme 2.21. The ozonolysis and Wittig procedure producing **1.62** and the stabilised ylide **2.44**

2.4 The synthesis of enantiomerically pure (-)-1.63

2.4.1 The synthetic target

With the successful production of **1.62**, modification of the route was carried out to enable the production of unique ambuic acid analogues. It was initially decided to modify the procedure outlined above to enantioselectively produce the (-)-analogue **1.63** (Figure 2.12).[163] **1.63** will be produced to determine whether stereochemistry has an effect on the biological activity of staphylococcal *agr*-mediated quorum sensing activity.
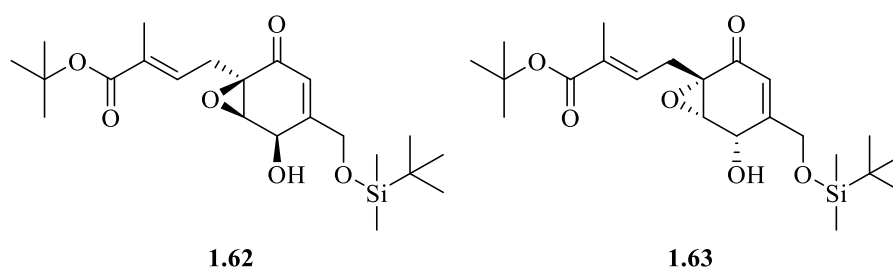
Figure 2.12. The synthetic target, the (-)-analogue **1.63**.

2.4.2 Synthesis of target 1.63

Broadly, the synthetic route to **1.63** is similar to that of **1.62** with the main modification to the procedure being that of alteration of the highly enantioselective Diels-Alder reaction. The reaction was modified by utilising (*S*)-(-)-*o*-tolyl-CBS oxazaborolidene **1.68** instead of (*R*)-(+)-*o*-tolyl-CBS oxazaborolidene **1.56** catalyst (Scheme 2.22).

Utilisation of (*S*)-(-)-*o*-tolyl-CBS oxazaborolidene catalyst **1.68** allows for formation of the desired (-)-adduct **1.67** in reasonable yield (56%) with good enantioselectivity observed, $[\alpha]_D^{25} = +81.4$. The (+)-adduct has a value of $[\alpha]_D^{25} = -70.3$. Steric occlusion of the suprafacial π-orbitals of the reaction substrate **1.54** by the bulky tolyl group within (*S*)-(-)-*o*-tolyl-CBS oxazaborolidene **1.68** aids in the enantioselectivity of this reaction (Figure 2.13).
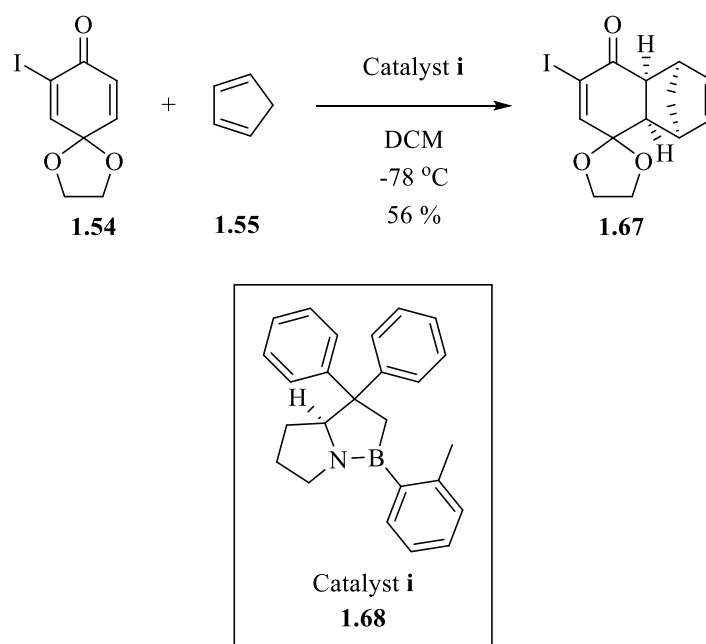
Scheme 2.22. The enantioselective Diels-Alder reaction selectively forming the (-)-adduct **1.67** and the chiral catalyst **1.63**.

With the successful production of (-) Diels-Alder adduct **1.67**, the remainder of the synthesis of target **1.63** proceeded in a similar manner to the production of **1.62**, as outlined previously in this chapter.

The allyl group was installed via Stille coupling in a good yield (69%) to furnish **1.69** (Scheme 2.23). The lower ketone was then de-protected with dilute H_2SO_4 affording the dione **2.45** in an excellent yield (91%). **2.45** was then treated with H_2O_2 in the presence of Na_2CO_3 to afford the epoxide **1.70** in a good yield (76%). The primary alcohol was then installed α- to the lower ketone of **1.70** using DBU and aqueous formaldehyde to provide alcohol **1.71** in a good yield (87%, Scheme 2.23). The primary alcohol was then utilised for the reduction of the lower ketone to the desired secondary alcohol, yielding the diol **1.72** in adequate yield (57%) with good enantioselectivity, $[\alpha]_D^{25} = +43.9$. The corresponding (+)-diol **1.60** was found to have a value of $[\alpha]_D^{25} = -44.4$. The primary alcohol was then protected as a *t*-butyl-dimethyl silyl ether, affording **2.46** in a good yield (79 %). The Diels-Alder adduct was then dismantled by heating **2.46** in diphenyl ether to liberate cyclopentadiene giving quinone derivative **1.73** in poor yield (38 %, Scheme 2.23). As discussed in more detail in chapter 3, yields observed in this retro Diels-Alder reaction were often variable, with poor yields being associated with the formation of side products, potentially through thermolysis and/or oxidation. Attempts to improve this reaction are discussed in chapter 3.
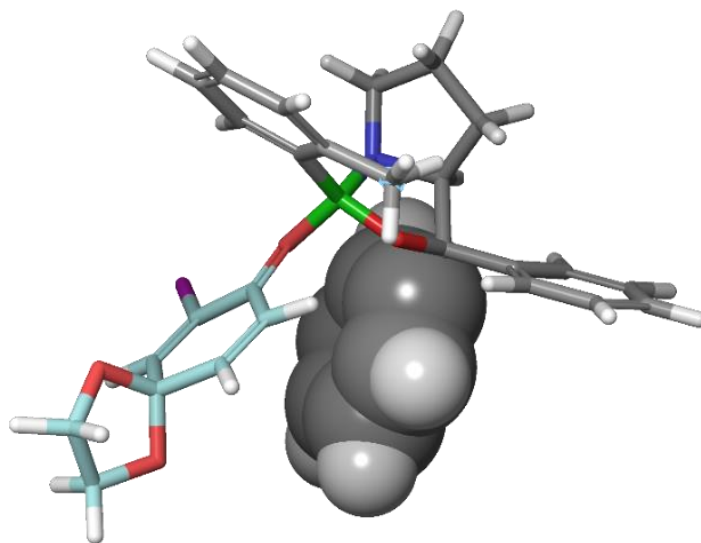
Figure 2.13. Catalytic complex formed between the activated (*S*)-(-)-*o*-tolyl-CBS oxazaborolidene **2.33** (grey) and reaction substrate, 2.9 (turquoise). Through action as a Lewis acid, the boron within the CBS catalyst can coordinate to the carbonyl, allowing for occlusion of the suprafacial π-orbitals by the bulky tolyl group (highlighted) within the catalyst. This prevents orbital alignment of the diene (cyclopentadiene) and the dienophile (reaction substrate) and favours formation of the (-)-adduct.

1.73 was taken into the two-step ozonolysis and Wittig procedure, outlined in more detail previously in this chapter, producing the target compound **1.63** in 36 % yield. The total yield for the production of **1.63** from 2-iodophenol is 0.6 % in an 11 step synthetic route (53 mg of **1.63** was produced in total). **1.63** was taken forward for biological assessment in chapter 4.
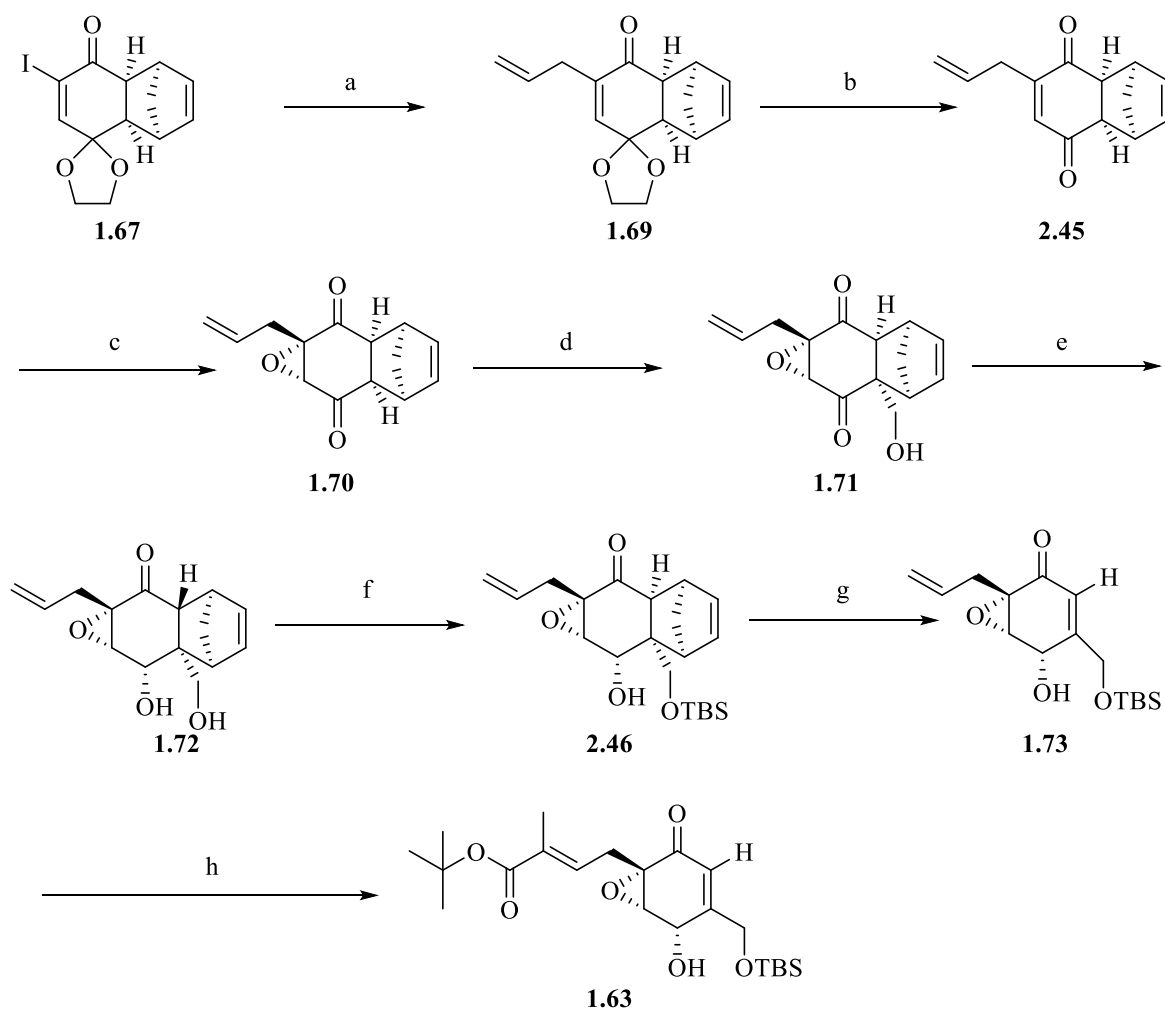
Scheme 2.23. The synthesis of target **1.63** from the Diels-Alder adduct **1.67**. (a) Pd(PPh₃)₄, allyltributyl stannane, THF, 10 min, 110 ℃, 150 W MW radiation, 69%; (b) 1 N H₂SO₄, acetone, THF, 30 min, rt., 91%; (c) 10% (w/v) Na₂CO₃, 30% (v/v non-stab.) H₂O₂, acetone, 30 min, 0 ℃, 76%; (d) 37% (w/v) aqueous formaldehyde, DBU, THF, 30 min, 0 ℃, 87%; (e) DIBAL-H, THF, 30 min, -78 ℃, 57%; (f) TBDMSCl, imidazole, DMF, 4 h, 0 ℃, 79%; (g) Ph₂O, 4 h, 230 ℃, 38%; (h) O₃, dimethylsulfide, MeOH, -78 ℃, 30 min then Ph₃P=C(Me)CO₂t-Bu, DCM, 2 h, -40 ℃, 36%.

2.5 The attempted synthesis of ether analogues of the primary alcohol

2.5.1 The Synthetic Targets

With the finding that racemate **1.52** was active against staphylococcal *agr* mediated quorum sensing activity, it was decided to produce a range of analogues of enantiomerically pure **1.62** to determine how chemical modification of the primary alcohol affects biological activity. Initial attempts of derivatisation were to synthesise a range of ether analogues [shown by general structure **1.64**, (Figure 2.14)] of the primary alcohol (protected as the *t*-butyl dimethyl silyl ether) within **1.62**. This was done as a means to explore the chemical space around the primary alcohol of **1.52** and the silyl ether of **1.62**.
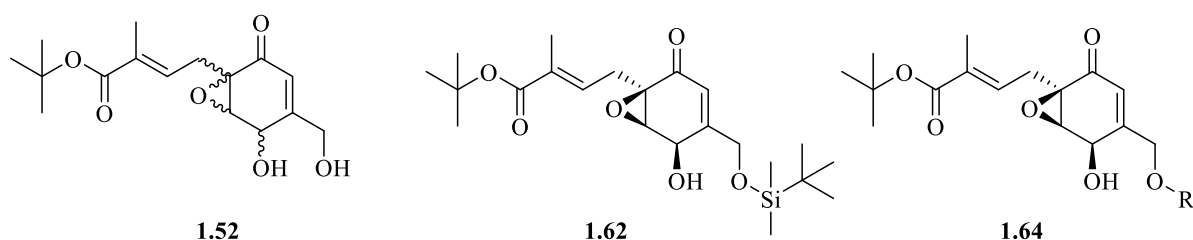
Figure 2.14. Racemate **1.52**, enantiomerically pure '(+)' enantiomer **1.62** and general structure of the ether analogue synthetic target **1.64**.

2.5.2 Synthesis- Attempted Williamson Etherification

Initial attempts at the production of the asymmetric ether employed a modified Williamson ether synthesis procedure, one of the oldest named synthetic transformations in organic chemistry.[189]

Compound **1.60** was initially chosen as the substrate for the production of a range of ether analogues as it is simpler and less time consuming to produce than quinolone derivative **1.62** (Figure 2.15).

1.60
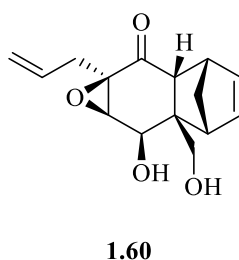
Figure 2.15. The intermediate **1.60** used as the reaction substrate for Williamson ether synthesis.
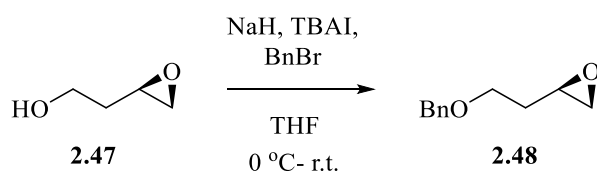
Scheme 2.24. The Liang et al procedure for the production of an asymmetric ether.[190]

Initial conditions tested were based on a modified literature procedure from Liang *et al.* (Scheme 2.24), utilised in their synthesis of both 11-α-methoxycurvularin and 11-β-methoxycurvularin.[190] Alcohol **2.47** is treated with NaH and tetra-*n*-butyl ammonium iodide (TBAI) as a phase transition catalyst to install benzyl ether, giving **2.48** (Scheme 2.24)**.** Their procedure allows for near quantitative formation of a benzyl ether in the presence of an epoxide, thus, it was decided to use their conditions for this application to preserve the epoxide.

The key intermediate **1.60** was stirred with NaH to deprotonate the primary alcohol, in THF in the presence of the phase transition catalyst TBAI and bromomethyl cyclohexane in order to generate the desired asymmetric ether **2.51** (Scheme 2.25, Table 2.1 condition 1).
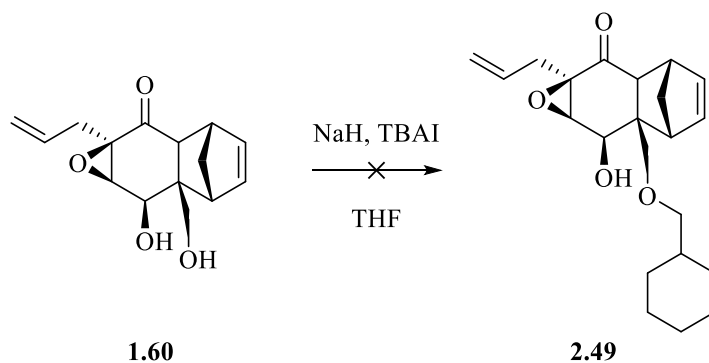
Scheme 2.25. Attempted synthesis of the methyl cyclohexyl asymmetric ether analogue **2.49** from diol **1.60**.

Unfortunately, the modified condition from Liang *et al.* failed to produce the desired product **2.49**, with no reaction occurring (by change in TLC) even after some 2 days of stirring at ambient temperature.

Table 2.1. Conditions trialled for the synthesis of desired asymmetric ether **2.75**

Condition	Solvent	Base	Other
1	THF	Sodium hydride (excess)	TBAI
2	THF	Sodium hydride (excess)	15-Crown-5 ether (1 eq.)
3	THF	Potassium *t*-butoxide (excess)	N/A

The poor reaction outcome could potentially be attributed to the primary alcohol being sterically hindered. Thus, modification of the procedure was required. Aspinall *et al.* report the improvement of etherification of sterically hindered alcohols, when sodium hydride was used as base, through the use of 15-crown-5 ether **2.50** (Figure 2.16).[191] They stated that using traditional methods, utilising sodium hydride as base, often leads to outcomes which are 'unacceptable' in terms of yield and timescale.[191] Furthermore, these methods often necessitate the use of polar aprotic solvents such as DMF or DMSO, which are both problematic in terms of toxicity and ease of removal.[191] Therefore, 15-crown-5 ether was utilised for this application to try and improve the reaction outcome.

2.50
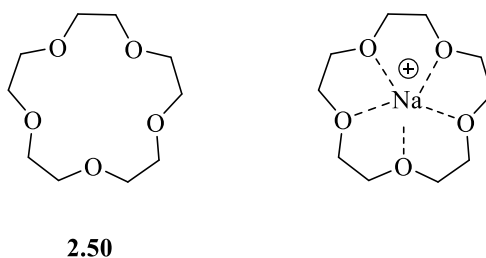
Figure 2.16. 15-Crown-5 ether **2.50** and 15-crown-5 ether chelating a sodium cation.

15-Crown-5 ether chelates the sodium cation, aiding its solvation and increasing the availability of hydride for deprotonation (Figure 2.16). Additionally, coordination of the sodium cation would also prevent it from interacting with the alkoxide which would weaken it as a nucleophile.

Starting material **1.60** was stirred with sodium hydride and 15-crown-5 ether, before the addition of bromomethylcyclohexane (Table 2.1, condition 2). Unfortunately the reaction failed to proceed despite stirring again for several days.

In a final attempt to generate the desired methyl cyclohexyl ether, the strong, non-nucleophilic base potassium *t*-butoxide was used in place of sodium hydride (Table 2.1, condition 3).

Unfortunately, this also failed to improve the reaction outcome and even after 2 days of stirring, no change in the reaction mixture was observed by TLC.

With the failure of these conditions to produce the desired ether **2.49**, it was postulated there may be a factor adversely affecting the reaction. One possibility that might account for the poor reaction outcome could be the secondary alcohol potentially acting as a hydrogen bond donor and bonding with the alkoxide, reducing its nucleophilicity **2.51** (Figure 2.17).
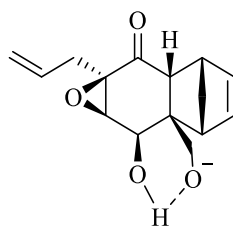
2.51

Figure 2.17. Potential six-membered ring formed between the alkoxide and the adjacent secondary alcohol **2.51**

To see if this was indeed the case, it was decided to utilise the dione **1.59** as the reaction substrate as the ketone is unable to act as a hydrogen bond donor. Thus, dione **1.59** was treated as previous (with sodium hydride, 15-crown-5 ether and bromomethylcyclohexane in THF) to form the ether **2.52**. *Post*-workup, ^{1}H-NMR and LC/MS analysis revealed that the observed product was a diastereoisomeric mixture of the diol **2.53** (Scheme 2.26), indicative of sodium hydride-mediated reduction of the ketones. With the failure of Williamson-like etherification, an alternate synthetic strategy was required.
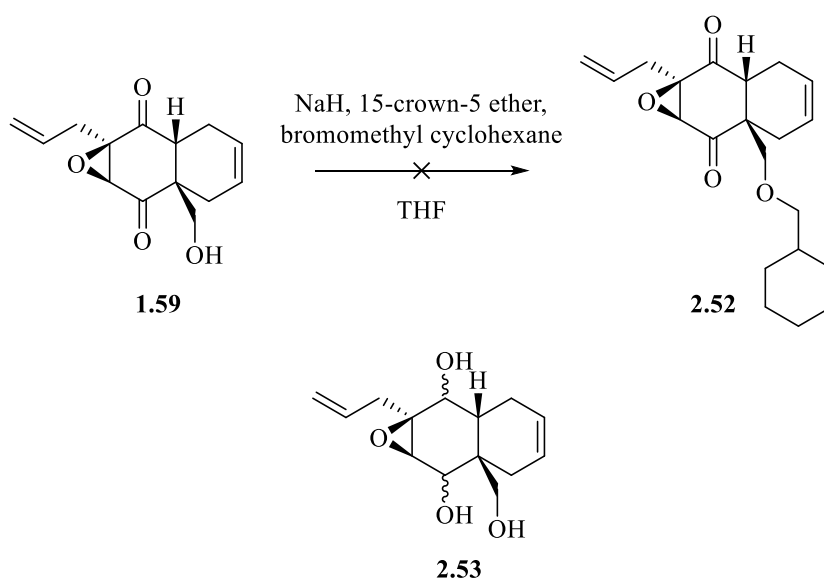
Scheme 2.26. The attempted synthesis of methyl cyclohexyl ether **2.52** from dione starting material **1.59**. Reaction formed undesired diastereoisomeric mix of diol **2.53**

2.5.3 Attempted Modification of Hydroxymethylation Step to Install the Ether Directly

With the difficulties experienced in the production of an ether via a modified Williamson ether synthesis, it was decided to attempt to install the ether directly through modification of the hydroxymethylation procedure.
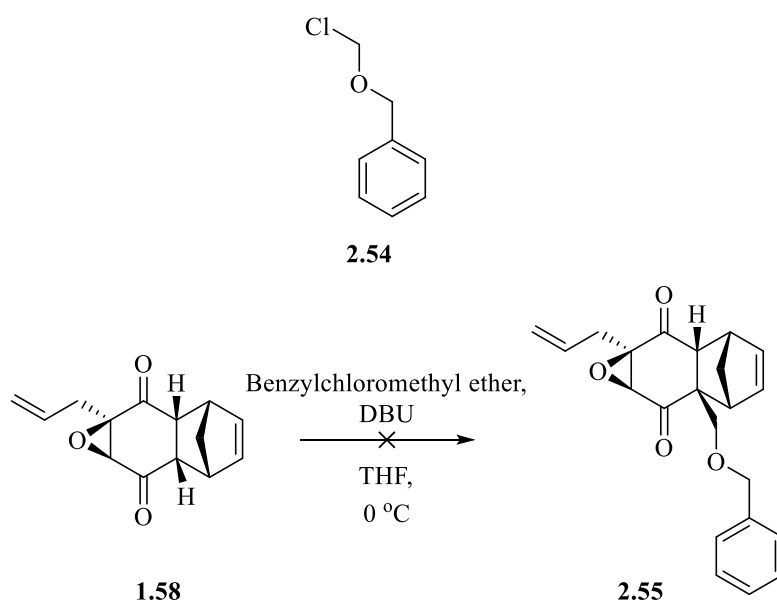
Scheme 2.27. Benzylchloromethyl ether **2.54** and the attempted installation of the benzyl ether to yield **2.55**.

Hence, the dione **1.58** was treated with DBU followed by 1.5 equivalents of benzylchloromethyl ether **2.54** in THF at 0 ℃ (Scheme 2.27). It was hoped that the carbanion formed when **1.58** is treated with DBU would act as a nucleophile and attack the δ-positive carbon adjacent to the chlorine within **2.54**.

Initially, the reaction was attempted at 0 ℃ with gradual warming to ambient temperature. However, Thin-layer chromatography (TLC) failed to show any change in the reaction mixture. The reaction was subsequently heated to 90 ℃ with 150 W microwave radiation for 30 minutes. Unfortunately, this failed to facilitate the formation of **2.55**, thus it was heated again for a further 90 minutes. No change was observed by TLC or LC-MS. The failure of these conditions could be due to steric occlusion of the carbanion, caused by the adduct and/or the size of the benzylchloromethyl ether.

2.5.4 Conversion of the Primary Alcohol to a Leaving Group

With the failure of above model studies, an alternative strategy was required. The conversion of the primary alcohol to a leaving group, allowing for nucleophilic substitution with an alcohol (forming the desired ether) was deemed to be the next suitable strategy.

Initially, it was decided to produce propyl ether **2.56** (to be converted to the final compound) from dione **1.59** in a one pot reaction with a mesylate intermediate **2.57** (Figure 2.18).
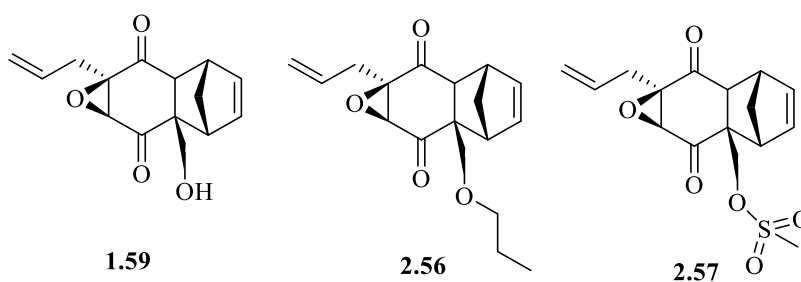
Figure 2.18. Dione **1.59**, the desired propyl ether **2.56** and the mesylate intermediate **2.57**

Hence, the intermediate **1.59** was treated with 1.5 equivalents of Et$_3$N and mesyl chloride for 2 h at -78 ℃ using a procedure modified from the literature (Table 2.2, condition 1).[192] After stirring, an excess of anhydrous propan-1-ol was added and the reaction mixture was stirred for 72 h at ambient temperature. After stirring for 72 h, TLC analysis showed a change in

reaction mixture and the potential product was purified. However upon analysis by ^{1}H NMR, this compound was found to be the mesylate **2.57**.

Thus, the mesylate **2.59** was treated with an excess of anhydrous propan-1-ol, which had previously been treated with sodium hydride to generate the alkoxide nucleophile in an attempt to aid the reaction. Unfortunately, after further stirring, LC-MS analysis failed to show any change in the reaction mixture.

Table 2.2. Conditions tested to convert the primary alcohol into a good leaving group

Condition	Solvent	Temperature (^{o}C)	Reagents
1	DCM	-78	Et$_3$N (1.5 eq.), mesyl chloride (1.5 eq.), propan-1-ol (excess)
2	DCM	75, 150 W microwave radiation	Imidazole (1.1 eq.), iodine (1.1 eq.), triphenylphosphine (1.1 eq.)

Due to the failure of production of an asymmetric propyl ether with a mesylate intermediate, it was decided to convert the primary alcohol into an iodide, **2.58** (Table 2.2, condition 2). This was attempted using an Appel reaction (Figure 2.19).

A

B

2.58
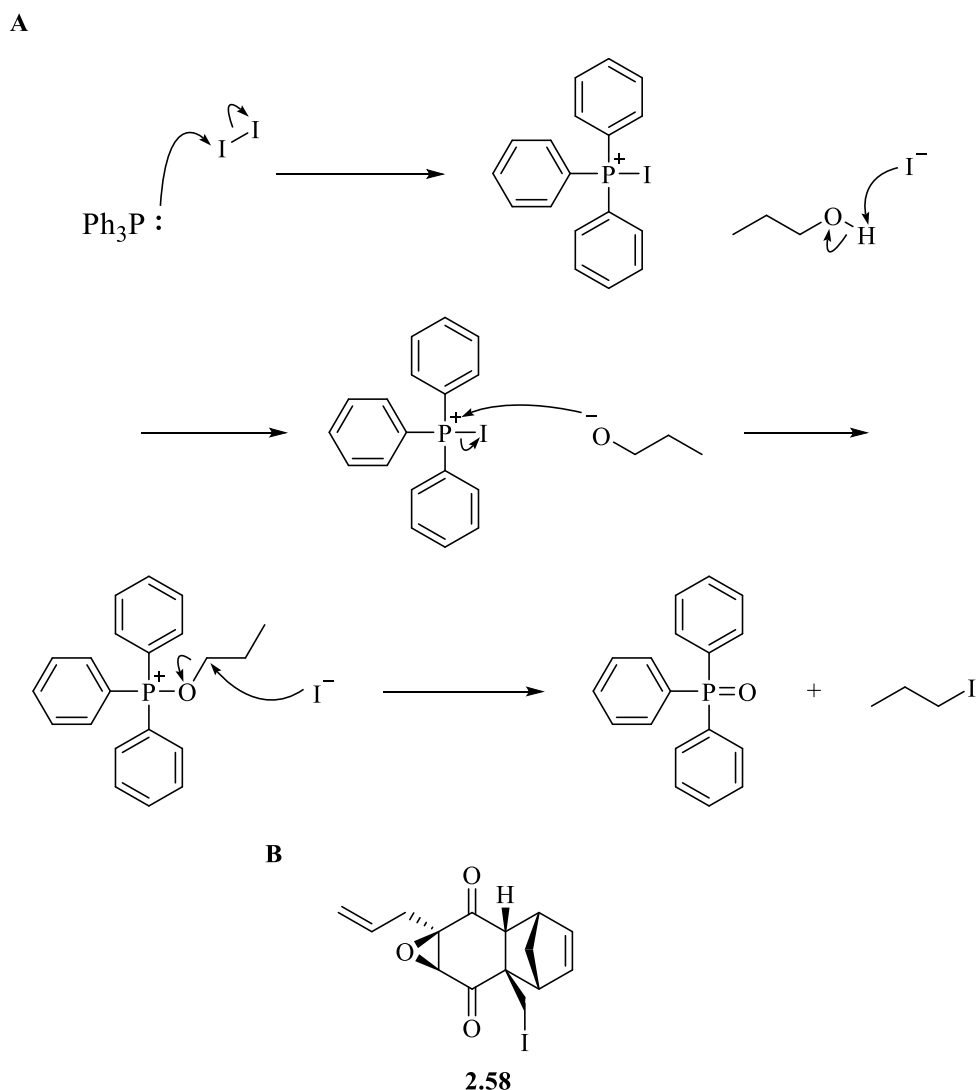
Figure 2.19. (**A**) Mechanism of the Appel reaction, for the conversion of an alcohol to an iodide. The formation of the strong P=O bond provides an enthalpic driving force for the reaction. (**B**) The target iodide **2.58**

The Appel reaction is the conversion of an alcohol to a halide using triphenylphosphine and a source of halide, for example carbon tetrachloride or elemental iodine (Figure 2.19).[193-194] Initial formation of the phosphonium salt and deprotonation of the alcohol allows for subsequent displacement of the iodide by the generated alkoxide (Figure 2.19). Through an S_N2 mechanism, the iodo ion can react to form the alkyl halide and triphenylphosphine oxide, the strong P=O bond formation providing an enthalpic driving force for the reaction (Figure 2.19).

A procedure was adapted from the literature (Table 2.2, condition 2) to produce the iodide.[195] Alcohol **1.59** was stirred with imidazole (acting as a sink for the HI generated in the reaction, forming the imidazolium iodide), triphenylphosphine and iodine (all 1.1 eq.) and the reaction

mixture was stirred overnight.[195] Unfortunately, no reaction was observed when the reaction was monitored by TLC. Thus, the reaction mixture was heated for 2 h at 75 ºC with 150 W microwave radiation. Heating the reaction mixture caused the formation of triphenylphosphine oxide precipitate, an indicator that the reaction had proceeded. Furthermore a change in the reaction mixture was observed by TLC. Thus, workup and purification of the reaction mixture was carried out. Unfortunately, it was not possible to purify the iodide, it may have degraded during silica gel chromatography.

With the exhaustive testing of numerous synthetic strategies and conditions to produce a range of asymmetric ether analogues and the failure of these conditions, it was decided to discontinue the production of these analogues.

2.6 Production of silyl ether analogues of the primary alcohol

2.6.1. The synthetic targets

With the failure to produce ether analogues, it was decided to produce a range of silyl ether analogues of the primary alcohol **1.65** (Figure 2.20). Silyl ether analogues were chosen due to the facile nature of their installation.[182]
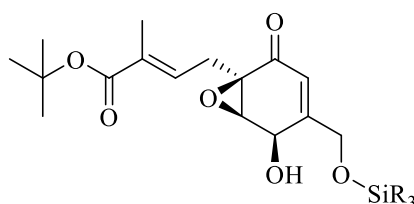
1.65

Figure 2.20. The general structure of a silyl ether synthetic target **1.65**.

The incorporation of silicon into small molecular inhibitors is uncommon in medicinal chemistry.[196-197] As of 2018, no drugs containing silicon were approved in Western Europe or the United States.[197] The only example of an approved drug containing silicon is silabolin **2.59** (Figure 2.21) which is used in Eastern Europe.[196-197] Silabolin is a steroid used for the treatment of muscle wasting disorders which is administered as a trimethyl silyl ether pro-drug.[196-197]
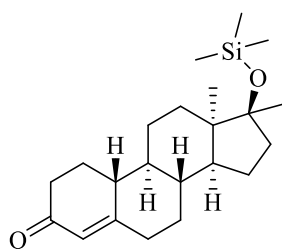
2.59

Figure 2.21. The trimethyl silyl ether pro-drug silabolin.**2.59**

Silyl ethers are typically used as protecting groups and as such have well-defined chemical properties.[182, 198] The Si-O bond is thermodynamically stable, but under acidic and aqueous conditions proves kinetically labile.[198] The steric environment around the silicon atom dictates the lability of the silyl ether. [198] This property is useful in the design of prodrugs such as silabolin, **2.59** as well as in synthetic strategies for the selective protection of alcohols.[198] The trimethyl silyl ether within silabolin is labile under mildly acidic conditions, whereas more

complex silyl ethers such as *t*-butyldimethyl silyl ethers are more resistant to hydrolysis under both mildly basic and acidic conditions.[199]

The silyl ethers, whilst rare in final compounds of interest within the literature, have been used previously to improve the clinical potential of withaferin A **2.60**, which is cytotoxic against several ovarian cancer cell lines (Figure 2.22).[200] Perestelo *et al.* found the incorporation of silyl ethers in **2.61** enhances the pharmacological properties of withaferin A.[200] They noted that slight modifications on the silyl ether substituent had substantial effects on the compound activity.[200] For example, the incorporation of a triethyl silyl ether gave improved cytotoxic activity against the human cisplatin resistant ovarian cancer cell line A2780/CP70 when compared to the free alcohol **2.60** with IC_{50} values of 20 nM and 32 nM respectively for the silyl ether and free alcohol.[200]
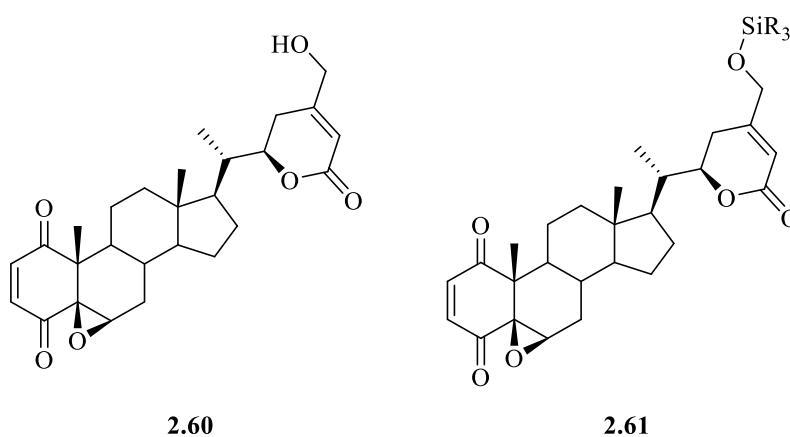
Figure 2.22. Withaferin A **2.60** and general structure of a silyl ether analogue **2.61** reported by Perestelo *et al.*.[200]

The incorporation of silicon into inhibitors can provide the resulting compound with unique medicinal chemical properties.[196, 198, 200] Silicon containing compounds have increased lipophilicity which could enhance cell penetration.[198] Furthermore, silicon is more electropositive than carbon, potentially generating an electron deficient centre within the compound.[196, 198] Within the target structures here (**1.65**), the incorporation of silicon generates an ether with increased polarity compared to an ether with a C-O-C bond. This may prove interesting in terms of compound activity.

The previous utilisation of silyl ethers to improve the activity of withaferin A **2.60** and the interesting medicinal chemical properties imparted by the inclusion of silicon make this an

interesting and novel approach for the design and synthesis of a range of analogues. Thus, the synthesis of a focussed range of unique silyl ether analogues will be attempted herein (Figure 2.23). These analogues will incorporate a range of chemical functionalities, including short linear and branched chain alkanes as well as aromatics (Figure 2.23). In addition, the silyl ethers were synthesised to explore the chemical space around the silyl ether of **1.62**.
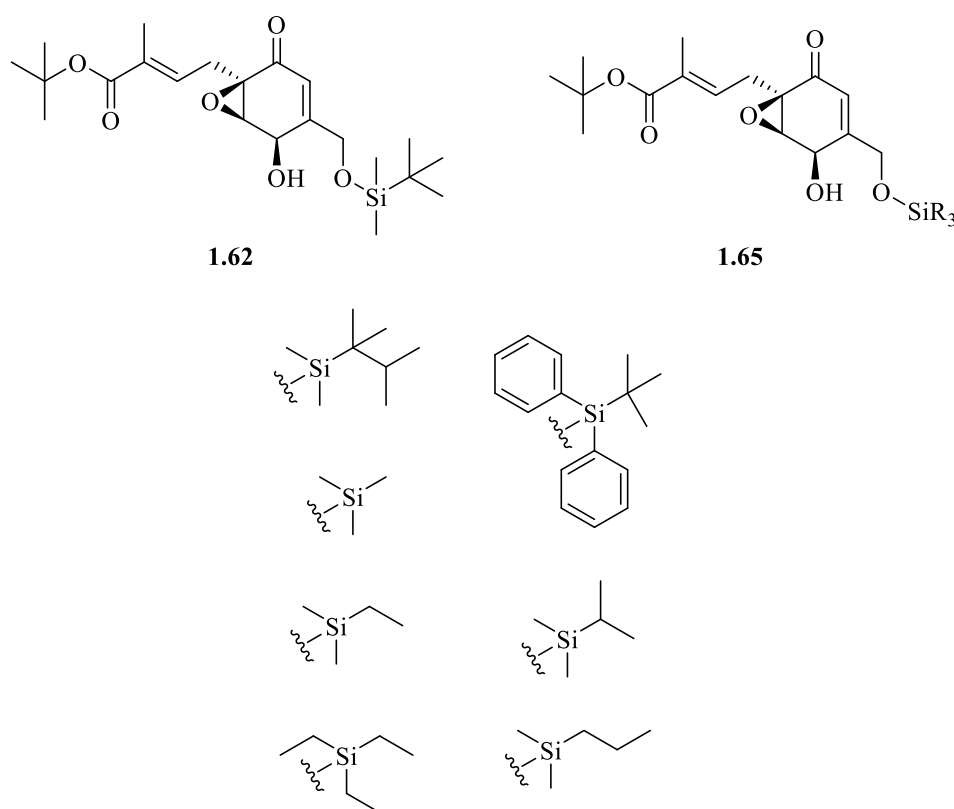
Figure 2.23. The initial silyl ether analogue **1.62** (LB151), the general target silyl ether structure **1.65** and the proposed silyl groups to be incorporated.

Furthermore, with the synthesis of enantiomerically pure **1.62** by Dr Leonardo Baldasarre, the production of further silyl ether analogues could provide useful information about the effect on biological activity of ambuic acid analogues modified at the primary alcohol.

2.6.2 The synthesis of silyl ether analogues

The synthesis of the unique silyl ether analogues broadly follows the synthesis of **1.62**, which has been outlined in detail previously in this chapter. Following the synthetic route, the *t*-butyl dimethyl silyl ether, **1.62** was first cleaved exposing the free alcohol to yield diol **1.74** (Scheme 2.28). The diol **1.74** was then treated with a silyl chloride in the presence of imidazole to furnish the desired silyl ether analogue (Scheme 2.28).
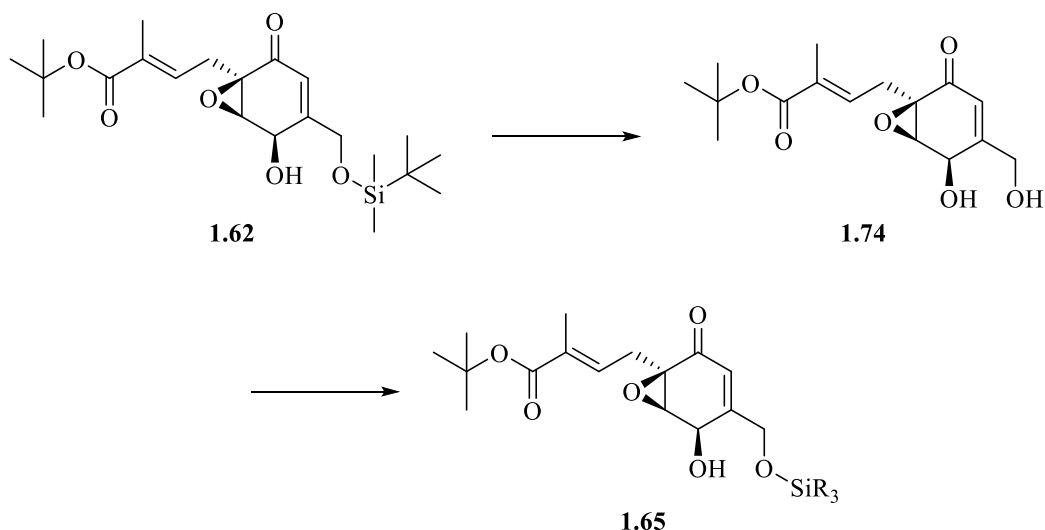
Scheme 2.28. Proposed synthetic route to silyl ether analogues. Cleavage of silyl ether of **1.62** followed by subsequent reaction to form desired silyl ether.

Initial attempts at deprotection of the TBS-protected primary alcohol utilised 2 equivalents of tetra-*n*-butyl ammonium fluoride (TBAF) (Table 2.3, condition 1). TBAF is a source of the fluoride ion which can attack the electron deficient silicon atom within **1.62** cleaving the silyl ether. With 4 h stirring at 0 ºC, TLC analysis confirmed consumption of the starting material and the formation of a more polar product, indicative of the formation of the desired diol **1.74**. Unfortunately, following purification by silica gel chromatography, the diol **1.74** was obtained in a low yield of 37%. For the production of a range of analogues, an efficient deprotection method is required as the production of the substrate for the reaction **1.62** requires a significant investment of both reagents and time. To avoid wasting of reagents, the deprotection method needs to be as efficient as possible.
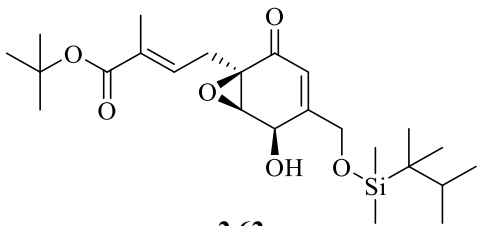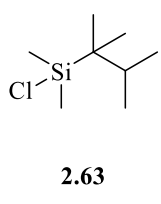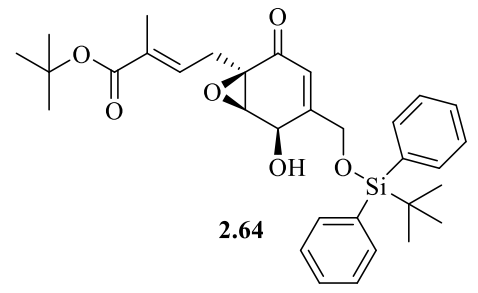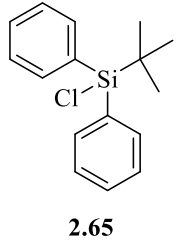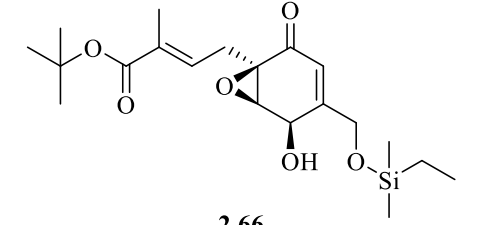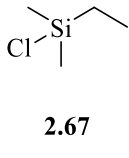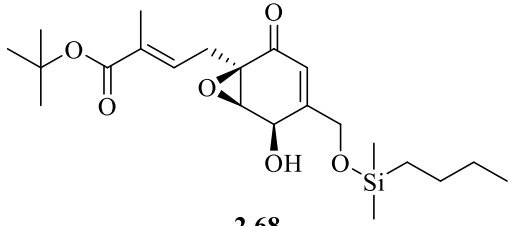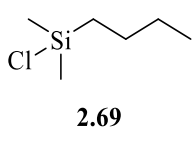
Table 2.3. Conditions for the cleavage of the t-butyl dimethyl silyl ether within **1.62**

Condition	Solvent	Reagents	Yield (%)
1	THF	2 eq. TBAF	37
2	-	1:2:1 mix of diethyl ether, acetic acid and dH₂O	54

Thus, **1.62** was treated with a 1:2:1 mixture of diethyl ether, acetic acid and dH$_2$O to dismantle the ether (Table 2.3, condition 2). **1.62** was stirred in the mixture overnight, which produced the desired diol **1.74** in an improved yield (54%).

With a more efficient production of diol, the subsequent step is the installation of the silyl ether. This was carried out using a standard procedure for installing silyl ethers. Thus, the diol **1.74** was first stirred with imidazole in DMF before addition of the relevant silyl chloride (Table 2.4).

Table 2.4. The silyl chlorides used to produce the final silyl ether analogues and their yields

Target Compound	Silyl Chloride	Yield (%)
2.62	**2.63**	23 (4 mg)
2.64	**2.65**	6 (1.5 mg)
2.66	**2.67**	-
2.68	**2.69**	-

Upon exposure of the diol **1.74** to dimethylthexyl silyl chloride **2.63** the dimethylthexyl silyl ether **2.62** was obtained in a low yield (23 %). In contrast, the production of the *t*-butyldiphenyl silyl ether proved more challenging, with a yield of 6 % of the desired product **2.64** (Table 2.4). This poor yield could be attributed to the steric hindrance incurred by the two bulky phenyl

groups within silyl chloride **2.65**. The amount of compound *t*-butyl diphenyl silyl ether **2.64** generated was insufficient to fully characterise by NMR.

The production of ethyl dimethyl and *n*-butyl dimethyl silyl ethers proved more problematic (**2.66** and **2.68**, respectively) (Table 2.4). Upon reaction of diol **1.74** with the appropriate silyl chloride (either **2.67** or **2.69**), no change in reaction mixture was observed by either LC-MS or TLC.

With the failure of the reaction utilising imidazole as the base, it was decided to investigate whether changing the base would improve the reaction outcome. Thus, 2,6-lutidine was used as the base for the reaction in an attempt to form the desired *n*-butyldimethyl silyl ether **2.68**. This again failed to cause a change in reaction mixture. Likewise, in an attempt to form the ethyldimethyl silyl ether, 2,6-lutidene was again used to try and aid formation of the product **2.70**, again, no change was observed. Thus, pyridine was added to the reaction mixture, which again failed to cause a change in the reaction mixture even with stirring overnight.

With the failure of these reactions, it was decided to discontinue with this approach of producing analogues. The dimethyl thexyl silyl chloride **2.62** (Figure 2.24) was taken forward for characterisation of anti-virulence activity, described in chapter 4.

2.62
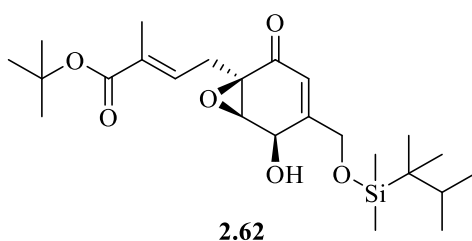
Figure 2.24. The synthesised silyl ether analogue **2.62** to be taken forward for biological testing

2.7 Ketal analogues

2.7.1 The synthetic targets

The production of several ketal analogues, cross-linking the diol of **1.74**, may provide some valuable pharmacological data about the anti-virulence activity of ambuic acid and the synthetic analogues. Firstly replacement of the alcohols, with two ethers, which comprise the ketal may yield some interesting information regarding the inhibition of staphylococcal *agr*-mediated quorum sensing. Secondly, the formation of a cyclic ketal would impart a level of rigidity within the structure of the modified compound, which may alter compound activity.

A family of drugs containing a ketal moiety is the azole anti-fungals, including ketoconazole **2.70** (Figure 2.25). Ketoconazole **2.70** is a broad spectrum anti-fungal known to inhibit the production of steroids, required for correct fungal membrane synthesis.[201] Ketoconazole **2.70** can be used for oral treatment of both superficial and deeper fungal infections.[202] In addition, ketoconazole is also used for the treatment of systemic *Candida albicans* infection (candidiasis) which can prove fatal.[202-203]
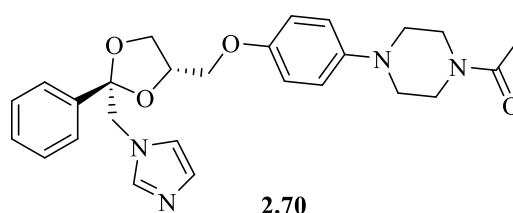
Figure 2.25. The azole anti-fungal drug ketoconazole **2.70**

A further example of a drug molecule containing a ketal moiety is topiramate **2.71** (Figure 2.26). **2.71** is widely used for the treatment of epilepsy and migranes.[204-205] In the treatment of epilepsy, **2.71** is believed to function through a number of modes of action, including inhibition of carbonic anhydrase and increasing the frequency of opening of GABA-mediated chloride ion channels.[206-207] Compound **2.71** is a fructose derivative, initially synthesised in a study to produce compounds for the treatment of hypoglycaemia.[204] It was found that **2.71** had no direct effect on blood sugar levels however, it was found to have efficacy against several types of human seizures.[204] The ketals within **2.71** are known to enhance the central-nervous system uptake of the compound through masking of the hydrophilic hydroxyl groups within the fructose ring, leading to a bioavailability of ~80%.[204, 208]
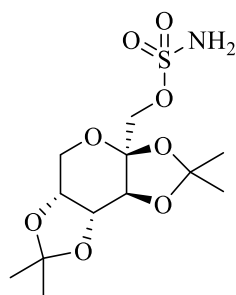
2.71

Figure 2.26. The known anti-epileptic and migrane treatment topiramate **2.71**

The previous utilisation of the ketal functionality within known drug molecules makes the synthesis of ketal analogues a viable route for the production of novel analogues of ambuic acid. It was decided to initially produce the dimethyl (**2.72**), diethyl (**2.73**) and cyclohexyl (**2.74**) ketals (Figure 2.27). As discussed in section 2.3, the diethyl **2.73** and cyclohexyl **2.74** ketals were prepared from the racemic Diels-Alder adduct **2.38**. Thus, the two ketals **2.73** and **2.74** are both racemic.
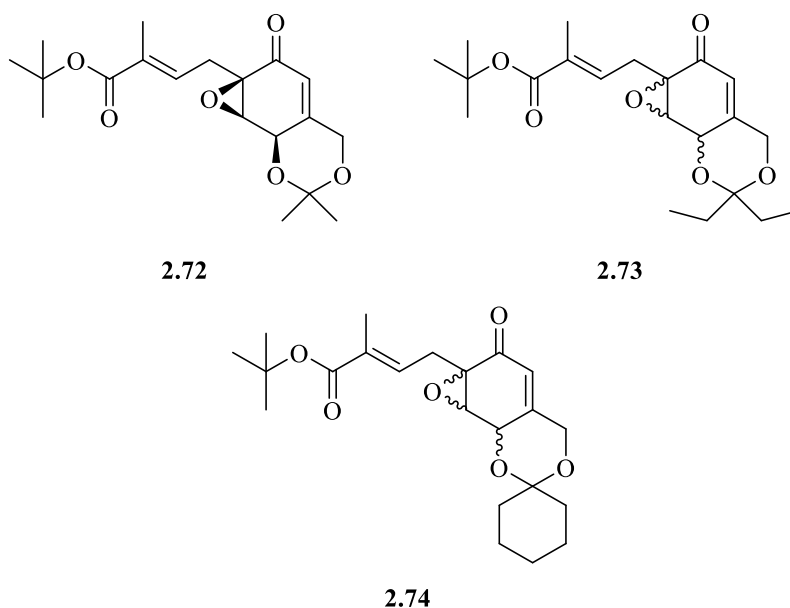
2.72   **2.73**

2.74

Figure 2.27. The structures of the target ketal compounds, dimethyl **2.72**, diethyl **2.73** and cyclohexyl **2.74**.

2.7.2 The synthesis of the ketal analogues

The synthesis of the ketal analogues follows a similar route to the production of the silyl ether analogues, as discussed above. The diol is produced by the cleavage of the *t*-butyl dimethyl

silyl ether with a 1:2:1 mix of dH$_2$O, acetic acid and diethyl ether. With production of the diol **1.74**, the ketal (given as general structure **1.66**) will be installed using a procedure modified from Jin *et al.* (Scheme 2.29 and Scheme 2.30).[209] Jin *et al*. treated **2.75** with a solution of *p*-toluenesulfonic acid (0.2 mg/ mL) in acetone at room temperature, which afforded the dimethyl ketal **2.76** in a good yield (71 %).[209]
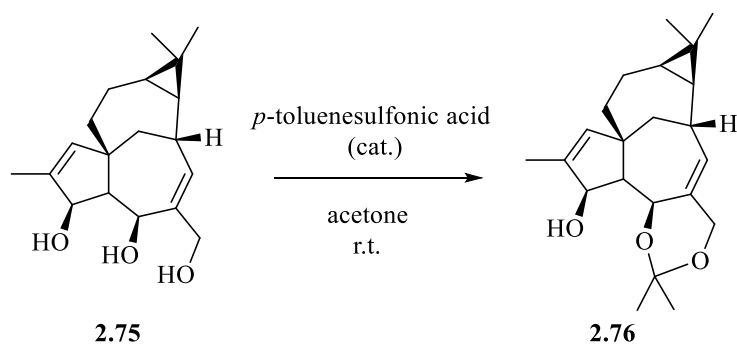
Scheme 2.29. The installation of the dimethyl ketal carried out by Jin *et al.*.[209]

The dimethyl ketal **2.72** was produced by treating diol **1.74** with acetone and catalytic *p*-toluenesulfonic acid (0.2 mg/mL) at 60 ℃. The reaction proceeded smoothly, with formation of product observed by LC-MS. The reaction was worked-up and the product was purified initially by preparative-TLC, to yield a yellow oil (6 mg, 20 % yield) with recovery of 32 % of starting material (confirmed by LC-MS) (Scheme 2.31). HPLC purification yielded 2 mg of the desired dimethyl ketal **2.72** which will be taken for biological testing in chapter 4.
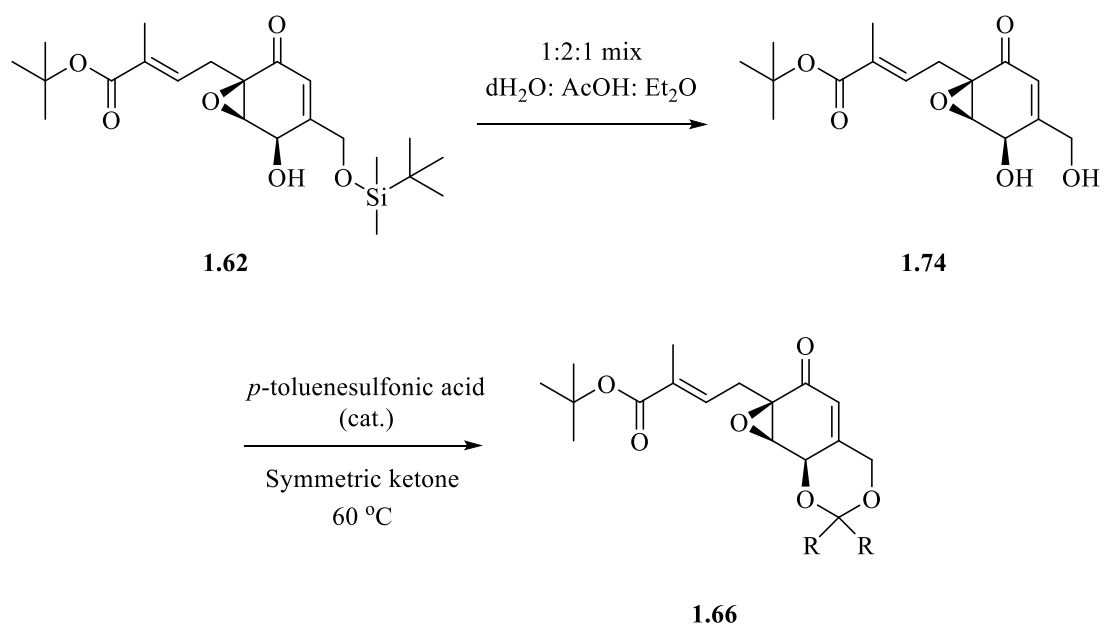
Scheme 2.30. The proposed synthetic route for the production of ketal analogues. The silyl ether of **1.62** is dismantled yielding diol **1.74**, followed by installation of the desired ketal forming **2.5** using a procedure adapted from Jin *et al.*.[209]
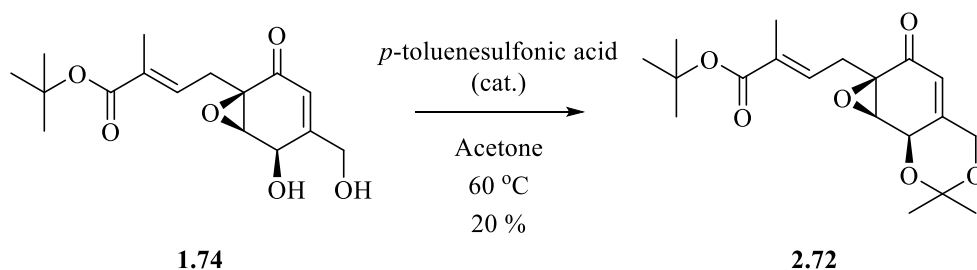
Scheme 2.31. Production of dimethyl ketal **2.72** from diol **1.74**

The racemic diethyl ketal **2.73** was to be produced in a similar manner. Thus, the racemic diol **2.77** was dissolved in a solution of *p*-toluenesulfonic acid (0.4 mg/mL) in pentan-3-one and heated to 100 ℃ (Scheme 2.32). After stirring overnight, TLC analysis of the reaction mixture indicated ~50 % conversion of starting material **2.77**, with the appearance of a spot of increased hydrophobicity. The reaction mixture was worked up and the product **2.73** was purified by column chromatography yielding 12 mg of a yellow oil (15 %, Scheme 2.32). The poor yield could be attributed to steric hindrance, potentially by pentan-3-one and/or the reaction substrate **2.77**. The diethyl ketal **2.73** was taken forward for biological testing in chapter 4.
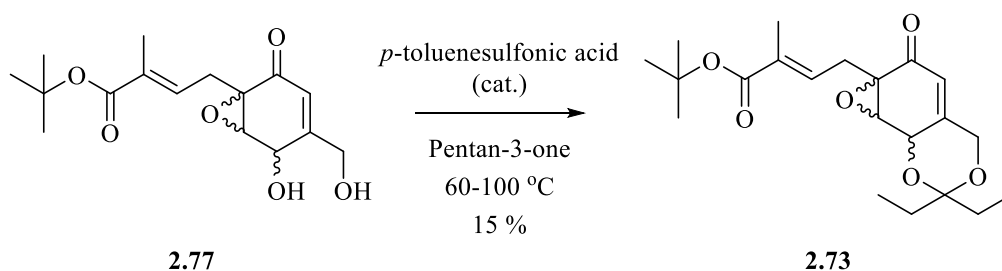
Scheme 2.32. The production of the diethyl ketal **2.73** from diol **2.77**.

The same procedure was also attempted for the installation of the cyclohexyl ketal, to give the racemic cyclohexyl ketal **2.74**. Thus, the racemic diol **2.77** was dissolved in a solution of *p*-toluenesulfonic acid (0.2 mg/mL) in cyclohexanone and heated to 60 ℃. After 2 h of heating, no change in the reaction mixture was observed by TLC and LC-MS, thus the reaction was raised to 80 ℃ for 1 h. Again, no change was observed, so the reaction was heated to 100 ℃ overnight (Scheme 2.33). No change was observed, so the reaction was worked up in order to recover the starting material. The reaction failure could be potentially attributed to steric occlusion, imparted by both starting material and cyclohexanone.

119
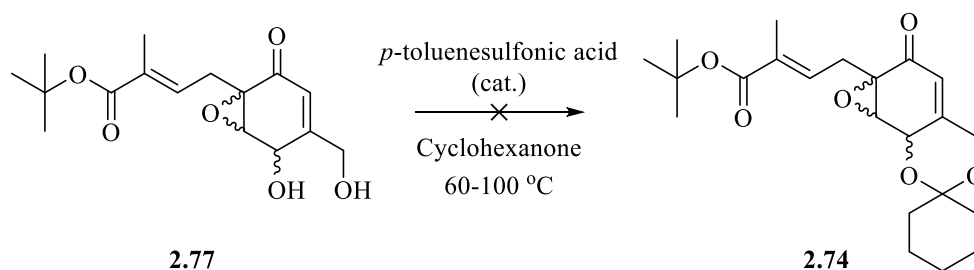
Scheme 2.33. The attempted production of cyclohexyl ketal **2.74** by cyclohexanone method

An alternative route to **2.74** was investigated. A *trans*-acetalation/ketalation route was evaluated in an attempt to improve the reaction outcome. Alternative routes to ketals have been studied previously.[210-211] Lorette *et al.* successfully produced a range of dimethyl ketals utilising 2,2-dimethoxypropane in place of acetone.[211] Thus, it was anticipated that replacement of cyclohexanone with 1,1-dimethoxycyclohexane may improve the reaction outcome, potentially facilitated by the production of the reactive oxonium ion intermediate (Scheme 2.34). Hence, the diol **2.77** was dissolved in a solution of *p*-toluenesulfonic acid (0.4 mg/ mL) in 1,1-dimethoxycyclohexane and heated to 60 ℃ for 1.5 h with stirring (Scheme 2.35). This led to a change in reaction mixture, observed by TLC and LC-MS, with ~80 % conversion of starting material. This coincided with the appearance of a spot of increased hydrophobicity when analysed by TLC. The product was purified by column chromatography yielding 30 mg of a clear oil (31 %). The cyclohexyl ketal **2.74** was taken forward for biological testing in chapter 4.
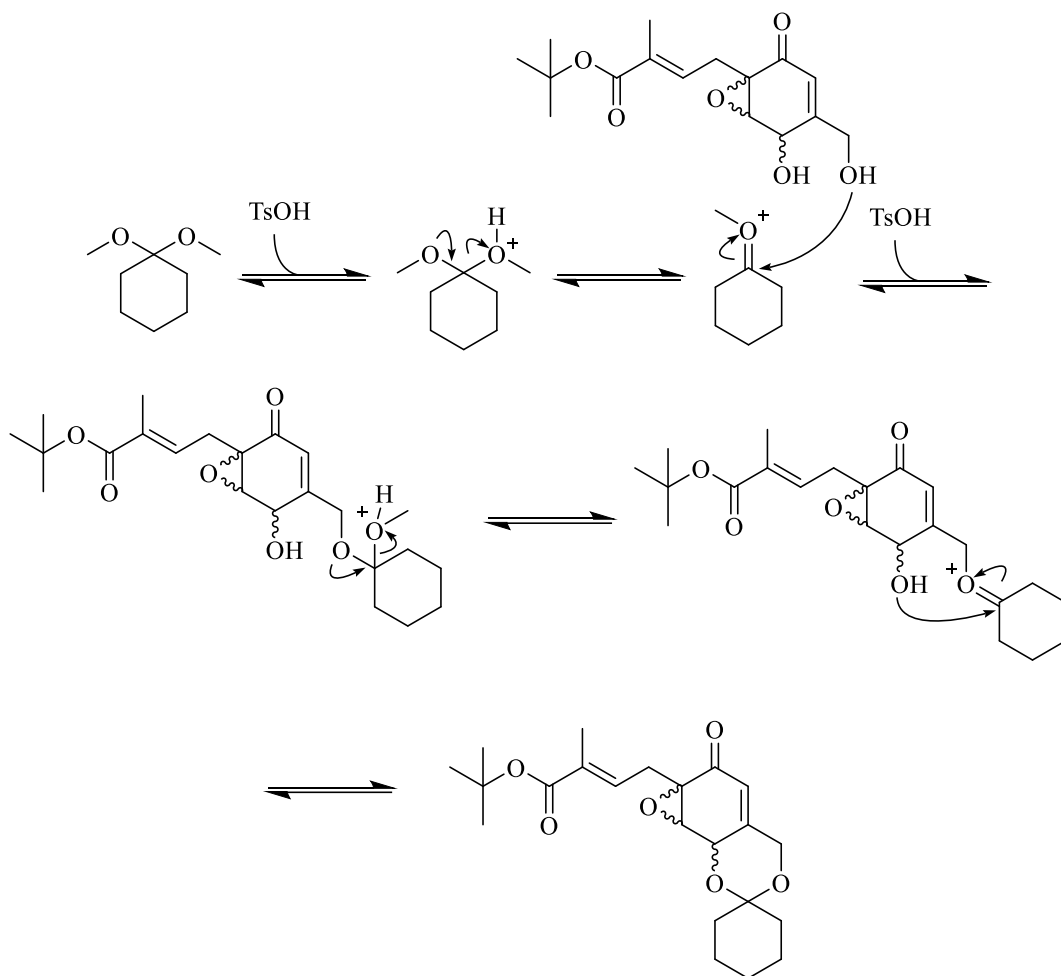
Scheme 2.34. Proposed mechanism of the *trans*-acetalation/ketalation reaction.

As described previously in this chapter, both the diethyl **2.73** and cyclohexyl **2.74** ketals were synthesised from a racemic preparation of the bromo Diels-Alder adduct **2.38** ($[\alpha]_D^{25} = 0.0$). Optical rotation values of both the diethyl **2.73** and cyclohexyl **2.74** ketals were both $[\alpha]_D^{25} = 0.0$, again indicative of the final compounds being racemic.
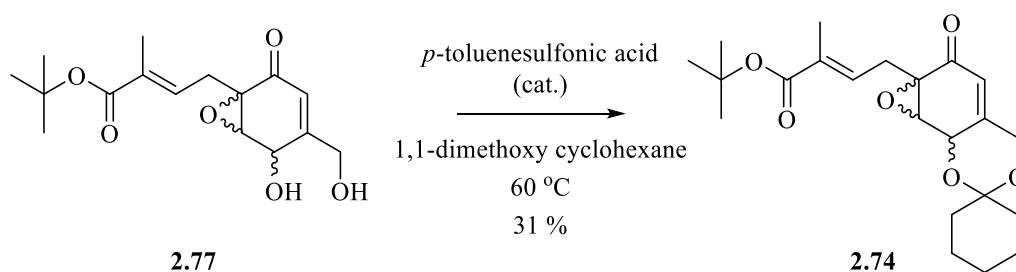
Scheme 2.35. The production of the cyclohexyl ketal **2.74** from diol **2.77** by the *trans*-acetalation/ketalation method

In addition, [1]NMR analysis of both the diethyl **2.73** and cyclohexyl **2.74** ketals revealed a diastereoisomeric mix of compounds. For the diethyl ketal **2.73**, a 1:1 ratio was observed by ^{1}H NMR (Figure 2.28) and for the cyclohexyl ketal **2.74**, a 9:1 ratio was observed (Figure 2.30).

The ^{1}H NMR of diethyl ketal **2.73** showed duplication of peaks corresponding to protons at positions 4 and 5 within the epoxycyclohexenone ring (Figure 2.28 B) each with an integral of ~0.5 each, suggesting a 1:1 mix of compounds. Additionally, duplication of the signal assigned to the α-proton within the ring was observed, with each signal again integrating to ~0.5 protons (Figure 2.28 C). Additionally, there is a signal indicative of a CH_2 at δ 2.43 (Figure 2.28 A), which through the use of COSY 2D NMR, was found to couple to the terminal CH_3 at δ 1.06 (Figure 2.29). The other CH_2 is under and adjacent to the methyl peak within the left hand of the molecule (Figure 2.28 A). The difference in chemical shift of the CH_2 peaks is indicative that they are in two different chemical environments, further suggesting a diastereomeric mix of compounds.
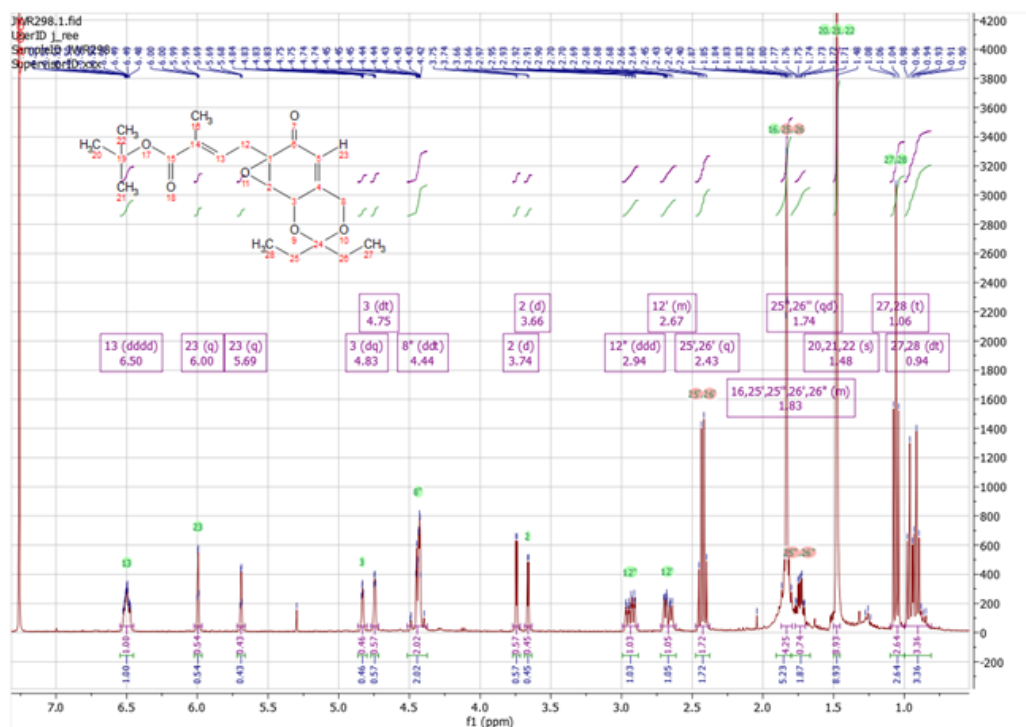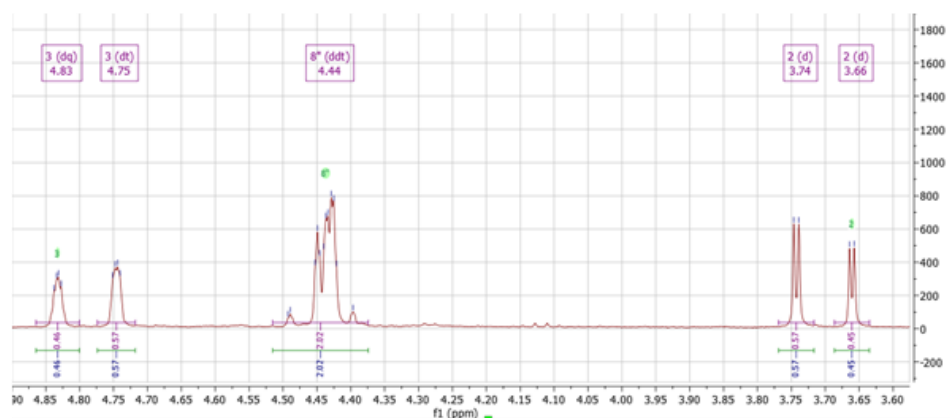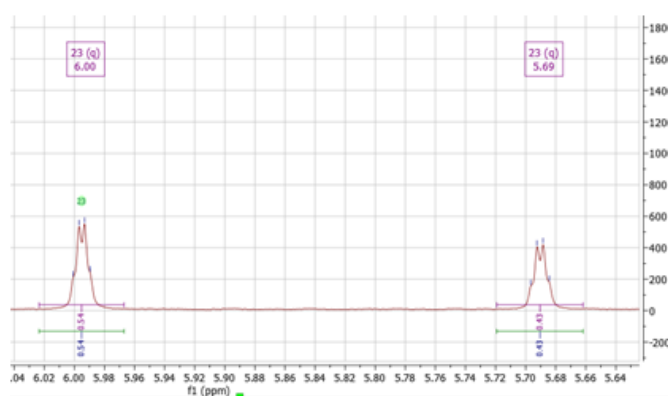
Figure 2.28. ^{1}H NMR of the diethyl ketal **2.73**. (**A**) Full ^{1}H NMR of diethyl ketal **2.73**, note the CH$_2$ at 2.43 ppm, indicative of one of the CH$_2$ moieties within the diethyl ketal. (**B**) Magnified region of ^{1}H NMR showing the duplication of signals corresponding to the protons within the epoxy cyclohexene ring in ~1:1 ratio, indicative of a 1:1 mixture. (**C**) Magnified region of ^{1}H NMR showing the duplication of signals corresponding to the α-proton.
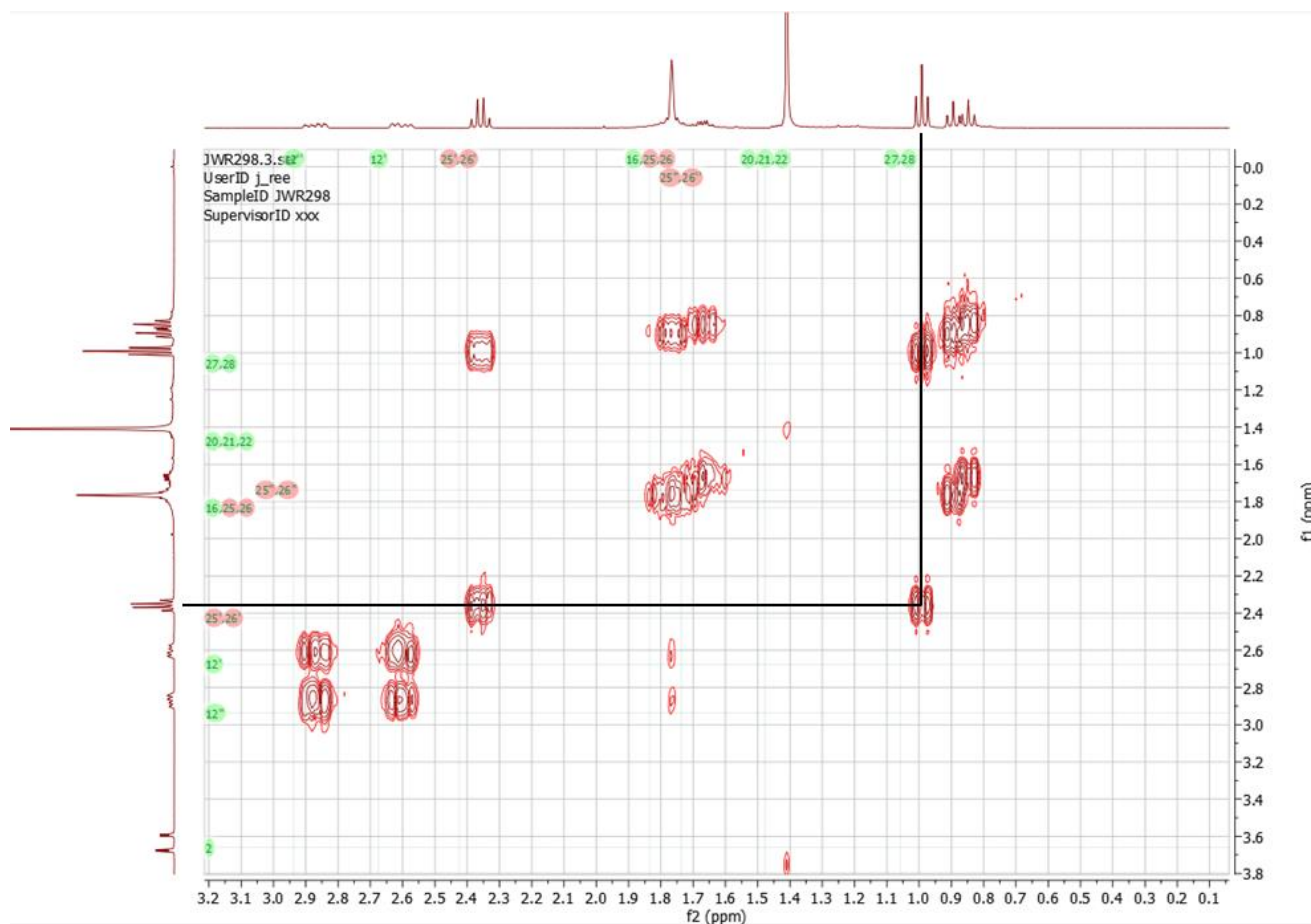
Figure 2.29. Magnified region of the 2D COSY NMR of the diethyl ketal **2.73** showing the CH_2 at 2.43 ppm coupling to the CH_3 peak at 1.06 ppm. Line denotes the correlation.

In the case of the cyclohexyl ketal analogue **2.74**, there is again evidence of ^1H NMR signal duplication for protons within the epoxy cyclohexenone ring as well as the α-proton (Figure 2.30 B), however in this instance, the integration gives an approximate ratio of 9:1 (Figure 2.30 B), which suggests the formation of one diasteroemer is favoured over the other.
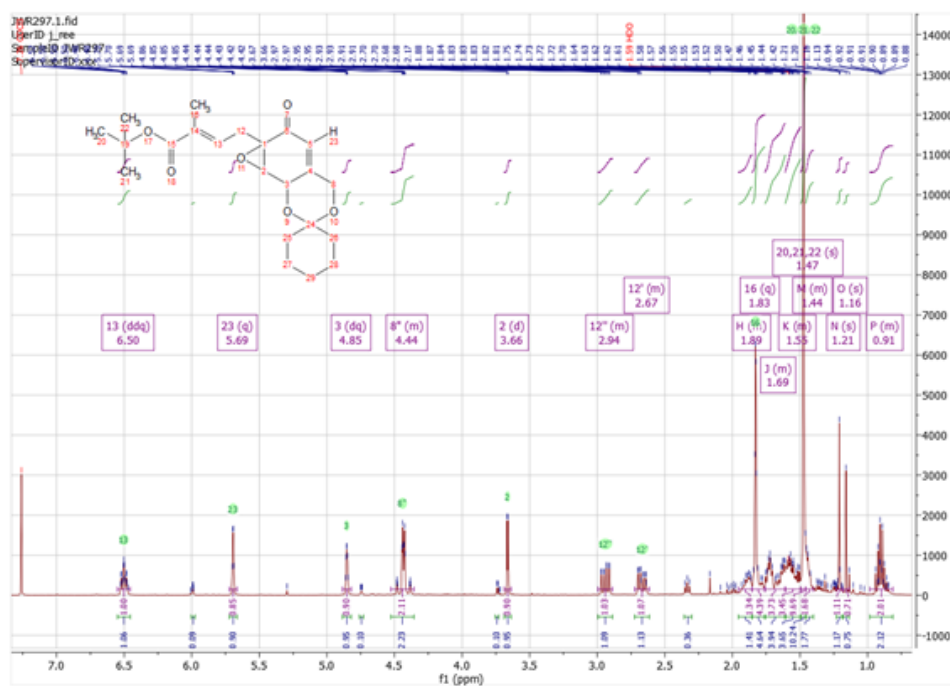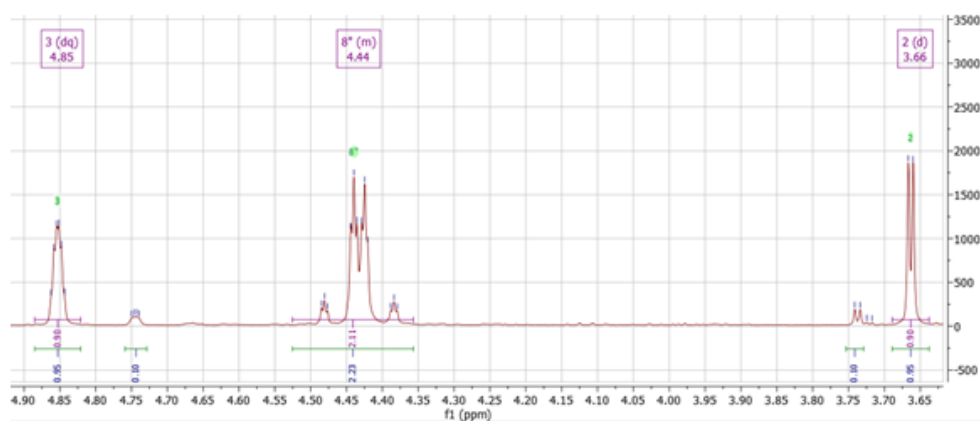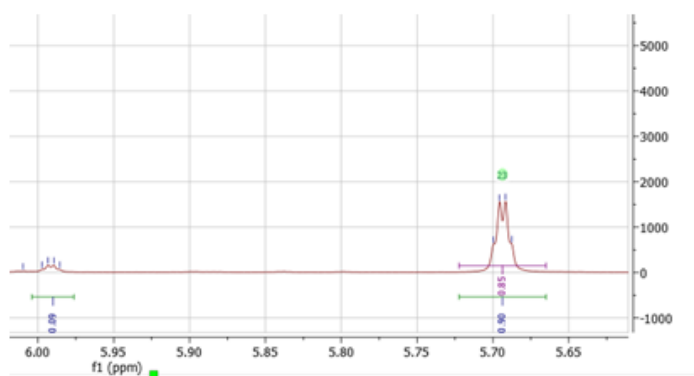
Figure 2.30. (A) ^{1}H NMR of the cyclohexy ketal **2.74**. **(B)** Magnified region of ^{1}H NMR showing the duplication of signals corresponding to the protons within the epoxy cyclohexene ring in an approximate ratio of 9:1 (by integral). **(C)** Magnified region showing the duplication of the signals corresponding to the α-proton, again in an approximate ratio of 9:1.

The *trans*-acetalation/ketalation approach yielded the desired cyclohexyl ketal in improved yield when compared to the previous approach, which had been successfully used for the production of the dimethyl **2.72** and diethyl **2.73** ketals. This is pleasing, as the cyclohexyl ketal requires a more sterically encumbered substrate (1,1-dimethoxyxyclohexane) when compared to the production of the dimethyl (acetone) and diethyl (pentan-3-one) ketals. As such, for the future preparation of similar compounds, the *trans*-acetalation/ketalation approach should be used. Dimethyl ketal (**2.72**), diethyl ketal (**2.73**) and cyclohexyl ketal (**2.74**) were taken forward for biological testing, outlined in chapter 4.

2.8 Conclusions

This chapter has outlined the attempted synthesis of a range of unique analogues of ambuic acid.
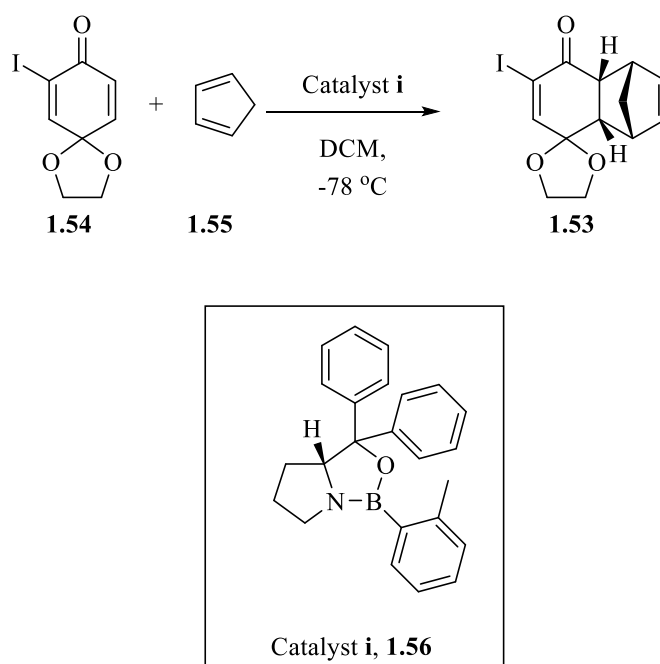
Scheme 2.36. The key Diels-Alder reaction providing the key intermediate (+)-adduct **1.53**.

The general synthesis of **1.62**, utilising an efficient procedure optimised by Dr Leonardo Baldessarre has been outlined here. This involved the use of a key Diels-Alder reaction between cyclic ketal and cyclopentadiene in the presence of (R)-(+)-o-tolyl-CBS-oxazaborolidine **1.56** catalyst which afforded the adduct **1.53** in good yield with good enantioselectivity (Scheme 2.36). With the successful synthesis of adduct **1.53**, production of the final compound **1.62** could proceed. Stille cross-coupling allowed for the installation of the allyl functionality giving **1.57**, epoxidation through the use of H_2O_2 gave the desired epoxide **1.58** (Scheme 2.37). A procedure adapted from Mehta *et al.* and Jung *et al.* allowed for the installation of the primary alcohol to afford **1.59** (Scheme 2.37).[163, 168] The lower ketone was then enantioselectivly reduced using a modified procedure from Jung *et al.* utilising DIBAL-H which afforded diol **1.60**.[163] The primary alcohol is then protected as the *t*-butyl dimethyl silyl ether **2.27**. The Diels-Alder adduct of **2.27** is subsequently dismantled giving the quinilone derivative **1.61** which is then taken into the ozonolysis and Wittig procedure to afford the final *t*-butyl ester **1.62**.
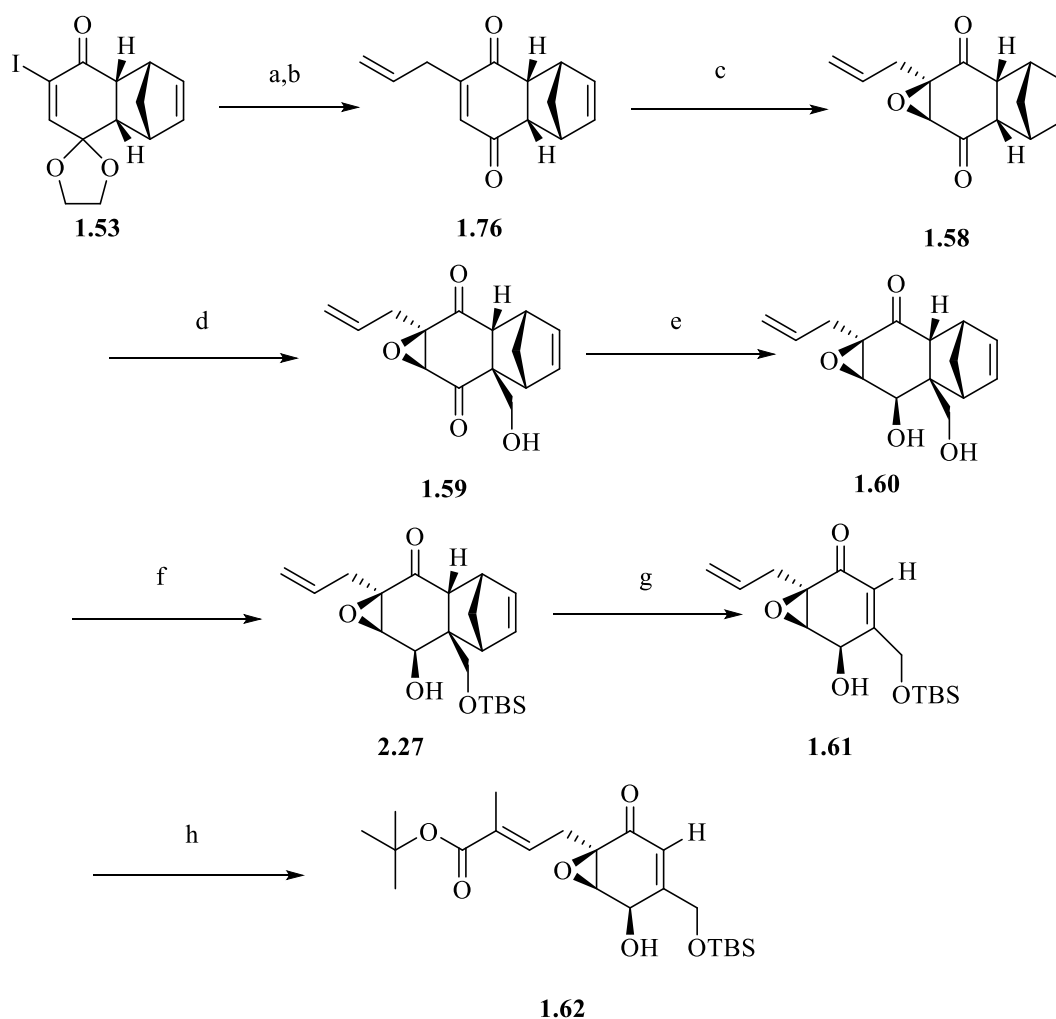
Scheme 2.37. The route to enantiometrically pure **1.62** which has been carried out in this study. (a) Pd(PPh₃)₄, allyltributyl stannane, THF, 10 min, 110 ℃, 150 W MW radiation, 68%; (b) 1 N H₂SO₄, acetone, THF, 30 min, rt., 96%; (c) 10% (w/v) Na₂CO₃, 30% (v/v non-stab.) H₂O₂, acetone, 30 min, 0 ℃, 83%; (d) 37% (w/v) aqueous formaldehyde, DBU, THF, 30 min, 0 ℃, 79%; (e) DIBAL-H, THF, 30 min, -78 ℃, 43%; (f) TBSCl, imidazole, DMF, 4 h, 0 ℃, 83%; (g) Ph₂O, 4 h, 230 ℃, 73%; (h) O₃, dimethylsulfide, MeOH, -78 ℃, 30 min then Ph₃P=C(Me)CO₂t-Bu, DCM, 2 h, -40 ℃, 25%.

The compound **1.63**, the corresponding (-)-enantiomer of **1.62** has been prepared to determine how stereochemistry affects the anti-virulence activity of the compounds. Production was mediated through the modification of the key Diels-Alder reaction to produce the (-)-adduct **1.67**. This was carried out using (*S*)-(-)-*o*-tolyl-CBS oxazaborolidene catalyst 1.**68**. This provided the adduct **1.67** with good enantioselectivity and reasonable yield (Scheme 2.38). With the successful production of adduct **1.67**, subsequent transformations yielded the desired final compound **1.63**. This route broadly follows the route to **1.62**.
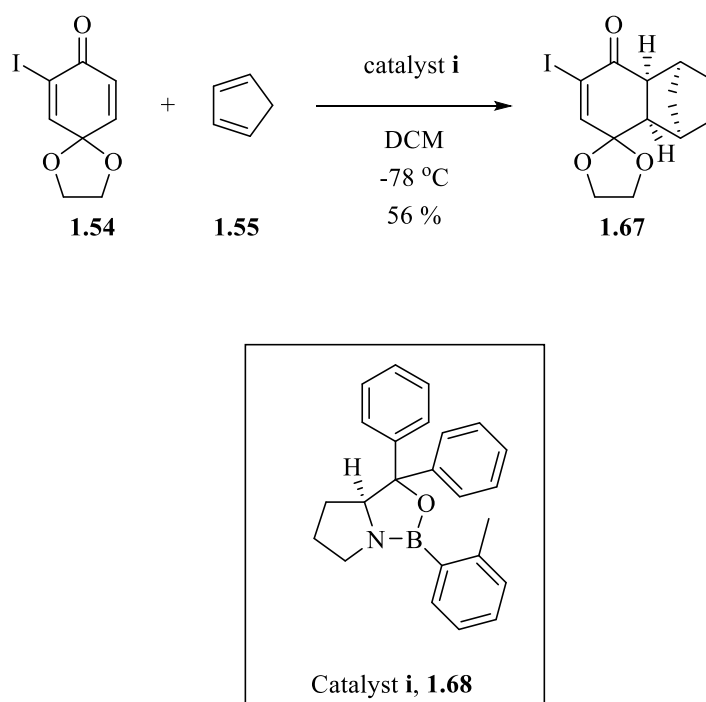
Scheme 2.38. The chiral Diels-Alder reaction providing the key intermediate, (-)-adduct **1.67**

The attempted production of a range of ether analogues was also outlined. Numerous approaches to modify a Williamson ether synthesis failed to afford the desired asymmetric ether. It was decided to discontinue with this branch of analogues.

The synthesis of numerous silyl ether analogues was attempted. Perestelo *et al.* suggests that the production of a range of silyl ether analogues may be an interesting series of analogues to synthesise.[200] Unfortunately, the production of several silyl ethers proved problematic and it was only possible to produce one, **2.62** in sufficient yield for biological assessment (Figure 2.31).
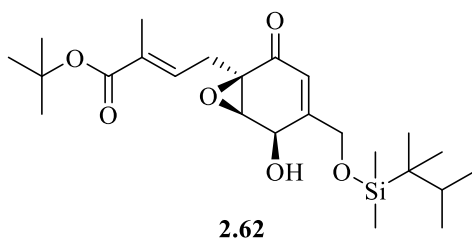
Figure 2.31. The dimethylthexyl silyl ether **2.62**

A focussed range of ketal analogues have been synthesised. Dimethyl (**2.72**), diethyl (**2.73**) and cyclohexyl (**2.74**) ketals have been successfully synthesised. These were produced from the reaction of the diol **1.74** with the desired ketone in the presence of catalytic p-toluenesulfonic acid. This procedure afforded the dimethyl and diethyl ketals however failed in the production of the more sterically encumbered cyclohexyl ketal. Thus an efficient trans-acetalation/ketalation route for the production of the cyclohexyl ketal has been established. This utilises the 1,1-dimethoxy variant of the ketone as a more reactive substrate for reaction. This procedure could be utilised in future applications for the production of further sterically encumbered ketals. Furthermore, NMR analysis of the diethyl **2.73** and cyclohexyl **2.74** ketals indicated a diasteromeric mixture of compounds in a 1:1 ratio for the diethyl ketal and a 9:1 ratio for the cyclohexyl ketal.

The successfully synthesised compounds (Figure 2.32) were taken forward for biological assessment of anti-virulence activity against the *agr* system in chapter 4.

1.63

2.62

2.72

2.73

2.74
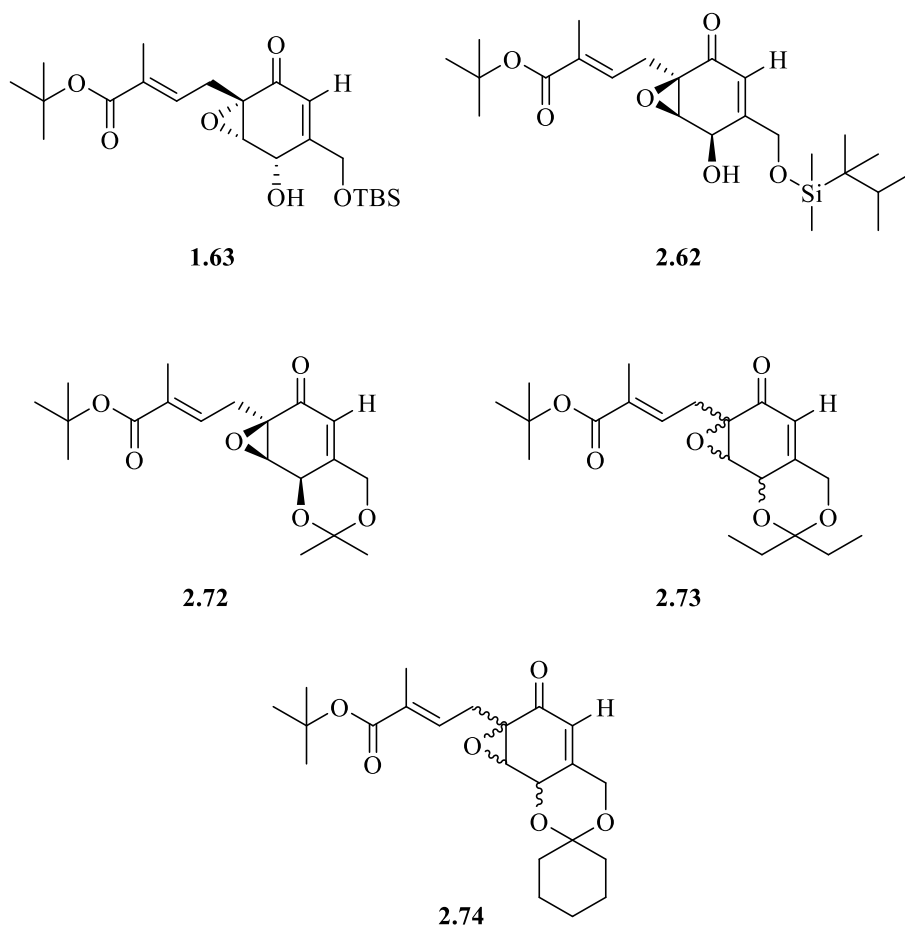
Figure 2.32. The compounds successfully produced in this chapter to be taken forward for biological testing. The (-) enantiomer **1.63**, the dimethylthexyl silyl ether **2.62** and the dimethyl (**2.72**), diethyl (**2.73**) and cyclohexyl (**2.74**) ketals.

Chapter 3. The total synthesis of a cyclpropyl analogue of a lead ambuic acid analogue

3.1 Chapter outline

This chapter outlines the synthesis of an isosteric analogue of ambuic acid, in which the epoxide moiety is replaced with a cyclopropyl group. The cyclopropyl analogue **1.75** is required to elucidate the mode of action of ambuic acid and its analogues. This chapter discuses the installation of the cyclopropyl ring and the subsequent chemical transformations to generate the desired product **1.75**, which is based on the ambuic acid analogue **1.62**, the synthesis of which is previously reported in chapter 2.
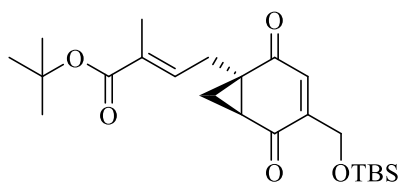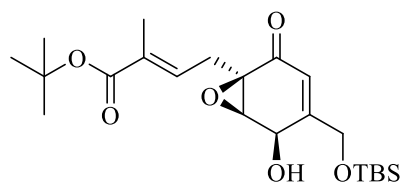
1.75   **1.62**

3.2 Introduction

3.2.1 AgrB, a cysteine protease

As previously outlined in chapter 1, AgrB is a putative, membrane-bound cysteine protease that is responsible for the removal of the C-terminal region of AgrD, in a process which is coupled to the formation of the AIP thiolactone macrocycle. The macrocyclic structure is critical for AIP activity.[103, 122-123, 152]

In summary, AgrD, an AIP pre-pro peptide consists of a core AIP sequence flanked N-terminally by an amphipathic helix and C-terminally by an AgrB recognition motif consisting of hydrophilic residues.[120, 122, 212] AgrB catalytically excises the C-terminal recognition region of AgrD which yields an enzyme-substrate thioacyl intermediate involving the key catalytic Cys77 residue of AgrB.[120, 122, 212] Subsequent intramolecular nucleophilic attack of this intermediate by an absolutely conserved cysteine within the core AIP sequence generates the thiolactone macrocycle, releases the AgrD thiolactone pro-peptide, and regenerates the active site of AgrB (described in greater detail in chapter 1).[152]

The AgrD thiolactone pro-peptide is then N-terminally processed by the putative CAAX metalloprotesae MroQ producing the mature AIP molecule which is then secreted into the extracellular milieu[124].

3.2.2 Disorders and inhibitors of cysteine proteases

Cysteine proteases are found extensively in nature and fulfil a wide range of biological roles. A number of cysteine proteases have been identified in the genomes of both veterinary and human parasites.[213] Clan CA (papain family) and Clan CD asparaginyl endopeptidases (legumains) are amongst those used by parasites such as metazoan and protozoa.[213] Parasites, such as *Trypanosoma sp.* and *Plasmodium falciparum* utilise cysteine proteases for the propagation of infection.[214-216] *P. falciparum* utilises cysteine proteases for a range of functions, including the breakdown of haemoglobin and the invasion and rupture of erythrocytes.[214]

Cysteine proteases are not unique to parasites and examples are found in vertebrates, including the human and animal hosts infected by the parasite.[213, 217] Mammalian cysteine proteases include cathepsins, which are often found at high concentrations within intracellular organelles, such as lysosomes for the degradation of unwanted proteins and caspases, which play a key

part in apoptosis- controlled cell death.[213, 217] More recently, there is a growing field of evidence suggesting that cysteine proteases function beyond lysosomes and have a range of pathological and physiological functions.[217] For example, cathepsin activity is often elevated in the heart and arterial walls of patients with cardiovascular disease.[217] Furthermore, the loss of function of calpain 3 is linked to the onset of limb-girdle muscular dystrophy.[159]

Due to the importance cysteine proteases play in numerous pathological conditions, inhibitors have been widely studied and several have been validated as potential therapeutics.[159] Both covalent and non-covalent inhibitors of cysteine proteases have been previously studied.[162] Covalent inhibitors of cysteine proteases either acylate or alkylate the key nucleophilic cysteine within the active site of the protease target.

3.2.3 Acylating inhibitors

Examples of inhibitors which acylate the key nucleophilic cysteine of cysteine proteases are the aza-peptides **3.1** (Figure 3.1).[162, 218] Aza-peptides are peptides wherein one of the amino acids has its α-carbon substituted for a nitrogen.[162, 219] It is thought that aza-peptides inhibit cysteine proteases through 'direct acylation' of the key nucleophilic cysteine within the active site of the cysteine protease.[162] Initial attack at the aza-amino acid carbonyl by the active site thiol leads to the formation of a covalent carbazyl intermediate (Scheme 3.1).[162] With a natural peptide substrate, a thioester is formed (Scheme 3.1).[162] Inhibition of the protease by aza-peptides occurs due to the nature of the carbazyl enzyme-substrate intermediate.[162] The carbazyl carbonyl is less susceptible to nucleophilic attack by water, i.e. by hydrolysis, due to the trigonal geometry and delocalisation of the α-nitrogen lone pair into the carbonyl system.[162] This leads to a slower rate of hydrolysis relative to the ester intermediate formed with the natural substrate and subsequent inhibition.[162]
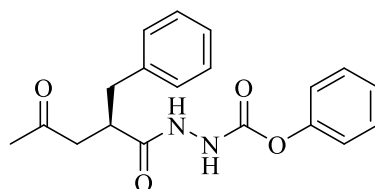
3.1

Figure 3.1. An example of an azapeptide ester from Magrath et al..[218]

Despite formation of the relatively stable carbazyl intermediate, aza-peptide inhibition can still be surmounted by hydrolysis and hence, proteolytic activity can be recovered.[162]
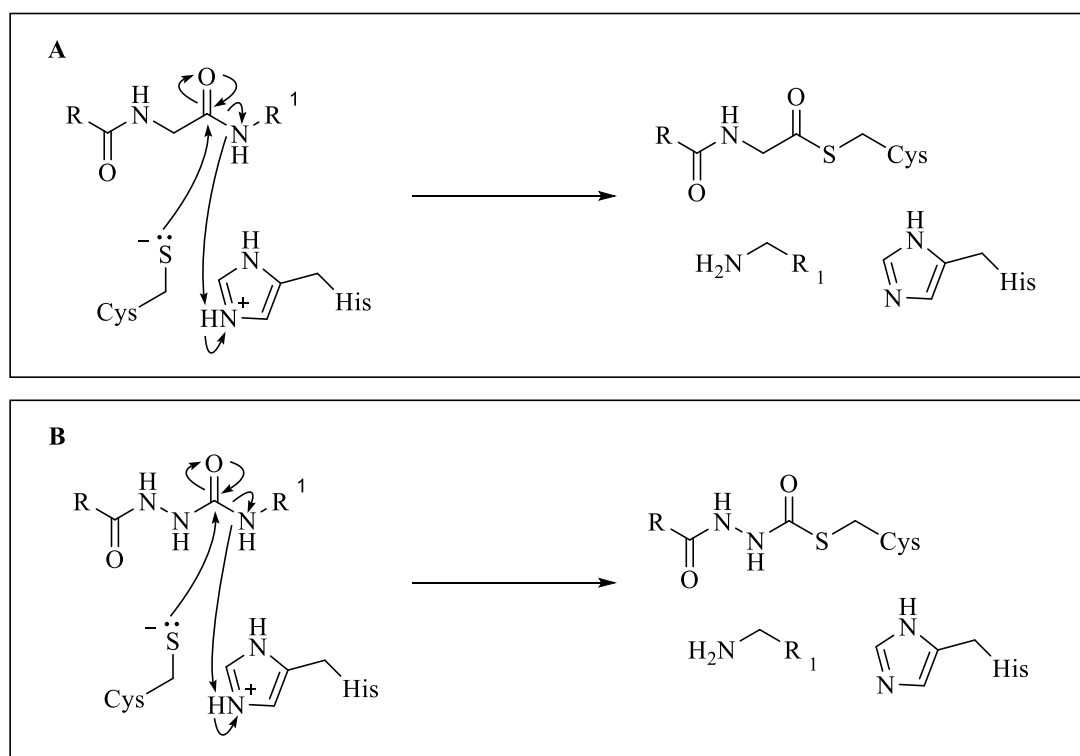
Scheme 3.1. The mechanism of lysis of a peptide bond by a cysteine protease, **(A)** by forming a thioester intermediate and **(B)** the mechanism of action of aza-peptide inhibitors of cysteine proteases; note the carbazyl intermediate, less readily hydrolysed than the thioester formed when the protease reacts with the natural peptide substrate.

3.2.4 Alkylating inhibitors

3.2   **3.3**
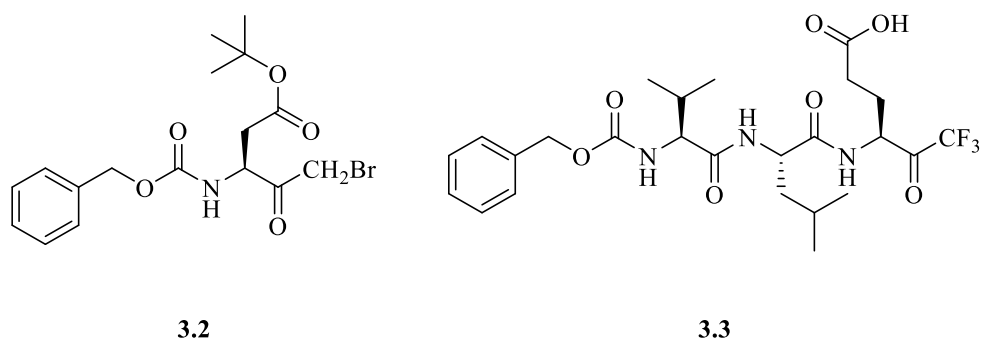
Figure 3.2. Examples of halomethylketone inhibitors of the coronavirus 3CL^{pro} main protease.

Examples of alkylating inhibitors of cysteine proteases include halomethyl ketones and epoxysuccinates.[162] The compounds **3.2** and **3.3** (Figure 3.2) are examples of inhibitors of the

coronavirus 3CL^{pro} main protease which carry the halomethyl ketone electrophilic warhead which facilitates the formation of a thiolether adduct with the key catalytic cysteine within the active site of the target protease (Scheme 3.2).[220] The resultant thiolether is resistant to hydrolysis, overcoming the enzyme reactivation pathway typically associated with other acylating agents.[162]
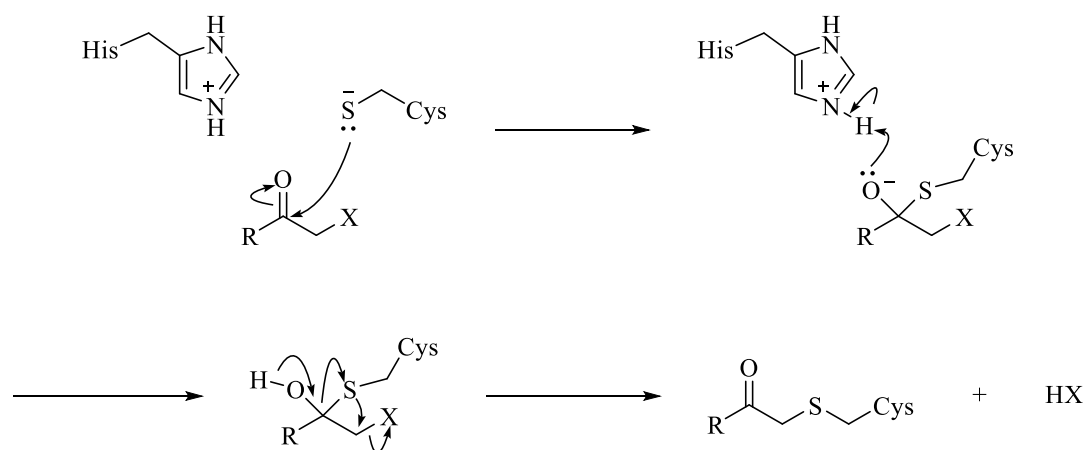
Scheme 3.2. Mechanism of inhibition of halomethyl ketones alkylating a cysteine protease as suggested by Bacha et al..[220]

Epoxysuccinates (**3.4** and **3.5**) (Figure 3.3) are a further class of covalent, alkylating inhibitors of cysteine proteases which utilise the epoxydione electrophilic warhead to irreversibly modify the nucleophilic cysteine within the protease active site (Scheme 3.3).[159, 221] Nucleophilic attack at either carbon of the epoxide opens the strained 3-membered heterocycle, leading to alkylation mediated by the formation of a thiolether and inhibition surmountable only by *de novo* protein synthesis.[162]

3.4   **3.5**
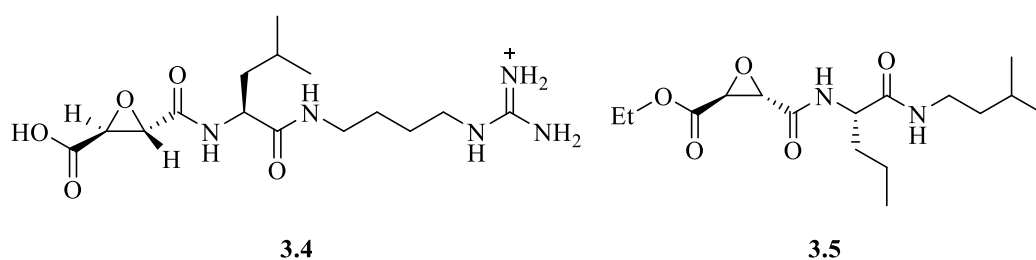
Figure 3.3. Examples of epoxysuccinate inhibitors.

Epoxysucinates have previously been shown to be a useful family of cysteine protease inhibitors with the pro-drug E-64d (**3.5**) having reached phase-III clinical trials for the treatment of muscular dystrophy (Figure 3.3).[159]
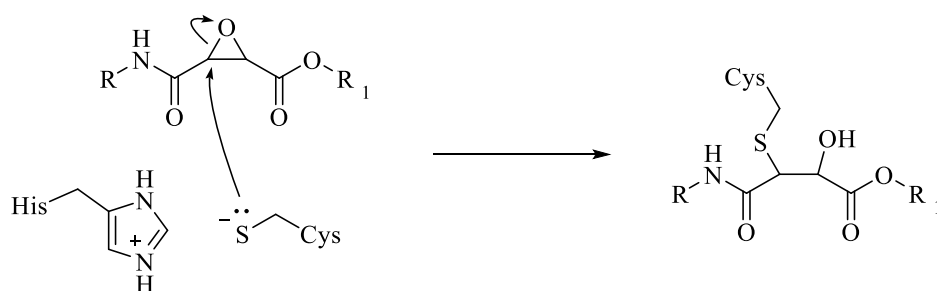
Scheme 3.3. A potential mechanism of inhibition of epoxysuccinates which alkylate the key nucleophilic cysteine within the active site.

3.2.5 Is ambuic acid a covalent inhibitor of AgrB?

Despite the mechanism of ambuic acid attenuation of staphylococcal *agr*-mediated virulence remaining unknown, the presence of the epoxide moiety which is shared with the known family of cysteine protease inhibitors such as **3.4** and **3.5** may suggest a potential mode of action. It is hypothesised that ambuic acid covalently modifies the catalytic Cys84 in AgrB forming a thiolether-bound enzyme-inhibitor covalent adduct (Scheme 3.4). This leads to inhibition of AgrB, surmountable only by *de novo* protein synthesis.
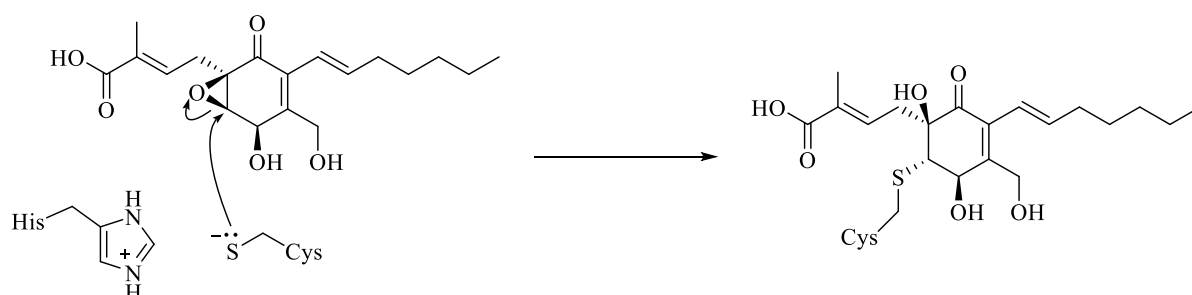
Scheme 3.4. A proposed mechanism of inhibition of AgrB by ambuic acid.

 To determine whether ambuic acid and the unique synthesised analogues function in the manner proposed in Scheme 3.4, a cyclopropyl isostere **1.75** of a lead analogue **1.62** was synthesised. The isosteric replacement of the epoxide with a cyclopropyl ring may go some way towards the determination of a mechanism of action for ambuic acid analogues, which is interest as there is currently no published mechanism within the literature.

3.3 Synthesis of the cyclopropyl analogue

3.3.1 Methods for cyclopropylation

In order to produce the final cyclopropyl isostere **1.75**, a method for the stereoselective installation of the cyclopropyl ring was required. Compound **2.27** (Figure 3.4), the synthesis of which is outlined in chapter 2 was chosen as the substrate for the cyclopropylation reaction. In the synthesis of the epoxide-containing equivalent **1.62**, compound **2.27** is the substrate for the Julia-Colona epoxidation. Hence, **2.27** was chosen as the point of divergence from the general synthesis discussed in chapter 2 to enable the synthesis of the cyclopropyl analogue **1.75**.

2.27
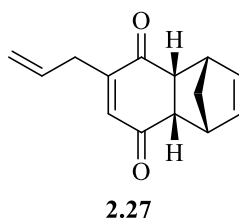
Figure 3.4. Substrate for cyclopropylation

Despite their strained nature, cyclopropyl rings are present in a diverse range of natural products such as pheromones and terpenes.[222] Hence, synthetic methods to introduce cyclopropyl rings have been extensively explored. For example, multiple methods have been developed for the installation of cyclopropyl rings, including the Simmons-Smith and Corey-Chaycovsky reactions.[165-166, 223-224]

The original Simmons-Smith reaction utilises iodomethylzinc iodide (prepared from CH_2I_2 and elemental zinc) and an olefin for the production of a cyclopropane compound (Figure 3.5).[223-225] Modifications to the procedure which utilise diethylzinc have also been developed and remain widely used in synthetic applications.[225]
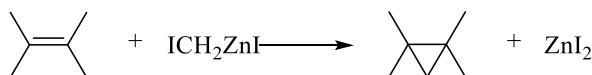
Figure 3.5. Equation of the Simmons-Smith reaction

Despite the discovery of the Simmons-Smith reaction occurring in the 1950s, the exact mechanism by which the reaction occurs remains undetermined and is beyond the scope of this thesis.[225]
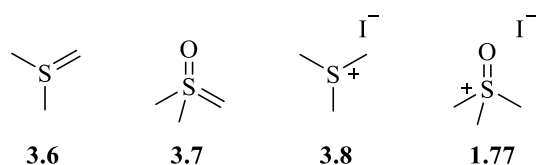
Figure 3.6. Structures of sulphur ylides dimethylsulfonium methylide **3.6** and dimethylisulfoxonium methylide **3.7**, and their respective precursors, trimethylsulfonium iodide **3.8** and trimethylsulfoxonium iodide **1.77**.

In the early 1960s, Corey and colleagues reported the ability of two sulphur ylides; dimethylsulfonium methylide **3.6** and dimethylsulfoxonium methylide **3.7** (Figure 3.6) to transfer methylene group to a range of unsaturated electrophilic centres, such as C=O, C=S, C=N and α,β-unsaturated olefins. Since these early findings, several methods have been reported leading to them becoming versatile reagents, suitable for a range of synthetic applications.[226-227] The ylides **3.6** and **3.7** are prepared from trimethylsulfonium iodide (**3.8**) and trimethylsulfoxonium iodide (**1.75**) respectively by stirring with a base, typically sodium hydride (Figure 3.6).
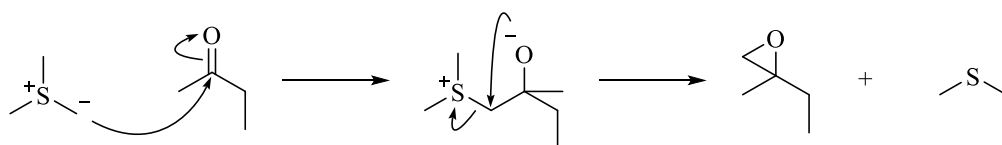
Scheme 3.5. Mechanism of Corey-Chaycovsky epoxidation.

.

In early studies, **3.6** was first found to react with ketones and aldehydes to produce oxiranes (Scheme 3.5).[165-166] Ylide **3.7** can also react with ketones to give the oxirane (Scheme 3.6 A). However in the presence of an electrophilic olefin, such as in an α,β-unsaturated system (e.g. an enone), **3.7** will selectively react to give the cyclopropane with no formation of the corresponding oxirane (Scheme 3.6 B).[165-166, 228-229] However, reaction of **3.6** with an α,β-unsaturated olefinic system does not give the cyclopropane. Computational studies of the reaction mechanism, carried out by Xiang *et al.* suggested that **3.7** favours the formation of the cyclopropyl ring due to the high activation energy of the rate determining, ring closure event required for the formation of the oxirane (Scheme 3.6).[230] Furthermore, the sulfoxonium may delocalise the negative charge of the ylide **3.7**, softening it as a nucleophile favouring HOMO-

LUMO interaction leading to 1,4-conjugate addition at the electrophilic olefin compared to direct 1,2 addition.

A
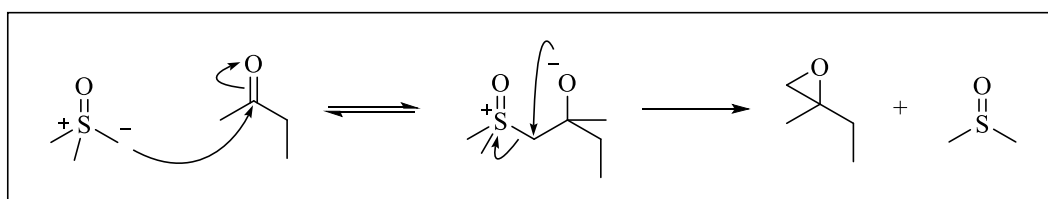
B
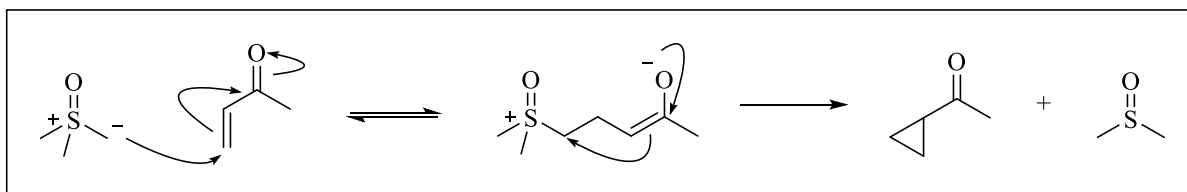
Scheme 3.6. Mechanism of Corey-Chaycovsky **(A)** epoxidation with dimethylsulphoxonium methylide **3.7** and the Corey-Chaycovsky **(B)** cyclopropylation.

3.3.2 Production of the cyclopropyl ring

Of the above two cyclopropylation reactions, it was decided to install the cyclopropyl moiety using a modified Corey-Chaycovsky reaction with dimethylsulfoxonium methylide **3.7**. The Corey-Chaycovsky procedure allows for the selective cyclopropylation of α,β-unsaturated systems, the target in this synthetic application, whereas the Simmons-Smith reaction may react with the other alkenes within the reaction substrate **1.76**. Furthermore, Corey-Chaycovsky cyclopropylation proceeds as a 1,4-addition, akin to the Julia-Colona (Weitz-Scheffer) epoxidation described in chapter 2 and it is hoped that the level of conservation of mechanism between the two reactions may lead to the cyclopropane product sharing the same *endo* stereochemistry as the epoxide (Scheme 3.7). Additionally, it was hoped that the chiral Diels-Alder adduct would confer stereoselectivity on the reaction through steric occlusion, preventing formation of the non-desired *exo-* enantiomer.

1.76   **1.78**
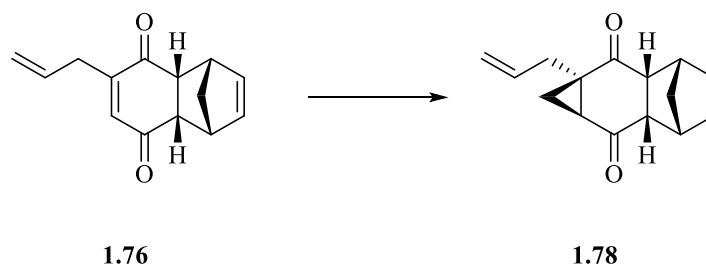
Scheme 3.7. Installation of the cyclopropyl ring

Thus, a procedure by Lee *et al.* which was used for their installation of a cyclopropyl ring on a cyclohexenone was modified for this application (Scheme 3.8).[231] Initially 1 eq. of trimethylsulfoxonium iodide (**1.77**) was stirred with 1.1 eq. of NaH in DMSO at -78 ℃ to generate the active sulphur ylide species **3.7**. Then, the substrate **1.76** in DMSO was titrated into the methylide suspension (Table 3.1, condition 1). The reaction was monitored by HRMS and the correct mass of the desired product **1.78** was observed. However, upon purification, the overall yield was < 10 % and upon analysis by ^{1}H-NMR, the isomer **3.9** was found to be the major product in a ratio of 85.5:14.5 (ratio calculated by ^{1}H NMR) with the minor product being the desired cyclopropane **1.78** (Scheme 3.9, Figure 3.7 **A**).
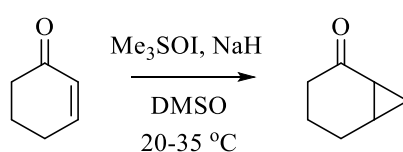
Scheme 3.8. The Corey-Chaycovsky cyclopropylation reaction as used by Lee et al..[231]

It was postulated that a small excess of base may be the cause for this isomerisation, so in an attempt to alleviate this, 2 eqv. of trimethylsulfoxonium iodide were employed to ensure that all NaH within the reaction mixture had reacted (Table 3.1, condition 2). Unfortunately, this condition still afforded the isomer in extremely poor yield (Scheme 3.9, Table 3.1).

Table 3.1. Table of tested conditions of Corey Chaycovsky-cyclopropylation. * 1 eq. of Me$_3$SOI used.

Condition	Source of methyl (2 eqv.)	Base (1 eqv.)	Additive	Solvent	Temperature (℃)	Yield (%)
1	Me$_3$SOI *	NaH	-	DMSO	20-50	<10
2	Me$_3$SOI	NaH	-	DMSO	20-50	<10
3	Me$_3$SOI	-	-	THF	20	-
4	Me$_3$SOI	*t*-BuOK	TBAI (cat.)	DCM	20	4
5	Me$_3$SOI	*n*-BuLi	-	DCM	-76-20	-
6	Me$_3$SOI	*n*-BuLi	-	DMSO/THF	-76-20	16
7	Me$_3$SOI	*n*-BuLi	-	THF	-76-20	45
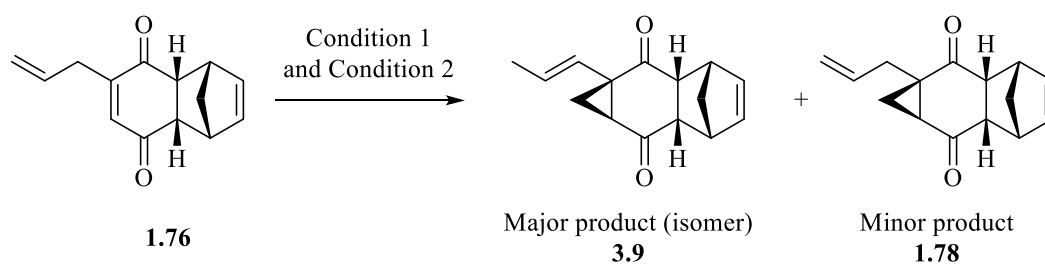
Scheme 3.9. The reaction of conditions 1 and 2 from Table 3.1, gave the undesired isomer **3.9** (major product) and desired cyclopropane **1.78**.

In order to alleviate the problem, it was decided to prepare the dimethylsulfoxonium methylide species *ex situ* (Table 3.1, condition 3). Methylide species **3.7** was prepared by stirring a suspension of trimethylsulfoxonium iodide with NaH in THF, before addition of this suspension to a solution of substrate **1.76**. However, upon addition to **1.76**, no change in reaction mixture was observed by TLC even with stirring overnight. The reactive methylide species may have degraded prior to the addition of **1.76**. With the failure of this condition, it was decided to continue to prepare the methylide *in situ*.

In conditions 1-3 (Table 3.1) it was observed that the dimethylsulfoxonium methylide was in suspension in the reaction solvent. In an effort to improve the solubility and therefore availability of the methylide **3.7** for cyclopropanation, an alternate method was devised. Initially, the decision was made to change the reaction solvent to DCM in an attempt to better solvate the dimethylsulfoxonium and improve the reaction outcome (Table 3.1, condition 5). Unfortunately this condition failed to cause any change in the reaction mixture when monitored by TLC and HRMS.

With the failure of the above condition, a procedure developed by Ng *et al.*, which was established to eliminate the hazards associated with NaH in a scale-up reaction, was modified for use here, wherein NaH is replaced with *t*-BuOK.[232-233] Moreover, the changes made included using the solvent DCM in place of DMSO and the use of tetra-*n*-butylammonium iodide (TBAI) as a phase transition catalyst to aid solubility (Table 3.1, condition 4). TBAI had been shown to be beneficial in cyclopropanation reactions previously, albeit in aqueous systems.[233] Unfortunately, the reaction failed to proceed to completion (monitored by TLC) and upon analysis, the product again proved to be the isomer **3.9** with a yield of 4%. Again, the reaction mixture was observed to be a suspension, even with the addition of TBAI, a possible explanation for the undesirable outcome observed in this study. Next, *n*-BuLi was used as the

base to produce the active methylide species (Table 3.1, condition 5). Unfortunately these conditions failed to react.

A further method for cyclopropylation utilises a mixture of DMSO/THF as the solvent system.[233] The procedure was subsequently modified utilising *n*-BuLi as the base to produce the methylide active species from trimethylsulfoxonium iodide (Table 3.1, condition 6). The substrate **3.9** was added and the reaction proceeded to completion. It was pleasing to see that upon purification, ^{1}H NMR found that the desired cyclopropane **1.78** had been selectively formed with no formation of the undesired isomer **3.9**. However, the overall yield was still poor at 16 %. As there are numerous subsequent steps to convert the cyclopropane **1.78** to the final compound, an improvement of the reaction yield was required.
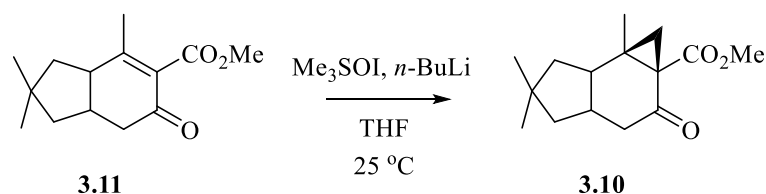
Scheme 3.10. The Corey-Chaycovsky cyclopropylation conditions optimised by Thompson et al., utilised in their synthesis of sesquiterpenes.

Thompson *et al*., in their synthesis of marasmane and lactarane sesquiterpenes developed a method for cyclopropanation using THF as the reaction solvent (Scheme 3.10). [234] Cyclopropane **3.10** was prepared through treatment of cyclohexenone **3.11** with **3.7** that had been prepared through the reaction of **1.77** with *n*-BuLi (Scheme 3.10). With the observed benefit of THF in Condition 6 (Table 3.1), it was decided to use THF as the solvent in this application (Table 3.1, condition 7). Gratifyingly, a dramatic improvement in the reaction outcome was observed, with a yield of 45 % of the desired cyclopropane and no evidence of isomerisation or formation of the oxirane found by ^{1}H NMR analysis (Figure 3.7, B). Thompson *et al*. also experienced a notable improvement in yield using THF.[234] They suggested that the sulfoxonium enolate intermediate (, B) formed in the reversible 1,4-addition may be stabilised in DMSO. If this is the case, they proposed that the stabilised sulfoxonium enolate may cyclise less readily relative to the reverse reaction yielding starting material **1.76** and dimethylsulfoxonium methylide.[234]
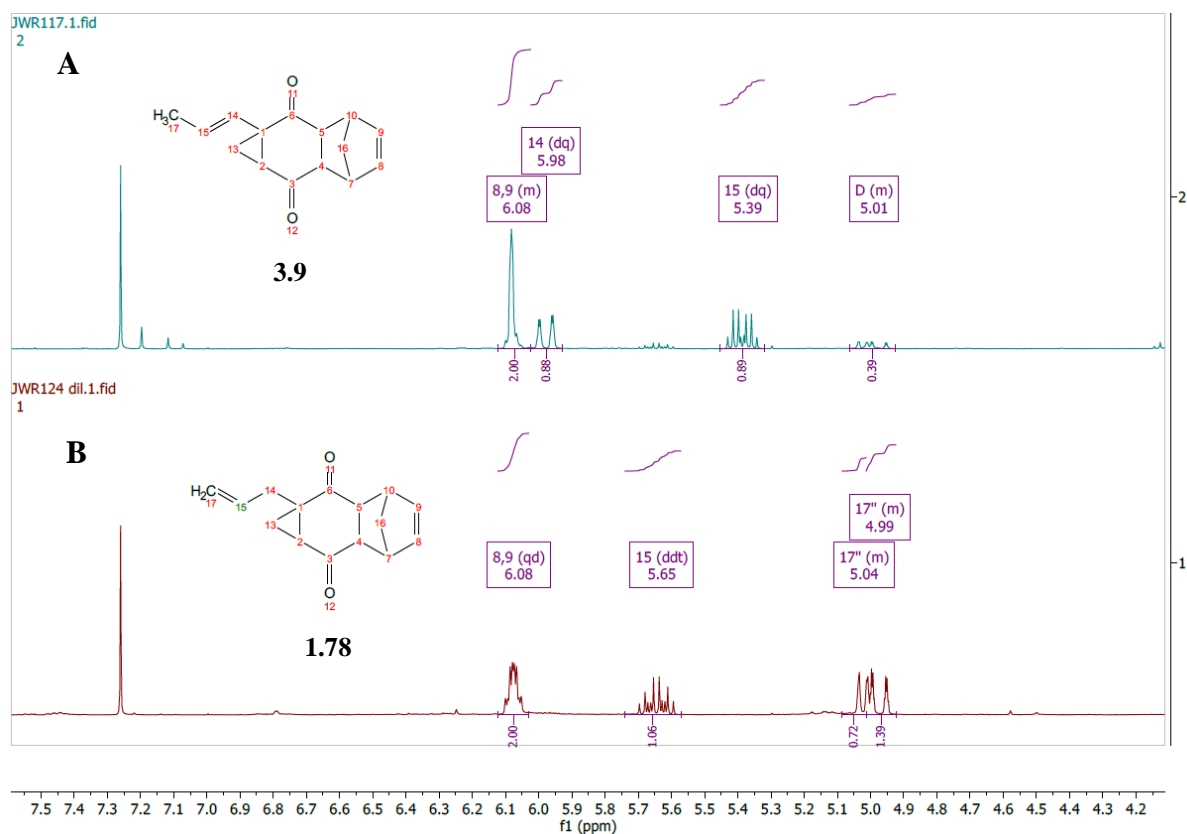
Figure 3.7. ¹H NMR of region of interest of spectra of the undesired isomer **3.9 (A)** and the desired product **1.78 (B).** Additional peak in spectra **A** at ppm 1.68 (dd, J= 6.5, 1.7 Hz, 3H)- not shown here indicative of terminal Me in isomer **3.9**

In addition to selective formation of the desired cyclopropane **1.78**, Nuclear Overhauser Effect Spectroscopy (NOESY) confirmed the relative stereochemistry of the cyclopropyl ring (Figure 3.8). It was observed that the cyclopropyl ring was installed *endo* with respect to the Diels-Alder adduct bridgehead. NOE interaction was found between the protons of the CH₂ within the cyclopropyl ring and the two α-protons to the right of the ketones (Figure 3.8). This shows that these protons are sufficiently close to each other to allow for observation of a NOE cross-peak, indicating that they are on the same face of the molecule. Furthermore, there is no observable correlation between the α-protons either side of the lower ketone, suggesting that they are too far from each other, indicative that the two protons are on opposing faces of the molecule (Figure 3.8). These data suggest that the cyclopropyl ring has installed with the desired stereochemistry.

Since a suitable condition for the installation of a cyclopropyl ring had been established a scale-up the reaction was evaluated. Initial tests of the cyclopropylation procedure, as outlined above, were carried out at a 1 mmol scale. Initial trials to scale-up the reaction were carried out at a 2

mmol scale. Unfortunately, when a scale-up was attempted, a reduction in yield was observed. As such, it was decided to carry out the cyclopropylation in batches to produce sufficient material for the completion of the synthesis of cyclopropyl analogue **1.75**.
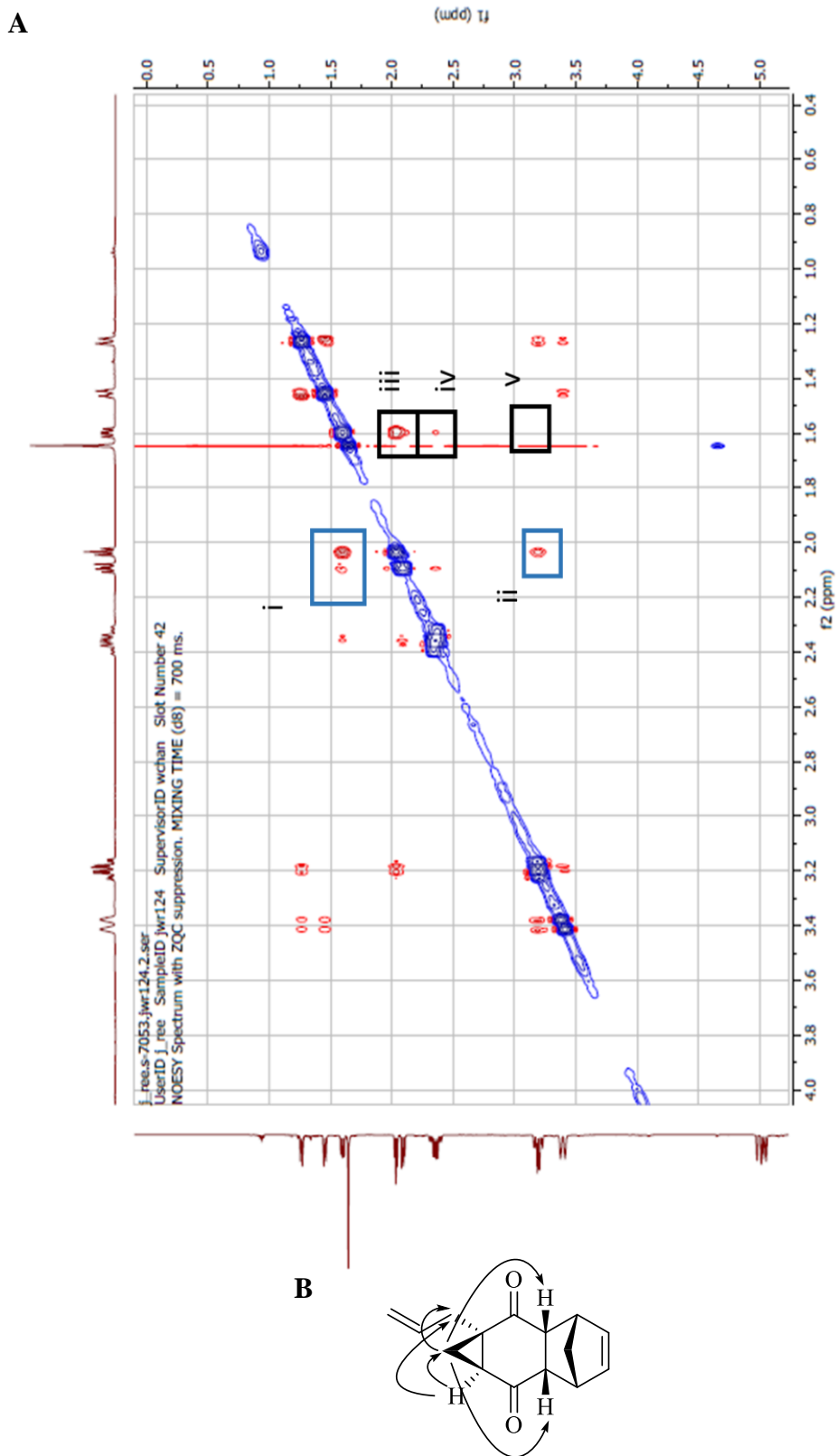
Figure 3.8. **(A)** NOESY NMR spectra showing ROI for stereochemical assignment of cyclopropyl ring and **(B)** schematic of correlations. **(A)** Correlations between **(i)** cyclopropyl CH_2 to allyl CH_2; **(ii)** cyclopropyl CH_2 and two α-protons to right of ketones; **(iii)** α-proton adjacent to cyclopropyl ring and cyclopropyl CH_2; **(iv)** and the allylic CH_2; **(v)** no correlation between α-protons either side of ketones, too far, suggests correct stereochemistry.

3.3.3 Synthetic strategy for producing the final cyclopropyl analogue
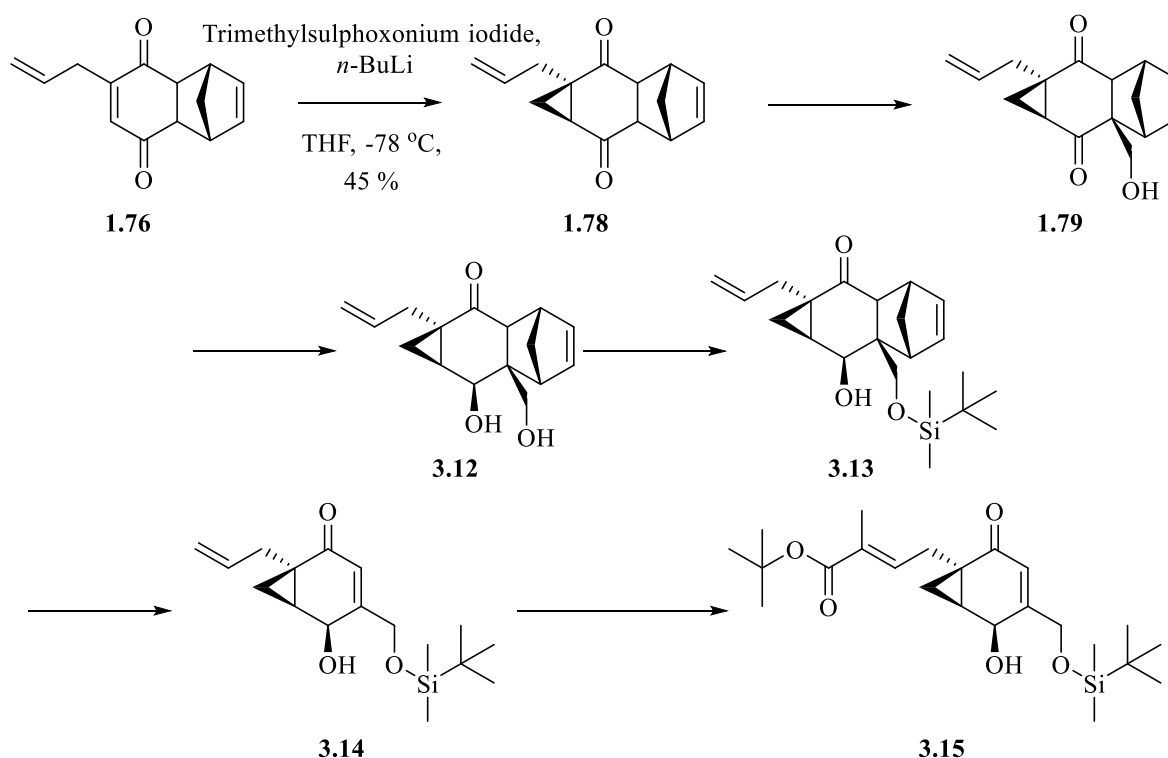
Scheme 3.11. Proposed route to the final cyclopropyl analogue of a modified ambuic acid.

With the successful establishment of a stereoselective cyclopropylation method, a route to the final cyclopropyl analogue **3.15** was required. Scheme 3.11 outlines the proposed synthetic route, which broadly follows the same synthetic strategy used for the total synthesis of the corresponding epoxide-containing analogues, outlined in Chapter 2. Thus, the cyclopropane **1.78** will be treated in an α-hydroxymethylation procedure to install the primary alcohol to yield **1.79**. The lower ketone will then be stereoselectivly reduced to the secondary alcohol to afford the diol **3.12**. The primary alcohol of **3.12** will then be protected at the *t*-butyldimethylsilyl ether **3.13** for subsequent transformations. Silyl ether **3.13** will then be treated in a retro Diels-Alder procedure to dismantle the adduct giving **3.14**. The intermediate **3.14** will be treated in an ozonolysis procedure to give the aldehyde, which will be taken into a Wittig olefination to yield final compound **3.15**.

3.3.4 Optimisation of the synthesis of target 3.1
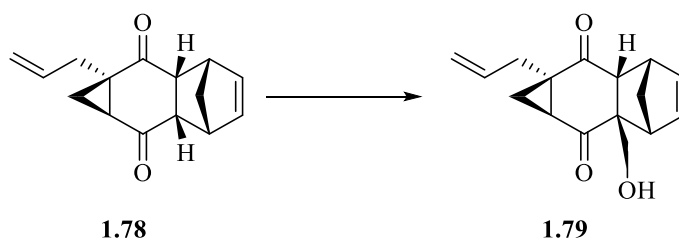
Scheme 3.12. Transformation of cyclopropane **1.78** to the desired alcohol **1.79**.

After the cyclopropylation and production of the desired cyclopropane **1.78**, the subsequent step was the installation of the primary alcohol α to the lower ketone (Scheme 3.12). Initially, a procedure previously employed by Metha *et al.*, Jung *et al.* and previously in this study was evaluated.[163-164] Initial attempts made using the same conditions (Table 3.2, condition 1) proved to yield alcohol **1.79** in a poor yield (4%).

Modifications to this procedure included doubling the number of equivalents of aqueous formaldehyde and increasing the reaction time (up to 24-48 h) improved the reaction outcome and generated the desired alcohol **1.79** (Table 3.2, condition 2). Unfortunately, the yield of the product **1.79** proved variable, with yields of 12-62 % observed (Table 3.2, condition 2). However this was an improvement over the previous condition, sufficient for use here.

Table 3.2. Table of conditions for installation of primary alcohol

Condition	DBU (mol %)	Eq. Formaldehyde (aq.)	Yield (%)
1	20	5	4
2	20	10	12-62

With the successful production of the desired alcohol **1.79**, the next step was to stereoselectivly reduce the lower ketone to the corresponding secondary alcohol (Scheme 3.13).
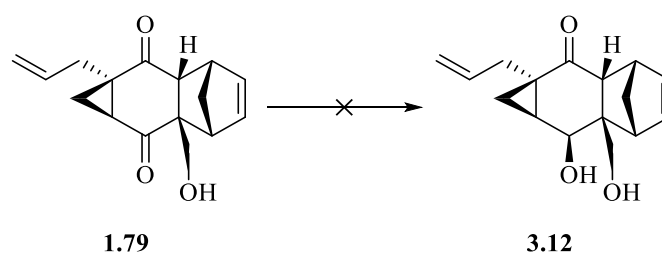
Scheme 3.13. Reduction of the lower ketone to the secondary alcohol.

Initial attempts at the stereoselective reduction used the same conditions as had previously been successfully employed for the production of epoxide containing analogues in Chapter 2. Hence, 0.5 eq. of DIBAL-H were added to **1.79** and stirred (Table 3.3, condition 1). No change in the reaction mixture was observed, therefore a further ~0.5 eq. DIBAL-H was added. Unfortunately this also failed to improve the reaction outcome with no formation of product (established by using HRMS).
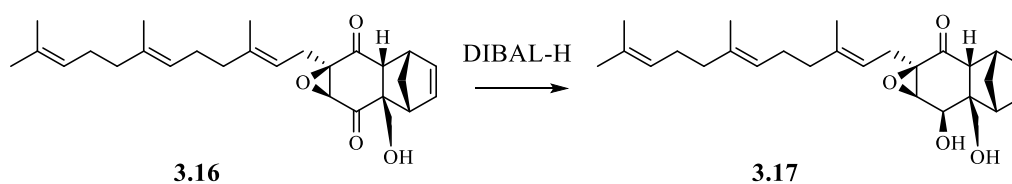
Scheme 3.14. The reduction wherein Mehta *et al.*suggest that the primary alcohol is required for the stereoselective reduction of the ketone of **3.16** giving diol **3.17**.[180]

Mehta *et al.* in their synthesis of yanuthones, a family of epoxy cycyclohexenones suggest that the carbonyl and primary alcohol are important for the stereoselective reduction of the ketone **3.16** giving diol **3.17** through the coordination of the aluminium within DIBAL-H (Scheme 3.14).[180] In this study, isosteric replacement of the epoxide with a cyclopropyl ring has a clear effect on the reaction outcome, suggesting that the epoxide may play a role in the stereoselective reduction of the lower ketone, contrary to the ideas postulated by Mehta *et al.*.[180]

Table 3.3. Table of conditions for the reduction of lower ketone to the corresponding secondary alcohol

Condition	Reducing Agent	Equivalents	Yield (%)
1	DIBAL-H	0.5 (with further addition of 0.5)	-
2	LiAlH$_4$	0.5	- Diasteroisomeric mix of alcohols

In an attempt to improve the reaction outcome and due to the lack of any change in the reaction mixture observed with DIBAL-H, it was decided to use the stronger reducing agent LiAlH$_4$ to stereoselectively reduce the ketone.

Thus, 0.5 eq. LiAlH$_4$ was added to a stirring solution of alcohol **1.79**. The reaction proceeded slowly and required stirring for 48 h, which is unexpected for this type of reaction. However upon completion, it was found that a mix of products had been generated (Table 3.3, condition 2). Upon purification, it was found that the products were a diastereoisomeric mix of both the secondary alcohols. Furthermore, some starting material was also observed. It was clear that LiAlH$_4$ was unsuitable for this application.

Other methods of reduction such as a Leusch are available, however, they are not suitable for this application as selectivity for the lower ketone cannot be guaranteed.
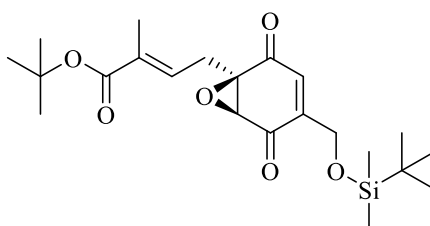
3.18

Figure 3.9. The dione analogue **3.18** produced by Dr Leonardo Baldessarre, found to be as active against *agr* activity as **1.62**.

At this time, it had been found that the dione **3.18** produced by Dr Leonardo Baldassarre, formerly of this research group (Figure 3.9) showed anti-virulence activity comparable to that of the alcohol **1.62** and as such, it was decided to produce the dione version of the cyclopropyl analogue **1.75**, negating the need for this reduction.
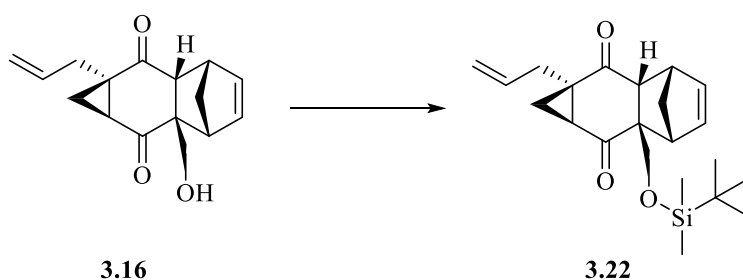
Scheme 3.15. Installation of the *t*-butyldimethylsilyl ether

Subsequently, dione **1.79**, was taken into the silyl ether protection step. Initial attempts at protecting the primary alcohol as the silyl ether **1.80** (Scheme 3.15) proved surprisingly problematic for a reaction of this type with yields of 23-38 % observed. Initially, 5 equivalents of TBDMSCl and imidazole were used to install the silyl ether (Table 3.4, condition 1). Unfortunately the reaction yield proved surprisingly poor (23-38 %).

An improvement of the reaction outcome proved to be facile. Simply increasing the number of equivalents of TBDMSCl and imidazole to 10 and increasing the reaction time allowed for a dramatic improvement in the reaction outcome with an observed yield of 82% (Table 3.4, condition 2).

Table 3.4. Table of conditions for installation of TBDMS silyl ether

Condition	Reagents	Equivalents	Yield (%)
1	TBDMSCl, imidazole	5	23-38
2	TBDMSCl, imidazole	10	82

With the successful production of silyl ether **1.80**, the Diels-Alder adduct was to be dismantled in a retro Diels-Alder procedure (Scheme 3.16).

1.80   **1.81**
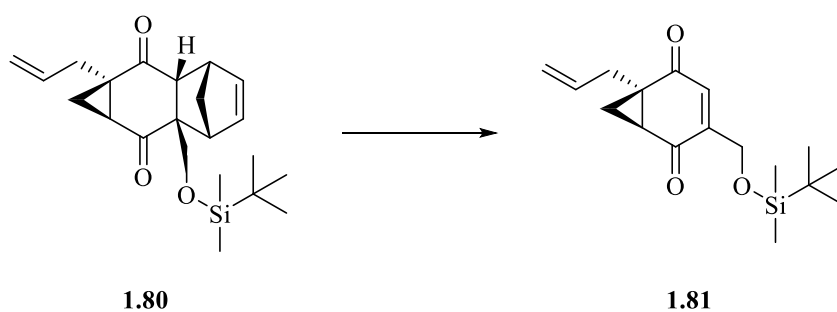
Scheme 3.16. Retro Diels-Alder reaction to dismantle the adduct.

Previously, the retro Diels-Alder reaction had given variable yields (~30-60%) in the production of epoxide-containing analogues based on **1.62**. The reaction conditions, as previously discussed in chapter 2 are harsh, requiring the heating of substrate in Ph_2O for 2-3 h at 230 ºC. Poor yields were often characterised by the appearance of multiple products, as observed by TLC. This could be indicative of pyrolysis of the starting material and indeed the desired product when formed. Pyrolysis could be due to the harsh reaction conditions. Furthermore, oxidation of compounds may have occurred despite best efforts to maintain an inert atmosphere. Thus, it was decided to employ microwave-assisted chemistry in an attempt to improve the variable yields observed. Microwave chemistry has previously been used to great success in a wide array of synthetic applications.[235]

Thus, the starting material **1.80** was dissolved in Ph_2O and the microwave reaction vessel was flushed with argon before heating to 200 ºC for 15 min with 250 W microwave radiation (Table 3.5, condition 1). It was found that the microwave struggled to heat the reaction mixture to a temperature in excess of 140-150 ºC. Nevertheless, TLC analysis indicated that the reaction had proceeded relatively cleanly. There was some evidence of compound degradation with the formation a by-product that did not migrate on TLC analysis, typical of what had been experienced previously using conventional heating methods. Upon purification, it was found that the desired product **1.81** had indeed been formed however the yield of the reaction proved poor (26 %). This poor yield could be attributed to compound degradation.

Table 3.5. Table of conditions for retro Diels-Alder reaction.

Condition	Solvent	Microwave Conditions	Yield (%)
1	Ph$_2$O	250 W μW, 140-150 °C, 15 min	26
2	MeCN	200 W μW, 140 °C, 30 min	80-91

A review of literature found that methodologies for retro Diels-Alder reactions with unstable reaction substrates utilised MeCN as the reaction solvent, albeit with conventional oven heating.[236] It was decided to utilise MeCN as the solvent for this application.

Thus, the substrate **1.80** was dissolved in MeCN and heated to 140 °C with 200 W microwave radiation (Table 3.5, condition 2). TLC and HRMS analyses found that after 30 minutes of heating, the starting material **1.80** had been consumed and that the desired product **1.81** had formed. A small amount of degradation product appeared to be present on the baseline of the TLC. Relative to Table 3.5, condition 1, the level of degradation product appeared minimal. In-order to remove the degradation by-product, the reaction mixture was filtered through a silica plug before concentration *in vacuo*. Pleasingly, this gave the desired product **1.81** in excellent yield (80-91%). Potentially, the improved outcome may be due to the increased polarity of MeCN, aiding heating by the microwave. It was also pleasing to note that the reaction had proceeded so cleanly (determined by NMR) that the crude filtrate could be used for the next synthetic step without need for further purification.
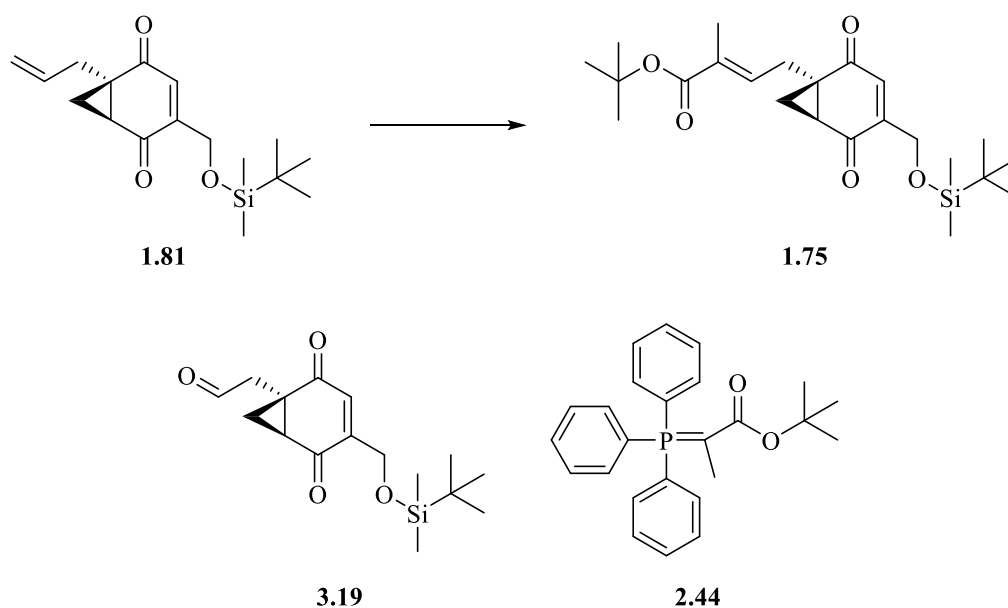
Scheme 3.17. Production of the final compound **1.75** through a 2-step procedure, ozonolysis followed by Wittig olefination. The aldehyde intermediate **3.19** and ylide **2.44** are shown here.

After the optimisation of the retro Diels-Alder reaction, compound **1.81** was treated in an ozonolysis procedure with a reductive workup to generate the aldehyde **3.19** before a final stabilised Wittig reaction with ylide **2.44** to install the *t*-butyl ester moiety to generate the final compound **1.75** in 40 % yield (Scheme 3.17, Figure 3.10). In summary, the desired compound **1.75** was produced in 5 steps with a total yield of 3.8 % from starting material **1.76**.
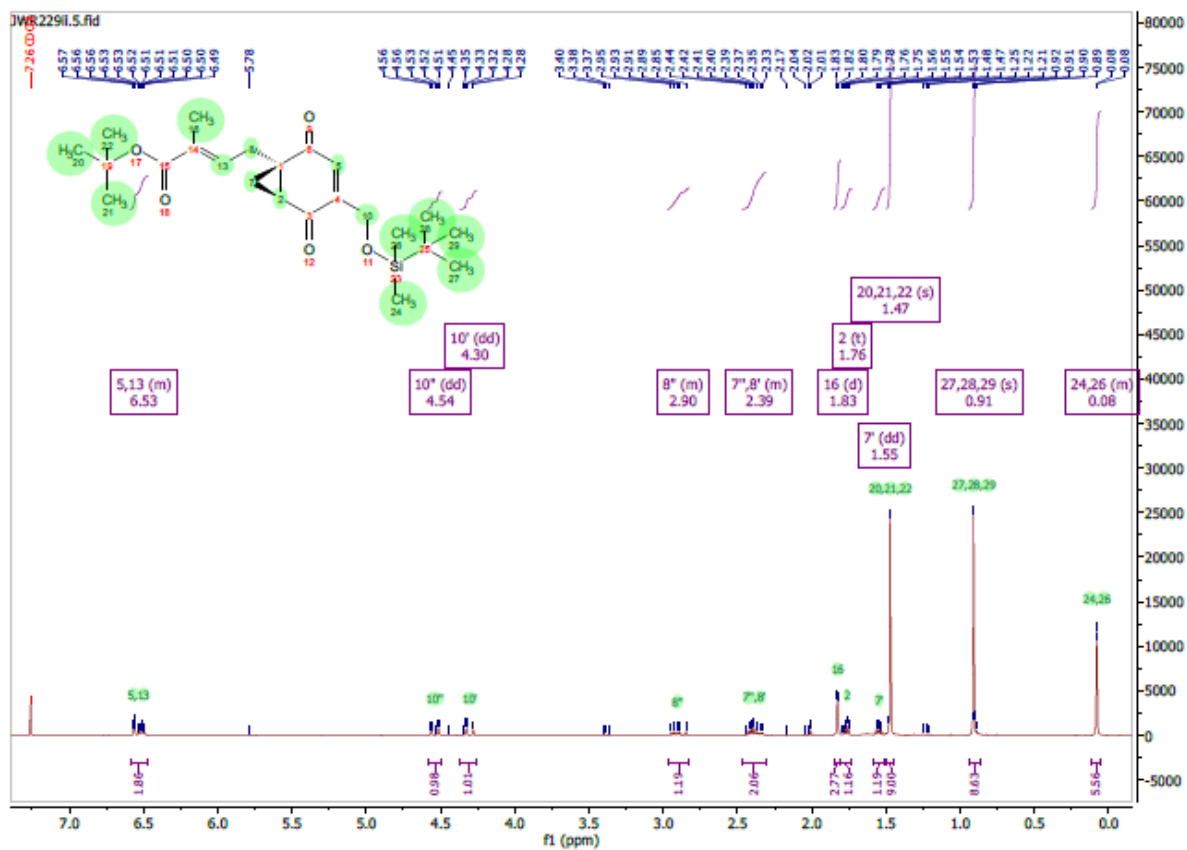
Figure 3.10. ^{1}H NMR of final cyclopropyl analogue

3.4 Conclusions

This chapter has described the production of a novel cyclopropyl analogue **1.75** of the epoxide containing compound **1.62**. An efficient and facile synthetic route to **1.75** has been established (Scheme 3.18).

The production of **1.75** necessitated the development of a Corey-Chaycovsky cyclopropylation reaction to facilitate the stereoselective installation of the cyclopropyl ring, providing cyclopropane **1.78**. Thorough optimisation of this key, synthetic transformation has been carried out utilising numerous procedures adapted from the literature. Pleasingly, the reaction of dione **1.76** in THF with the methylide species **3.7**, produced by treatment of trimethylsulfoxonium iodide **1.77** with *n*-BuLi, gave the desired compound in a good yield of 45 % (Scheme 3.18). Furthermore, NOESY spectroscopy confirmed that the cyclopropyl ring of **1.78** had installed *endo* with respect to the Diels-Alder adduct bridgehead.

The optimisation of the subsequent synthetic steps to afford the final cyclopropane **1.75** has also been carried out. Modification of the hydroxymethylation and subsequent TBDMS protection steps (previously used in Chapter 2) proved facile, with an increase in the number of reagent equivalents and reaction time providing the desired products in satisfactory yields (Scheme 3.18).

In addition, a highly efficient and reliable microwave-catalysed retro Diels-Alder reaction has been developed. Previous approaches, requiring harsh conditions, gave the desired product **1.81** with poor yield. With microwave assisted heating and relatively mild conditions, **1.81** was provided in an excellent yield, observed to be 80-91 % (Scheme 3.18). The microwave-catalysed reaction is a dramatic improvement upon previous conditions which have been utilised within this study and is makes the production of **1.75** more facile.

The cyclopropyl analogue **1.75** will be taken forwards for biological assessment as an inhibitor of staphylococcal *agr* activity. Determining the biological activity of **1.75** will be of great interest as it may prove insightful in the determination of the mode of action of ambuic acid and the analogues synthesised in this thesis. If **1.75** is inactive, it shows that the epoxide is the key functional group required for inhibition. Conversely, if **1.75** is active against the *agr* system, it would suggest that the epoxide is not necessary for inhibition. In this instance,

replacement of the epoxide (which can irreversibly alkylate a range of nucleopiles) would make the compound an improved candidate compound in the production of a novel therapeutic agent.
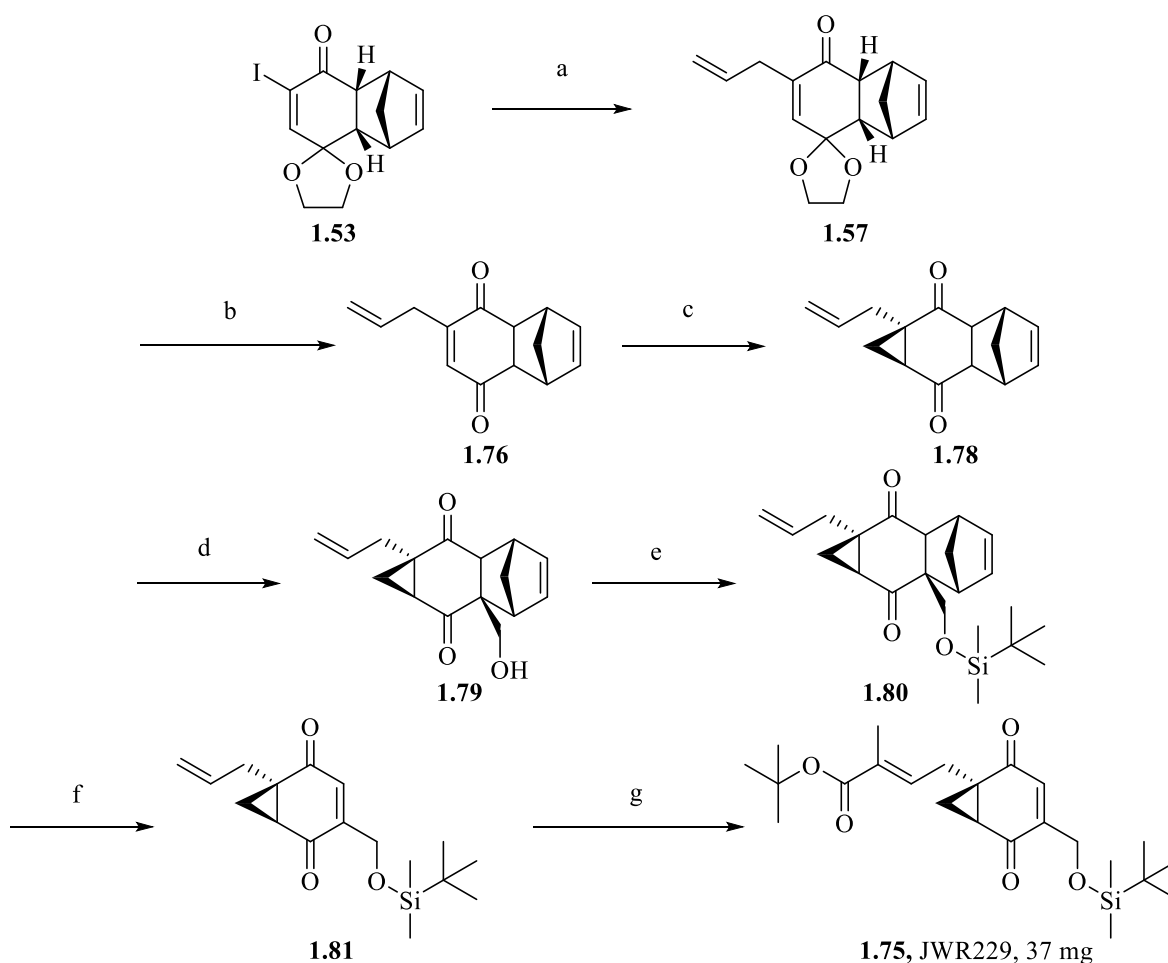
Scheme 3.18. The optimised route to the cyclopropyl analogue **1.75**. (a) Pd(PPh₃)₄, allyltributyl stannane, THF, 100 °C, 150 W µW radiation, 68%; (b) 1 N H₂SO₄, acetone, THF, 30 min, rt., 96%; (c) Me₃SOI, *n*-BuLi, THF, -78 °C 45%; (d) 37% (w/v) aqueous formaldehyde, DBU, THF, 30 min, 0 °C, 62%; (e) TBSCl, imidazole, DMF, 4 h, 0 °C. 82%; (f) MeCN, 140 °C, 200 W µM radiation, 91%; (g) O₃, dimethylsulfide, MeOH, -78 °C, 30 min then Ph₃P=C(Me)CO₂*t*-Bu, DCM, 2 h, -40 °C, 40%.

Chapter 4. Biological assessment of analogues

4.1 Chapter outline

The characterisation of the anti-virulence activity of analogues of ambuic acid, which have been synthesised is outlined in this chapter. In addition, compounds synthesised by Dr Leonardo Baldassarre will also be tested herein. Furthermore, the *agr*-inhibitory activity of ambuic acid will also be fully characterised.

The *agr*-inhibitory activity of the compounds will be assessed using a bioluminescent *lux*-based reporter strain of *agr* activity. Analogues which are found to be potent inhibitors of *agr* in the bioluminescence assay will be assessed for their ability to inhibit the production of α-haemolysin and AIP-I, both of which are phenotypically relevant markers of *agr* activity.

4.2 Introduction

The highly functionalised epoxycyclohexenone ambuic acid **1.1** has been previously assessed for anti-virulence properties in several studies.[153, 155] Through the use of anti-virulence screening of fungal extracts, Nakayama *et al.* identify ambuic acid **1.1** as an inhibitor of quorum sensing-mediated gelatinase production in *Enterococcus faecalis*, with an inhibitory concentration of approximately 10 µM.[153] Furthermore, no effect on bacterial growth was observed, even with concentrations up to 1 mM.[153]

In order to investigate the mechanism by which ambuic acid inhibits gelatinase biosynthesis, Nakayama *et al.* investigated the effect of ambuic acid has on gelatinase biosynthesis-activating protein (GBAP), an AIP analogue in *E. faecalis* (described in more detail in the chapter 1). To do this, they cultured the GBAP-negative strain of *E. faecalis* OU510 in media containing GBAP (to induce gelatinase expression) in the presence and absence of ambuic acid **1.1**.[153] Gelatinase expression is mediated by the *fsr* quorum sensing system (outlined in greater detail in chapter 1) and gelatinase activity can be used as a reporter of *fsr* activity. Nakayama *et al.* found that treatment of OU510 cells with ambuic acid had no effect on the observed level of gelatinase activity, thus it was suggested that ambuic acid has no effect on the ability of *E. faecalis* to sense the GBAP signal quorome molecule.[153] This is indicative of ambuic acid inhibition of GBAP production.[153]

In addition to investigating inhibition of GBAP signalling in *E. faecalis*, Nakayama *et al.* probed the effect of ambuic acid **1.1** on quorum sensing in other Gram-positive bacteria, namely *S. aureus* and *Listeria innocua*.[153] They found that ambuic acid inhibits *agr* quorum sensing in *S. aureus* and the biosynthesis of cyclic peptide quoromes in *L. innocua*.[153]

Todd *et al.* further investigated the effect of ambuic acid **1.1** on *agr* activity in *S. aureus*.[155] They found that ambuic acid functioned as an inhibitor of AIP-I biosynthesis in a strain where AIP-I biosynthesis is de-coupled from quorum sensing.[155] Inhibition of AIP-I biosynthesis by ambuic acid was observed in the MRSA strain USA300 (IC$_{50}$= 2.5 ± 0.1 µM) as well as the constitutively producing AIP-I strain, thus indicating the inhibition of AIP-I biosynthesis.[155] To further confirm this, the authors investigated inhibition of AIP-I production in the

constitutively producing strain with the known inhibitor of AgrC, AIP-II.[155] Todd *et al.* found that AIP-II was unable to inhibit production of AIP-I in this strain.[155]

Todd *et al.* further showed the promise of ambuic acid as an inhibitor by assessing its *in vivo* inhibitory activity in a mouse murine dermal infection model of MRSA.[155] With a single dose of ambuic acid (either 5 µg or 25 µg), delivered in conjunction with MRSA challenge, a reduction in skin ulcer formation was observed, in a dose-dependent manner.[155] Furthermore, when the mice were challenged with an *agr*-driven *lux* containing strain, the authors observed a reduction in virulence in animals treated with ambuic acid.[155]

These data demonstrated that ambuic acid **1.1** is an anti-virulence compound of some utility. Thus, the anti-virulence activity of ambuic acid and the activity of numerous unique synthetic analogues will be discussed herein.

4.3 The characterisation of the anti-virulence properties of ambuic acid

The initial testing of ambuic acid was carried out using the methicillin-sensitive *S. aureus* SH1000 (EJM82) native *agr* activity assay, as outlined in chapter 5.1. The SH1000 *S. aureus* cells with an intact *agr* locus are modified at the *attB2* ectopic locus with a re-engineered *lux* cassette from *Photorhabdus luminescens*, which is under the direct control of the *agrP3* promoter.[237-238] This provides a real-time, luminescent reporter of transcriptional activity from the native *agrP3* promoter (Figure 4.1).

The *lux* cassette is under the direct transcriptional control of the *agrP3* promoter and thus, an increase in luminescence is indicative of increased *agr* activity. Conversely, a decrease in the observed luminescent signal, relative to the solvent only control is indicative of inhibition of *agr* activity. The EJM82 strain contains an intact *agr* (group-I) system and the only source of AIP is that which is produced by the cells. This is termed native AIP production assay herein.
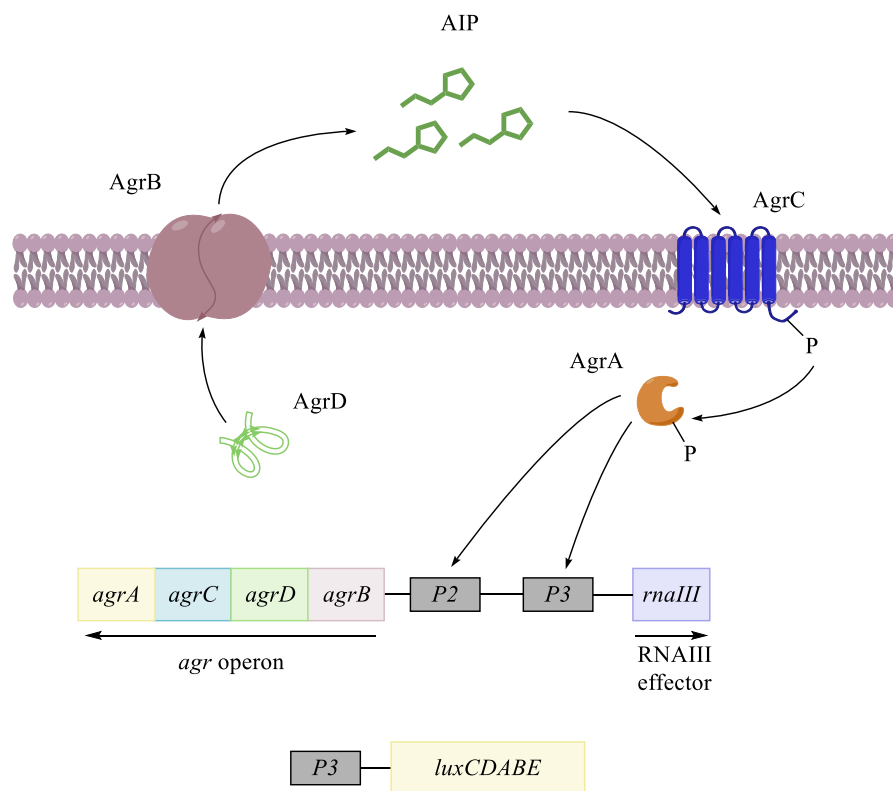
Figure 4.1. A schematic of the EJM82 reporter strain used for assessment of anti-agr activity of the test compounds.

Using the native AIP production assay, it was found that ambuic acid **1.1** was a potent inhibitor of *agr* activity (Figure 4.2) as a result of inhibition of AIP production. The IC$_{50}$ value was calculated to be 0.95 ± 0.13 μM with complete shutdown of *agr* activity observed at concentrations exceeding 10 μM (Figure 4.2). The IC$_{50}$ observed experimentally in this study corroborates with those reported by Todd *et al*. (2.5 ± 0.1 μM).[155]
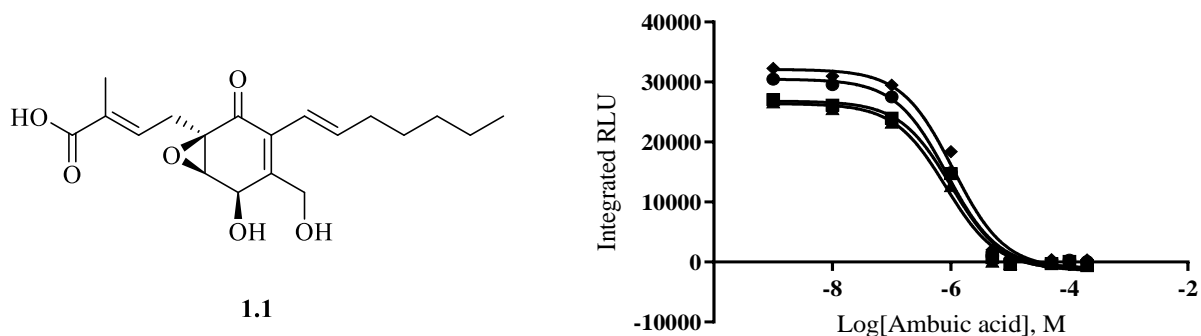
Figure 4.2. Ambuic acid **1.1**. and the IC$_{50}$ curve generated from the EJM82 native production assay assay (IC$_{50}$ 0.95 ± 0.13 μM, n= 4). Integrated RLU was calculated by dividing the luminescence value by the corresponding OD$_{600}$ value and plotting against time for the duration of the assay, the area under the curve was measured at t > 210 mins, giving integrated RLU.

It was important to establish whether the effect caused by ambuic acid **1.1** (Figure 4.2) in the native AIP production assay was a real effect on *agr* activity, or non-specific inhibition of *lux* by ambuic acid. In order to achieve this, a Δ*agr* strain of *S. aureus* RN4220 with a plasmid based pxyl/ tet inducible *lux* cassette, was utilised. Within these cells, the *lux* bioluminescent signal is de-coupled from regulation by *agr* activity (as in the EJM82 cells) and is instead, under the direct control of a tetracycline inducible promoter, wherein treatment with tetracycline gives a bioluminescent signal.

Thus, the cells were treated with a range of concentrations of anhydrous tetracycline (1-100 ng/ mL) and ± 20 µM ambuic acid. Increasing the concentration of anhydrous tetracycline was found to increase the bioluminescent signal. Importantly, upon analysis of bioluminescent signal, when comparing treatment with 20 µM ambuic acid to the DMSO only control, no significant difference is observed (Figure 4.3). This suggests that ambuic acid has minimal effect on the *lux* bio reporter, implying that the effect observed in the native AIP production assay (Figure 4.2) was inhibition of *agr* activity and not a non-specific effect on the *lux* reporter.
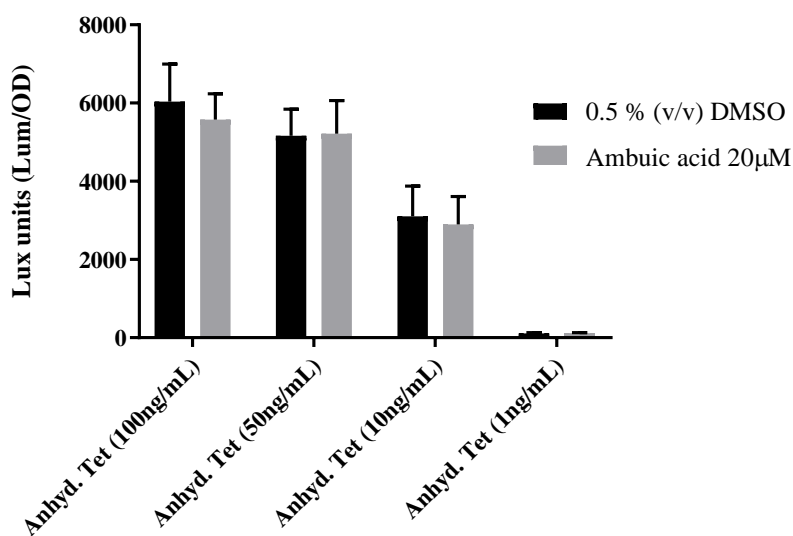
Figure 4.3. Bar chart showing levels of inducible lux luminescence ± 20 µM ambuic acid (n= 3, bars denote SD).

In addition to the observed decrease in the bio-reporter signal in the native AIP production assay, it was important to determine whether ambuic acid has an effect on the level of toxin production, with the focus here on α-haemolysin. As described in chapter 1, activation of *agr* leads to the upregulation of the production of numerous exotoxins, such as α-haemolysin. Investigation of the effect of ambuic acid **1.1** on α-haemolysin production thus provides a further, viable readout for the effect of ambuic acid on *agr* activity.

In order to investigate the effect of ambuic acid on the production of α-haemolysin, the CA-MRSA strain USA300_LAC was grown with shaking in the presence of increasing concentrations of ambuic acid, from 1-40 µM. These concentrations of ambuic acid were selected as full shutdown of *agr* activity was observed in the native AIP-I production assay with concentrations >10 µM (Figure 4.2). 1 µM was also chosen as it is near the experimentally observed IC$_{50}$ (Figure 4.2).

After 8 h of bacterial growth, the growth media were collected and assessed for α-haemolysin content by Western blotting. It was found that increasing concentrations of ambuic acid caused a decrease in the level of α-haemolysin in culture supernatant relative to the solvent (DMSO) control (Figure 4.4).
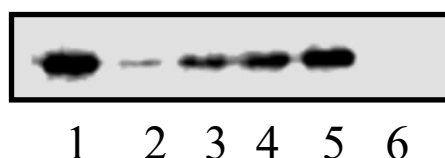
Figure 4.4. Western blot showing inhibition of α-haemolysin by the *S. aureus* CA-MRSA strain USA300_LAC (1) 0.5 % (v/v) DMSO, (2) ambuic acid 40 µM, (3) ambuic acid 20 µM, (4) ambuic acid 10 µM, (5) ambuic acid 1 µM, (6) AIP-95 1 µM (positive control).

With the finding that ambuic acid **1.1** has promising inhibitory activity towards the *agr* system, ambuic acid **1.1** was assessed for anti-bacterial properties. As described in chapter 1, the disruption of bacterial growth is problematic in the development of anti-virulence compounds, as anti-growth activity would impart a selective pressure for the development of resistance to the compound. It was found that ambuic acid **1.1** has minimal effect on *S. aureus* growth (Figure 4.5)
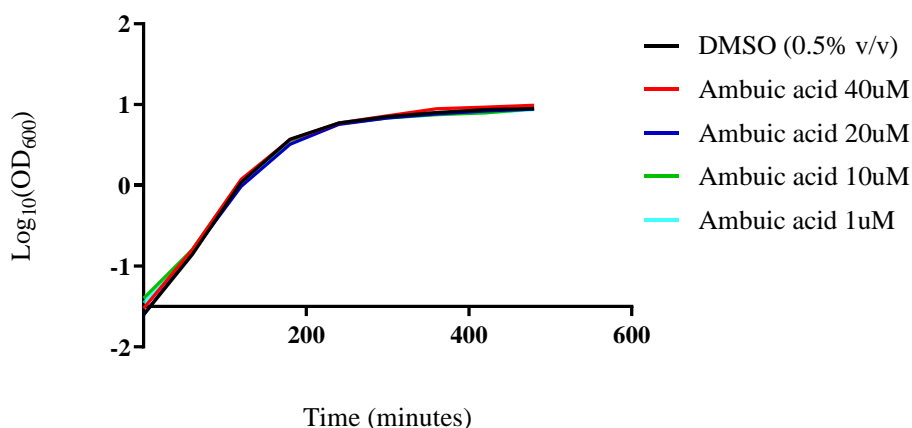
Figure 4.5. Growth curve of *S. aureus* USA300_LAC in the presence of increasing concentrations of ambuic acid.

It was also important to determine whether ambuic acid **1.1** was having an effect on the sensing of the extracellular AIP-I signal molecule by the transmembrane cognate receptor AgrC1. Investigation as to whether ambuic acid has an effect on the AgrC1 receptor will aid in the identification of the molecular target of ambuic acid.

To investigate whether ambuic acid **1.1** has an effect on the AgrC1 receptor, the *S. aureus* ROJ143 strain was utilised. This strain is a Δ*agr* background containing *agrP3 lux* and *agrP2agrC1agrA* and has previously been reported by Jensen *et al.*.[121] This bacterial construct is incapable of synthesising AIP-I as it lacks the required cellular machinery (AgrB and AgrD) for AIP-I synthesis. ROJ143 is, however capable of sensing AIP-I as it contains AgrC1 and AgrA1. These cells are capable of producing a *lux* bioluminescent signal in response to exogenous AIP as they contain the *luxABCDE* cassette under the direct transcriptional control of the *agrP3* promoter. Providing ROJ143 with exogenous AIP-I within the growth medium elicits a biomluminescent response. This strain is used for specifically investigating inhibitors of AgrC and AgrA, the proteins involved in the sensing of AIP-I. Thus, ROJ143 cells were treated with increasing concentrations of AIP-I (agonist) to generate an EC_{50} curve (Figure 4.6). Additionally, the cells were treated with 1 μM and 10 μM ambuic acid. 10 μM ambuic acid was chosen as the highest concentration in this assay, as in the native AIP production assay (Figure 4.2), full shutdown of *agr* activity was observed at this concentration.

164
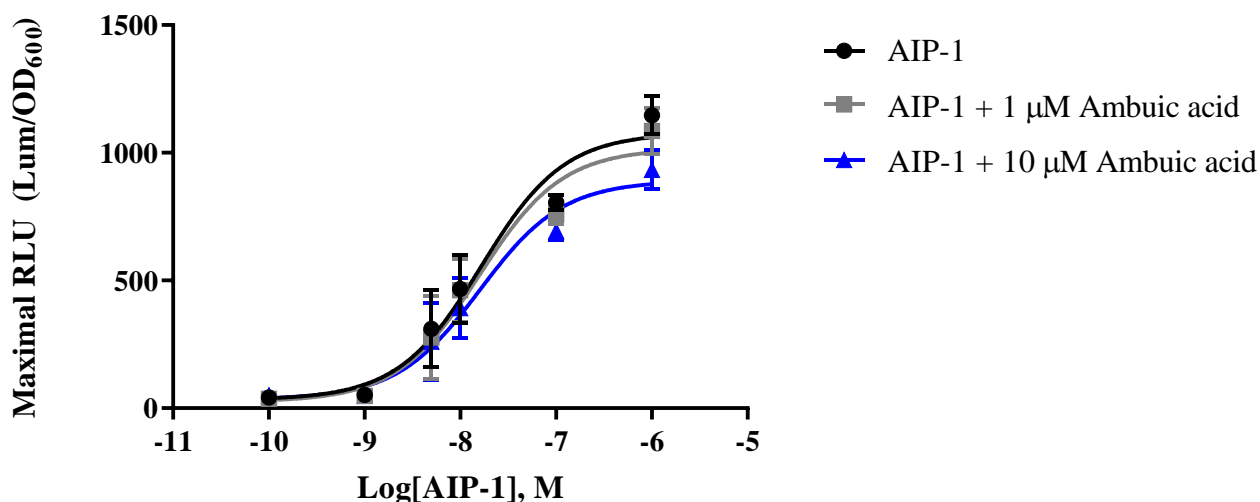
Figure 4.6. EC$_{50}$ curves of AIP generated from the ROJ143 assay in the presence of ambuic acid. EC$_{50}$ AIP-I alone= 16.52 ± 31.06 nM. EC$_{50}$ AIP-I and 1 µM ambuic acid= 15.83 ± 24.93 nM. AIP-I and 10 µM ambuic acid EC$_{50}$= 15.99 ± 29.45 nM. (n= 3, bars denote SD).

The data generated from the ROJ143 assay found that ambuic acid has minimal effect on the sensing of AIP-I by cognate AgrC1 (Figure 4.6). No evidence was observed of competitive inhibition, potentially of AgrC1 with comparable EC$_{50}$ values with and without ambuic acid. This data suggests that ambuic acid targets the biosynthesis of the AIP molecule, which corroborates with data reported by both Nakayama *et al.* and Todd *et al.*.[153, 155]

These data showed that ambuic acid is a promising, potent inhibitor of virulence in *S. aureus* whilst exhibiting minimal effect on bacterial growth. This makes it a promising compound for study.

1.1
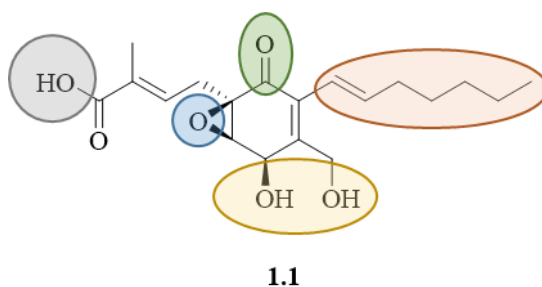
Figure 4.7. Regions of ambuic acid **1.1** to be modified. Grey, compare the free acid against the t-butyl ester. Blue, production of an inert isostere of the epoxide. Green, modification of the ketone within the epoxycyclohexenone ring. Orange, removal of the right-hand heptenyl chain. Yellow, modification at the primary and secondary alcohols.

Having established that ambuic acid **1.1** is a potent inhibitor of *agr* activity via inhibition of AIP production, chemical modification of the compound was undertaken to produce unique

analogues. The main areas of modification within this study are: (a) the carboxylic acid moiety, (b) the ketone within the epoxycyclohexenone ring, (c) the epoxide, (d) the right hand (*E*)-heptene chain and (e) modification of the two alcohols (Figure 4.7). Analogues investigating how modification of the above position have been synthesised as part of this study (outlined in chapters 2 and 3) as well as those synthesised by Dr Leonardo Baldassarre.

4.4 Evaluation of truncated ambuic acid analogues

Racemate **1.52** (LB75) (Figure 4.8), synthesised by Dr Leonardo Baldessarre was tested in the EJM82 native AIP production assay. It was found to be active, though lower in potency (Figure 4.8) and thus further analogues were synthesised. Analogues of this compound were synthesised to determine the importance of the heptenyl moiety.
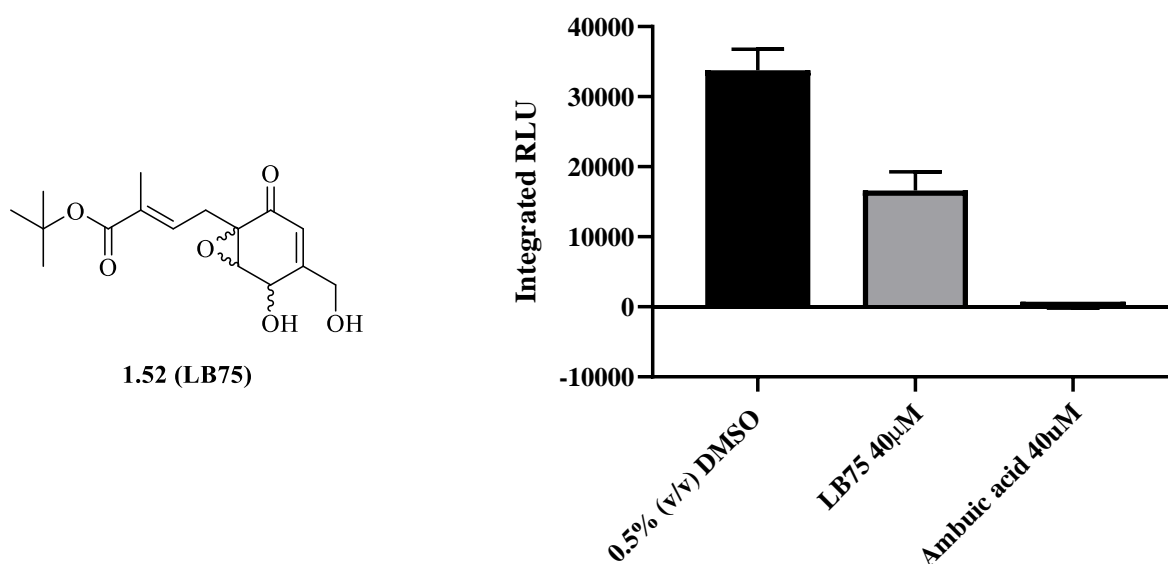
Figure 4.8. Racemate **2.44** (LB75) and a bar chart showing results of an EJM82 native AIP production assay where cells treated with a single concentration of compound (n= 3, bars denote SD, values blanked with Δagr 0.5 % (v/v) DMSO).

With the initial promise of racemate **1.52** (LB75) as a weak inhibitor of *agr*-mediated virulence, enantio-selective syntheses of the (+) and (-) variants were carried out to yield compounds **1.74** (LB153), **1.62** (LB151) and **1.63** (JWR28) (Figure 4.9). The compounds **1.62** (LB151) and **1.63** (LB153) were synthesised by Dr Leonardo Baldassarre. These compounds were tested using the EJM82 native AIP production assay and were found to be potent inhibitors of *agr* expression (Figure 4.9).

A

1.74 (LB153)
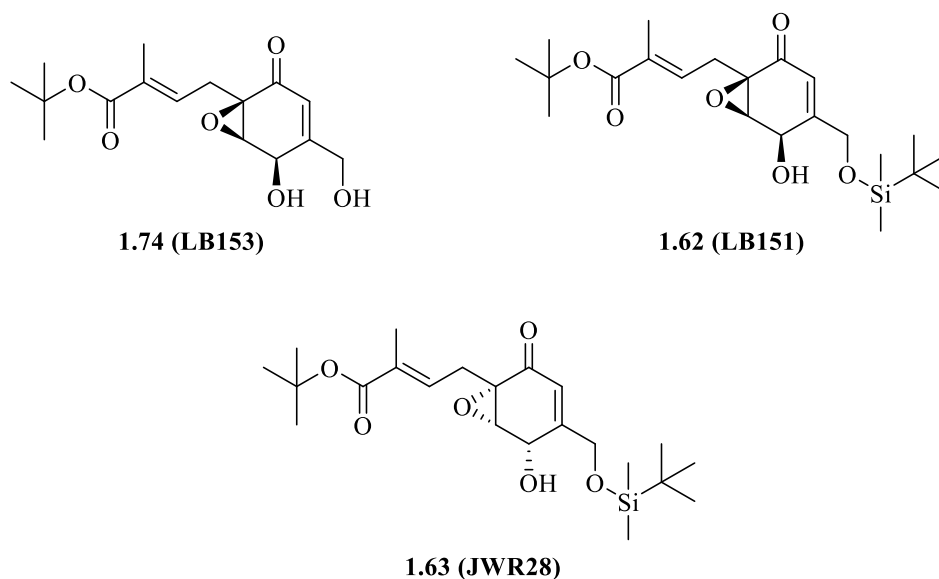
1.62 (LB151)

1.63 (JWR28)

B
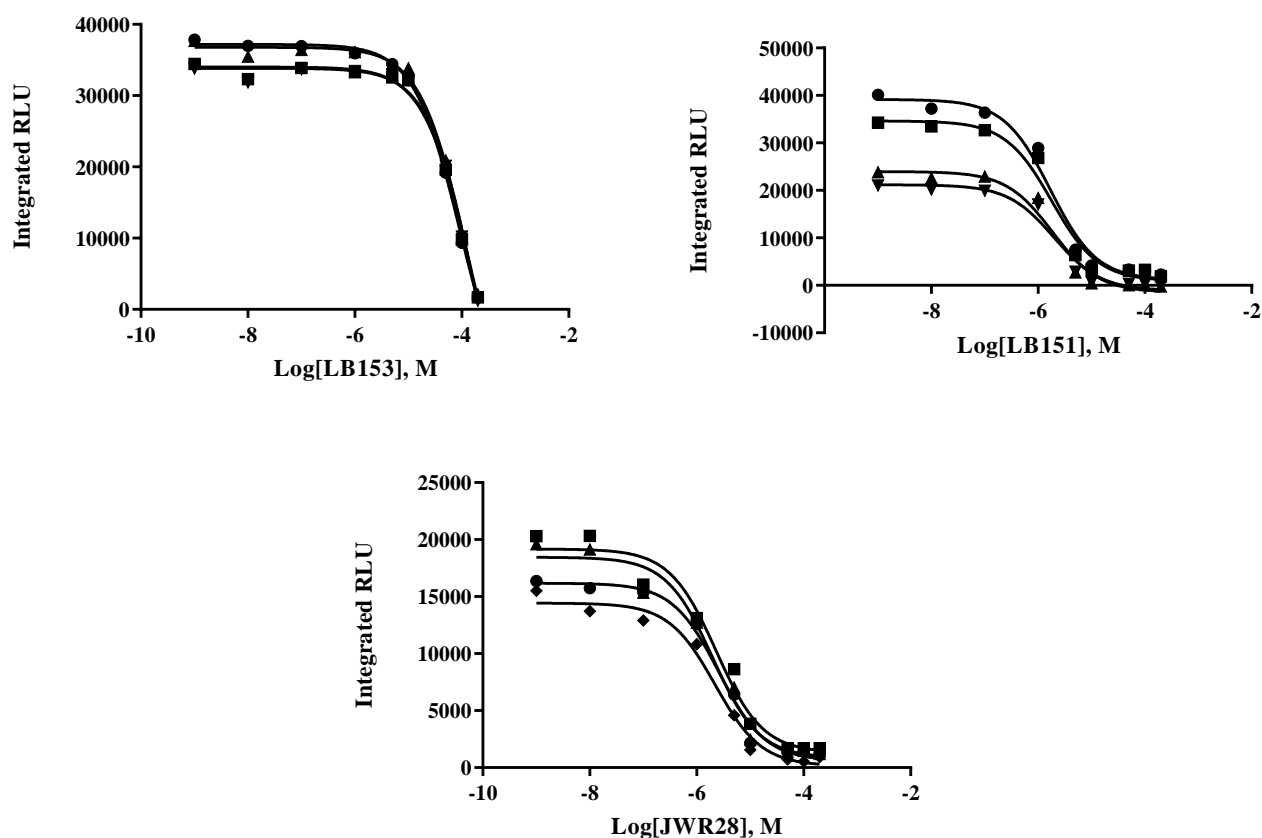
Figure 4.9. Enantiomerically pure analogues of the promising inhibitor **1.74**. **(A)** The (+) enantiomer **1.74** (LB153), the silyl ether analogue **1.62** (LB151) and the (-) enantiomer **1.63** (JWR28). **(B)** IC_{50} curves of the above compounds generated from the EJM82 native AIP production assay. The IC_{50} values are: **LB153:** 133.95 ± 33.80 µM, **LB151:** 1.84 ± 0.13 µM and **JWR28:** 2.27 ± 0.25 µM with 7 % residual activity (n= 4 for all IC_{50} curves)

167

Table 4.1. IC$_{50}$ values of the LB75 analogues

Compound	IC$_{50}$ (µM)	Residual activity (% maximal)	cLogP
1.74 (LB153)	133.95 ± 33.80	-	0.57
1.62 (LB151)	1.84 ± 0.13	-	3.98
1.63 (JWR28)	2.27 ± 0.25	7	3.98

The diol **1.74** (LB153), the (+)- enantiomer of **1.52** (LB75) was found to inhibit *agr* activity with an IC$_{50}$ of 133.95 ± 33.80 µM, which is ~140 times less potent than the parent natural product ambuic acid **1.1** (IC$_{50}$ = 0.95 ± 0.13 µM). The silyl ether compounds **1.62** and **1.63**, the (+)- and (-)-silyl ether precursors to **1.74**, respectively were also tested in the same assay. Unexpectedly, both of these compounds were found to be potent inhibitors of *agr* mediated virulence with IC$_{50}$ values of a similar order to that of ambuic acid **1.1** (Table 4.1).

Hence, although the removal of the heptenyl moiety has a dramatic effect on the inhibitory potency of **1.74**, it is clear that there is a trend in lipophilicity and potency. For example, compound **1.74** with a low cLogP value of 0.57 has a lower potency than compounds **1.62** and **1.63**, both of which have cLogP values of 3.98 (Table 4.1). The lower potency of **1.74** relative to these compounds could potentially be explained by poor cell penetration and/or poor membrane localisation for interaction with the putative target AgrB, imparted by a lower level of lipophilicity. Whereas the higher level of lipophilicity of **1.62** and **1.63** may enhance cell penetrative properties, thus allowing for increased potency due to increased compound access to the target.

In addition to the trends observed with change in lipophilicity, these data provide additional information about ambuic acid. Firstly, all compounds show inhibition of the *agr* system and they all lacked the heptenyl chain, which is present in ambuic acid **1.1**. Particularly focussing on **1.62** and **1.63** which have comparable IC$_{50}$ values to ambuic acid, loss of the heptenyl chain has minimal effect on compound activity (**1.62** IC$_{50}$= 1.84 ± 0.13 µM, **1.63** IC$_{50}$= 2.27 ± 0.25 µM). This suggests that the heptenyl chain is not involved in a specific inter-molecular (drug-target) interaction, as, if this were the case, an effect on compound activity would be expected. The heptenyl chain may however be beneficial in enhancing the cell-penetrative properties of ambuic acid through a general increase in lipophilicity. The fact that compounds **1.62** and **1.63** have similar activities to ambuic acid and when the silyl ether is dismantled in **1.74**, causing a

loss of potency is further evidence of this. This suggests that a level of lipophilicity is required for a potent inhibitor of *agr* activity.

Secondly, stereochemistry affects the overall compound efficacy, not potency. Directly comparing compounds **1.62** and **1.63** (Figure 4.9,Table 4.1), both compounds have a comparable potency with IC$_{50}$ values of a similar order. The difference in activities is in overall efficacy. The compound **1.62** causes complete shutdown of *agr* activity whereas **1.63** inhibition leaves ~7 % residual activity (Figure 4.9, Table 4.1).
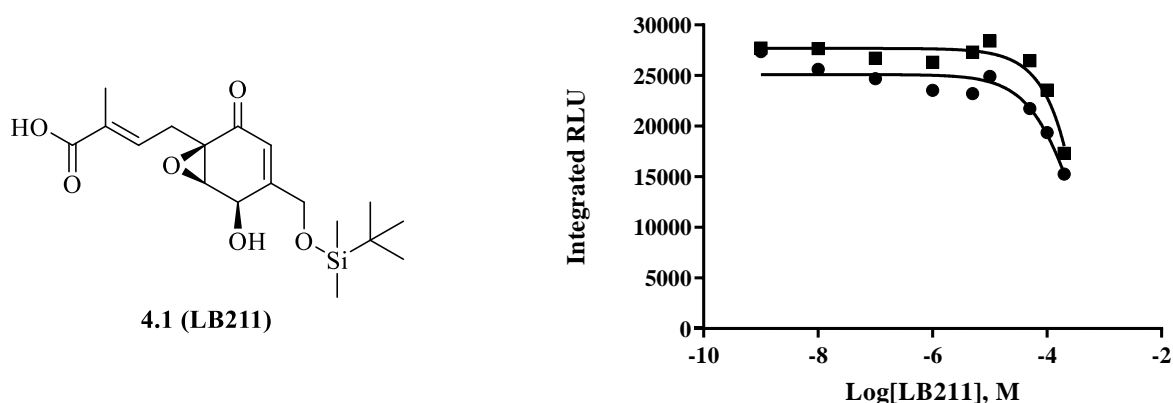
Figure 4.10. The free acid variant of **2.1**, **4.1** (LB211) and the IC$_{50}$ curve generated from the EJM82 native AIP production assay (IC$_{50}$ = >200 µM, n= 2). cLogP of LB211= 2.2922

Dismantling the *t*-butyl ester to afford the free acid **4.1** (LB211, produced by Dr Leonardo Baldassarre), like the removal of the silyl ether led to a large effect on compound activity when assessed in the EJM82 native AIP production assay (Figure 4.10). Free acid **4.1** has an IC$_{50}$ of >200 µM, several hundred fold higher than both of the more potent corresponding analogue **1.62** and the parent natural product ambuic acid **1.1**. The loss of hydrophobicity may be detrimental to the cell penetrative properties of the compound, having a negative effect on compound potency.

With the initial promise of silyl ether 1.62, and the previous utilisation of silyl ethers within theliterature to improve the activity of withaferin A **2.60** (described previously in chapter 2), it was decided to synthesise a number of unique silyl ether analogues, outlined in chapter 2. Unfortunately, the synthesis proved problematic and it was only possible to produce one analogue, compound **2.62** (JWR99), the dimethyl thexyl silyl ether (Figure 4.11). The incremental increase in hydrophobicity compared to the *t*-butyl dimethyl silyl ether **1.62** (cLogP **2.62** = 4.41, **1.62**= 3.98) leads to a small increase in potency (IC$_{50}$ **2.62**= 0.65 ± 0.07

μM, IC$_{50}$ **1.62**= 1.84 ± 0.13 μM). This is further evidence that a level of hydrophobicity is required for the compound to be a potent inhibitor of *agr*.
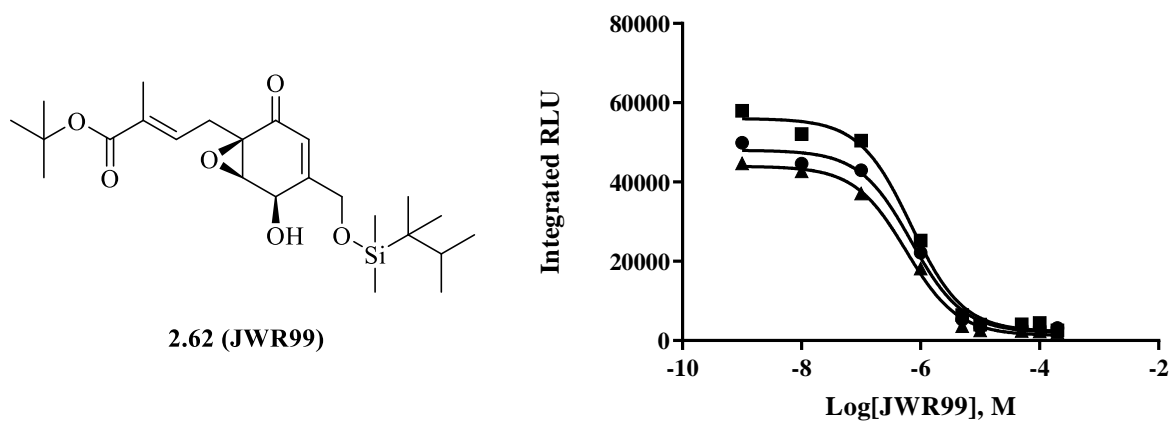
2.62 (JWR99)

Figure 4.11. The dimethyl thexyl silyl ether **2.62** (JWR99) and the IC$_{50}$ curve generated from the EJM82 native AIP production assay. IC$_{50}$ = 0.65 ± 0.07 μM (n= 3).

A range of ketal analogues based on the racemate **2.88** were also synthesised. The synthesis of the ketals is outlined in chapter 2. These compounds have the potential to yield some interesting SAR information about ambuic acid. Replacement of the two alcohols with cyclic ethers may yield interesting information about how these positions are involved in drug-target interactions.
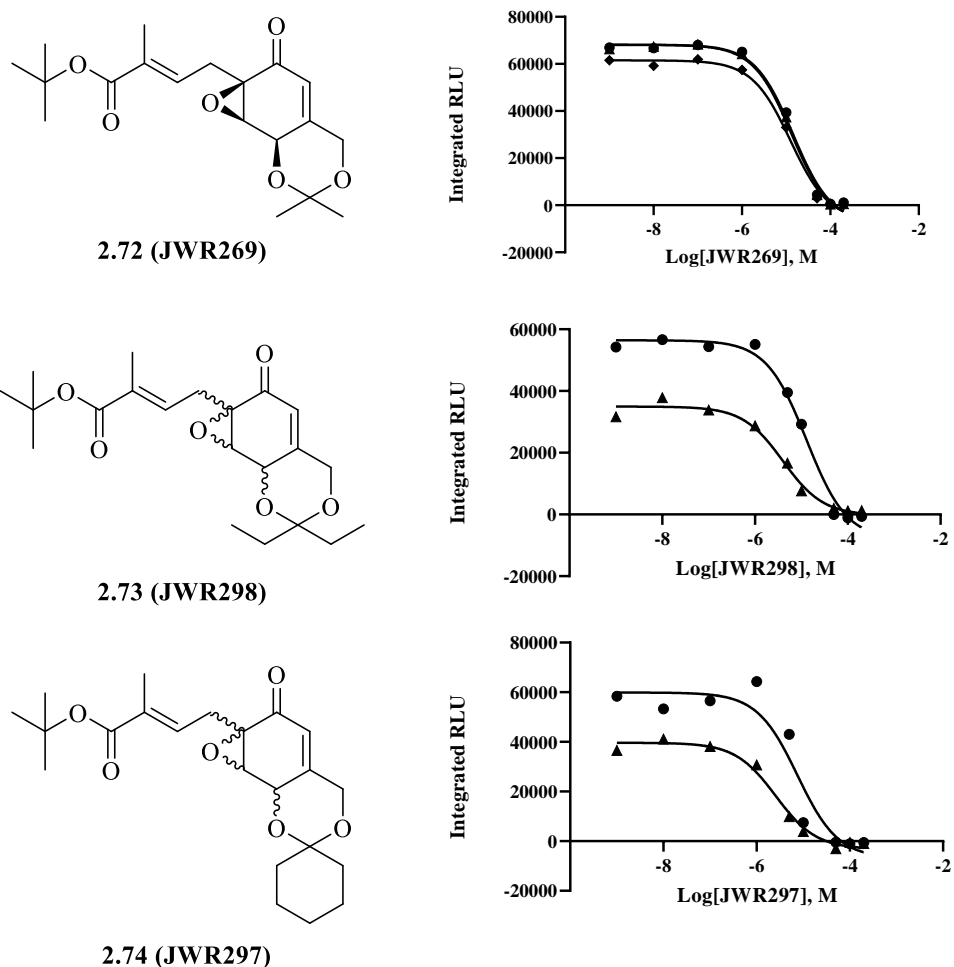
Figure 4.12. The structures and IC_{50} curves from the native AIP-I production assay of the ketal analogues, the dimethyl ketal **2.72** (JWR269), the diethyl ketal **2.73** (JWR298) and the cyclohexyl ketal **2.74** (JWR297). The IC_{50} curves of the above compounds were generated using the EJM82 native AIP-I production assay. The IC_{50} values are: **JWR269:** 13.34 ± 0.08 µM (n=3), **JWR298:** 8.47 ± 6.32 µM (n=2), **JWR297:** 5.06 ± 3.52 µM (n=2).

Table 4.2. The IC_{50} values of the ketal analogues

Compound	IC_{50} (µM)	cLogP
2.72 (JWR269)	13.34 ± 0.08	2.54
2.73 (JWR298)	8.47 ± 6.32	3.59
2.74 (JWR297)	5.06 ± 3.52	3.49

The bioactivity of the ketal analogues (Figure 4.12) was assessed in the EJM82 native AIP assay (kindly carried out by Dr Ewan Murray of the Chan/Williams group due to COVID-19 restrictions). Dimethyl ketal **2.72** was found to inhibit *agr* activity with an IC_{50} of 13.34 ± 0.08 µM, approximately 13 fold less potent than ambuic acid and the potent synthetic analogue **2.1** (Figure 4.12, Table 4.2). In contrast to **1.62**, compound **2.72** is less lipophilic, which again correlates to a loss of potency (Table 4.2). Additionally, the replacement of the secondary alcohol within **1.62** with the dimethyl ketal in **2.72** may be a cause of this loss of potency. Additionally, the formation of the new six-membered ketal ring, containing the two cyclic ethers may have a detrimental effect on compound activity. This ring may adopt two conformers (chair/boat) and one/both of the conformers may be detrimental to compound binding, having a negative effect on the activity of **2.72**.

Interestingly, dimethyl ketal **2.72** was found to have an effect on the growth of the bacterial cells. Increasing concentrations of compound caused a delay in the onset of bacterial log phase growth (Figure 4.13), with the most pronounced effect being observed when the cells are treated with 200 µM **2.72** which resulted in a clear dose-dependent effect. Comparing 200 µM **2.72** with untreated 0.5 % (v/v) DMSO, the delay of onset of log phase growth is ~150 minutes (Figure 4.13). **2.73** and **2.74** both also had a minor effect on bacterial growth (data not shown), albeit less of an effect than **2.72**.
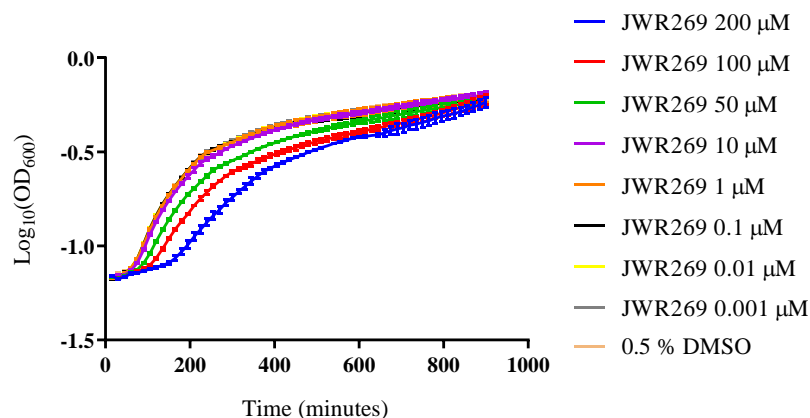
Figure 4.13. Growth curves of EJM82 cells, grown in a TECAN plate reader in the presence of increasing concentrations of dimethyl ketal **2.72** (JWR269) in 0.5 % (v/v) DMSO

The bioactivity of both the diethyl (**2.73**) and cyclohexyl (**2.74**) ketals was assessed in the EJM82 native AIP-I assay (again, kindly undertaken by Dr Ewan Murray due to COVID-19 restrictions). Both compounds **2.73** and **2.74** were found to be potent inhibitors of *agr* activity with IC_{50} values of 8.47 ± 6.32 µM and 5.06 ± 3.52 µM respectively (Figure 4.12, Table 4.2).

Comparing the dimethyl ketal (**2.72**) with the diethyl ketal (**2.73**), the increase in alkyl chain length has a positive effect on compound potency (Table 4.2). The incremental increase in lipophilicity may be the cause of this. Interestingly, the cyclohexyl ketal **2.74** was also found to be a potent inhibitor, this is of particular interest as **2.74** contains a unique, tricyclic structure, not present in any of the other synthesised analogues. Like the diethyl ketal (**2.73**) the cyclohexyl ketal (**2.74**) again shows improved potency when compared to the dimethyl ketal (**2.72**), this could be attributed to its relative increase in lipophilicity (Table 4.2).

Further information can be gained from the diol **4.2** (LB221) (Figure 4.14) where the alcohol at position 1 of the epoxycyclohexenone ring is a mixture of the (*S*) and (*R*) stereoisomers. Reduction of the ketone to the alcohol equates to ~13 fold loss of anti-virulence potency (Figure 4.14). This may indicate that the ketone may be a key molecular contact between drug and target. Additionally, as **4.2** is a diastereoisomeric mix of (*S*) and (*R*) alcohols, one of the two enantiomers may have a detrimental effect on the anti-virulence activity of the compound.

173
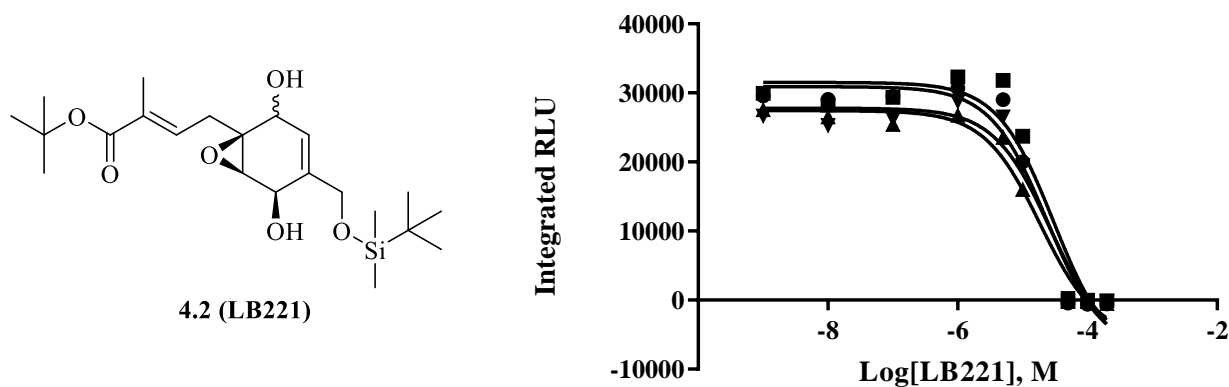
Figure 4.14. The diol **4.2** (LB221) and the IC_{50} curve from the EJM82 assay. $IC_{50} = 24.67 \pm 4.84$ μM (n= 4).

Furthermore, in a comparison between **1.62** and diol **4.2**, loss of the Michael acceptor, a possible site of covalent, conjugate addition of the key catalytic cysteine within the postulated target AgrB, leads to ~ 20 fold loss of potency. Within **1.62**, the cyclic enone may facilitate conjugate addition of the thiol of the key catalytic Cys84 within AgrB at the β-carbon of the Michael system. This would lead to alkylation of the Cys84 residue leading to inhibition of proteolytic activity. Within the diol **4.2**, the Michael system is destroyed through reduction of the ketone to the corresponding secondary alcohol, loss of this conjugation prevents conjugate addition of the thiol of Cys84 to the β-carbon. The loss of potency when comparing cyclic enone **1.62** and diol **4.2** could suggest that conjugate addition might be involved in inhibitory activity.

To further investigate this, it was decided to synthesise an unreactive, cyclopropyl analogue of the epoxide in order to determine whether the epoxide was the key functional group, or whether Michael addition may be the cause of inhibition.

4.5 Bioactivity of the cyclopropyl analogue
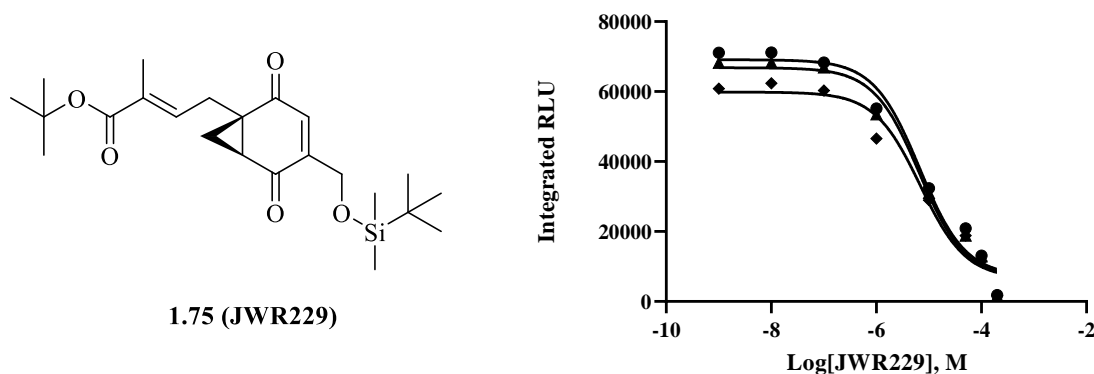
Figure 4.15. The cyclopropyl isostere **1.75** (JWR229) of the lead truncated ambuic acid analogue **1.62** and the IC$_{50}$ curve generated from the EJM82 native AIP production assay. IC$_{50}$ = 6.69 ± 0.14 µM (n= 3)

The cyclopropyl analogue **1.75** (JWR229), (Figure 4.15) the total synthesis of which is outlined in chapter 3 may provide some interesting information about the mechanism by which the analogues inhibit *agr* mediated virulence. As outlined within the introduction and chapter 3, it is postulated that ambuic acid is a covalent inhibitor of the membrane bound cysteine protease AgrB, and with a conserved mechanism to the epoxysuccinates uses the epoxide electrophilic centre to irreversibly alkylate the key catalytic cysteine. It was anticipated that isosteric replacement of the epoxide of the lead ambuic acid analogue **2.1** with a cyclopropyl ring would lead to substantial attenuation of inhibitory activity.

The *agr*-inhibitory properties of **1.75** (JWR229) were assessed as above using the EJM82 native AIP production assay (kindly carried out by Dr Ewan Murray of the Williams/Chan group, due to COVID-19 restrictions). Unexpectedly, the cyclopropyl analogue **1.75** was found to be active against the *agr* system with an IC$_{50}$ value of 6.69 ± 0.14 µM. This is approximately 6-fold less than the epoxide containing equivalent.

Retention of potent activity may suggest one of two things. Firstly, that the epoxide is not critical to inhibitory activity because the compounds function by a different mode of action. Replacement of the electrophilic epoxide centre with a less reactive cyclopropyl isostere caused only a ~6 fold reduction in compound potency when compared to LB151, suggesting a different mechanism of inhibition than postulated in chapter 3. Secondly, that there may be sufficient non-covalent interactions between **1.75** and the putative target AgrB to allow for non-covalent inhibition.

175

The observed bioactivities of diol **4.2** (LB221) and the cyclopropyl analogue **1.75** (JWR229) at present prove inconclusive in the determination of a possible covalent mode of action of the ambuic acid analogues. At present, further study is required to determine the mode of action of the compounds and whether they are covalent inhibitors.

4.6 Ambuic acid analogues

In addition to the truncated ambuic acid analogues tested above, analogues of full ambuic acid have been synthesised by Dr Leonardo Baldessarre. Firstly, analogues of ambuic acid **2.32** (LB163) and **4.3** (LB182) were synthesised by Dr Leonardo Baldessarre and tested in the EJM82 native AIP production assay (Figure 4.16). The silyl ether **2.32** was found to be toxic to the cells, potentially due to hydrophobicity and disruption of the membrane (cLogP= 7.44) (Figure 4.16). However compound **4.3**, shows potent inhibitory activity of the *agr* system with an IC_{50} of 1.53 ± 0.17 μM, comparable to that of the natural product ambuic acid (IC_{50} 0.95 ± 0.13 μM). Masking of the acid within ambuic acid as a *t*-butyl ester has minimal effect on the ability of the compound to act as a potent inhibitor of *agr*. This suggests that the acid may not be critical for compound activity.
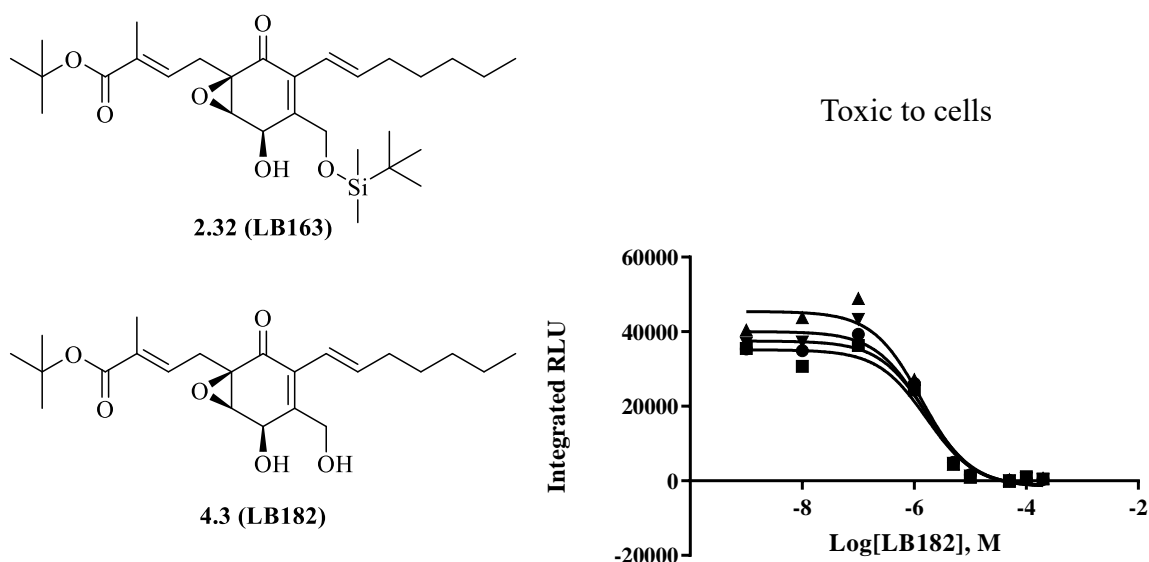
Figure 4.16. The structures and IC_{50} curves of ambuic acid analogues **2.32** (LB163) and **4.3** (t-butyl ester ambuic acid). IC_{50} LB182= 1.53 ± 0.17 μM (n= 4)

176

4.7 Testing compounds in the presence of exogenous AIP

Having established that ambuic acid **1.1** was a potent inhibitor of *agr* activity in the native AIP production assay, it was decided to investigate how inhibition was affected when the SH1000 EJM82 cells were treated with exogenous AIP-I. The *agr* system in these cells is effectively primed for activity with the presence of exogenous AIP. Cells were treated with 100 nM AIP-I, far above the EC_{50} for AgrC activation and a range of concentrations of ambuic acid and **1.62**, one of the most promising synthetic analogues to generate an IC_{50} curve.

Ambuic acid **1.1** and LB151 **1.62** were both found to still be potent inhibitors of *agr* activity even in the presence of 100 nM AIP-I as IC_{50} values are comparable $\pm$ exogenous AIP-I. There is however a notable difference in the overall efficacy of **1.62** (Figure 4.17). Complete shutdown of *agr* was observed when the cells were treated with ambuic acid **1.1**, however, when the cells were treated with **1.62** approximately 15 % residual was observed, even when the cells were treated with the highest concentration of compound (Figure 4.17), indicating that inhibition is incomplete with **1.62**.
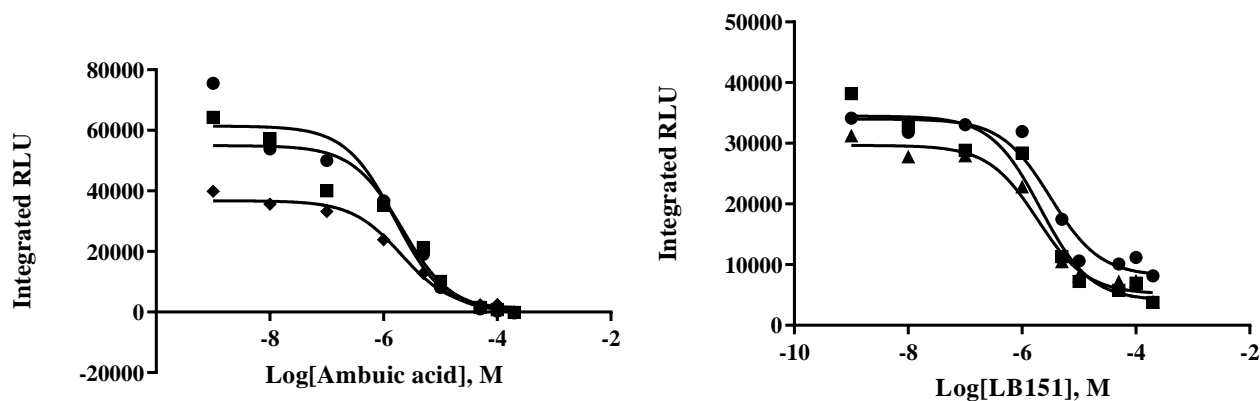
Figure 4.17. IC_{50} curves generated from the EJM82 assay in the presence of 100 nM exogenous AIP-I. IC_{50} Ambuic acid= 1.92 ± 0.29 µM. IC_{50} **1.62** (LB151)= 2.34 ± 0.68 µM with 15 % residual activity. n= 3 for both.

4.8 Effect on AIP-I and toxin production

Further to the use of the *lux* reporter as a means to determine *agr* inhibitory activity, it is important to determine how the tested compounds affect levels of AIP-I and *exo*-toxin production, both of which are physiologically relevant in *S. aureus* infections. The methicillin-sensitive strain of *S. aureus* SH1000 was grown in the presence of several of the compounds tested above for 9 h in shaker culture. At 2, 4 and 9 h into bacterial growth, samples of culture supernatant were taken and the biomass was pelleted. The cell-free supernatant was diluted 1:20 for analysis using the *S. aureus* ROJ143 assay, outlined previously within this chapter. *S. aureus* ROJ143 is a *Δagr* background with a chromosomal copy of *agrP3::luxABCDE* and plasmid based *agrP2::agrC1agrA1*.[121] These cells cannot biosynthetically synthesise AIP-I. They are however, capable of responding to AIP-I and generate a bioluminescent signal, the amplitude of which is relatable to the level of AIP-I present in the growth media.

The compounds tested in this assay were ambuic acid **1.1**, **1.62** (LB151) and **4.3** (LB182). Both **1.62** and **4.3** were selected as they had shown potent inhibitory activity in the native AIP production assay with IC$_{50}$ values of 1.84 ± 0.13 µM and 1.53 ± 0.17 µM, respectively. Thus, SH1000 cells were treated with 100 µM of desired compound. The cells were also treated with 1 µM AIP-95, a known inhibitor of AgrC as a positive control for inhibition. During preparation of the assay conditions, it was observed that LB151 and LB182 appeared to be poorly soluble (in 0.5 % DMSO (v/v) in LB growth media), as both formed a cloudy suspension, however the samples were both taken forward for the assay.

Initial findings from this experiment showed that none of the test compounds exhibit any bacteriostatic or bactericidal effects, even at 100 µM. No difference was observed between treatment and DMSO control (Figure 4.18A).

Samples taken from the bacterial growth culture after 2 h were taken forward into the ROJ143 assay (Figure 4.18 B). The data shows little AIP-I present in the test medium, which is expected given the early stage in bacterial growth at which it was taken. Samples taken at 4 h showed an increase in bioluminescence, indicative of an increase in AIP-I production, which is expected given the samples were taken at late-log phase when the *agr* system is typically activated (Figure 4.18 C). A slight increase in luminescence is observed when ROJ143 cells are treated

with culture supernatant taken at 9 h into SH1000 growth, again indicative of an increase in AIP-I production (Figure 4.18 C).

After 2 h of bacterial growth, there is a minor effect on the level of AIP-I when the cells are treated with test compounds, however, the overall signal is too low to interpret any inhibitory effects. After 4 h, both 100 µM ambuic acid and 1 µM AIP-95 shown inhibition of AIP-I production (Figure 4.18 C), with near full shutdown of bioluminescence observed. 100 µM **1.62** (LB151) proves ineffective, with levels of luminescence observable comparable to DMSO control (Figure 4.18 C). The observed poor solubility of **1.62** could be the cause of this loss of inhibition. 100 µM **4.3** (LB182), which also showed a level of insolubility shows a level of inhibition of AIP-I production, however full arrest of AIP-I production was not observed.

After 9 h (Figure 4.18 D), AIP-95 again shows near full shutdown of AIP-I, with low bioluminescence observed in the ROJ143 assay. Ambuic acid appears to lose activity as AIP-I appears to be produced due to the increase in bioluminescence (Figure 4.18 D) when compared to 4 h (Figure 4.18 C). This suggests that ambuic acid loses potency over time.

In addition to the challenge of SH1000 with test compounds at the start of the growth curve, untreated SH1000 cells were treated with 100 µM ambuic acid 2 h into bacterial growth. This was done to determine how late addition with ambuic acid altered its inhibitory activity. As shown in Figure 4.18 C, at 4 h, the later addition of ambuic acid shows a loss in activity relative to treatment from the start. At 9 h (Figure 4.18 D), the level of inhibition between late addition of ambuic acid and addition at the start of the assay is comparable.9

Investigation into how treatment affected the overall secretome of SH1000 was carried out by SDS-PAGE. Coomassie Blue stained gel (Figure 4.18 E) shows that at 4 h, for all treatments and DMSO control, very little secreted protein is present, due to early stage in growth. After 9 h, ambuic acid, **4.3** and AIP-95 show a decrease in the overall level of secreted protein relative to the DMSO control (Figure 4.18 E).

Western blot analysis was carried out to assess media content for α-haemolysin (Figure 4.18 F). After 4 h, no toxin was observed (Figure 4.18 F). After 9 h, inhibition of α-haemolysin production was observed was observed in samples from SH1000 cells which had been treated

with ambuic acid, **4.3** and AIP-95 (Figure 4.18 F). This correlates to the observed reduction of AIP-I production in Figure 4.18 C and D.

These data show that ambuic acid and **4.3** (LB182) have an effect on the level of AIP-I produced by the cells as well as the secreted exotoxin α-haemolysin. This, taken with the data from the native AIP production assays together show that these are promising anti-virulence compounds.
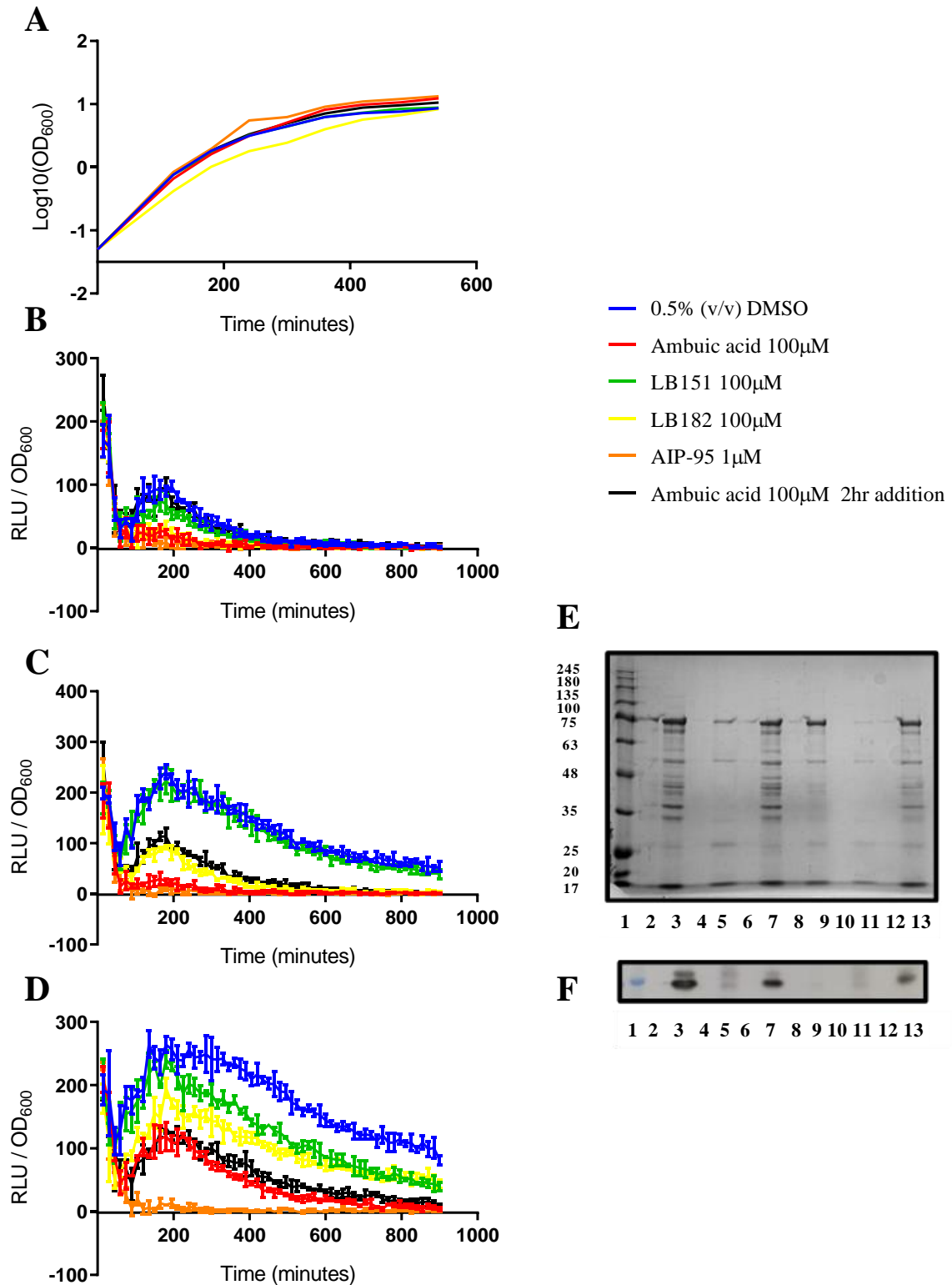
Figure 4.18. (A) *S. aureus* SH1000 growth curve, (B) luminesence profile from *S. aureus* ROJ143 assay with samples taken at 2 h, (C) 4 h and (D) 9 h after start of growth SH1000 growth. (E) Coomassie stained 12 % acrylamide gel showing secretome profile, F) Western blot against α-haemolysin. For both (E) and (F) (1) NEB pre-stained protein standard, (2) 0.5 % DMSO 4 h, (3) 0.5 % DMSO 9 h, (4) ambuic acid 100 μM 4 h, (5) ambuic acid 100 μM 9 h, (6) 1.62 (LB151) 100 μM 4 h,(7) 1.62 (LB151) 100 μM 9 h, (8) 4.3 (LB182) 100 μM 4 h, (9) 4.3 (LB182) 100 μM 9 h, (10) AIP-95 1 μM (11) AIP-95 1 μM (12) ambuic acid 100 μM late addition 4 h, (13) ambuic acid 100 μM late addition 9 h.

4.9 Conclusions
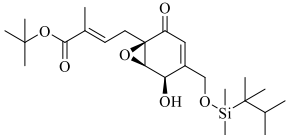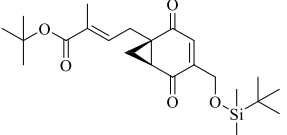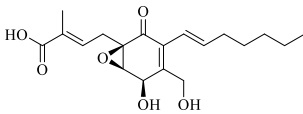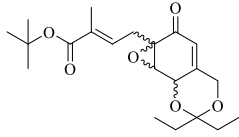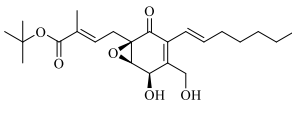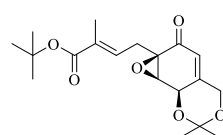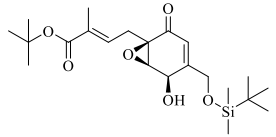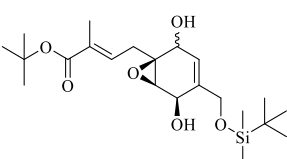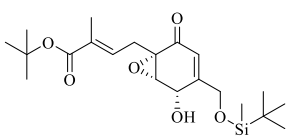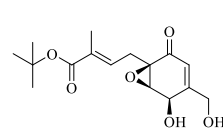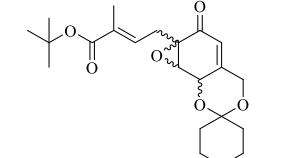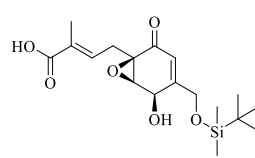
The anti-*agr* activity of ambuic acid **1.1** has been assessed in this chapter. It has been found to be a potent inhibitor of *agr* activity in the native AIP-I production assay, with no adverse effect on bacterial growth, comparable to the IC_{50} value previously reported by Todd *et al.*.[155] In addition, the inhibitory activity was found not to be non-specific inhibition of the *lux* bio-reporter. Furthermore, ambuic acid treatment reduced the production of α-haemolysin in the MRSA strain USA300. The ROJ143 assay shows evidence that ambuic acid inhibits the bio-synthesis of the AIP-I signal molecule, with only a very minor effect on sensing. These data have shown that ambuic acid is a potent inhibitor of *agr* activity, with an observable effect on the production of α-haemolysin, making it a promising molecule for producing analogues as novel anti-virulence therapies.

Analogues of ambuic acid have also been assessed using the native AIP production assay and several have been found to be potent inhibitors of *agr* activity (Table 4.3). Compounds **1.74**, **1.62** and **1.63** reveal that the right-hand (*E*)-heptenyl chain of ambuic acid **1.1** is not specifically required for compound activity as these compounds are active against *agr*. It is also clear that increasing lipophilicity has a positive effect on compound activity. Comparing **1.74** and **1.62**, loss removal of the lipophilic *t*-butyldimethylsilyl ether moiety in **1.74** leads to a significant loss of compound potency (Table 4.3). It was also found that comparing **1.63** and **1.62**, stereochemistry had a minimal effect on compound potency, with comparable IC_{50} values for both compounds, however there was a slight loss in the overall efficacy of the (-)- enantiomer JWR28 (Table 4.3).

The free acid analogue **4.1** of **1.62** has also been tested in the EJM82 assay (Table 4.3). It was found that removal of the *t*-butyl ester led to a significant negative effect on compound potency, with the IC_{50} of **4.1** found to be >200 µM (Table 4.3).

The novel silyl ether analogue **2.62** was also tested in the EJM82 native AIP production assay and found to be a potent inhibitor of *agr* activity, with an IC_{50} of 0.65 ± 0.07 µM. Comparing **2.64** to **1.62**, the slight increase in lipophilicity of **2.64** relative to **1.62** has a positive effect on compound potency (Table 4.3).

Table 4.3. The structures of the compounds which have been tested as part of this study in the EJM82 and their IC$_{50}$ values which have been experimentally found in the EJM82 native AIP production assay.

Compound	IC$_{50}$ (μM)	Compound	IC$_{50}$ (μM)
2.62 (JWR99)	0.65 ± 0.07	**1.75** (JWR229)	6.69 ± 0.14
1.1 (ambuic acid)	0.95 ± 0.13	**2.63** (JWR298)	8.47 ± 6.32
4.3 (LB182)	1.53 ± 0.17	**2.72** (JWR269)	13.34 ± 0.08
1.62 (LB151)	1.84 ± 0.13	**4.2** (LB221)	24.67 ± 4.84
1.63 (JWR28)	2.27 ± 0.25 (7 % residual activity)	**1.74** (LB153)	133.95 ± 33.80
2.74 (JWR297)	5.06 ± 3.52	**4.1** (LB211)	>200

A number of ketal analogues have also been assessed for *agr* inhibitory activity in the EJM82 native AIP production assay (Table 4.3). Dimethyl (**2.72**), diethyl (**2.73**) and cyclohexyl (**2.74**) ketals were all found to be potent inhibitors of *agr* activity. Comparing **2.72** and **2.73**, the increase in the ketal chain length from methyl to ethyl was found to be beneficial in terms of compound potency. Compound **2.74**, containing a unique tricyclic structure was also found to be a potent inhibitor of *agr* activity (Table 4.3).

The cyclopropyl analogue **1.75**, the synthesis of which is outlined in chapter 3 was found to be a potent inhibitor of *agr* activity (Table 4.3). Replacement of the epoxide with an inert cyclopropyl ring was carried out in an attempt to determine the mode by which ambuic acid and the synthetic analogues function. The cyclopropyl analogue **1.75** was found to be a potent inhibitor of *agr* activity ($IC_{50} = 6.69 \pm 0.14$ µM). This suggests that the epoxide is not required for potent inhibition of *agr* activity. Further study of the mechanism by which the inhibitors function is required.

Ambuic acid and the truncated analogue **1.62** (LB151) were both found to be potent inhibitors in the EJM82 assay when the cells were treated with exogenous AIP-I. Potency was comparable ± AIP-I for both compounds, however a loss of overall efficacy of LB151 was found when the cells were also treated with AIP-I.

The most potent compounds **1.62** (LB151), **4.3** (LB182) as well as ambuic acid **1.1** were tested to determine whether they inhibit AIP-I production. Ambuic acid and **4.3** were found to inhibit the production of AIP-I as well as reduced the level of production of α-haemolysin. It was also found that after growth for 9 h, ambuic acid loses inhibitory activity.

The data above showed that the tested compounds are promising inhibitors of staphylococcal virulence and are promising therapeutic agents for the treatment of serious multi-drug resistant infection. It is proposed that **1.62** is a hit compound which would be the basis for further structure-activity exploration.

Taken together, the data presented here represents the first study of analogues of ambuic acid as anti-virulence compounds targeting *S. aureus*.

Chapter 5. Summary and future work

5.1 General conclusions

The aims of this thesis were to discover novel anti-virulence compounds that target the staphylococcal *agr* system as a modality to treat serious, multi-drug resistant *S. aureus* infections. To achieve this, three key aims have been investigated. Firstly, the synthesis of a focused range of analogues of the natural fungal product ambuic acid **1.1**. Second, the synthesis of a cyclopropyl isostere of the epoxide within an ambuic acid analogue to investigate how it alters activity. Thirdly, the *in vitro* biological characterisation of the synthesised analogues.
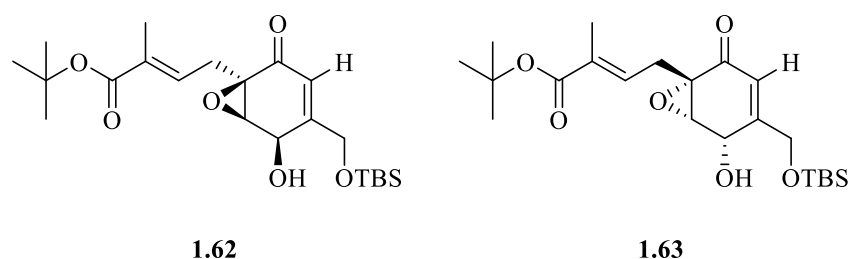
Figure 5.1. The truncated ambuic acid analogue **1.62** and the corresponding (-)-enantiomer **1.63**.

The synthesis of a range of analogues of the truncated ambuic acid analogue **1.62** has been carried out (Figure 5.1). A synthetic route, adapted from the Jung *et al*. total synthesis of ambuic acid by Dr Leonardo Baldassarre, formerly of the Williams/Chan group has been utilised as the main synthetic route.[163] Modification of this route has been carried out to afford a number of unique analogues.
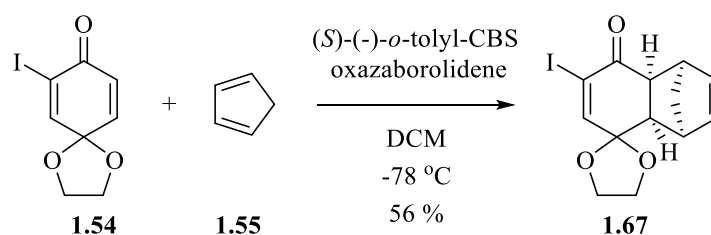
Scheme 5.1. The key Diels-Alder reaction to produce the (-)-adduct **1.67** which confers stereoselectivity on subsequent steps through steric occlusion of formation of the undesired enantiomer.

Firstly, a route to the (-)-enantiomer of **1.63** (Figure 5.1) has been established through the modification of a key Diels-Alder reaction, by forming a, chiral Diels-Alder adduct intermediate **1.67** which can confer stereoselectivity on subsequent chemical transformations through steric occlusion of the undesired enantiomer (Scheme 5.1). Diels-Alder adduct **1.67** was produced with good enantioselectivity, $[\alpha]_D^{24} = +81.4$ and reasonable yield (56 %). The opposing enantiomer, the (+)-adduct has a value of $[\alpha]_D^{24} = -70.3$, which is comparable to the

186

known value in the literature.[163] With the successful production of adduct **1.67**, subsequent synthetic transformations yielded the final compound **1.63**. These included the DIBAL-H mediated enantioselective reduction of the ketone moiety within **1.71**, a procedure pioneered by Mehta *et al.* and Jung *et al.* utilising DIBAL-H to afford diol **1.72** with good enantioselectivity (Scheme 5.2), $[\alpha]_D^{24} = +43.9$. The corresponding (+)-enantiomer has a value of $[\alpha]_D^{24} = -44.4$, which is comparable to the literature.[163] Final compound **1.63** was successfully produced and taken into biological assessment.
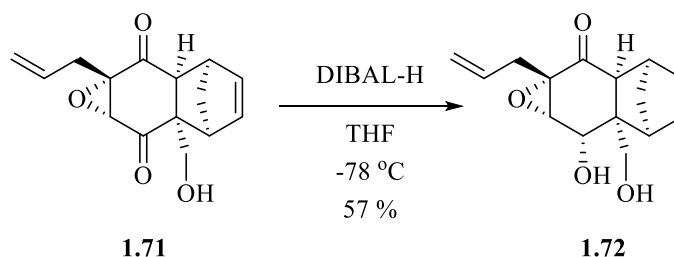
Scheme 5.2. The enantioselective reduction of the ketone of **1.71** to the corresponding secondary alcohol **1.72**.

Attempts were also made to produce ether analogues through modification of the primary alcohol in enantiomerically pure **1.62**. Unfortunately, exhaustive testing of ether formation conditions failed to yield the desired asymmetric ethers.

The synthesis of numerous silyl ether analogues was also attempted. These compounds were synthesised by dismantling of silyl ether **1.62** to afford the key diol intermediate **1.74** (Figure 5.2), followed by subsequent reaction with a silyl chloride to give the corresponding silyl ether analogues. Unfortunately, it was only possible to produce dimethylthexyl silyl ether **2.62** (Figure 5.2). The failed condensation reactions are likely due to steric hindrance of commercially available silyl chlorides (such as TBDPSCl) and the starting material.
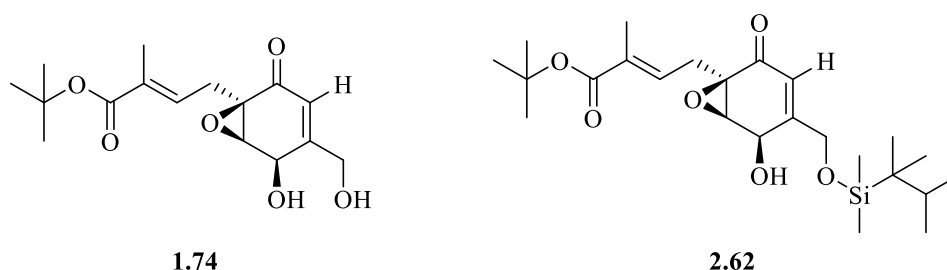
Figure 5.2. The key diol intermediate **1.74** and the successfully synthesised dimethylthexyl silyl ether **2.62**.

The synthesis of several ketal analogues of **1.62** has also been carried out. Dimethyl (**2.72**), diethyl (**2.73**) and cyclohexyl (**2.74**) ketals have been successfully synthesised utilising the key diol intermediate **1.74/2.77** (Figure 5.3). Reaction of diol **1.74/2.77** with symmetric ketone afforded the desired ketal. Moreover, an efficient *trans*-acetalation/ketalation procedure was established, which utilised the *O,O*-dimethoxy variant of the ketone to afford even sterically encumbered ketals, such as the cyclohexyl ketal **2.74** with reasonable yield (31%).

2.72   **2.73**

2.74
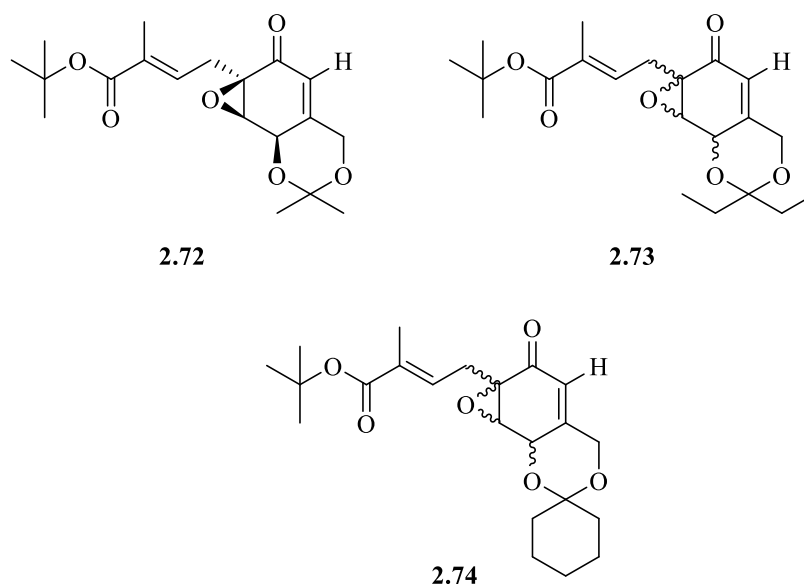
Figure 5.3. The ketal analogues. Dimethyl ketal **2.72**, diethyl ketal **2.73** and cyclohexyl ketal **2.74**.

The second aim was to produce a novel cyclopropyl isostere **1.75** of a truncated ambuic acid analogue **2.1** (Figure 5.4). This was carried out to determine whether the epoxide electrophilic warhead is required for potent inhibition of the putative cysteine protease AgrB. It was predicted that no inhibition would be observed with replacement of the reactive epoxide.

1.75
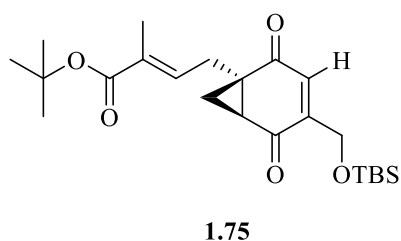
Figure 5.4. The cyclopropyl isostere **1.75**.

The production of the cyclopropyl isostere **1.75** was achieved through the optimisation of a key Corey-Chaycovsky cyclopropylation reaction using trimethylsulfoxonium iodide in the presence of *n*-BuLi for the enantioselective installation of the cyclopropyl ring to afford **1.78** (Scheme 5.3). Enantioselective insertion of the cyclopropyl ring was confirmed through

NOESY NMR. With the successful installation of the cyclopropyl ring, the optimisation of subsequent synthetic steps has been carried out to afford the final compound. Notably, advancements have been made through the development of a highly efficient microwave-assisted retro Diels-Alder reaction to dismantle the adduct **1.80** in order to yield **1.81**, typically with a yield of 80-91 % with the requirement of relatively mild conditions (Scheme 5.4).
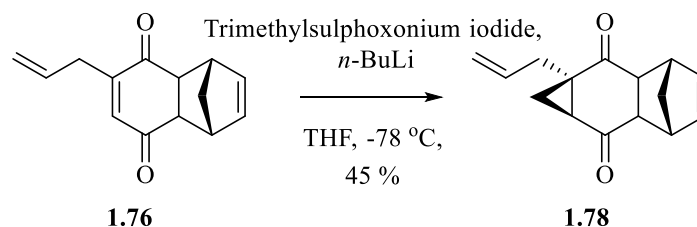
Scheme 5.3. The Corey-Chaycovsky cyclopropylation reaction used here to install the cyclopropyl ring giving key intermediate **1.78**.

Third, the successfully synthesised analogues were also assessed for their *in vitro* anti-*agr* activity. As outlined in chapter 4, a bioluminescence reporter has been utilised to determine the anti-virulence properties of numerous analogues.
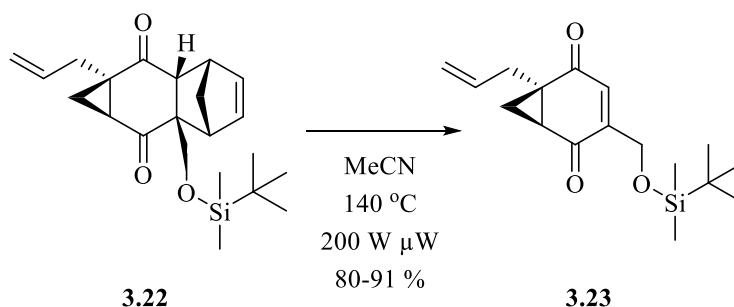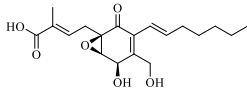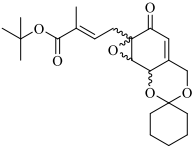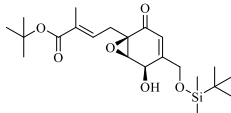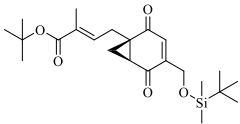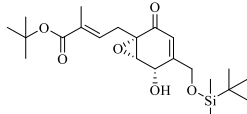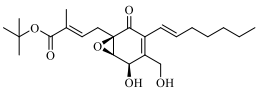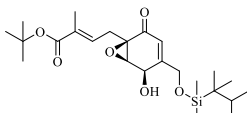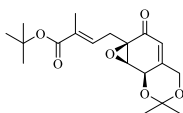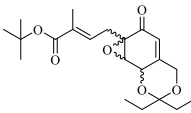
Scheme 5.4. The optimised conditions for the retro-Diels-Alder reaction giving the key intermediate **3.23**.

Initially, selected anti-*agr* properties of ambuic acid (**1.1**) were characterised. It was found to be a potent inhibitor of *agr* mediated virulence in the native AIP production bioluminescent reporter assay with an IC_{50} of 0.95 ± 0.13 µM (Table 5.1), which agrees with the literature (2.5 ± 0.1 µM).[155] Furthermore, ambuic acid was found to cause an observable reduction in the level of the secreted exotoxin, α-haemolysin. These data show that ambuic acid is a potent inhibitor of an *agr*-regulated virulence factor. In addition, the ROJ143 AIP-I sensing assay indicates that ambuic acid inhibits the biosynthesis of the AIP-I signal molecule instead of antagonism of the AgrC receptor.

Synthetic analogues of ambuic acid have also been assessed using the native AIP-I production assay. Several analogues have been found to be potent inhibitors of *agr* activity including **2.62** (JWR99), **1.62** (LB151) and **1.63** (JWR28) (Figure 5.5 and Table 5.1). The opposing enantiomers (**1.62** and **1.63**) of a truncated ambuic acid analogue (Figure 5.1, Table 5.1) were both found to be potent inhibitors of *agr* activity. Stereochemistry was found to effect the overall efficacy of the compounds, with minimal effect on the potency.

Significantly, the dimethylthexyl silyl ether **2.62** (JWR99) was found to have improved activity when compared to ambuic acid **1.1** (IC$_{50}$ of JWR99= 0.65 ± 0.07 µM; ambuic acid= 0.95 ± 0.13 µM).

Table 5.1. The structures and IC$_{50}$ values of the synthetic analogues of ambuic acid. The IC$_{50}$ values were calculated in the EJM82 native AIP production assay.

Compound	IC$_{50}$ (µM)	Compound	IC$_{50}$ (µM)
1.1 (ambuic acid)	0.95 ± 0.13	2.74 (JWR297)	5.06 ± 3.52
1.62 (LB151)	1.84 ± 0.13	1.75 (JWR229)	6.69 ± 0.14
1.63 (JWR28)	2.27 ± 0.25 (7 % residual activity)	4.3 (LB182)	1.53 ± 0.17
2.62 (JWR99)	0.65 ± 0.07		
2.72 (JWR269)	13.34 ± 0.08		
2.73 (JWR298)	8.47 ± 6.32		

Ambuic acid (**1.1**) and the potent truncated analogue **1.62** (LB151) have also both been found to be potent inhibitors of *agr* activity even when the *agr* system within the reporter strain was primed with exogenous AIP-I.
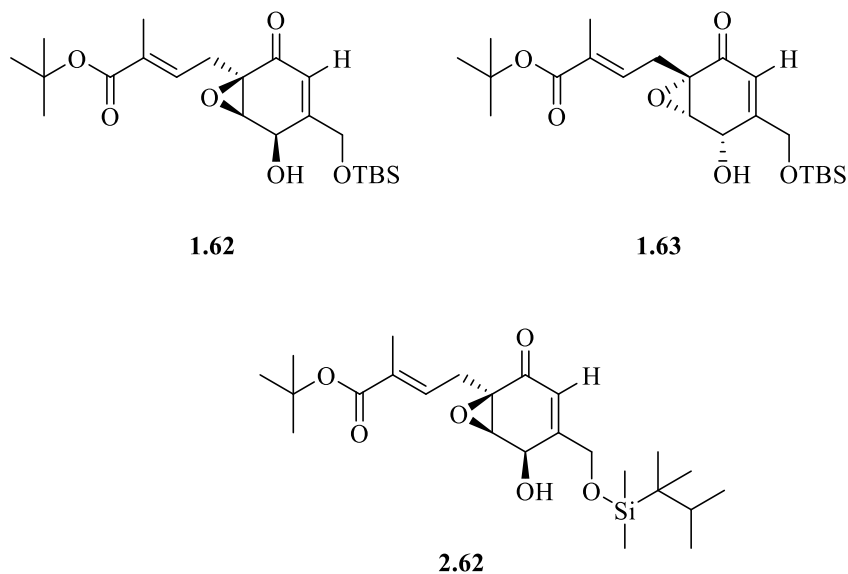
Figure 5.5. The structures of **1.62** (LB151), **1.63** (JWR28) and the silyl ether analogue **2.62** (JWR99).

The ketal analogues **2.72**, **2.73** and **2.74** were also assessed for anti-*agr* activity using the native AIP-I production assay (Figure 5.6). All three ketal analogues were found to have inhibitory activity against the staphylococcal *agr* system (Table 5.1). Of these analogues, the cyclohexyl ketal **2.74** was found to be the most potent, with an IC$_{50}$ of 5.06 ± 3.52 μM (Table 5.1).

2.72

2.73

2.74
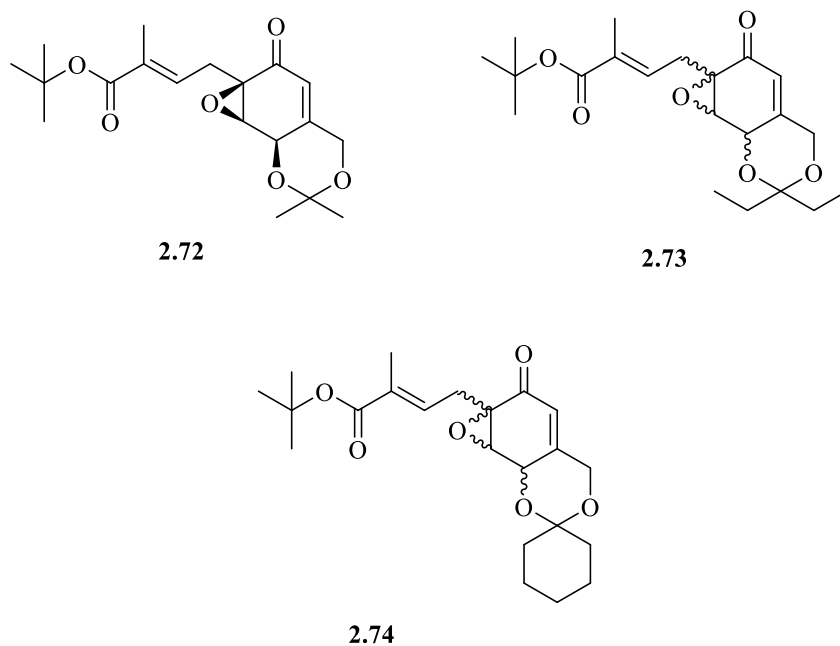
Figure 5.6. The structures of the ketal analogues, **2.72** (JWR269), **2.73** (JWR298) and **2.74** (JWR297).

The cyclopropyl analogue JWR229 **1.75** (Figure 5.7) was assessed for anti-virulence activity in the native AIP-I production assay. Unexpectedly, the cyclopropyl analogue **1.75** was found to be a potent inhibitor of *agr* mediated virulence with an $IC_{50} = 6.69 \pm 0.14\ \mu M$. This suggests that the electrophilic epoxide centre is not required for potent inhibitory activity. At present, further study of the mechanism by which the inhibitors can elicit an effect is required.

1.75
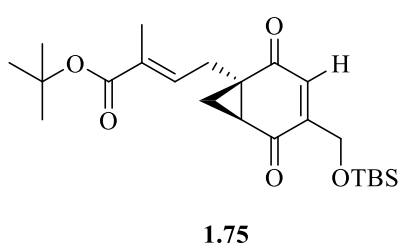
Figure 5.7. The cyclopropyl isostere **1.75** (JWR229).

A number of the most potent compounds, **1.62** (LB151), **4.3** (LB182, Figure 5.8) and ambuic acid (**1.1**) were also tested to determine whether they inhibit the production of AIP-I and the secreted α-haemolysin. Both ambuic acid and **4.3** were both found to inhibit AIP-I production. In addition, they were both able to inhibit production of α-haemolysin. It is also important to note, that over time, the efficacy of ambuic acid appears to reduce.
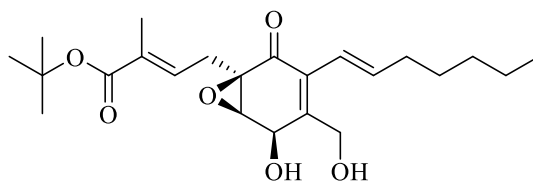
4.3

Figure 5.8. LB182 **4.3** (LB182), *t*-butyl ester analogue of ambuic acid

In summary, the biological characterisation of ambuic acid and the synthetic analogues has shown that they are inhibitors of some promise as future therapies for the treatment of serious, multi-drug resistant *S. aureus* infections. This work represents the first study of analogues of the natural product ambuic acid as inhibitors of the virulence of *S. aureus*.

5.2 Future work

5.2.1 Ambuic acid analogues

The work outlined in this thesis has described the synthesis and biological characterisation of the anti-virulence properties of numerous truncated analogues of the natural product ambuic acid. The synthesis of analogues has been focused on the production of analogues of **2.1**. Herein, possible future directions for work focusing on development of ambuic acid analogues will be discussed.

The right hand (*E*)-heptene moiety of ambuic acid **1.1** could be replaced with a range of lipophilic groups to afford a range of unique analogues. The installation of such lipophilic groups could provide some useful data on the inhibitory activity of ambuic acid. To this end, a number of target structures are shown in Figure 5.9.

R= H
R= *t*-butyl
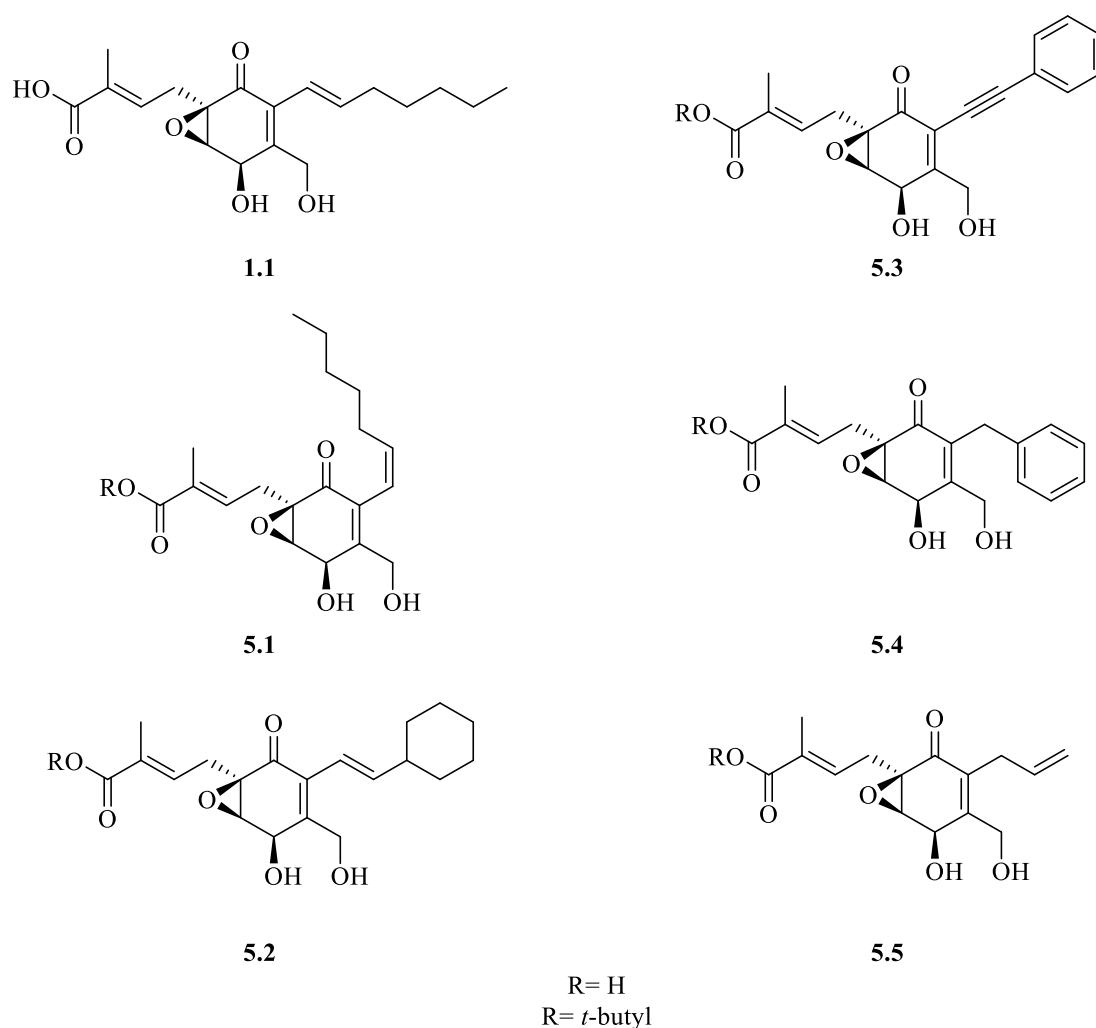
Figure 5.9. Ambuic acid **1.1** and the target right hand chain analogues. Both the free acid and t-butyl ester analogues could be synthesised.

The proposed structures incorporate an array of chemical functionalities, including the *cis*-isomer of the heptene chain **5.1** (*trans* in natural ambuic acid **1.1**), a cyclohexyl ring **5.2**, alkynyl **5.3** (imparting rigidity), benzyl **5.4** and short alkene chains **5.5** (Figure 5.9).

The proposed route to the above series of analogues would initially follow the synthesis of truncated ambuic acid analogue **1.62**. Modification is required for the installation of the right hand chain. Thus, the silyl ether **2.27** will be treated in an α-bromination reaction previously utilised by Jung *et al*. to yield the bromo compound **2.28** (Scheme 5.5).[163] The Diels-Alder adduct of **2.28** will subsequently be dismantled giving bromo-quinolone derivative **2.29**, which will then be taken into an ozonolysis and Wittig procedure to afford the key intermediate **2.31** (Scheme 5.5). The intermediate **2.31** will then be taken into a Stille cross-coupling with the appropriate stannane to furnish the compound with the desired right-hand chain **5.6** (Scheme 5.5). This will be followed by sequential de-protection of the silyl ether (giving *t*-butyl ester compounds **5.7**) and final dismantling of the *t*-butyl ester giving final free acid **5.8** (Scheme 5.5). Progress towards the production of these compounds has been made, however it was unfortunately curtailed due to the COVID-19 pandemic.
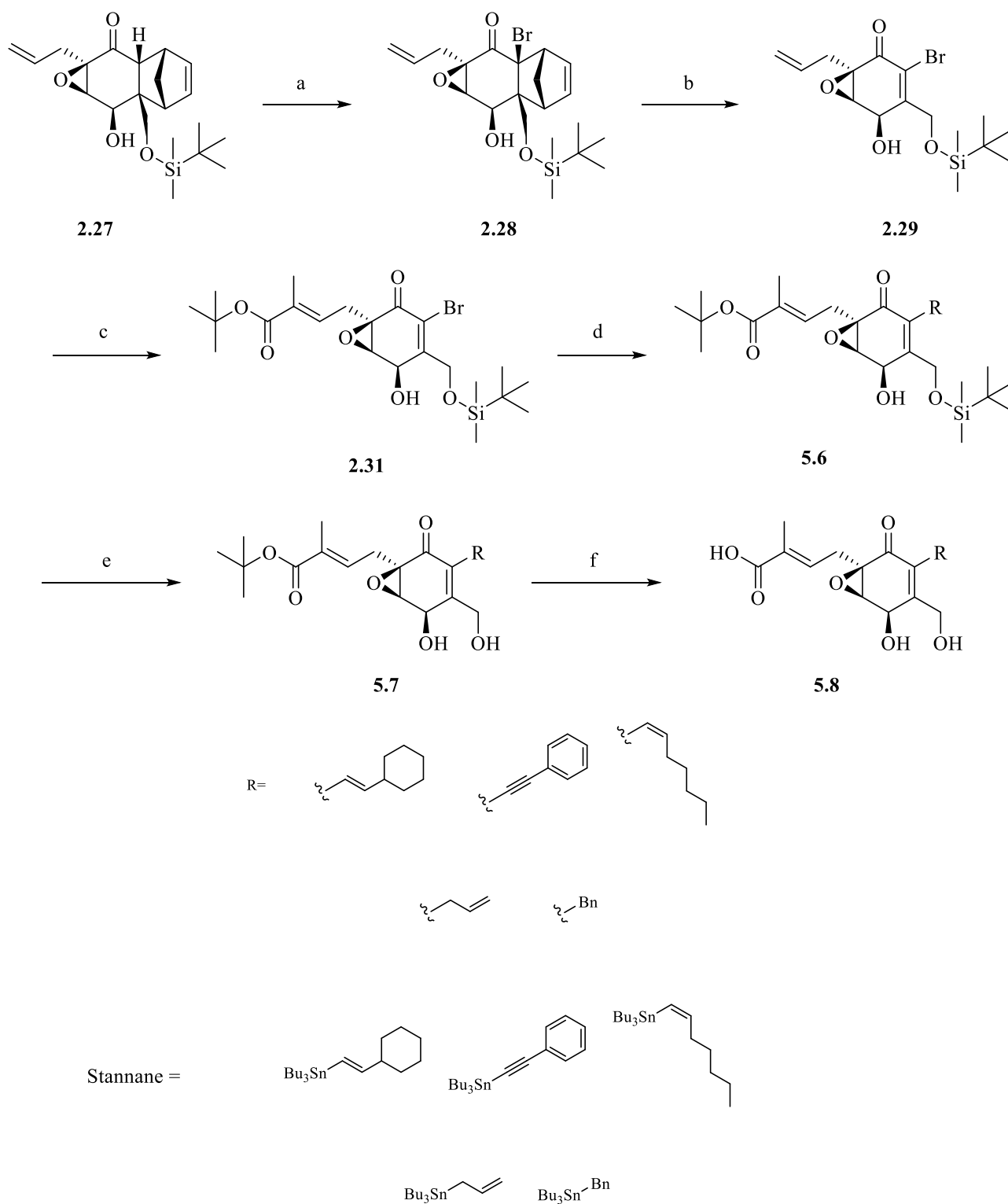
Scheme 5.5. The proposed route to the right-hand analogues. (a) DBU, 1,2-dibromotetrachloroethane; (b) Ph₂O, heat; (c) O₃, dimethylsulphide then Ph₃P=C(Me)CO₂t-Bu; (d) SnBuR₃, Pd(PPh₃)₄, μW radiation; (e) acetic acid, Et₂O, dH₂O; (f) trifluoroacetic acid

Steps towards the production of these analogues have been undertaken. Thus, the *t*-butyl dimethyl silyl ether **2.27**, was treated in an α-bromination procedure, adapted from Jung *et al.* in their total synthesis of ambuic acid.[163] Silyl ether **2.27** was stirred with DBU (20 mol %) to remove the α-proton and before subsequent reaction with 1,2-dibromotetrachloroethane. This produced the desired bromide **2.28** in excellent yield (85 %, Scheme 5.6). The α-bromination procedure affords a key bromide intermediate that enables facile access to a range of analogues via Stille cross-coupling. However, when the bromide **2.28** was treated in the retro Diels-Alder reaction to dismantle the adduct, the quinolone derivative **2.29** was obtained in poor yield (Scheme 5.7). Nevertheless, with the successful production of **2.29**, the subsequent step was the ozonolysis and Wittig procedure, previously described in this chapter to produce *t*-butyl ester **2.31**. This unfortunately yielded **2.31** in poor yield (10%, Scheme 5.8).
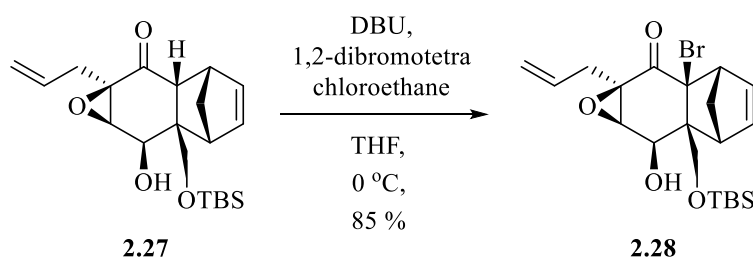
Scheme 5.6. The α-bromination procedure adapted from Jung *et al.* allowing successful production of bromide **2.28**.[163]

t-butyl ester **2.31** was taken forward for Stille cross-coupling to install the desired right hand chain. The installation of he (*Z*)-hept-1-enyl and (*E*)-cyclohexyl vinylic right-hand chains, to afford **5.9** and **5.10** proceeded smoothly (Figure 5.10). However, installation of the benzylic, allylic and alkynyl side chains proved problematic and production of the corresponding compounds failed.
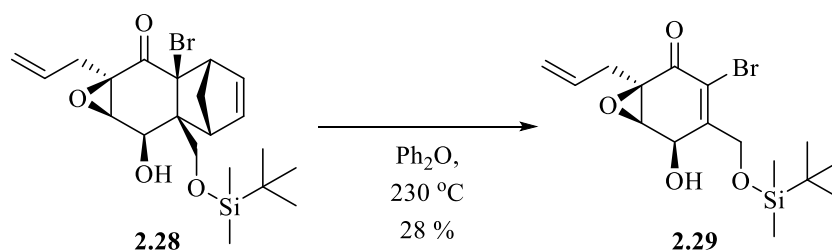
Scheme 5.7. Retro Diels-Alder reaction, dismantling adduct of **2.29** giving **2.29**.
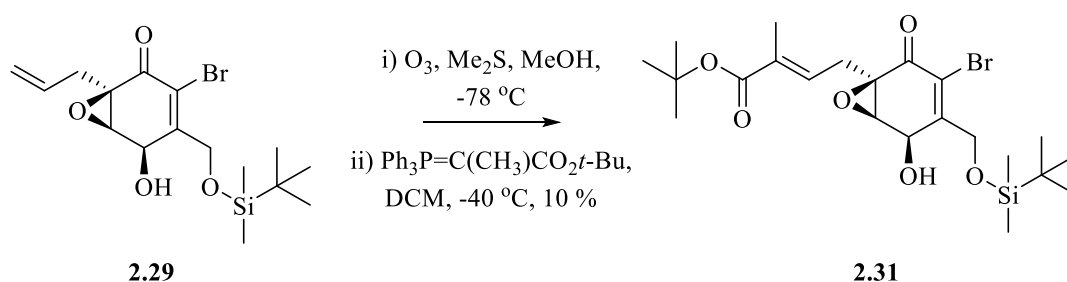
Scheme 5.8. The ozonolysis and Wittig procedure installing the t-butyl ester moiety providing **2.31** in poor yield, 10%.

With the installation of the desired right-hand chain giving both **5.9** and **5.10**, subsequent sequential deprotection gave the desired final compounds. Unfortunately, the amount of compound was insufficient to allow for full characterisation and biological testing. However, the route pioneered here is a promising starting point for the production of further analogues of ambuic acid and future optimisation
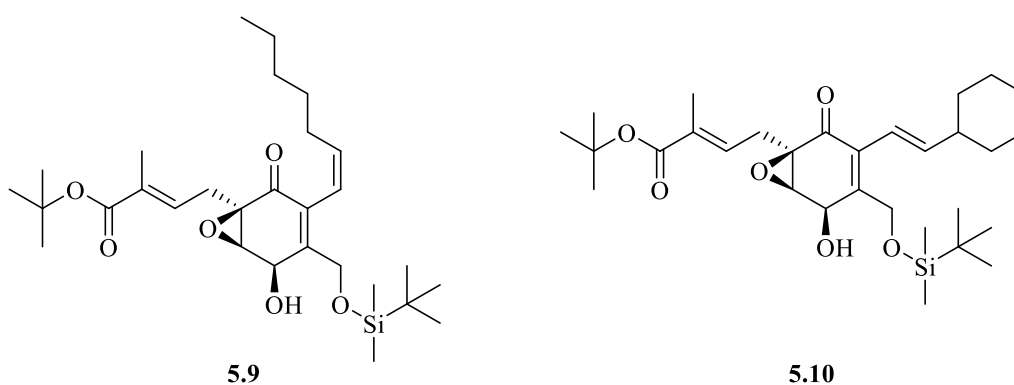
Figure 5.10. The (*Z*)-hept-1-ene **5.9** and (*E*)-cyclohexyl vinyl **5.10** products produced by the Stille reaction.

5.2.2 Cyclopropyl analogues

As outlined in chapter 3, the synthesis of a novel cyclopropyl isostere of the epoxide within a truncated ambuic acid analogue has been achieved. The cyclopropyl isostere was synthesised to determine whether loss of the epoxide electrophilic centre has a negative effect on the anti-virulence activity of the compound.

The next logical step in the production of cyclopropyl analogues would be to take steps towards the production of cyclopropyl ambuic acid **5.11**, through adaptation of the synthesis of cyclopropyl analogue **1.75**.
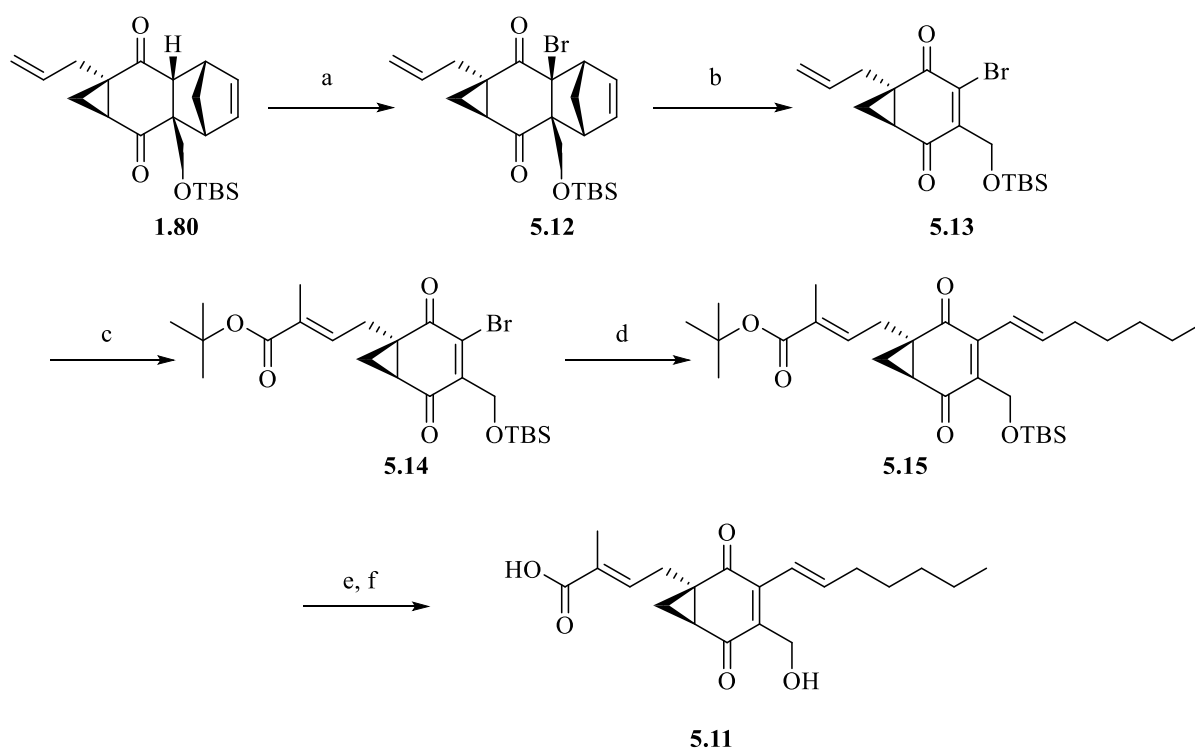
Scheme 5.9. The proposed route to the ambuic acid analogue **5.11** through adaptation of the route to cyclopropy isosotere **1.75**. (a) 1,2-dibromotetrachloroethane, DBU; (b) Ph$_2$O, heat; (c) O$_3$, dimethylsulphide then Ph$_3$P=C(Me)CO$_2$t-Bu; (d) tributyl (*E*)-hept1-enyl stannane, Pd(PPh$_3$)$_4$; (e) acetic acid : Et$_2$O : dH$_2$O 1:2:1; (f) trifluoroacetic acid.

The proposed route (Scheme 5.9) to cyclopropyl ambuic acid **5.11** requires modification of the route to the cyclopropyl analogue **1.75** outlined in chapter 3. It would be necessary to produce the dione variant as reduction of lower ketone to the corresponding secondary alcohol was not successful in Chapter 3, even after testing several conditions.

Silyl ether **1.80** will be treated using an α-bromination procedure adapted from Jung *et al.* to provide the bromo compound **5.12** (Scheme 5.9).[163] Dismantling of the Diels-Alder adduct will subsequently be carried out using procedures previously utilised in this study giving **5.13** which in turn will be treated in an ozonolysis and Wittig olefination procedure to yield the *t*-butyl ester **5.14**. Subsequently, a Stille cross-couping will enable the installation of the (*E*)-hept-1-ene chain, giving **5.15** (Scheme 5.9). Sequential de-protection of the silyl ether and *t*-butyl ester would yield the final compound **5.11**.

The cyclopropyl analogue **1.75** was synthesised as an attempt to elucidate the mechanism by which the inhibitors studied in this thesis function. It was postulated that replacement of the

electrophilic warhead with an inert cyclopropyl ring would lead to loss of inhibitory activity. However, upon biological testing outlined in chapter 4, **1.75** was unexpectedly found to be a potent inhibitor of *agr* activity. This suggested that the epoxide is not required for potent inhibitory activity. Thus, further study is required to elucidate the mechanism-of-action of these compounds.

One potential method could be the fluorescent labelling of ambuic acid through the modification of the free carboxylic acid. Fluorescent ambuic acid could then be incubated with *S. aureus* culture expressing AgrB, which could then be purified for analysis. If ambuic acid is a covalent inhibitor of AgrB, it would be expected that fluorescently labelled ambuic acid would co-purify with AgrB.

Du *et al*. developed a 6-oxo-(acetyl piperazine) fluorescein **5.16** (Figure 5.11) label for the selective labelling of free-fatty acids within human sera.[239] In their study, they utilise this fluorescein label to determine the level of seven free-fatty acids through HPLC in a highly sensitive manner.[239] Du *et al*. find that they could detect levels as low as 0.1-6.4 nM.[239]

They found that the piperazine moiety within **5.16** reacts with free carboxylic acids under mild conditions in the presence of EDC to give fluorescently labelled carboxylic acid.[239] The free acid of ambuic acid **1.1** could be labelled this way, giving **5.17** and indeed, the *t*-butyl ester of cyclopropyl analogue **1.75** could be dismantled and the resultant free acid could be reacted with **5.16** to give the corresponding fluorescently labelled cyclopropyl analogue **5.18** (Figure 5.11).

As the epoxide containing analogues are thought to irreversibly alkylate the key catalytic cysteine within the active site of AgrB, reaction with fluorescently labelled ambuic acid should yield fluorescently labelled drug-target covalent complex. In contrast, if the cyclopropyl analogue does not covalently modify AgrB, no signal should be observed.

Like the Du study, fluorescence could be monitored though the use of HPLC.[239] Reversed-phase HPLC (RP-HPLC) can be used to give high-resolution separation of membrane proteins.[240] An issue is that the solvents and the resins used can denature peptides.[240] Thus, RP-HPLC is typically used for analytical purification of membrane proteins.[240] If the fluorescent labelled compound is covalently bound to the target protein, the protein would effectively be

fluorescently labelled. Monitoring of the eluent of the RP-HPLC column for fluorescein fluorescence (494/512 nm excitation/emission) could provide a readout for this potential assay.

5.16

5.17

5.18

Figure 5.11. The fluorescein derivative **5.16** produced by Du *et al*. and the proposed fluorescein labelled ambuic acid **5.17** and cyclopropyl **5.18** analogues.[239]

5.2.3 Biological assessment of the compounds

As outlined within chapter 4, a number of synthetic analogues of ambuic acid have been tested as inhibitors of *agr* in *S. aureus*. At present, compounds have only been tested in *agr* group-I and there is a need to determine whether the compounds are able to inhibit different *agr* groups.

To determine the activity of the synthesised analogues in different *agr* groups, a method from the Nakayama study of ambuic acid inhibition could be adapted.[153] Nakayama *et al*. utilise LC/MS to monitor the biosynthesis of a variety of quorum sensing signal molecules ± treatment with ambuic acid.[153] Nakayama *et al*. use this method to assess the ability of ambuic acid to inhibit the production of the signal molecule in a number of bacterial species, including *L. innocua* and *S. aureus*.[153]

The desired organism would be grown ± ambuic acid and a sample could be taken, filtered and analysed using LC/MS, with monitoring of the liquid-chromatography eluent of the desired *m/z* of the molecular ion of the relevant signal molecule/ This could be achieved through adapting methods utilised by Nakayama *et al.*.[153] Treatment could be compared against un-treated control to determine the effect of ambuic acid on the ability of the bacterium to produce their corresponding signal molecule. This would allow for the screening of numerous organisms in a relatively facile manner. Test organisms could include *Enterococcus faecalis, Clostridium difficile, Listeria innocua* and further species of staphylococci, such as *Staphylcoccus pseudointermedius*. These experiments have the potential to further show the utility of ambuic acid **1.1**, and indeed the synthetic analogues produced as part of this study as pan-inhibitors of Gram-positive virulence via inhibition of AIP biosynthesis.

Chapter 6. Materials and Methods

6.1 Table of strains

Table 6.1. Table of strains.

Name	Genotype	Selection	Source
S. aureus SH1000 EJM82	*attB agrP3::luxABCDE*	Km	Dr. Ewan Murray
S. aureus SH1000 EJM83	*Δagr::Erm attB agrP3::luxABCDE*	Km	Dr. Ewan Murray
S. aureus ROJ143	Δagr::Erm pAgr-lux/p2AgrC1agrA	Cm	Jensen et al. (2008)
Inducible *lux* *S. aureus* RN4220	*Pxyl/tet:gfp:luxABCDE pUNK*	Cm	This laboratory
S. aureus SH1000	Wild-type	-	Bei Resources
S. aureus USA300_LAC	Wild-type	-	Bei Resources

6.2 Measurement of *agrP3* promoter by bioluminescence (EJM82 native AIP production assay)

S. aureus EJM82 and *S. aureus* EJM83 (Table 6.1) were grown overnight in Luria-Bertani (LB) broth containing 100 µg/ mL kanamycin in shaker culture (37 ℃, 200 rpm). Cells were pelleted (12,000 × G) and washed 3 times with LB broth. After final wash and suspension, the culture was diluted to OD_{600} 0.05 with LB broth containing 100 µg/ mL kanamycin and grown for 4 h at 37℃, 200 rpm. After growth, the culture was washed as above and diluted 1 : 20 in LB broth for inoculation of a 96-well Greiner microtiter plate which had been treated with a range of concentrations of test compounds (0-200 µM) in DMSO, such that final DMSO assay concentration didn't exceed 0.5 % (v/v). EJM83 (Δ*agr*) was also plated with 0.5 % (v/v) DMSO as a negative control for bioluminescence.

6.3 *S. aureus* ROJ143 AgrC inhibition bioreporter assay

The AIP-I bioreporter strain *S. aureus* ROJ143 (Table 6.1) was grown overnight in shaker culture (37 ℃, 200 rpm) in LB broth containing 10 µg/mL chloramphenicol. The overnight culture was diluted to an OD_{600} of 0.05 in LB broth containing 10 µg/mL chloramphenicol and grown for 4 hours. After growth, the culture was diluted 1:20 for inoculation of a 96-well Greiner microtiter plate, which had been treated with a range of concentrations of AIP-I to generate an EC_{50} curve ± ambuic acid.

6.4 *S. aureus* RN4220 non-specific *lux* inhibition assay

The tetracycline inducible *lux* reporter strain of RN4220 (Table 6.1) was grown in BHI medium for 4 h (37 ℃, 200 rpm) and diluted 1:500 in BHI before inoculation of a Greiner microtiter plate. The plate had previously been treated with a range of concentrations of anhydrotetracycline (100-1 ng/ mL in H_2O) to induce bioluminescence and either ambuic acid (20 µM in 0.5 % (v/v) DMSO) or vehicle (0.5 % (v/v) DMSO). The level of bioluminescence was measured as described in section 6.5.

6.5 The measurement of *lux* bioluminescence

S. aureus EJM82 is able to produce AIP-I and can produce a luminescent signal, the amplitude of which is dependent on the level of *agr* activity. *S. aureus* ROJ143 cannot produce AIP-I but it can respond to exogenous AIP-I and as such, when grown in the presence of AIP-I, a luminescent signal is observed.

Bioluminescence production from the *S. aureus* EJM82, *S. aureus* ROJ143 and RN4220 non-specific lux inhibition assays were measured using a Tecan Infinite F200 plate reader. Cells were grown under static conditions. Cellular growth was monitored at OD_{600} every 15 min for 15 h. Bioluminescence of EJM82 cells was measured with an integration time of 4,000 ms every 15 min for 15 h. ROJ143 and RN4220 bioluminescence was measured with an integration time of 1000 ms every 15 minutes for 15 h.

Bioluminescence was determined by dividing each luminescence value by the corresponding OD_{600} value. Integrated luminescence was calculated by measuring the area under the luminescence curve from time > 210 min. For *S. aureus* EJM82 assays, integrated luminescence was blanked by subtracting the value from the Δagr strain *S. aureus* EJM83 (background) from each test value.

6.6 *S. aureus* USA300_LAC and SH1000 growth curves

The MRSA strain of *S. aureus* USA300_LAC or the MSSA strain SH1000 (Table 6.1) were grown overnight in LB broth in shaker culture (37 ºC, 200 rpm). Overnight culture was washed 3 times in LB (12,000 × G) and diluted to OD_{600} 0.05 in LB ± treatment with compound in a final assay concentration of DMSO of 0.5 % (v/v). The cells were grown for 9 h in shaker culture (37 ºC, 200 rpm). OD_{600} measured every hour (from 2 h).

6.7 Preparation of samples from *S. aureus* SH1000 growth culture for *S. aureus* ROJ143 assay

At 2, 4 and 9 h into the *S. aureus* SH1000 growth curve, 200 μL of culture suspension was taken and the bio mass was pelleted (20,000× G). The supernatant was taken and stored at -20 ºC until required

6.8 Preparation of secreted protein Samples from *S. aureus* USA300_LAC Growth Culture

At 4 h and 9 h into the *S. aureus* USA300_LAC growth curve, samples of culture were taken and the cells were pelleted at $20,000 \times G$. The supernatant removed and stored at -20 ºC until required.

Samples of supernatant were thawed and protein was precipitated in 20 % (v/v) trichloroacetic acid for 15 min at 0 ºC. Protein was pelleted at $20,000 \times G$ and protein pellets were washed 3 times with acetone ($20,000 \times G$). Acetone was evaporated after the final wash and the pellets were suspended in $2 \times$ SDS loading buffer (100 mM Tris-Cl, 2.5 M glycerol, 4 % (v/v) SDS, 0.005 % (w/v) bromophenol blue and 200 mM β-mercaptoethanol). Volume of loading buffer was varied to normalize samples to the lowest OD_{600} from the growth curves. Samples were heated to 95 ºC for 10 minutes and the debris was pelleted ($20,000 \times G$). Samples were stored at -20 ºC until required.

6.9 *S. aureus* ROJ143 AIP-I production bioreporter assays

The AIP-I bioreporter strain *S. aureus* ROJ143 (Table 6.1) was grown overnight in shaker culture (37 ºC, 200 rpm) in LB broth containing 10 µg/mL chloramphenicol. The overnight culture was diluted to an OD_{600} of 0.05 in LB broth containing 10 µg/mL chloramphenicol and grown for 4 h. After growth, the culture was diluted 1:20 for inoculation of a 96-well Greiner microtiter plate, treated with 10 µL of test supernatants obtained from the *S. aureus* SH1000 growth curve. Final dilution of supernatants 1:20. Bioluminescence was measure as described in section 6.5.

6.10 SDS-PAGE, Coomassie staining and Western blotting of *S. aureus* α-haemolysin

SDS-PAGE on protein samples was carried out using 12 % acrylamide SDS-PAGE gels. Resolving gel (12 % (v/v) acrylamide, 380 mM Tris-base pH 8.8, 0.1 % (w/v) SDS, 0.1 % (w/v) ammonium persulphate and 0.14 mM tetramethylethylenediamine in dH_2O) were poured and isopropanol was used to level. When the gel had set, isopropanol was removed and stacking

gel (6 % (v/v) acrylamide, 78 mM Tris-base pH 6.8, 0.12 % (w/v) SDS, 0.12 % (w/v) ammonium persulphate and 0.12 mM tetramethylethylenediamine in dH$_2$O) was poured.

Samples and NEB protein standard molecular weiht markers (NEB prestained protein ladder, broad molecular weight) loaded and gel run at 50 mA in 1 × SDS-PAGE running buffer (0.19 mM glycine, 0.027 mM Tris-base, 0.1 % (w/v) SDS in dH$_2$O) until the loading buffer front had reached the bottom of the gel. Proteins were visualized with Coomassie Blue (GelCode^{TM}) and destained with H$_2$O. Imaged using GelDoc^{TM} (Biorad).

S. aureus α-haemolysin was detected using Western blotting. Protein transferred from gel to 0.4 µm nitrocellulose membrane in transfer buffer (20 % (v/v) methanol, 0.25 mM Tris-base, 0.2 mM glycine) at 200 V for 1 h.

Blocking carried out either overnight at 4 ℃ or for 2 h at ambient temperature in 5 % (w/v) skimmed milk in TBS-Tween20 (26 mM Tris-base, 72 mM NaCl and 0.1 % (v/v) Tween20, pH 7.6 in dH$_2$O). Primary anti α-haemolysin monoclonal antibody (kind gift from Prof. Lindy Durrant, School of Medicine, University of Nottingham) was diluted 1 : 5,000 in 0.5 % (w/v) skimmed milk in TBS-Tween20 and incubated for 1 h at ambient temperature. Membrane washed with TBS-Tween20. Secondary antibody- *S. aureus* protein-A conjugated to horseradish peroxidase (Sigma) diluted 1 : 5,000 in 5 % (w/v) skimmed milk in TBS-Tween20 and incubated with membrane for 45 min at ambient temperature. Membrane washed with TBS-Tween20.

S. aureus α-haemolysin visualized with ECL^{TM} or ECL^{TM} prime detection reagents (Amersham Bioscience). Photographic film exposed to membrane and developed.

Chapter 7. Chemical Experimental

7.1 General synthetic chemistry procedures

All reagents, unless otherwise stated were purchased from Sigma Aldrich, Merck, VWR, Thermo Scientific and Acros Organics.

Reactions carried out at r.t., 0 ℃, -40 ℃ and -78 ℃.. 0 ℃ achieved with ice, -40 ℃ with acetonitrile and dry ice and -78 ℃ with acetone and dry ice. For reactions requiring heating, a hotplate was used. Where microwave radiation was required, a CEM Discover-S microwave digestion system was utilised.

Moisture sensitive reactions were carried out in flame-dried or oven dried glassware under inert nitrogen atmosphere.

All reactions monitored by analytical thin-layer chromatography (Merck 60 F254, pre-coated, aluminium backed plates), high-resolution mass spectrometry (BruckerTM microTOF mass spectrometer by positive electrospray ionization), compounds dissolved in methanol and liquid-chromatography/ mass-spectrometry. Thin-layer chromatography visualized with short wavelength (254 nm) UV light and stained with potassium permanganate stain.

Silica gel chromatography was performed using Sigma Aldrich technical grade silica gel, 60 Å, 230-400 nm mesh, 40-63 µm.

Preparative TLC (pTLC) carried out on commercially available Merck PLC silica gel 60, 0.5 mm glass-backed plates.

Chemical structures verified by ^{1}H and ^{13}C NMR. Compound purity (>95 %) verified by NMR spectrometry. ^{1}H and ^{13}C spectra samples dissolved in chloroform-d and recorded using Brüker Avance-400 operating at 400 MHz for ^{1}H and 100 MHz for ^{13}C spectra. NOESY spectra recorded on Brüker AV(III) 500 MHz spectrometer. Chemical shifts reported in ppm and referenced to internal solvent standard (chloroform-d ^{1}H- 7.26 ppm, ^{13}C 77.16 ppm). Coupling constants reported in Hz. COSY and HSQC 2D spectra used for assignment.

Optical rotation was measured using a Bellingham & Stanley ADP-220 polarimeter in a 0.25 dm cuvette. Concentration (c) of the compound was given in g/100 mL.

Semi-preparative RP-HPLC was carried out using a Waters HPLC system equipped with binary pump modules and a dual wavelength UV detector (detection at 214 nm and 254 nm). The mobile phase consisted of solvent A (Milli-Q ± 0.06% TFA) and solvent B (MeCN/Milli-Q 9:1 ± 0.06% TFA). Semi-preparative RP-HPLC carried out using a Hichrom Kromasil 100 5-C^8 (150 × 10 mm, 5 µm) column at 4 mL/min.

Melting points recorded using a Gallenkamp melting point apparatus, values given in degrees Celsius (^{o}C) and are uncorrected.

7.2 Full synthetic procedures

7.2.1. (1'S,4'R,4a'S,8a'R)-7'-iodo-1',4',4a',8a'-tetrahydro-8'H-spiro[[1,3]dioxolane-2,5'-[1,4]methanonaphthalen]-8'-one (Compound 1.53)
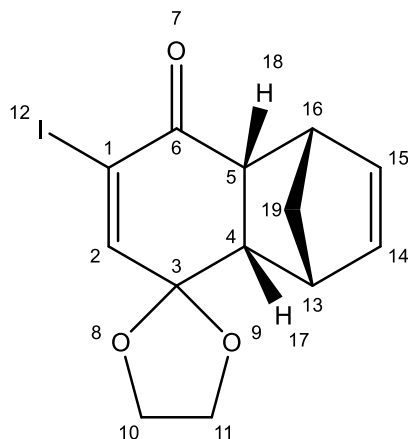
Triflic acid (8.77 mL, 0.2 M) in dry DCM was added dropwise to a solution of (*R*)-(+)-*o*-tolyl-CBS oxazaborolidene in toluene (4.2 mL, 0.5 M) at -78 ℃ and stirred for 15 minutes. A solution of **1.54** (3.16 g, 11.3 mmol) in dry DCM (12 mL) and freshly distilled cyclopentadiene (1.12 mL) were added dropwise to the stirring solution. Reaction monitored by TLC (hexane/EtOAc 3:1). Upon completion, reaction quenched with TEA (1 mL). Crude mixture was concentrated under reduced pressure. Product purified by silica gel chromatography (PET ether/ EtOAc 3:1) yielding the title compound as a yellow/ brown oil (3.44 g/ 88 %). R_f = 0.5 (hexane/EtOAc 3:1). $[\alpha]_D^{25}$ = -70.3 (*c* 1, CHCl$_3$). MS: *m/z* (+ESI) exact mass calc'd for C$_{13}$H$_{13}$IO$_3$ [M + Na]+ 366.9807 found 366.9802. ^{1}H NMR (400 MHz, Chloroform-*d*) δ 7.04 (d, *J* = 1.3 Hz, 1H, C2-H), 6.06 (dd, *J* = 5.7, 2.9 Hz, 1H, C14-H), 5.82 (dd, *J* = 5.6, 2.8 Hz, 1H, C15-H), 4.10 (ddd, *J* = 6.4, 5.6, 3.7 Hz, 1H, OCH$_2$CH$_2$O), 4.07 – 3.89 (m, 3H, OCH$_2$CH$_2$O), 3.29 (dq, *J* = 4.2, 1.4 Hz, 1H, C5-H), 3.26 (dd, *J* = 8.4, 4.2 Hz, 1H, C16-H), 3.19 (dp, *J* = 3.5, 1.7 Hz, 1H, C13-H), 2.81 (ddd, *J* = 8.4, 3.6, 1.3 Hz, 1H, C4-H), 1.38 (dt, *J* = 8.6, 1.8 Hz, 1H, C19-H), 1.34 – 1.27 (m, 1H, C19-H). 13C NMR (101 MHz, Chloroform-*d*) δ 193.53, 153.87, 135.93, 133.39, 108.73, 105.41, 65.54, 64.49, 50.86, 48.62, 46.61, 46.59, 46.42.

7.2.2. 7-iodo-1,4-dioxaspiro[4.5]deca-6,9-dien-8-one (COMPOUND 1.54)
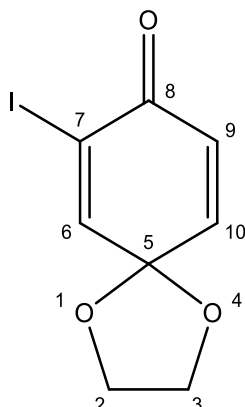
Anhydrous DME (44.8 mL) was added dropwise to compound **2.34** at -78 ºC. BF$_3$Et$_2$O (1.86 mL, 15 mmol) and ethylene glycol (4.2 mL, 75 mmol) were added and the reaction was stirred for 2 h, with gradual raising to ambient temperature. The reaction was monitored by TLC (hexane/EtOAc 3:1). When completed, reaction was quenched with sat. NH$_4$Cl (aq.). The organic layer was extracted with DCM (3 × 20 mL) and dried over anhydrous MgSO$_4$. Mixture was filtered and the crude mixture was concentrated under reduced pressure. Product purified by silica gel chromatography (PET ether/ EtOAc 3:1) yielding the title compound as a yellow powder (3.33 g, 81 %). R$_f$ = 0.35 (hexane/EtOAc 3:1). m.p. 94-96 ºC. MS: *m/z* (+ESI) exact mass calc'd for C$_8$H$_7$IO$_3$ [M + Na]+ 300.9332 found 300.9345.^{1}H NMR (400 MHz, Chloroform-*d*) δ 7.38 (d, *J* = 2.8 Hz, 1H, C6-H), 6.65 (dd, *J* = 10.0, 2.9 Hz, 1H, C9-H), 6.31 (d, *J* = 10.0 Hz, 1H, C10-H), 4.13 (s, 4H, C2/3-H).^{13}C NMR (101 MHz, Chloroform-*d*) δ 178.68, 152.02, 143.86, 126.23, 104.97, 99.65, 65.98.

7.2.3. (Iodine route) (1'S,4'R,4a'S,8a'R)-7'-allyl-1',4',4a',8a'-tetrahydro-8'H-spiro[[1,3]dioxolane-2,5'-[1,4]methanonaphthalen]-8'-one (Compound 1.57)
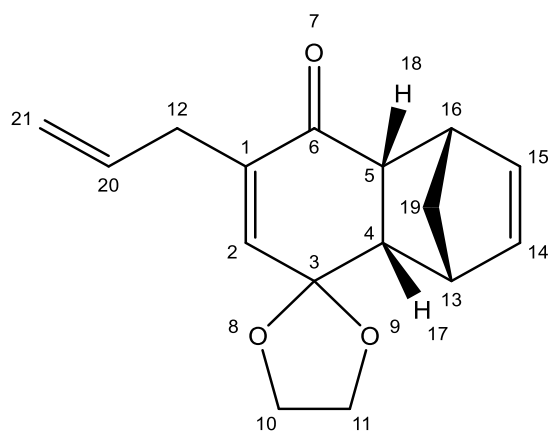
Pd(PPh$_3$)$_4$ (863 mg, 7.5 mol%) and allyltributyl tin (6.2 mL, 20 mmol) were added to a solution of **1.53** in degassed THF (10 mL) under nitrogen. The reaction mixture was heated to 110 ºC with microwave radiation (150 W) and stirred for 10 min. The reaction monitored by TLC (hex/EtOAc 3:1). Upon completion, the reaction was cooled to ambient temperature and quenched with sat. NH$_4$Cl (aq.). Organic layer extracted with EtOAc (3 × 10 mL). Crude mix concentrated under reduced pressure. Product was purified by silica gel chromatography (PET ether/EtOAc 9:1) yielding the title compound as a brown oil (1.78 g, 68 %). R$_f$ = 0.5 (hexane/EtOAc 3:1). MS: *m/z* (+ESI) exact mass calc'd for C$_{16}$H$_{18}$O$_3$ [M + Na]+ 281.1154 found 281.1157. ^{1}H NMR (400 MHz, Chloroform-*d*) δ 6.08 – 6.00 (m, 2H, CH=CH), 5.80 (dd, *J* = 5.6, 2.9 Hz, 1H, C2-H), 5.78 – 5.64 (zm, 1H, C20-H), 5.11 – 5.01 (m, 2H, C21-H), 4.16 – 4.05 (m, 1H, OCH$_2$CH$_2$O), 4.05 – 3.91 (m, 3H, OCH$_2$CH$_2$O), 3.31 (dhept, *J* = 4.2, 1.4 Hz, 1H, C13-H), 3.17 (dh, *J* = 3.5, 1.7 Hz, 1H, C16-H), 3.06 (dd, *J* = 8.8, 4.3 Hz, 1H, C4-H), 2.87 (dq, *J* = 6.9, 1.3 Hz, 2H, C12H), 2.82 (ddd, *J* = 8.8, 3.6, 1.4 Hz, 1H, C5-H), 1.41 (dt, *J* = 8.5, 1.8 Hz, 1H, C19-H), 1.35 – 1.28 (m, 1H, C19-H). ^{13}C NMR (101 MHz, Chloroform-*d*) δ 199.63, 141.86, 140.74, 135.58, 134.53, 133.48, 117.36, 104.57, 65.49, 64.19, 50.41, 48.91, 47.88, 46.67, 46.14, 33.15.

7.2.4. (1aR,2aR,3S,6R,6aS,7aS)-1a-allyl-1a,2a,3,6,6a,7a-hexahydro-3,6-methanonaphtho[2,3-b]oxirene-2,7-dione (Compound 1.58)
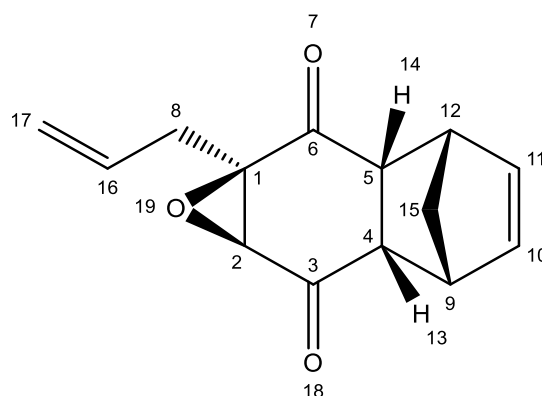
10 % (w/v) Na$_2$CO$_3$ (aq.) (3.81 mL) and H$_2$O$_2$ (7.83 mL, non-stabilised, 30 % v/v) were added to a solution of **1.57** (1.38 g, 6.4 mmol) in acetone at 0 ºC and stirred for 30 min. Reaction monitored by TLC (hexane/EtOAc 3:1). Upon completion, reaction was quenched with saturated NH$_4$Cl (aq.) and the organic layer was extracted with DCM (3 × 10 mL). Organic fractions combined and dried over anhydrous MgSO$_4$. The mixture was filtered and the crude was concentrated under reduced pressure. Product purified by flash chromatography (PET ether/EtOAc 9:1) yielding title compound as a brown/ red oil (1.24 g, 83 % yield). R$_f$ = 0.74 (hexane/EtOAc 3:1). MS: *m/z* (+ESI) exact mass calc'd for C$_{14}$H$_{14}$O$_3$ 253.25282 found 253.0833. ^{1}H NMR (400 MHz, Chloroform-*d*) δ 6.05 (t, *J* = 1.8 Hz, 2H, C10-H/C11-H), 5.70 – 5.55 (m, 1H, C16-H), 5.16 – 5.04 (m, 2H, C17-H), 3.57 – 3.42 (m, 2H, C9-H/C12-H), 3.39 (s, 1H, C2-H), 3.29 (ddh, *J* = 4.9, 3.3, 1.5 Hz, 2H, C4-H/C5-H), 2.71 (ddt, *J* = 15.1, 6.4, 1.4 Hz, 1H, C8-H), 2.56 (ddt, *J* = 15.3, 7.5, 1.2 Hz, 1H, C8-H), 1.48 (dt, *J* = 8.8, 2.0 Hz, 1H, C15-H), 1.30 (dt, *J* = 8.6, 1.5 Hz, 1H, C15-H). ^{13}C NMR (101 MHz, Chloroform-*d*) δ 204.91, 204.89, 136.68, 136.63, 130.14, 119.99, 66.26, 62.04, 50.52, 50.00, 46.67, 43.41, 43.22, 31.71.

7.2.5. (1aR,2aR,3S,6R,6aS,7aS)-1a-allyl-6a-(hydroxymethyl)-1a,2a,3,6,6a,7a-hexahydro-3,6-methanonaphtho[2,3-b]oxirene-2,7-dione (Compound 1.59)
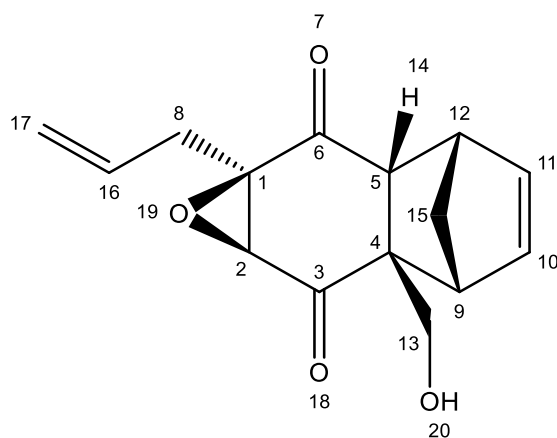
DBU (165 μL, 20 mol %) and aqueous formaldehyde (2.06 mL, 37 % (w/v)) were added to a solution of **1.58** (1.24 g, 5.3 mmol) in anhydrous THF at 0 ℃. Reaction was allowed to proceed for 30 min and was monitored by TLC (hexane/EtOAc 3:1). When complete, reaction was quenched with saturated NH$_4$Cl (aq.) and organic layer extracted in EtOAc (3 × 10 mL). Organic layers were combined, dried over anhydrous MgSO$_4$, filtered and concentrated under reduced pressure. Product was purified by silica gel chromatography (PET ether/EtOAc 5:1) yielding title compound as a clear oil (1.09 g, 79 %). . R$_f$ = 0.2 (hexane/EtOAc 3:1). MS: *m/z* (+ESI) exact mass calc'd for C$_{15}$H$_{16}$O$_4$ [M + Na]$^+$ 283.0946 found 283.0949. ^{1}H NMR (400 MHz, Chloroform-*d*) δ 6.07 (t, *J* = 1.9 Hz, 2H, CH=CH), 5.71 – 5.55 (m, 1H, C16-H), 5.18 – 5.04 (m, 2H. C17-H), 4.35 (dd, *J* = 11.7, 4.5 Hz, 1H, C13-H), 3.81 (dd, *J* = 11.5, 4.2 Hz, 1H, C13-H), 3.46 (s, 1H, C2-H), 3.32 (ddq, *J* = 13.5, 3.7, 1.8 Hz, 2H, C9-H/C12-H), 2.87 (d, *J* = 3.7 Hz, 1H, C5-H), 2.76 – 2.55 (m, 2H, C8-H), 2.06 – 1.91 (m, 1H, CH$_2$OH), 1.53 (dt, *J* = 9.5, 1.6 Hz, 1H, C15-H), 1.46 (dt, *J* = 9.5, 1.8 Hz, 1H, C15-H). ^{13}C NMR (101 MHz, Chloroform-*d*) δ 205.24, 204.09, 138.11, 137.97, 129.95, 120.14, 68.27, 67.15, 61.92, 61.62, 53.80, 45.98, 44.44, 43.43, 31.73.

7.2.6. (1aR,2aR,3S,6R,6aS,7R,7aR)-1a-allyl-7-hydroxy-6a-(hydroxymethyl)-2a,3,6,6a,7,7a-hexahydro-3,6-methanonaphtho[2,3-b]oxiren-2(1aH)-one (Compound 1.60)
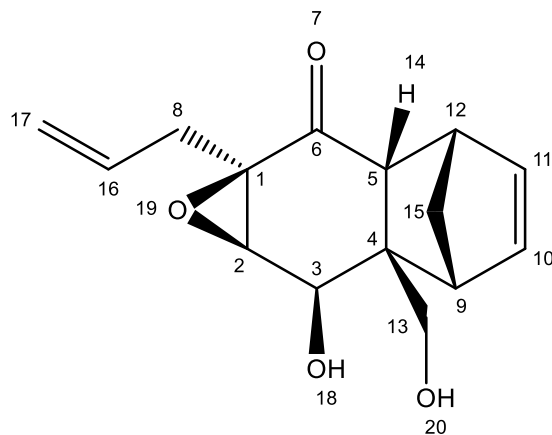
DIBAL-H (8.08 mL, 9.6 mmol, 1.2 M in toluene) was added dropwise to a solution of **1.59** (1.09 g, 4.2 mmol) in anhydrous THF at -78 ℃. Reaction stirred for 30 min, after which, additional DIBAL-H (2 mL, 2.3 mmol) added. Reaction monitored by TLC (hexane/EtOAc 2:1). Upon completion, reaction quenched with MeOH (3 mL) and HCl (21.7 mL, 1 M). Organic layers extracted with EtOAc (3 × 10 mL), dried over anhyd. $MgSO_4$, filtered and concentrated *in vacuo*. Product purified by flash chromatography (PET ether/ EtOAc 2:1) yielding the title compound as a clear solid (470 mg, 43 %). R_f = 0.17 (hexane/EtOAc 2:1). $[\alpha]_D^{25}$ = -44.4 (*c* 1, $CHCl_3$). MS: *m/z* (+ESI) exact mass calc'd for $C_{15}H_{18}O_4$ [M + Na]$^+$ 285.1103 found 285.1101. ^{1}H NMR (400 MHz, Chloroform-*d*) δ 6.29 (dd, *J* = 5.7, 3.0 Hz, 1H, C10-H), 6.11 (dd, *J* = 5.7, 3.2 Hz, 1H, C11-H), 5.71 − 5.56 (m, 1H, C16-H), 5.12 − 5.03 (m, 2H, C17-H), 4.68 (d, *J* = 11.5 Hz, 1H, C13-H), 3.97 (s, 1H, C3-H), 3.79 (dd, *J* = 11.5, 1.1 Hz, 1H, C13-H), 3.46 (s, 1H, C2-H), 3.31 (dt, *J* = 2.8, 1.4 Hz, 1H, C9-H), 3.25 − 3.18 (m, 1H, C12-H), 2.64 (ddt, *J* = 15.2, 6.6, 1.4 Hz, 1H, C8-H), 2.52 − 2.42 (m, 2H, C5-H/C8-H), 1.58 (dt, *J* = 9.3, 1.6 Hz, 1H, C15-H), 1.46 (dt, *J* = 9.3, 1.8 Hz, 1H, C15-H). ^{13}C NMR (101 MHz, Chloroform-*d*) δ 207.62, 140.20, 136.09, 131.11, 119.18, 73.07, 69.72, 66.41, 63.45, 55.09, 51.06, 46.27, 44.41, 44.05, 31.66.

7.2.7. (1R,5R,6R)-1-allyl-4-(((tert-butyldimethylsilyl)oxy)methyl)-5-hydroxy-7-oxabicyclo[4.1.0]hept-3-en-2-one (Compound 1.61)
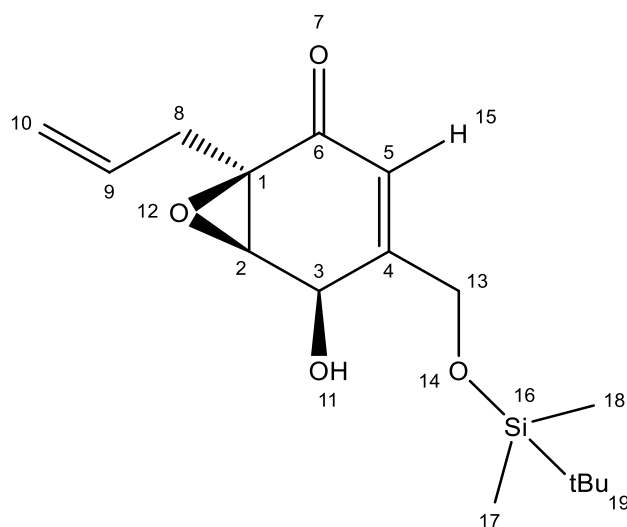
A solution of **2.27** (571 mg, 1.5 mmol) in diphenyl ether (10 mL) was heated for 4 h at 230 ℃. Reaction monitored by TLC (hexane/EtOAc 3:1). Upon completion, the reaction mixture was cooled to ambient temperature and product purified by flash chromatography, initially with PET ether, followed by PET ether:EtOAc 10:1 yielding the title compound as an off-white solid (333 mg, 73 %). R_f = 0.25 (hexane/EtOAc 3:1). MS: *m/z* (+ESI) exact mass calc'd for $C_{16}H_{26}O_4Si$ [M + Na]$^+$ 333.1498 found 333.1493. ^{1}H NMR (400 MHz, Chloroform-*d*) δ 6.00 (q, *J* = 1.7 Hz, 1H, C15-H), 5.73 (dddd, *J* = 16.9, 10.6, 7.5, 6.5 Hz, 1H, C9-H), 5.19 – 5.09 (m, 2H, C10-H), 4.65 (ddd, *J* = 9.1, 3.0, 1.3 Hz, 1H, C3-H), 4.49 – 4.34 (m, 2H, C13-H), 3.74 (d, *J* = 3.0 Hz, 1H, C2-H), 2.84 (ddt, *J* = 15.1, 7.6, 1.2 Hz, 1H, C8-H), 2.62 – 2.49 (m, 2H, C8-H/C11-H), 1.61, 0.91 (s, 9H, *t*Bu·H), 0.09 (d, *J* = 1.5 Hz, 6H, C17-H/C18-H). ^{13}C NMR (101 MHz, Chloroform-*d*) δ 193.19, 157.19, 131.32, 120.25, 119.25, 65.98, 63.12, 60.76, 59.17, 40.84, 32.07, 25.80, 23.83, 20.79, 18.26, 17.49, 17.30, 14.65, -5.47, -5.50.

7.2.8. tert-butyl (E)-4-((1R,5R,6R)-4-(((tert-butyldimethylsilyl)oxy)methyl)-5-hydroxy-2-oxo-7-oxabicyclo[4.1.0]hept-3-en-1-yl)-2-methylbut-2-enoate (Compound 1.62)
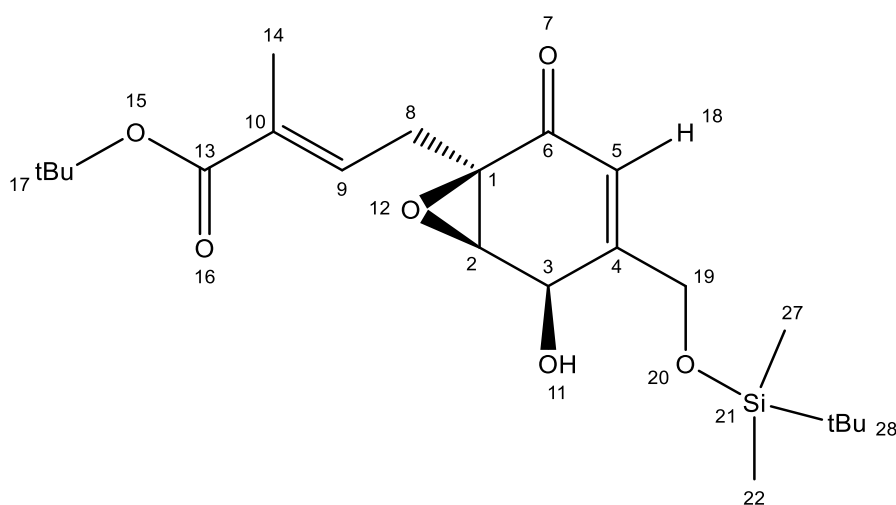
A solution of **1.61** (333 mg, 1.5 mmol) in MeOH (10 mL) was cooled to -78 ℃ and ozonloysed for 3 min. Dimethylsulphide (2.64 mL) was added and the reaction was allowed to proceed for 30 min with stirring and gradual warming to ambient temperature. Monitored by TLC (hexane/EtOAc 3:1). Upon completion, reaction mixture quenched with H_2O and organic phase extracted with DCM (3×10 mL) and organic layers concentrated under reduced pressure. To a solution of the crude aldehyde (280 mg, 0.89 mmol) in DCM (5 mL), a solution of $Ph_3P=C(CH_3)CO_2t$-Bu (567 mg, 1.45 mmol) in DCM (5 mL) was added dropwise at -40 ℃ with stirring. Reaction allowed to warm to -10 ℃ and stirred for 2 h. Monitored by TLC (hexane/EtOAc 10:1). When completed, product purified by silica gel chromatography (PET ether/EtOAc 10:1) yielding the title compound as a yellow/ brown oil (157 mg, 25 %). $R_f = 0.26$ (hexane/EtOAc 10:1); MS: m/z (+ESI) exact mass calc'd for $C_{22}H_{36}O_6Si$ [M + Na]$^+$ 447.5988 found 447.2182. ^1H NMR (400 MHz, Chloroform-d) δ H-9 6.50 (ddd, J = 8.3, 6.9, 1.5 Hz, 1H, C9-H), 6.01 (q, J = 1.7 Hz, 1H, C18-H), 4.67 (s, 1H, C3-H), 4.49 – 4.35 (m, 2H, C19-H), 3.73 (d, J = 3.0 Hz, 1H, C2-H), 2.95 (dd, J = 15.8, 8.0 Hz, 1H, C8-H), 2.66 (dd, J = 15.9, 7.0 Hz, 1H, C8-H), 1.84 (d, J = 1.4 Hz, 3H, C14-H), 1.48 (s, 9H, tBu17-H), 0.92 (s, 9H, tBu26-H), 0.10 (d, J = 1.4 Hz, 6H, C22-H/C27-H). ^{13}C NMR (101 MHz, Chloroform-d) δ 192.87, 166.89, 157.30, 132.95, 132.42, 120.15, 80.48, 65.96, 63.17, 60.51, 59.25, 28.10, 27.13, 25.80, 18.26, 12.83, -5.47, -5.49.

7.2.9. tert-butyl(E)-4-((1S,5S,6S)-4-(((tert-butyldimethylsilyl)oxy)methyl)-5-hydroxy- 2-oxo-7-oxabicyclo[4.1.0]hept-3-en-1-yl)-2-methylbut-2-enoate (Compound 1.63)
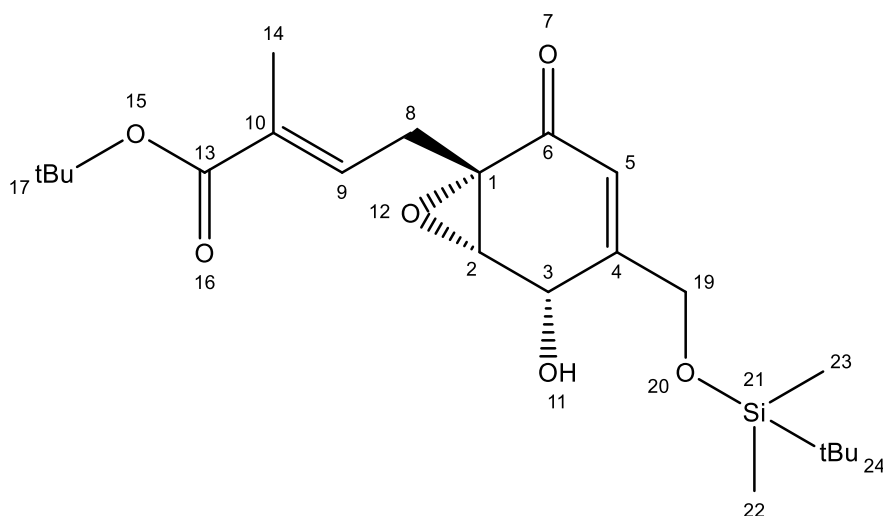
A solution of **1.73** (101 mg, 0.33 mmol) in MeOH (6.6 mL) was ozonolysed at -78 ℃ for 3 min. Dimethylsulphide (0.53 mL) was added and the reaction was allowed to proceed for 30 min whilst warming to ambient temperature. Monitored by TLC (hexane/EtOAc 3:1). When complete, the reaction was quenched with Milli-Q, the organic phase extracted into DCM (3 × 10 mL) and the crude was concentrated under reduced pressure.

A solution of Ph3P=C(CH3)CO2*t*-Bu (156 mg, 0.38 mmol) in DCM (1.3 mL) was cooled to -40 ℃ and a solution of the crude aldehyde (77 mg, 0.22 mmol) in DCM (2.3 mL) was added dropwise. The reaction was warmed to -10 ℃ and allowed to proceed for 2 h with stirring. Monitored by TLC (hexane/EtOAc 10:1). When complete, the product was purified by flash chromatography (PET ether/EtOAc 10:1) yielding the title compound as a clear oil (53 mg, 36 %). R_f = 0.3 (hexane/EtOAc 10:1). $[\alpha]_D^{25}$ = -23.9 (*c* 0.62, CHCl3). MS: *m/z* (+ESI) exact mass calc'd for $C_{22}H_{36}O_6Si$ [M + Na]+ 447.2179 found 447.2173. ^{1}H NMR (400 MHz, Chloroform-*d*) δ 6.53 (ddd, *J* = 8.3, 7.0, 1.6 Hz, 1H, C9-H), 6.04 (q, *J* = 1.7 Hz, 1H, C5-H), 4.73 – 4.66 (m, 1H, C3-H), 4.52 – 4.38 (m, 2H, C19-H), 3.75 (d, *J* = 3.0 Hz, 1H, C2-H), 2.97 (dd, *J* = 15.8, 8.0 Hz, 1H, C8-H), 2.68 (ddd, *J* = 15.9, 6.9, 1.3 Hz, 1H, C8-H), 2.58 (d, *J* = 8.9 Hz, 1H, C11-H), 1.86 (d, *J* = 1.5 Hz, 3H, C14-H), 1.50 (s, 9H, *t*Bu17-H), 0.94 (s, 9H, *t*Bu24-H), 0.12 (d, *J* = 1.3 Hz, 6H, C22-H/C23-H). ^{13}C NMR (101 MHz, Chloroform-*d*) δ 192.88, 157.32, 132.95, 132.43, 120.14, 65.95, 63.16, 60.50, 59.25, 28.10, 27.13, 25.80, 18.26, 12.83, -5.47, -5.49.

7.2.10. (1'R,4'S,4a'R,8a'S)-7'-iodo-1',4',4a',8a'-tetrahydro-8'H-spiro[[1,3]dioxolane-2,5'-[1,4]methanonaphthalen]-8'-one (Compound 1.67)
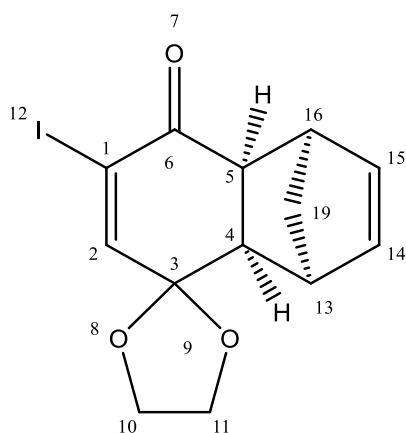
Triflic acid (9 mL, 0.2 M in dry DCM) was added dropwise over 30 sec to a solution of of (*S*)-(-)-*o*-Tolyl-CBS oxazoborolidine in toluene (4.3 mL, 0.5 M) at -78 ºC. After 15 min, a solution of **1.54** (3.26 g, 11.7 mmol) in dry DCM (12 mL) and freshly distilled cyclopentadiene (1.15 mL) were added. Monitored by TLC (hexane/EtOAc 3:1). Upon completion, reaction quenched with 1 mL TEA and warmed to ambient temperature. Crude concentrated *in vacuo* and product purified by silica gel chromatography (PET ether/EtOAc 3:1) yielding the title compound as a yellow/ brown oil (2.27 g, 56 %). R_f = 0.5 (hexane/EtOAc 3:1). $[\alpha]_D^{25}$ = +81.4 (*c* 1, CHCl₃). MS: *m/z* (+ESI) exact mass calc'd for $C_{13}H_{13}IO_3$ [M + Na]⁺ 366.9807 found 366.9807. ¹H NMR (400 MHz, Chloroform-*d*) δ 7.05 (d, *J* = 1.2 Hz, 1H, C2-H), 6.08 (dd, *J* = 5.7, 2.9 Hz, 1H, C14-H), 5.84 (dd, *J* = 5.7, 2.8 Hz, 1H, C15-H), 4.16 – 4.07 (m, 1H, OC$\underline{H}_2$CH₂O), 4.07 – 3.90 (m, 3H, OC$\underline{H}_2$C$\underline{H}_2$O), 3.31 (ddd, *J* = 4.6, 3.0, 1.5 Hz, 1H, C13-H), 3.27 (dd, *J* = 8.4, 4.2 Hz, 1H, C4-H), 3.21 (dq, *J* = 3.5, 1.9 Hz, 1H, C16-H), 2.87 – 2.79 (m, 1H, C5-H), 1.39 (dt, *J* = 8.7, 1.9 Hz, 1H, C19-H), 1.33 (d, *J* = 8.6 Hz, 1H, C19-H).¹³C NMR (101 MHz, Chloroform-*d*) δ 193.53, 153.84, 135.91, 133.42, 108.75, 105.43, 65.53, 64.49, 50.87, 48.62, 46.61, 46.42.

7.2.11. (1'R,4'S,4a'R,8a'S)-7'-allyl-1',4',4a',8a'-tetrahydro-8'H-spiro[[1,3]dioxolane-2,5'-[1,4]methanonaphthalen]-8'-one (Compound 1.69)
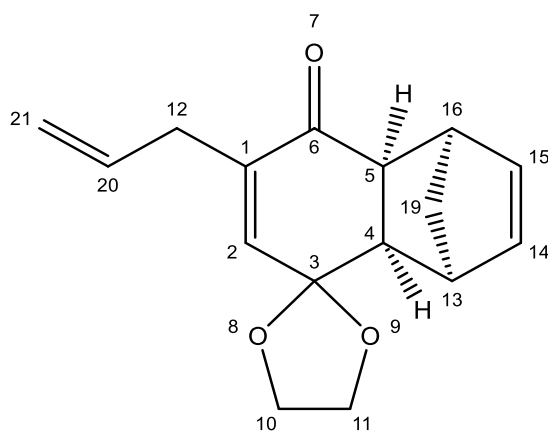
Pd(PPh$_3$)$_4$ (564 mg, 7.5 mol%) and allyltributyl tin (4 mL, 13.1 mmol) were added to a solution of **1.67** (2.23 g, 6.6 mmol) in degassed THF (10 mL) under nitrogen. The mixture was heated to 110 ºC with 150 W microwave radiation for 10 min with stirring. Monitored by TLC (hexane/EtOAc 3:1) and upon completion, the reaction mix was cooled to ambient temperature and quenched with saturated NH$_4$Cl (aq.). Organic phase extracted with EtOAc (3 × 10 mL). Crude concentrated under reduced pressure and product purified by silica gel chromatography (PET ether/EtOAc 9:1) yielding the title compound as a brown oil (1.18 g, 69 %). R$_f$ = 0.5 (hexane/EtOAc 3:1); MS: *m/z* (+ESI) exact mass calc'd for C$_{16}$H$_{18}$O$_3$ [M + Na]$^+$ 281.1154 found 281.1156. ^{1}H NMR (400 MHz, Chloroform-*d*) δ 6.08 – 6.00 (m, 2H, C<u>H</u>=C<u>H</u>), 5.80 (dd, *J* = 5.6, 2.8 Hz, 1H, C2-H), 5.78 – 5.64 (m, 1H, C20-H), 5.06 (ddq, *J* = 15.4, 3.5, 1.8 Hz, 2H, C21-H), 4.16 – 4.04 (m, 1H, OC<u>H</u>$_2$CH$_2$O), 4.04 – 3.91 (m, 3H, OC<u>H</u>$_2$C<u>H</u>$_2$O), 3.31 (dhept, *J* = 4.3, 1.4 Hz, 1H, C13-H), 3.17 (dh, *J* = 3.5, 1.7 Hz, 1H, C16-H), 3.06 (dd, *J* = 8.8, 4.3 Hz, 1H, C5-H), 2.91 – 2.86 (m, 2H, C12-H), 2.86 – 2.78 (m, 1H, C4-H), 1.41 (dt, *J* = 8.5, 1.8 Hz, 1H, C19-H), 1.35 – 1.28 (m, 1H, C19-H). ^{13}C NMR (101 MHz, Chloroform-*d*) δ 199.63, 141.86, 140.74, 135.58, 134.53, 133.48, 117.36, 104.57, 65.49, 64.19, 50.41, 48.91, 47.88, 46.67, 46.14, 33.15.

7.2.12. (1aS,2aS,3R,6S,6aR,7aR)-1a-allyl-1a,2a,3,6,6a,7a-hexahydro-3,6-methanonaphtho[2,3-b]oxirene-2,7-dione (Compound 1.70)
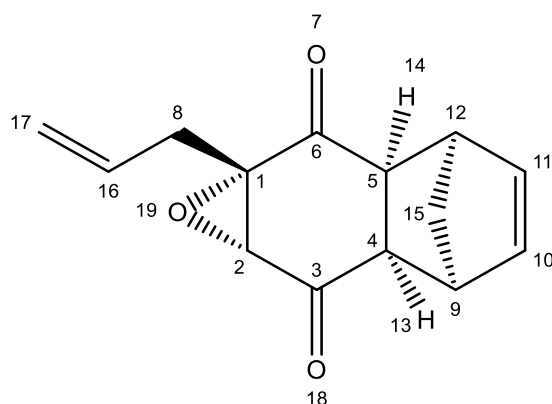
10 % Na_2CO_3 (2.57 mL, aq.) was added to a solution of **2.45** (918 mg, 4.2 mmol) and the mixture was stirred at 0 ℃. H_2O_2 (5.22 mL, non-stab., 30 % (v/v)) was then added dropwise and the reaction was allowed to proceed for 30 min at 0 ℃. Monitored by TLC (hexane/EtOAc 3:1). When complete, reaction quenched with sat. NH_4Cl (aq.) and the organic layer extracted into DCM (3 × 10 mL), dried over anhydrous $MgSO_4$, filtered and concentrated under reduced pressure. Product purified by silica gel chromatography (PET ether/EtOAc 9:1) yielding the title compound as a red/brown oil which (759 mg, 76 %). R_f = 0.50 (hexane/EtOAc 3:1). MS: m/z (+ESI) exact mass calc'd for $C_{14}H_{14}O_3$ [M + Na]+ 253.2528 found 253.0828. ^{1}H NMR (400 MHz, Chloroform-d) δ 6.04 (t, J = 1.8 Hz, 2H, CH=CH), 5.62 (dddd, J = 16.5, 10.9, 7.5, 6.4 Hz, 1H, C16-H), 5.16 – 5.06 (m, 2H, C17-H), 3.51 – 3.40 (m, 2H, C9-H/C12-H), 3.38 (s, 1H, C2-H), 3.28 (ddp, J = 4.9, 3.3, 1.7 Hz, 2H, C4-H/C5-H), 2.70 (ddt, J = 15.2, 6.5, 1.4 Hz, 1H, C8-H), 2.55 (ddt, J = 15.3, 7.6, 1.2 Hz, 1H, C8-H), 1.48 (dt, J = 8.8, 1.9 Hz, 1H, C15-H), 1.29 (dt, J = 8.6, 1.5 Hz, 1H, C15-H). ^{13}C NMR (101 MHz, Chloroform-d) δ 204.90, 204.89, 136.68, 136.62, 130.14, 119.99, 66.26, 62.04, 50.51, 49.99, 46.66, 43.40, 43.22, 31.70.

7.2.13. (1aS,2aS,3R,6S,6aR,7aR)-1a-allyl-6a-(hydroxymethyl)-1a,2a,3,6,6a,7a-hexahydro-3,6-methanonaphtho[2,3-b]oxirene-2,7-dione (Compound 1.71)
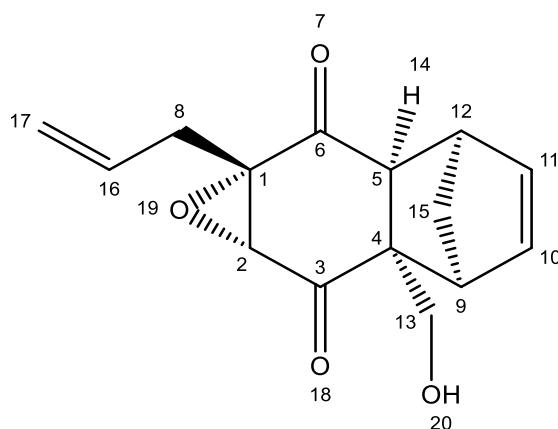
DBU (45 µL, 20 mol %) and aqueous formaldehyde (573 µL, 7.44 mmol, 37 % (w/v)) were added to a solution of **1.70** (759 mg, 3.2 mmol) in THF (10 mL) at 0 °C. The mixture was stirred for 30 min, after which additional formaldehyde (500 µL, 6.48 mmol, 37 % (w/v)) was added. The mixture was stirred for a further 30 min. Monitored by TLC (hexane/EtOAc 3:1). When complete, reaction quenched with sat. NH_4Cl (aq.), aqueous phase extracted with EtOAc (3×10 mL), dried over anhydrous $MgSO_4$, filtered and concentrated under reduced pressure. Product purified by silica gel chromatography (PET ether/EtOAc 5:1) yielding title compound as a white solid (730 mg, 87 %). $R_f = 0.2$ (hexane/EtOAc 3:1). MS: *m/z* (+ESI) exact mass calc'd for $C_{15}H_{16}O_4$ [M + Na]+ 283.0946 found 283.0947. ^{1}H NMR (400 MHz, Chloroform-*d*) δ 6.07 (t, *J* = 1.8 Hz, 2H, CH=CH), 5.62 (dddd, *J* = 16.9, 10.4, 7.4, 6.5 Hz, 1H, C16-H), 5.14 (dp, *J* = 5.2, 1.7 Hz, 1H, C17-H), H-17 5.12 – 5.04 (m, 1H, C17-H), 4.39 – 4.28 (m, 1H, C13-H), 3.82 (dd, *J* = 11.5, 4.6 Hz, 1H, C13-H), 3.45 (d, *J* = 5.3 Hz, 1H, C2-H), 3.31 (ddq, *J* = 11.9, 3.6, 1.8 Hz, 2H, C9-H/C12-H), 2.87 (d, *J* = 3.7 Hz, 1H, C5-H), 2.74 – 2.55 (m, 2H, C8-H), 1.52 (dt, *J* = 9.4, 1.6 Hz, 1H, C15-H), 1.45 (dt, *J* = 9.5, 1.8 Hz, 1H, C15-H). ^{13}C NMR (101 MHz, Chloroform-*d*) δ 205.25, 204.12, 138.10, 137.98, 129.95, 120.13, 68.25, 67.16, 61.92, 61.63, 53.82, 45.96, 44.42, 43.42, 31.72.

7.2.14. (1aS,2aS,3R,6S,6aR,7S,7aS)-1a-allyl-7-hydroxy-6a-(hydroxymethyl)-2a,3,6,6a,7,7a-hexahydro-3,6-methanonaphtho[2,3-b]oxiren-2(1aH)-one (Compound 1.72)
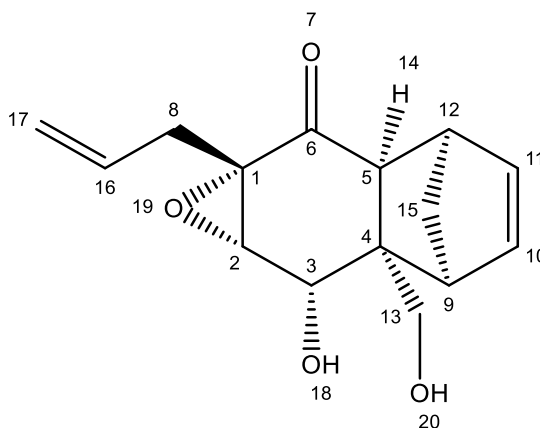
DIBAL-H (5.38 mL, 6.4 mmol, 1.2 M in toluene) was added dropwise to a solution of **1.71** (730 mg, 2.8 mmol) in dry THF at -78 ℃. Reaction was stirred for 30 min at -78 ℃. After 30 min, additional DIBAL-H (2 mL, 2.3 mmol) was added. Monitored by TLC (hexane/EtOAc 2:1). When complete, quenched with MeOH (3 mL) and HCl (14.45 mL, 1 M), organic phase extracted with EtOAc (3 × 10 mL), dried over anhydrous MgSO4, filtered and concentrated under reduced pressure. Product purified by silica gel chromatography (PET ether/ EtOAc 2:1) yielding the title compound as a clear solid (429 mg, 57 %). = 0.2 (hexane/EtOAc 2:1). $[\alpha]_D^{25}$ = 43.9 (*c* 59, CHCl$_3$). MS: m/z (+ESI) exact mass calc'd for C$_{15}$H$_{18}$O$_4$ [M + Na]+ 285.1103 found 285.1104. ^{1}H NMR (400 MHz, Chloroform-*d*) δ 6.30 (dd, *J* = 5.8, 2.9 Hz, 1H, C11-H), 6.12 (dd, *J* = 5.7, 3.2 Hz, 1H, C10-H), 5.65 (ddt, *J* = 18.0, 9.3, 7.0 Hz, 1H, C16-H), 5.13 – 5.04 (m, 2H, C17-H), 4.65 (d, *J* = 11.5 Hz, 1H, C13-H), 4.06 (s, 1H, 20 OH), 3.97 (s, 1H, C3-H), 3.83 (d, *J* = 11.5 Hz, 1H, C13-H), 3.47 (s, 1H, C2-H), 3.30 (s, 1H, C9-H), 3.24 (d, *J* = 4.5 Hz, 1H. C12-H), 2.93 (s, 1H, C13-H), 2.65 (dd, *J* = 15.1, 6.5 Hz, 1H, C8H), 2.55 – 2.43 (m, 2H, C8-H/C5-H), 1.58 (d, *J* = 9.2 Hz, 1H, C15-H), 1.47 (dt, *J* = 9.2, 1.9 Hz, 1H, C15-H). ^{13}C NMR (101 MHz, Chloroform-*d*) δ 207.41, 140.25, 136.10, 131.12, 119.18, 73.12, 70.00, 66.47, 63.52, 55.24, 51.10, 46.56, 44.44, 44.09, 31.67.

7.2.15. (1S,5S,6S)-1-allyl-4-(((tert-butyldimethylsilyl)oxy)methyl)-5-hydroxy-7-oxabicyclo[4.1.0]hept-3-en-2-one (Compound 1.73)
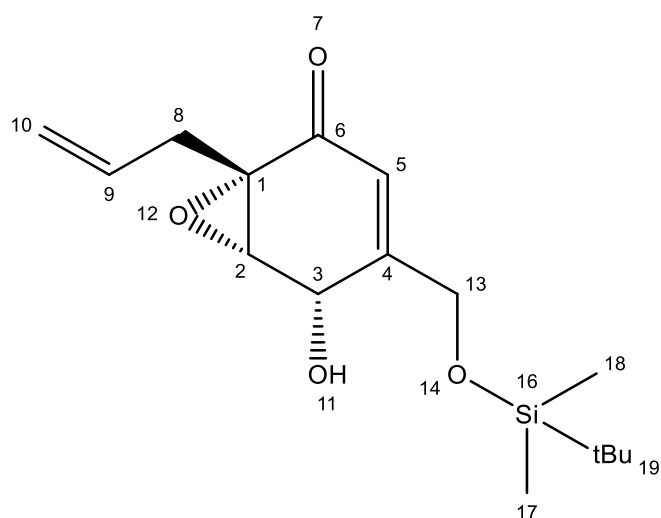
A solution of **2.46** (591 mg, 1.56 mmol) in diphenyl ether (10 mL) was heated for 4 h at 230 ℃ with stirring. Monitored by TLC (hexane/EtOAc 3:1). When complete, reaction allowed to cool and product purified by silica gel chromatography- initially with PET ether followed by PET ether:EtOAc 10:1 yielding the title compound as an off-white solid (206 mg, 38 %). R_f = 0.2 (hexane/EtOAc 3:1). MS: *m/z* (+ESI) exact mass calc'd for $C_{16}H_{26}O_4Si$ [M + Na]+ 333.1498 found 333.1493. ^{1}H NMR (400 MHz, Chloroform-*d*) δ 6.00 (q, *J* = 1.7 Hz, 1H, C5-H), 5.73 (dddd, *J* = 17.0, 10.6, 7.6, 6.5 Hz, 1H, C9-H), 5.19 – 5.09 (m, 2H, C10-H), 4.65 (ddd, *J* = 9.0, 3.0, 1.4 Hz, 1H, C3-H), 4.49 – 4.42 (m, 1H, C13-H), 4.42 – 4.35 (m, 1H, C13-H), 3.74 (d, *J* = 3.1 Hz, 1H, C2-H), 2.84 (ddt, *J* = 15.0, 7.6, 1.2 Hz, 1H, C8-H), 2.60 – 2.47 (m, 2H. C8-H/C11-H), 0.91 (s, 9H, C-*t*Bu-H), 0.09 (d, *J* = 1.5 Hz, 6H, C17-H/C18-H). ^{13}C NMR (101 MHz, Chloroform-*d*) δ 192.99, 156.96, 131.14, 120.10, 119.07, 65.81, 62.96, 60.58, 58.98, 31.90, 25.63, 18.09, -5.65, -5.67.

7.2.16. (TBAF route) tert-butyl (E)-4-((1R,5R,6R)-5-hydroxy-4-(hydroxymethyl)-2-oxo-7-oxabicyclo[4.1.0]hept-3-en-1-yl)-2-methylbut-2-enoate (Compound 1.74)
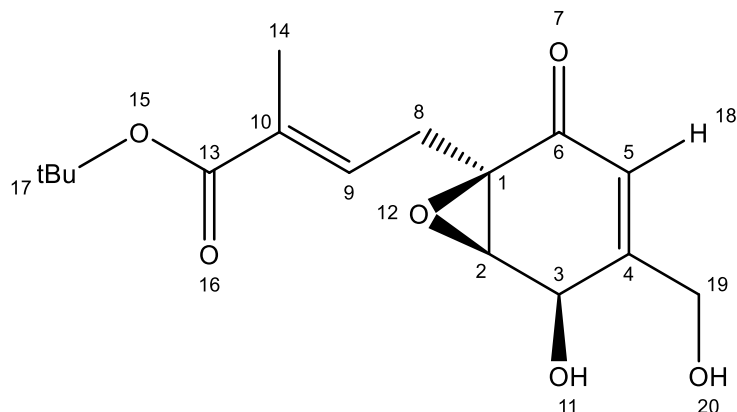
TBAF (800 µL, 0.8 mmol, 1 M in THF) was added to a solution of **1.62** (157 mg, 0.37 mmol) in dry THF (5 mL) at 0 ºC and the mixture stirred for 4 h. Monitored by TLC (hexane/EtOAc 1:1). Upon completion, the mixture was quenched with saturated NH_4Cl (aq.), organic layer extracted with EtOAc (3×10 mL), dried over $MgSO_4$, filtered and concentrated *in vacuo*. Product purified by silica gel chromatography (PET ether/ EtOAc 1:1) yielding the tile compound as a brown oil (41 mg, 40 %). R_f = 0.15 (hexane/EtOAc 1:1). MS: *m/z* (+ESI) exact mass calc'd for $C_{16}H_{22}O_6$ $[M + Na]^+$ 333.1314 found 333.1316. ^{1}H NMR (400 MHz, Chloroform-*d*) δ 6.49 (tt, *J* = 6.9, 1.5 Hz, 1H, C9-H), 5.99 (q, *J* = 1.5 Hz, 1H, C5-H), 4.73 (d, *J* = 5.3 Hz, 1H, C3-H), 4.42 (s, 2H, C19-H), 3.74 (d, *J* = 2.9 Hz, 1H, C2-H), 3.10 (s, 1H, C11-H), 2.98 – 2.86 (m, 1H, C8-H), 2.67 (ddd, *J* = 16.0, 7.0, 1.3 Hz, 1H, C8-H), 2.54 (s, 1H, C20-H), 1.83 (d, *J* = 1.5 Hz, 3H, C14-H), 1.47 (s, 9H, *t*Bu17-H). ^{13}C NMR (101 MHz, Chloroform-*d*) δ 192.79, 166.92, 156.95, 132.77, 132.30, 120.48, 80.52, 65.65, 62.75, 60.39, 59.11, 27.91, 26.87, 12.67.

7.2.17. (AcOH route) tert-butyl (E)-4-((1R,5R,6R)-5-hydroxy-4-(hydroxymethyl)-2-oxo-7-oxabicyclo[4.1.0]hept-3-en-1-yl)-2-methylbut-2-enoate (Compound 1.74)
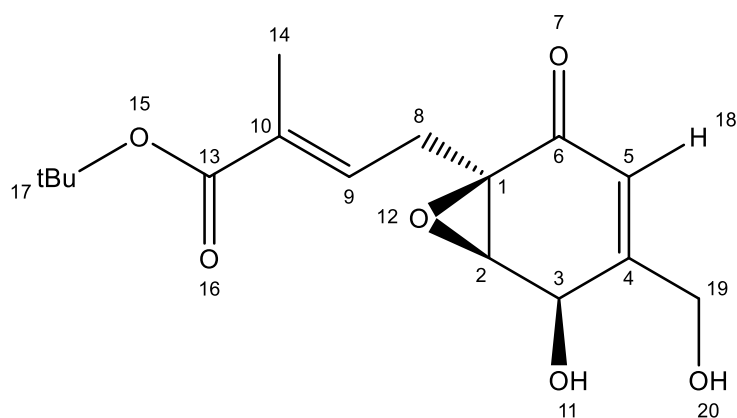
1.62 (393 mg/ 0.92 mmol) was dissolved in diethyl ether (2 mL) and cooled to 0 ºC. Once cooled, 4mL of acetic acid and 2 mL of Milli-Q were added and the reaction was stirred overnight with gradual warming to ambient temperature. The reaction was monitored by TLC (hexane/EtOAc 1:1). Upon completion, the reaction mixture was concentrated under reduced pressure yielding the title compound as a yellow oil (157 mg/ 54 %). $R_f = 0.16$ (hexane/ EtOAc 1:1). MS: m/z (+ESI) exact mass calc'd for $C_{16}H_{22}O_6$ [M + Na]$^+$ 333.1309 found 333.1312. ^{1}H NMR (400 MHz, Chloroform-d) δ 6.47 (ddd, J = 8.1, 6.8, 1.6 Hz, 1H, C9-H), 5.97 (d, J = 1.6 Hz, 1H, C5-H), 4.71 (s, 1H, C3-H), 4.38 (s, 2H, C19-H), 3.73 (d, J = 2.8 Hz, 1H, C2-H), 2.87 (dd, J = 15.9, 7.9 Hz, 1H, C8-H), 2.71 – 2.60 (m, 1H, C8-H), 1.81 (d, J = 1.4 Hz, 3H, C14-), 1.46 (s, 9H, t-butyl H). ^{13}C NMR (101 MHz, Chloroform-d) δ 193.36, 167.37, 157.98, 132.83, 132.78, 120.35, 80.86, 65.67, 62.57, 60.49, 59.48, 28.08, 27.06, 12.85.

7.2.18. tert-butyl-(E)-4-((1R,6S)-4-(((tert-butyldimethylsilyl)oxy)methyl)-2,5-dioxobicyclo[4.1.0]hept-3-en-1-yl)-2-methylbut-2-enoate (Compound 1.75)
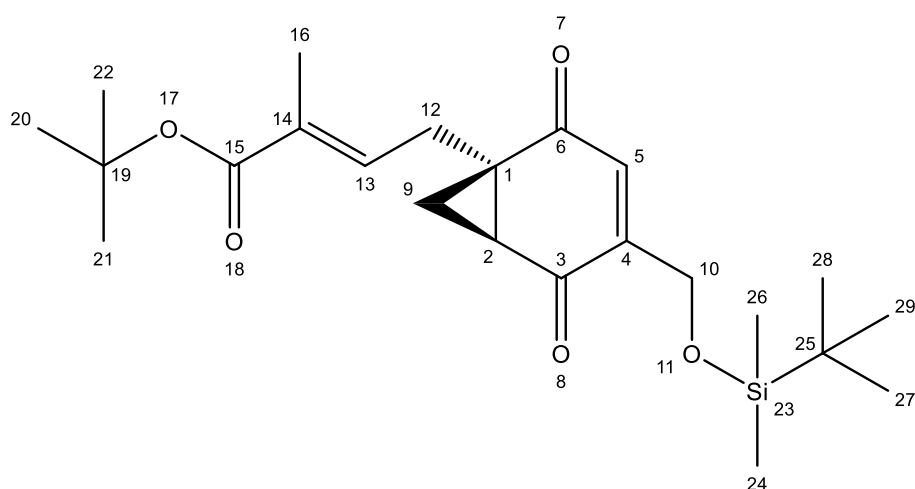
A solution of **1.81** (29 mg, 0.22 mmol) in MeOH (5 mL) was ozonolysed for 4 min at – 78 ºC with stirring. Dimethyl sulphide (414 µL) was added and the reaction was allowed to proceed for 30 min at r.t.. Monitored by TLC (hexane/EtOAc 3:1). When complete, reaction was quenched with Milli-Q and the organic layer was extracted with DCM (3 × 5 mL), dried over anhyd. MgSO$_4$, filtered and concentrated *in vacuo.*

A solution of Ph$_3$P=C(CH$_3$)CO$_2$*t*-Bu (9 mg) in dry DCM (5 mL) was cooled to -40 ºC and a solution of the crude aldehyde in dry DCM (5 mL) was added dropwise with stirring. The reaction was allowed to proceed for 2 h with gradual warming to -10 ºC. Monitored by TLC (hexane/EtOAc 10:1). Purified by preparatory TLC (hexane/EtOAc 3:1) yielding the title compound as a clear oil (37 mg, 0.088 mmol, 40 %). R$_f$ = 0.52 (hexane/EtOAc 3:1). MS: *m/z* (+ESI) exact mass calc'd for C$_{23}$H$_{36}$O$_5$Si [M + Na]$^+$ 443.2224, found 443.2233. ^{1}H NMR (400 MHz, Chloroform-*d*) δ 6.59 – 6.47 (m, 2H, C5-H, C13-H), 4.54 (dd, *J* = 18.5, 2.5 Hz, 1H, C10-H), 4.30 (dd, *J* = 18.5, 2.1 Hz, 1H, C10-H), 2.97 – 2.82 (m, 1H, C12-H), 2.47 – 2.31 (m, 2H C12-H/ C9-), 1.83 (d, *J* = 1.4 Hz, 3H C16-H), 1.76 (t, *J* = 5.0 Hz, 1H C2-H), 1.55 (dd, *J* = 8.9, 4.9 Hz, 1H C9-H), 1.47 (s, 9H COO*t*-Bu H), 0.91 (s, 9H *t*-Bu), 0.11 – 0.06 (m, 6H C24-H/ C25-H). ^{13}C NMR (101 MHz, Chloroform-*d*) δ 195.46, 195.32, 148.31, 134.90, 132.15, 131.24, 80.48, 59.26, 36.32, 32.85, 29.56, 28.10, 26.41, 25.83, 18.27, 12.77, -5.48, -5.50.

7.2.19. (1R,4S,4aR,8aS)-6-allyl-1,4,4a,8a-tetrahydro-1,4-methanonaphthalene-5,8-dione (Compound 1.76)
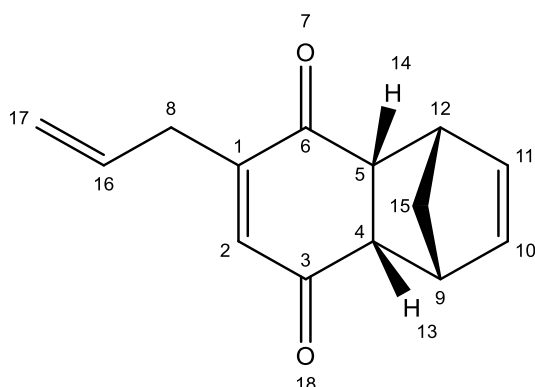
H$_2$SO$_4$ (8.08 mL, 1 N) and acetone (8.08 mL) were added to a solution of **1.57** (1.78 g, 6.8 mmol) in dry THF (5 mL) and the mixture was stirred for 30 min at ambient temperature. Reaction monitored by TLC (hexane/EtOAc 3:1). When complete, the organic phase was extracted with DCM (3 × 10 mL) and dried over anhydrous MgSO$_4$, filtered and concentrated under reduced pressure yielding title compound as a brown/ red waxy solid (1.38 g, 96%) which was used in the next step without further purification. R$_f$ = 0.5 (hexane/EtOAc 3:1). MS: *m/z* (+ESI) exact mass calc'd for C$_{14}$H$_{14}$O$_3$ 237.0891 found 237.0881. ^{1}H NMR (400 MHz, Chloroform-*d*) δ 6.45 (t, *J* = 1.5 Hz, 1H, C2-H), 6.05 (ddd, *J* = 18.0, 5.7, 2.8 Hz, 2H, CH=CH), 5.74 (ddt, *J* = 17.0, 10.1, 6.8 Hz, 1H, C16-H), 5.26 – 4.97 (m, 2H, C17-H), 3.54 (dh, *J* = 4.5, 1.4 Hz, 2H, C9-H/C12-H), 3.23 (t, *J* = 2.6 Hz, 2H, C8-H), 3.06 (dq, *J* = 6.9, 1.4 Hz, 2H, C4-H/C5-H), 1.49 (ddt, *J* = 40.3, 8.7, 1.7 Hz, 2H, C15-H). ^{13}C NMR (101 MHz, Chloroform-*d*) δ 199.26, 198.87, 153.38, 139.15, 135.47, 135.01, 132.91, 118.74, 49.01, 48.98, 48.89, 48.65, 48.54, 33.39.

7.2.20. (1aR,2aR,3S,6R,6aS,7aS)-1a-allyl-1a,2a,3,6,6a,7a-hexahydro-1H-3,6-methanocyclopropa[b]naphthalene-2,7-dione (Compound 1.78)
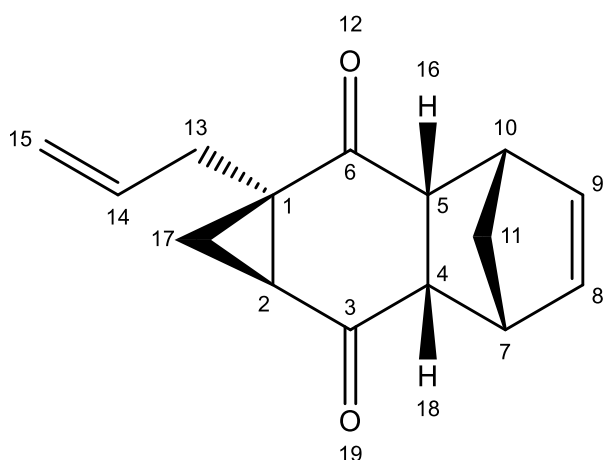
n-BuLi (520 μL, 1.3 mmol) was added dropwise to a stirring suspension of trimethylsulphoxonium iodide (568 mg, 2.6 mmol) in dry THF (10 mL) at − 76 ℃ and stirred for 1 h. After 1 h, a solution of **1.76** (271 mg, 1.3 mmol) in dry THF (10 mL) was added and the reaction was stirred for 1 h whilst warming to ambient temperature. Monitored by TLC (hexane/EtOAc 3:1). Upon completion, reaction quenched with Milli-Q, organic phase extracted with DCM (3 × 20 mL), dried over anhyd. MgSO$_4$, filtered and concentrated under reduced pressure. Product purified by silica gel chromatography (PET ether/EtOAc 3:1) yielding the title compound as a brown oil (133mg, 45 %). R$_f$ = 0.3 (hexane/EtOAc 3:1).). MS: *m/z* (+ESI) calc'd for C$_{15}$H$_{16}$O$_2$ [M + Na]$^+$ 251.1043 found 251.1039. ^{1}H NMR (500 MHz, Chloroform-*d*) δ 6.07 (qd, *J* = 5.6, 2.7 Hz, 2H, C8-H/ C9-H), 5.64 (ddt, *J* = 17.1, 10.2, 6.8 Hz, 1H, C14-H), 5.05 − 4.94 (m, 2H, C15-H), 3.42 − 3.32 (m, 2H, C7-H/ C10-H), 3.23 − 3.12 (m, 2H, C4H/ C5-H), 2.33 (qdt, *J* = 14.9, 6.8, 1.3 Hz, 2H, C13-H), 2.07 (dd, *J* = 8.4, 5.6 Hz, 1H, C17-H), 2.01 (t, *J* = 5.6 Hz, 1H, C17-H), 1.57 (dd, *J* = 8.4, 5.6 Hz, 1H, C2-H), 1.43 (dt, *J* = 8.8, 1.9 Hz, 1H, C11-H), 1.24 (dt, *J* = 8.8, 1.5 Hz, 1H, C11-H).^{13}C NMR (126 MHz, Chloroform-*d*) δ 205.91, 205.77, 136.87, 136.74, 133.37, 117.99, 49.59, 49.08, 46.64, 44.88, 44.59, 40.71, 37.78, 34.87, 19.45.

7.2.21. (1aR,3S,6R,6aS,7aS)-1a-allyl-6a-(((tert-butyldimethylsilyl)oxy)methyl)-1a,2a,3,6,6a,7a-hexahydro-1H-3,6-methanocyclopropa[b]naphthalene-2,7-dione (Compound 1.79)
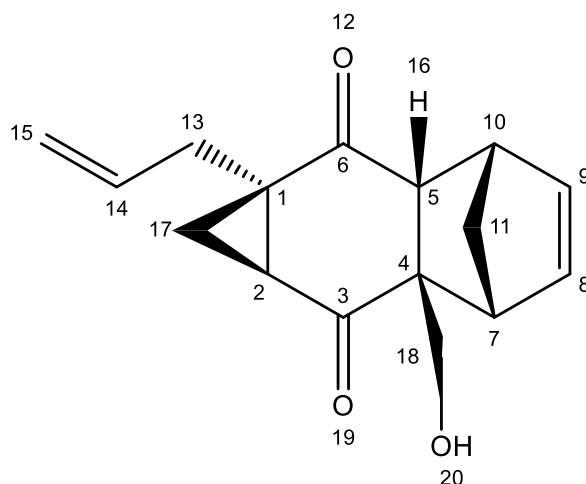
DBU (15 µL, 20 mol%) and aqueous formaldehyde (190 µL, 2.5 mmol, 37 % (w/v)) were added to a solution of **1.78** (122 mg, 0.5 mmol) in dry THF (5 mL) at 0 °C. The reaction was stirred for 2 h with gradual warming to ambient temperature. After 2 h, additional formaldehyde (190 µL, 2.5 mmol) was added and the reaction was stirred for a further 14 h at ambient temperature. Monitored by TLC (hexane/EtOAc 1:1). When complete, reaction quenched with sat. NH_4Cl (aq.), aqueous phase extracted with EtOAc (3 × 10 mL), organic layers combined, dried over anhyd. $MgSO_4$, filtered and concentrated under reduced pressure. Product purified by silica gel chromatography (PET ether/EtOAc 1:1) yielding the title compound as a light yellow oil (82 mg, 62 %). R_f = 0.17 (hexane/EtOAc 1:1). MS: *m/z* (+ESI) exact mass calc'd for $C_{16}H_{18}O_3$ [M + Na]$^+$ 281.1148 found 281.1147. ^{1}H NMR (400 MHz, Chloroform-*d*) δ 6.19 – 6.10 (m, 1H, C8-H), 6.08 (dd, *J* = 5.7, 2.8 Hz, 1H, C9-H), 5.61 (ddt, *J* = 17.2, 10.6, 6.9 Hz, 1H, C14-H), 5.11 – 4.95 (m, 2H, C15-H), 3.98 – 3.85 (m, 1H, C18-H), 3.74 (d, *J* = 10.8 Hz, 1H, C18-H), 3.50 (p, *J* = 2.1 Hz, 1H, C10-H), 3.26 (s, 1H, C7-H), 2.79 – 2.67 (m, 2H, C5-H, C13-H), 2.27 (q, *J* = 5.6 Hz, 1H, C17-H), 2.13 – 2.03 (m, 1H, C17-H), 1.93 (dd, *J* = 14.7, 6.9 Hz, 1H, C13-H), 1.51 – 1.28 (m, 3H, C2-H/ C11-H). ^{13}C NMR (101 MHz, Chloroform-*d*) δ 209.41, 206.14, 138.57, 136.98, 133.61, 118.09, 70.19, 59.59, 52.17, 50.88, 49.80, 48.51, 44.65, 40.52, 36.40, 35.59, 17.77.

7.2.22. (1aR,3S,6R,6aS,7aS)-1a-allyl-6a-(((tert-butyldimethylsilyl)oxy)methyl)-1a,2a,3,6,6a,7a-hexahydro-1H-3,6-methanocyclopropa[b]naphthalene-2,7-dione (Compound 1.80)
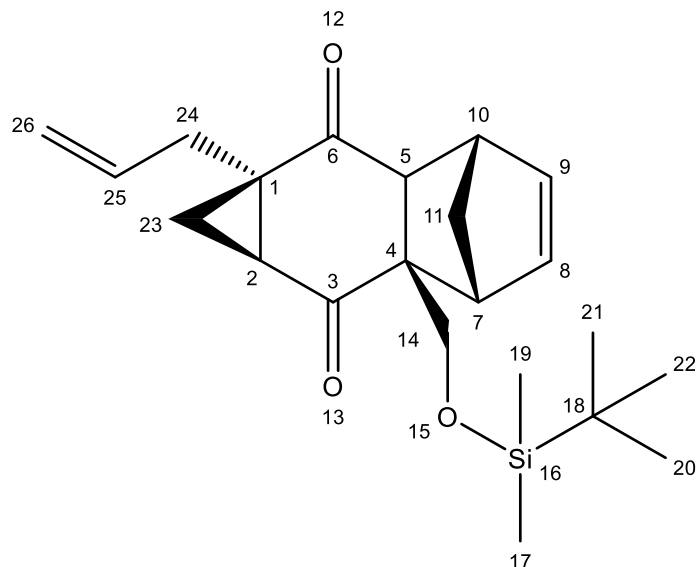
Imidazole (51 mg, 0.75 mmol) was added to a solution of **1.79** (30 mg, 0.16 mmol) in dry DMF (5 mL). Mixture was stirred at r.t. for 30 min, before cooling to 0 ℃ and addition of TBSCl (60 mg, 0.34 mmol). Stirred overnight with gradual warming to r.t.. Additional TBSCl (60 mg, 0.34 mmol) was added. Reaction progress monitored by TLC (hexane/EtOAc 9:1). Upon completion, reaction quenched with Milli-Q and organic layers extracted into hexane (3×10 mL). Organic layers were combined, dried over anhyd. $MgSO_4$, filtered and concentrated *in vacuo*. Product purified by silica gel chromatography (PET ether/EtOAc 15:1) yielding the title compound as a white solid (25 mg, 38 %). R_f = 0.54 (hexane/EtOAc 9:1). MS: *m/z* (+ESI) exact mass calc'd for $C_{22}H_{32}O_3Si$ [M + Na]$^+$ 395.2013 found 395.2021. ^{1}H NMR (400 MHz, Chloroform-*d*) δ 6.17 – 6.09 (m, 1H, C8-H), 6.09 – 6.00 (m, 1H, C9-H), 5.60 (ddt, *J* = 18.2, 9.3, 7.0 Hz, 1H, C25-H), 5.04 – 4.95 (m, 2H, C26-H), 4.13 – 4.01 (m, 1H, C14-H), 3.53 – 3.42 (m, 2H, C10-H/ C14-H), 3.02 (q, *J* = 2.0 Hz, 1H, C7-H), 2.98 – 2.89 (m, 1H, C5-H), 2.84 – 2.65 (m, 1H, C24-H), 2.60 (t, *J* = 5.3 Hz, 1H, C23-H), 2.03 (dd, *J* = 9.0, 5.5 Hz, 1H, C23-H), 1.87 (ddt, *J* = 14.7, 7.0, 1.3 Hz, 1H, C24-H), 1.51 – 1.38 (m, 1H, C11-H), 1.34 (t, *J* = 1.7 Hz, 1H, C11-H), 1.33 – 1.20 (m, 1H, C2-H, under EtOAc peak), 0.88 (s, 9H, *t*-Bu), 0.06 (d, *J* = 10.3 Hz, 6H, C17-H/ C19-H). ^{13}C NMR (101 MHz, Chloroform-*d*) δ 209.11, 206.96, 138.38, 136.90, 133.86, 117.89, 71.86, 60.03, 51.68, 51.57, 49.13, 45.51, 39.89, 36.33, 35.67, 26.06, 18.52, 16.16, -5.40, -5.48.

7.2.23. (Ph₂O route) 1-allyl-4-(((tert-butyldimethylsilyl)oxy)methyl)bicyclo[4.1.0]hept-3-ene-2,5-dione (Compound 1.81)
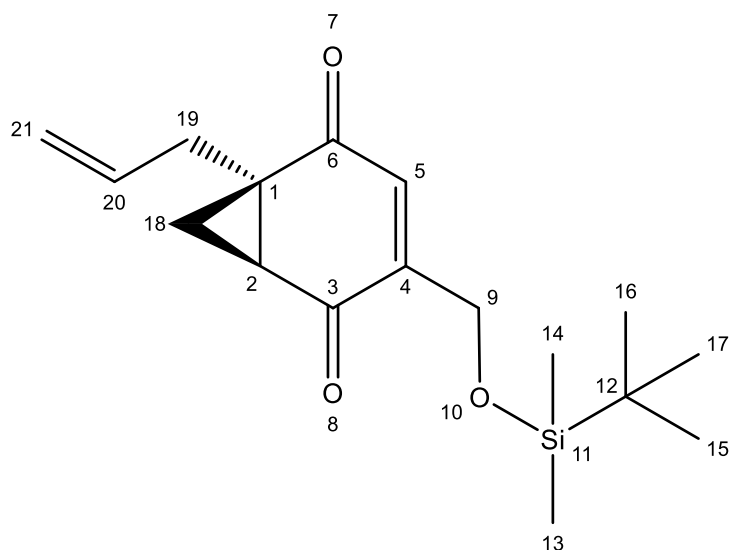
(25 mg, 0.06 mmol) of **1.80** was dissolved in Ph₂O (5 mL) and heated to 140 ºC with 250 W microwave radiation with stirring for 15 min under an argon atmosphere. Reaction monitored by TLC (hexane/EtOAc 8:2). Upon completion, reaction mixture allowed to cool to ambient temperature and product purified by silica gel chromatography, initially with neat hexane followed by Hexane/EtOAc 8:2 yielding title compound as a clear oil (5 mg, 26 %). $R_f = 0.82$ (hexane/EtOAc 8:2). MS: *m/z* (+ESI) exact mass calc'd for $C_{17}H_{26}O_3Si$ [M + Na]⁺ 329.1543 found 329.1555. ¹H NMR (400 MHz, Chloroform-*d*) δ 6.58 – 6.48 (m, 1H, C5-H), 5.75 (ddt, *J* = 17.2, 10.6, 6.9 Hz, 1H, C20-H), 5.12 – 5.02 (m, 2H, C21-H), 4.60 – 4.49 (m, 1H, C9-H), 4.37 – 4.22 (m, 1H, C9-H), 2.90 – 2.78 (m, 1H, C19-H), 2.40 (ddd, *J* = 8.8, 7.1, 5.1 Hz, 1H, C2-H), 2.28 – 2.18 (m, 1H, C19-H), 1.73 (t, *J* = 5.0 Hz, 1H, C18-H), 1.56 – 1.49 (m, 5H, C18-H under water peak), 0.90 (d, *J* = 8.8 Hz, 9H, *t*-Bu), 0.11 – 0.01 (m, 6H, C13-H/ C14-H). ¹³C NMR (101 MHz, Chloroform-*d*) δ 196.01, 195.78, 148.35, 133.45, 132.21, 131.49, 129.45, 118.46, 59.40, 36.72, 34.58, 32.86, 26.62, 25.97, 25.80, 18.42, 1.17, -5.34, -5.36.

7.2.24. (MeCN route) 1-allyl-4-(((tert-butyldimethylsilyl)oxy)methyl)bicyclo[4.1.0]hept-3-ene-2,5-dione (Compound 1.81)
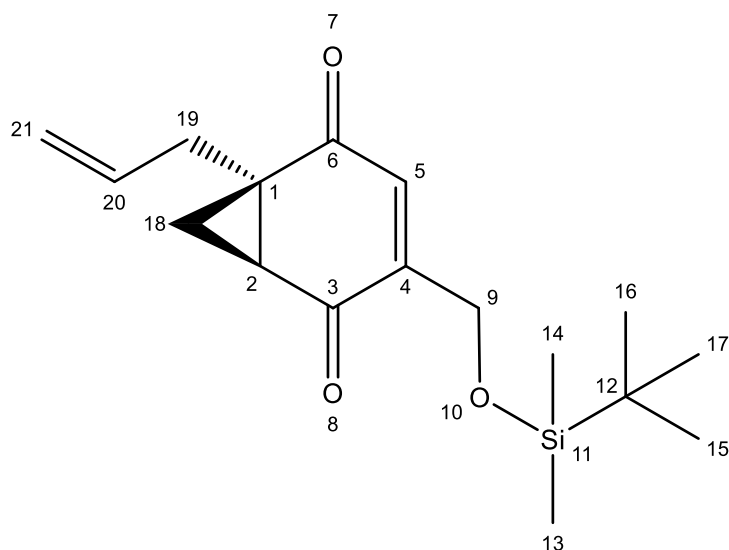
A solution of **1.80** (12 mg, 0.032 mmol) was dissolved in MeCN (1 mL) and heated to 140 ℃ with stirring with 200 W for 30 min. Reaction was monitored by TLC (hexane/EtOAc 4:1). When complete, the reaction mixture was filtered through a silica plug and washed through with diethyl ether. Filtrate was concentrated *in vacuo* yielding the title compound as a brown oil (9 mg, 0.029 mmol, 91 %). Rf= 0.56 (hexane/EtOAc 4:1). MS: *m/z* (+ESI) exact mass calc'd for $C_{17}H_{26}O_3Si$ [M + Na]$^+$ 329.1543 found 329.1558. ^{1}H NMR (400 MHz, Chloroform-*d*) δ 6.58 – 6.48 (m, 1H, C5-H), 5.75 (ddt, *J* = 17.2, 10.6, 6.9 Hz, 1H, C20-H), 5.12 – 5.02 (m, 2H, C21-H), 4.60 – 4.49 (m, 1H, C9-H), 4.37 – 4.22 (m, 1H, C9-H), 2.90 – 2.78 (m, 1H, C19-H), 2.40 (ddd, *J* = 8.8, 7.1, 5.1 Hz, 1H, C2-H), 2.28 – 2.18 (m, 1H, C19-H), 1.73 (t, *J* = 5.0 Hz, 1H, C18-H), 1.56 – 1.49 (m, 5H, C18-H under water peak), 0.90 (d, *J* = 8.8 Hz, 9H, *t*-Bu), 0.11 – 0.01 (m, 6H, C13-H/ C14-H). ^{13}C NMR (101 MHz, Chloroform-*d*) δ 196.01, 195.78, 148.35, 133.45, 132.21, 131.49, 129.45, 118.46, 59.40, 36.72, 34.58, 32.86, 26.62, 25.97, 25.80, 18.42, 1.17, -5.34, -5.36.

7.2.25. (1aR,2aR,3S,6R,6aS,7R,7aR)-1a-allyl-6a-((((tert-butyldimethylsilyl)oxy)methyl)-7-hydroxy-2a,3,6,6a,7,7a-hexahydro-3,6-methanonaphtho[2,3-b]oxiren-2(1aH)-one (Compound 2.27)
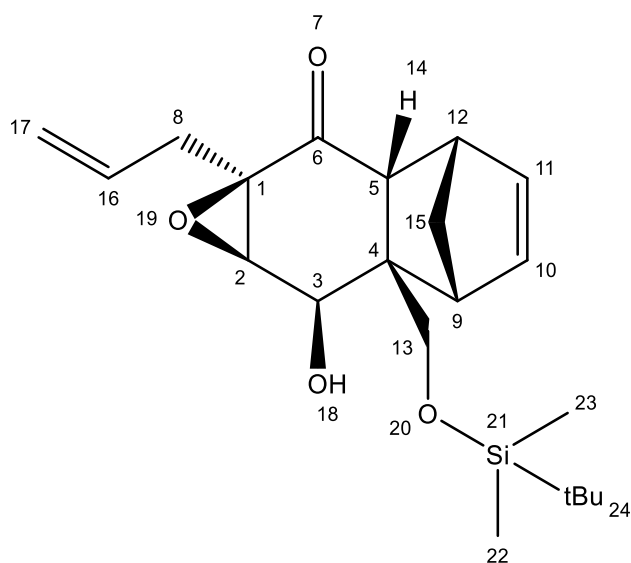
Imidazole (606 mg, 8.9 mmol) was added to a solution of **1.60** (470 mg, 1.8 mmol) in dry DMF (9 mL). After 30 min of stirring, the mixture was cooled to 0 °C and TBSCl (678 mg, 4.4 mmol) was added. The reaction was allowed to proceed for 4 h and progress was monitored by TLC (hexane/EtOAc 9:1). Upon completion, reaction was quenched with dH$_2$O and the aqueous phase was extracted with hexane (3 × 5 mL). Organic layers combined, dried with MgSO$_4$, filtered and concentrated under educed pressure. Product purified by silica gel chromatography (PET ether/EtOAc 15:1) yielding the title compound as a clear oil (571 mg, 83 %). R$_f$ = 0.5 (hexane/EtOAc 9:1); MS: *m/z* (+ESI) exact mass calc'd for C$_{21}$H$_{32}$O$_4$Si [M + Na]$^+$ 399.1968 found 399.1962. ^{1}H NMR (400 MHz, Chloroform-*d*) δ 6.26 (dd, *J* = 5.7, 2.9 Hz, 1H, C11-H), 6.13 (dd, *J* = 5.7, 3.2 Hz, 1H, C10-H), 5.73 – 5.58 (m, 1H, C16-H), 5.42 (d, *J* = 5.8 Hz, 1H, C3-H), 5.14 – 5.04 (m, 2H, C17-H), 4.89 (d, *J* = 10.6 Hz, 1H, C2-H), 3.90 (dd, *J* = 5.7, 1.4 Hz, 1H, C13-H), 3.73 (dd, *J* = 10.5, 1.4 Hz, 1H, C13-H), 3.53 (s, 1H, C18-H), 3.34 (d, *J* = 2.9 Hz, 1H, C12-H), 3.19 (dp, *J* = 5.1, 1.8 Hz, 1H, C9-H), 2.67 (ddt, *J* = 15.1, 6.6, 1.4 Hz, 1H, C8-H), 2.44 (ddt, *J* = 15.1, 7.5, 1.2 Hz, 1H, C8-H), 2.31 (d, *J* = 3.5 Hz, 1H, C14-H), 1.53 (dt, *J* = 9.2, 1.6 Hz, 1H, C15-H), 1.47 (dt, *J* = 9.2, 1.8 Hz, 1H, C15-H), 0.94 (s, 9H, *t*Bu-H), 0.13 (d, *J* = 7.6 Hz, 6H, C22-H/C23-H). ^{13}C NMR (101 MHz, Chloroform-*d*) δ 207.89, 139.44, 136.37, 131.28, 119.00, 72.78, 69.96, 67.16, 63.32, 54.40, 50.43, 45.58, 43.95, 43.75, 31.77, 25.76, 18.06, -5.64, -5.70.

7.2.26. 2-iodo-4,4-dimethoxycyclohexa-2,5-dien-1-one (Compound 2.34)
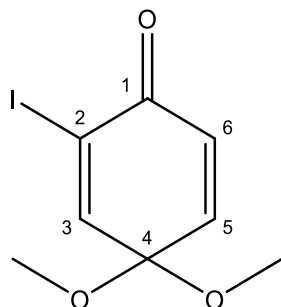
A solution of (diacetoxyiodo)benzene (16 g, 49.7 mmol) in dry MeOH (80 mL) was added dropwise over 2 h to a solution of 2-iodophenol (5.90 g, 26.8 mmol) in dry MeOH (43.7 mL) at 0 °C with stirring under nitrogen. The reaction was monitored by TLC (hexane/EtOAc 8:2). Upon completion, the reaction mixture was filtered over a silica gel pad and concentrated under reduced pressure. The product purified by silica gel chromatography (PET ether/EtOAc 9:1) yielding the title compound as a brown/red oil (4.15 g, 55 %). R_f = 0.38 (hexane/EtOAc 8:2). MS: m/z (+ESI) exact mass calc'd for $C_8H_9IO_3$ [M + Na]+ 302.9489 found 302.9491. ^{1}H NMR (400 MHz, Chloroform-d) δ 7.61 (d, J = 3.0 Hz, 1H, C3-H), 6.88 (dd, J = 10.3, 3.0 Hz, 1H, C6-H), 6.41 (d, J = 10.3 Hz, 1H, C5-H), 3.39 (s, 6H, $(OCH_3)_2$). ^{13}C NMR (101 MHz, Chloroform-d) δ 178.64, 152.30, 143.74, 126.98, 105.91, 94.30, 50.70.

7.2.27. 2-bromo-4,4-dimethoxycyclohexa-2,5-dien-1-one (Compound 2.36)
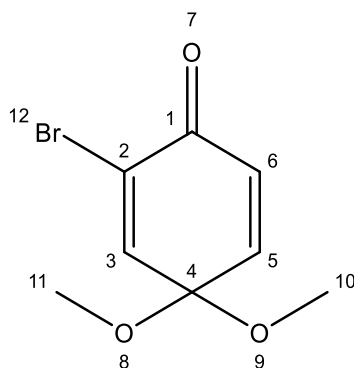
A solution of (diacetoxyiodo)benzene (14.9 g/ 46.3 mmol) in dry MeOH (80 mL) was added dropwise over 2 h to a stirring solution of 2-bromophenol (3 mL/ 25 mmol) in dry MeOH (40 mL) at 0 °C over the course of 2 h under nitrogen. The reaction was monitored by TLC (hexane/ EtOAc 8:2). Upon completion, the reaction mixture was filtered through a silica gel pad and the reaction mixture was concentrated under reduced pressure. The product was purified by silica gel chromatography (PET ether/ EtOAc 9:1) yielding the title compound as a brown oil (2.72 g/ 46 %). $R_f = 0.46$ (hexane/ EtOAc 8:2). MS: *m/z* (+ESI) exact mass calc'd for $C_8H_9BrO_3$ [M + Na]+ 254.9627 found 254.9629. ^{1}H NMR (400 MHz, Chloroform-*d*) δ 7.34 – 7.15 (m, 1H, C3-H), 6.85 (dd, *J* = 10.3, 3.0 Hz, 1H, C6-H), 6.39 (d, *J* = 10.3 Hz, 1H, C5-H), 3.39 (s, 6H, C10/11-H). ^{13}C NMR (101 MHz, Chloroform-*d*) δ 177.08, 144.11, 143.78, 128.41, 126.08, 94.58, 50.76.

7.2.28. 7-bromo-1,4-dioxaspiro[4.5]deca-6,9-dien-8-one (Compound 2.37)
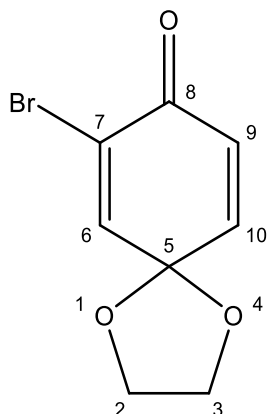
Anhydrous DME (35 mL) was added dropwise to **2.36** (2.72 g/ 11.6 mmol) at -78 ºC. To the solution, BF_3Et_2O (1.45 mL/ 11.7 mmol) was added dropwise, followed by subsequent addition of ethylene glycol (3.2 mL/ 57 mmol). The reaction was stirred for 2 h with gradual raising to ambient temperature. The reaction was monitored by TLC (hexane/ EtOAc 3:1). When complete, the reaction was quenched with saturated NH_4Cl (aq.) and the organic layer was extracted into DCM (3 × 20 mL) and dried over anhydrous $MgSO_4$. The mixture was filtered and the crude mixture was concentrated under reduced pressure. The product was purified by silica gel chromatography (PET ether/ EtOAc 3:1) yielding the title compound as a red/ yellow powder (1.9 g/ 71 %). R_f = 0.35 (hexane/ EtOAc 3:1). MS: *m/z* (+ESI) exact mass calc'd for $C_8H_7BrO_3$ [M + Na]+ 252.9471 found 252.9472. ^1H NMR (400 MHz, Chloroform-*d*) δ 7.06 (d, *J* = 2.9 Hz, 1H, C6-H), 6.64 (dd, *J* = 10.0, 2.8 Hz, 1H, C9-H), 6.29 (d, *J* = 10.0 Hz, 1H, C10-H), 4.15 (s, 4H, C2/3-H). ^{13}C NMR (101 MHz, Chloroform-*d*) δ 177.94, 143.88, 143.76, 127.52, 125.11, 99.92, 65.99.

7.2.29. 7'-bromo-1',4',4a',8a'-tetrahydro-8'H-spiro[[1,3]dioxolane-2,5'-[1,4]methanonaphthalen]-8'-one (Compound 2.38)
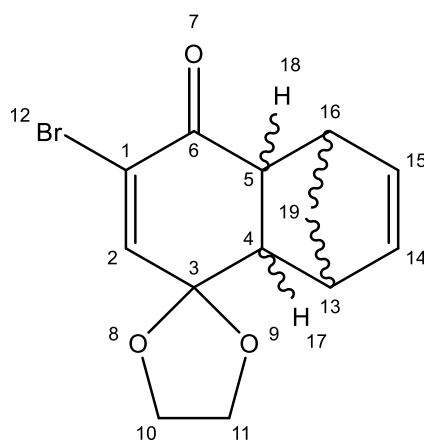
Triflic acid (14.1 mL, 0.2 M) in dry DCM was added dropwise to a solution of (*R*)-(+)-*o*-tolyl-CBS oxazaborolidene in toluene (6.72 mL mL, 0.5 M) at -78 ℃ and stirred for 15 minutes. A solution of **2.37** (4.26 g, 18.4 mmol) in dry DCM (26 mL) and freshly distilled cyclopentadiene (1.8 mL) were added dropwise to the stirring solution. Reaction monitored by TLC (hexane/EtOAc 3:1). Upon completion, reaction quenched with TEA (1 mL). Crude mixture was concentrated under reduced pressure. Product purified by silica gel chromatography (PET ether/ EtOAc 3:1) yielding the title compound as a yellow/ brown oil (4.02 g, 13.5 mmol 73 %). R_f = 0.5 (hexane/EtOAc 3:1). $[\alpha]_D^{25}$ = 0.0 (*c* 1, CHCl$_3$). MS: *m/z* (+ESI) exact mass calc'd for C$_{13}$H$_{13}$Br$_1$O$_3$ [M + Na]+ 318.9940, found 318.9950. ^{1}H NMR (400 MHz, Chloroform-*d*) δ 6.75 (d, *J* = 1.3 Hz, 1H, C2-H), 6.08 (dd, *J* = 5.6, 2.9 Hz, 1H, C15-H), 5.87 (dd, *J* = 5.6, 2.8 Hz, 1H, C14-H), 4.18 – 4.06 (m, 1H, C10/11-H), 4.06 – 3.90 (m, 3H, C10/11-H), 3.44 – 3.29 (m, 1H, C5-H), 3.26 – 3.11 (m, 2H, C13/16-H), 2.96 – 2.78 (m, 1H, C4-H), 1.42 (dt, *J* = 8.7, 1.8 Hz, 1H, C19-H), 1.32 (dt, *J* = 8.6, 1.5 Hz, 1H, C19-H). ^{13}C NMR (101 MHz, Chloroform-*d*) δ 192.59, 146.01, 136.09, 133.36, 128.01, 105.35, 65.64, 64.59, 51.02, 48.84, 47.89, 46.80, 46.73.

7.2.30. (Bromine route) 7'-allyl-1',4',4a',8a'-tetrahydro-8'H-spiro[[1,3]dioxolane-2,5'-[1,4]methanonaphthalen]-8'-one (Compound 2.40)
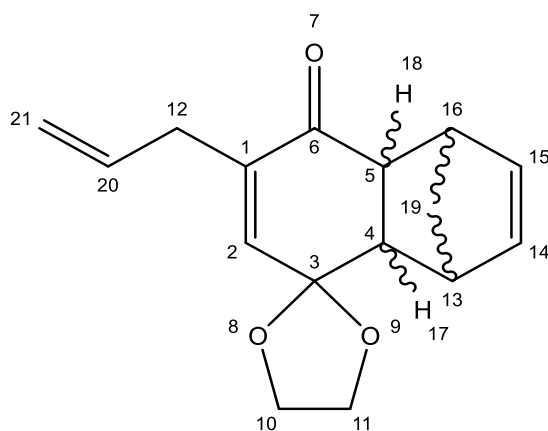
Pd(PPh$_3$)$_4$ (1.15 g, 7.5 mol%) and allyltributyl tin (**8.2** mL, **26.7** mmol) were added to a solution of **2.38** (4.02 g, 13.5 mmol) in degassed THF (20 mL) under nitrogen. The reaction mixture was heated to 110 ºC with microwave radiation (150 W) and stirred for 20 min. The reaction monitored by TLC (hex/EtOAc 3:1). Upon completion, the reaction was cooled to ambient temperature and quenched with sat. NH$_4$Cl (aq.). Organic layer extracted with EtOAc (3 × 10 mL). Crude mix concentrated under reduced pressure. Product was purified by silica gel chromatography (PET ether/EtOAc 9:1) yielding the title compound as a brown oil (2.62 g, 10.1 mmol, 75%). R$_f$ = 0.5 (hexane/EtOAc 3:1). MS: *m/z* (+ESI) exact mass calc'd for C$_{16}$H$_{118}$O$_3$ [M + Na]+ 281.1148, found 381.1152. ^{1}H NMR (400 MHz, Chloroform-*d*) δ 6.07 – 5.98 (m, 2H, C2-H, C15-H), 5.79 (dd, *J* = 5.6, 2.9 Hz, 1H, C14-H), 5.77 – 5.61 (m, 1H, C20-H), 5.11 – 5.05 (m, 1H, C21-H), 5.05 – 4.96 (m, 1H, C21-H), 4.13 – 4.05 (m, 1H, C10/11-H), 4.05 – 3.90 (m, 3H, C10/11-H), 3.29 (dtt, *J* = 4.2, 2.6, 1.3 Hz, 1H, C13-H), 3.15 (dh, *J* = 3.4, 1.7 Hz, 1H, C16-H), 3.05 (dd, *J* = 8.8, 4.3 Hz, 1H, C4-H), 2.86 (dq, J = 6.9, 1.4 Hz, 2H, C12-H), 2.81 (ddd, J = 8.8, 3.7, 1.4 Hz, 1H, C5-H), 1.43 – 1.22 (m, 2H, C19-H).13C NMR (101 MHz, Chloroform-d) δ 199.76, 141.92, 140.89, 135.68, 134.61, 133.55, 117.44, 104.64, 65.58, 64.28, 50.51, 49.00, 47.97, 46.76, 46.22, 33.24.

7.2.31. (1S,4R,4aS,8aR)-6-allyl-1,4,4a,8a-tetrahydro-1,4-methanonaphthalene-5,8-dione (Compound 2.45)
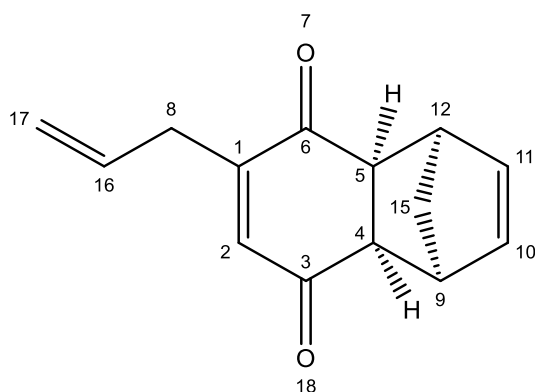
Acetone (5.46 mL) and H_2SO_4 (5.46 mL, 1 N) were added to a solution of **1.69** (1.18 g, 4.6 mmol) in THF (5 mL) and the mixture was stirred for 30 min at ambient temperature. Monitored by TLC (hexane/EtOAc 3:1). When complete, organic layer was extracted into DCM (3 × 10 mL), dried over anhydrous $MgSO_4$, filtered and concentrated under reduced pressure, yielding the title compound as a red/orange waxy solid (918 mg, 91 %) which was taken forward without further purification. R_f = 0.46 (hexane/EtOAc 3:1). MS: *m/z* (+ESI) exact mass calc'd for $C_{14}H_{14}O_2$ [M + Na]+ 237.0891 found 237.0876.^{1}H NMR (400 MHz, Chloroform-*d*) δ 6.45 (t, *J* = 1.4 Hz, 1H, C2-H), 6.10 – 6.00 (m, 2H, C17-H), 5.77 – 5.69 (m, 1H, C16-H), 5.20 – 5.07 (m, 2H, CH=CH), 3.55 (ddt, *J* = 5.6, 2.7, 1.4 Hz, 2H, C9-H/C12-H), 3.24 (t, *J* = 2.6 Hz, 2H, C4-H/C5-H), 3.07 (dq, *J* = 6.8, 1.3 Hz, 2H, C8-H), 1.58 – 1.42 (m, 2H, C15-H).^{13}C NMR (101 MHz, Chloroform-*d*) δ 199.27, 198.87, 153.39, 139.15, 135.47, 135.01, 132.91, 118.75, 49.02, 48.99, 48.90, 48.65, 48.54, 33.39.

7.2.32. (1aS,3R,6S,6aR,7S,7aS)-1a-allyl-6a-(((tert-butyldimethylsilyl)oxy)methyl)-7-hydroxy-2a,3,6,6a,7,7a-hexahydro-3,6-methanonaphtho[2,3-b]oxiren-2(1aH)-one (Compound 2.46)
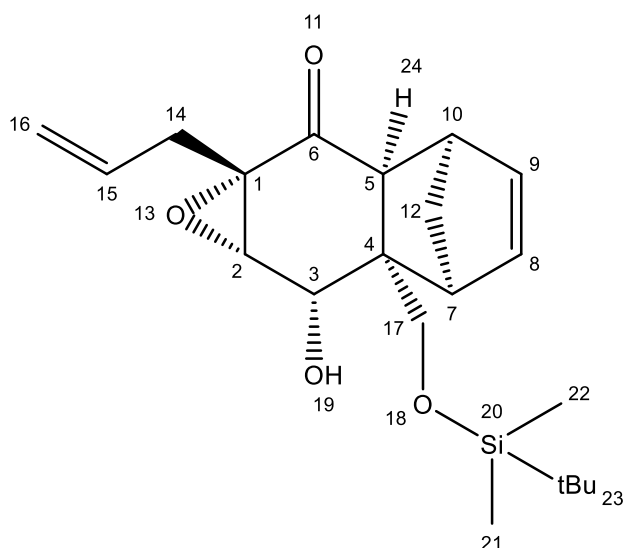
Imidazole (190 mg, 2.78 mmol) was added to a solution of **1.72** (148 mg, 0.56 mmol) in dry DMF (2.8 mL) and the mixture was stirred at ambient temperature for 30 min. The mixture was then cooled to 0 °C and TBDMSCl (210 mg, 1.38 mmol) was added and the reaction was stirred for 4 h at 0 °C. Monitored by TLC (hexane/EtOAc 9:1). When complete, reaction quenched with Milli-Q, organic phase extracted with hexane (3 × 5 mL), dried over anhyd. MgSO$_4$, filtered and concentrated under reduced pressure. Product purified by silica gel chromatography (PET ether/EtOAc 15:1) yielding the title compound as a clear oil (165 mg, 79 %). R$_f$ = 0.4 (hexane/EtOAc 9:1). MS: *m/z* (+ESI) exact mass calc'd for C$_{21}$H$_{32}$O$_4$Si [M + Na]+ 399.1968 found 399.1962. ^{1}H NMR (400 MHz, Chloroform-*d*) δ 6.26 (dd, *J* = 5.7, 2.9 Hz, 1H, C9-H), 6.13 (dd, *J* = 5.7, 3.2 Hz, 1H, C8-H), 5.73 – 5.58 (m, 1H, C15-H), 5.42 (d, *J* = 5.8 Hz, 1H, C3-H), 5.14 – 5.04 (m, 2H, C16-H), 4.89 (d, *J* = 10.6 Hz, 1H, C2-H), 3.90 (dd, *J* = 5.7, 1.4 Hz, 1H, C17-H), 3.73 (dd, *J* = 10.5, 1.4 Hz, 1H, C17-H), 3.53 (s, 1H, OH), 3.34 (d, *J* = 2.9 Hz, 1H, C10-H), 3.19 (dp, *J* = 5.1, 1.8 Hz, 1H, C7-H), 2.67 (ddt, *J* = 15.1, 6.6, 1.4 Hz, 1H, C14-H), 2.44 (ddt, *J* = 15.1, 7.5, 1.2 Hz, 1H, C14-H), 2.31 (d, *J* = 3.5 Hz, 1H, C5-H), 1.53 (dt, *J* = 9.2, 1.6 Hz, 1H, C12-H), 1.47 (dt, *J* = 9.2, 1.8 Hz, 1H, C12-H), 0.94 (s, 9H, *t*Bu-H), 0.13 (d, *J* = 7.6 Hz, 6H, C21-H/C22-H). ^{13}C NMR (101 MHz, Chloroform-*d*) δ 207.89, 139.43, 136.37, 131.27, 119.00, 72.78, 69.95, 67.14, 63.31, 54.39, 50.42, 45.58, 43.94, 43.74, 31.76, 25.75, 25.66, 18.06, -3.57, -5.65, -5.70.

7.2.33. tert-butyl (E)-4-((1R,5R,6R)-4-(((tert-butyldiphenylsilyl)oxy)methyl)-5-hydroxy-2-oxo-7-oxabicyclo[4.1.0]hept-3-en-1-yl)-2-methylbut-2-enoate (Compound 2.62)
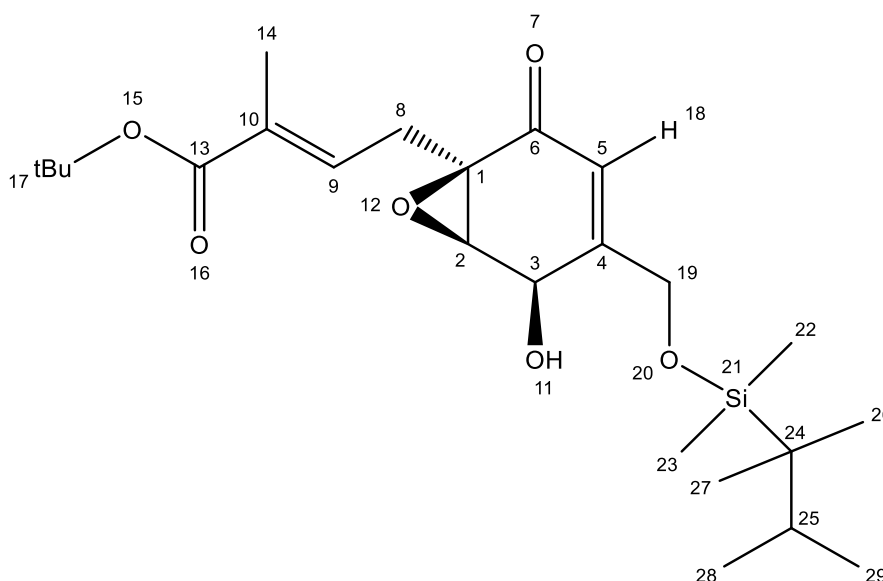
Imidazole (13 mg, 0.19 mmol) was added to a solution of **1.74** (12 mg, 0.038 mmol) in dry DMF (2 mL) and the mixture was stirred for 30 min. The mixture was then cooled to 0 °C and chloro(dimethyl)thexylsilane (18 µL, 0.095 mmol) added and the mixture was stirred for 4 h. Monitored by TLC (hexane/EtOAc 3:1). When complete, the reaction was quenched with dH$_2$O and organic layers extracted with hexane (3 × 5 mL). The layers were combined, dried over MgSO$_4$, filtered and concentrated *in vacuo*. Product purified by flash chromatography (hexane/EtOAc 3:1) yielding the title compound as a white oily solid (4 mg, 23 %). R$_f$ = 0.2 (hexane/EtOAc 3:1).MS: *m/z* (+ESI) calc'd for C$_{24}$H$_{40}$O$_6$Si [M + Na]$^+$ 475.2492 found 475.2504. ^{1}H NMR (400 MHz, Chloroform-*d*) δ 6.50 (ddd, *J* = 8.3, 6.9, 1.6 Hz, 1H, C9-H), 6.01 (q, *J* = 1.7 Hz, 1H, C18-H), 4.67 (d, *J* = 8.6 Hz, 1H, C3-H), 4.41 (t, *J* = 1.9 Hz, 2H, C19-H), 3.72 (d, *J* = 3.0 Hz, 1H, C2-H), 2.95 (dd, *J* = 15.8, 8.0 Hz, 1H, C8-H), 2.70 – 2.62 (m, 1H, C8-H), 2.56 (d, *J* = 8.8 Hz, 1H, C11-H), 1.84 (d, *J* = 1.4 Hz, 3H, C14-H), 1.48 (s, 9H, C17-H), 0.94 – 0.78 (m, 12H, C26-H/C27-H/C28-H/C29-H), 0.13 (d, *J* = 1.7 Hz, 6H, C22-H/C23-H).^{13}C NMR (101 MHz, Chloroform-*d*) δ 193.36, 167.36, 157.85, 133.39, 132.90, 120.61, 80.94, 66.44, 63.52, 60.94, 59.69, 34.56, 28.56, 27.60, 25.70, 20.72, 20.70, 18.96, 13.29, -3.06, -3.09.

7.2.34. tert-butyl (E)-4-((1R,5R,6R)-4-(((tert-butyldiphenylsilyl)oxy)methyl)-5-hydroxy-2-oxo-7-oxabicyclo[4.1.0]hept-3-en-1-yl)-2-methylbut-2-enoate (Compound 2.64)
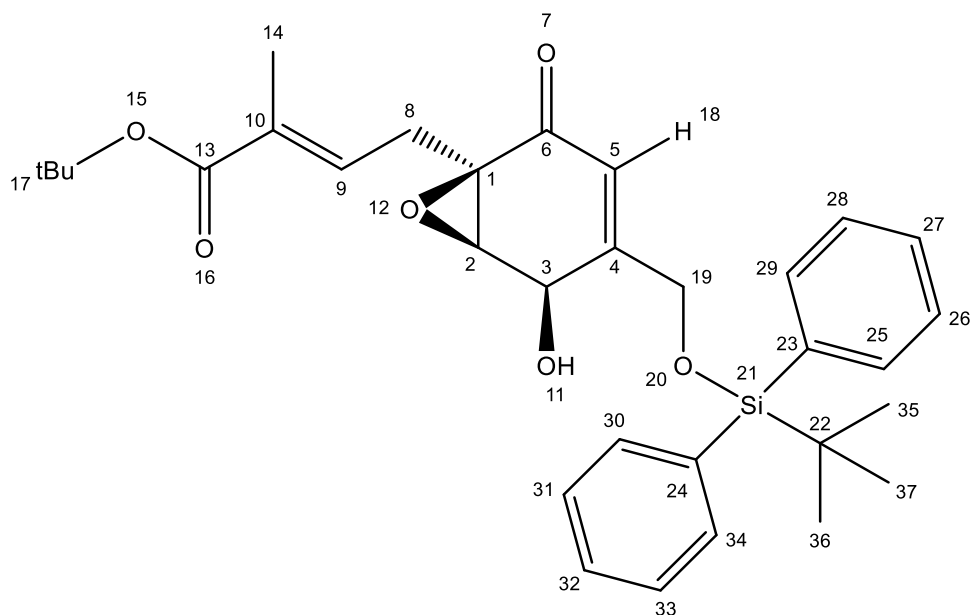
Imidazole (10 mg, 0.15 mmol) was added to a solution of **1.74** (10 mg, 0.013 mmol) in dry DMF (2 mL) and the mixture was stirred at ambient temperature for 30 min. The mixture was cooled to 0 °C and TBDPS (18 μL, 0.075 mmol) was added and the reaction mixture was stirred for 4 h. Monitored by TLC (hexane/EtOAc 3:1). When complete, the reaction was quenched with dH$_2$O, organic layer extracted with hexane (3 × 5 mL), dried with MgSO$_4$, filtered and concentrated *in vacuo*. Product purified by silica gel chromatography (PET ether/EtOAc 3:1) yielding the title compound as a white solid (1.5 mg, 6 %). R$_f$ = 0.26 (hexane/EtOAc 3:1). MS: *m/z* (+ESI) exact mass calc'd for C$_{32}$H$_{40}$O$_6$Si [M + Na]$^+$ 571.2492 found 571.2486. Shown to be the product by HRMS, ^{1}H and ^{13}C NMR could not verify due to amount produced.

7.2.35. tert-butyl (E)-4-((6aR,7aR,7bR)-2,2-dimethyl-6-oxo-4,6,7a,7b-tetrahydro-6aH-oxireno[2',3':5,6]benzo[1,2-d][1,3]dioxin-6a-yl)-2-methylbut-2-enoate (Compound 2.72)
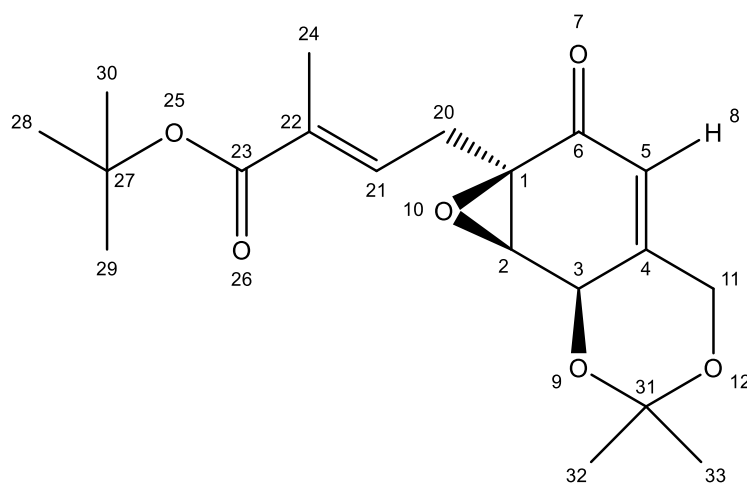
1.74 (38 mg, 0.1 mmol) was dissolved in a solution of *p*-toluene sulphonic acid in acetone (0.2 mg/ mL, 3 mL) and stirred at 60 ℃ for 1.5 h. Reaction monitored by TLC (hexane/ EtOAc 3:1). Upon completion, the reaction was quenched with the addition of 1mL saturated $NaHCO_3$ (aq.) and the mixture was concentrated under reduced pressure. The residue was subsequently re-dissolved in DCM and washed with brine. The organic layers were extracted into DCM (3 × 10 mL) and concentrated under reduced pressure. The product was purified by preparatory TLC (hexane/ EtOAc 1:1) yielding a yellow oil (6 mg, 20 %) which was subsequently purified by HPLC yielding a white solid (2 mg, 6 %). R_f = 0.44 (hexane/ EtOAc 3:1). MS: *m/z* (+ESI) exact mass calc'd for $C_{19}H_{26}O_6$ [M + Na]$^+$ 373.1622, found 373.1617. ^{1}H NMR (400 MHz, Chloroform-*d*) δ 6.50 (ddq, *J* = 8.5, 7.4, 1.5 Hz, 1H, C21-H), 5.71 (q, *J* = 1.7 Hz, 1H, C5-H), 4.83 (dq, *J* = 3.2, 1.7 Hz, 1H, C3-H), 4.44 (q, *J* = 1.9 Hz, 2H, C11-H), 3.65 (d, *J* = 2.7 Hz, 1H, C2-H), 3.00 – 2.89 (m, 1H, C20-H), 2.68 (ddd, *J* = 15.9, 7.1, 1.1 Hz, 1H, C20-H), 2.17 (s, 1H (acetone)), 1.83 (q, *J* = 1.1 Hz, 3H, C24-H), 1.54 (s, 3H, C32/33-H), 1.53 – 1.44 (m, 12H, *t*-butyl H, C32/33-H). ^{13}C NMR (101 MHz, Chloroform-*d*) δ 193.15, 166.89, 152.81, 133.05, 132.38, 117.81, 101.01, 80.49, 65.30, 61.66, 59.52, 56.02, 28.11, 26.86, 25.52, 22.57, 12.83.

7.2.36. tert-butyl (E)-4-(2,2-diethyl-6-oxo-4,6,7a,7b-tetrahydro-6aH-oxireno[2',3':5,6]benzo[1,2-d][1,3]dioxin-6a-yl)-2-methylbut-2-enoate (Compound 2.73)
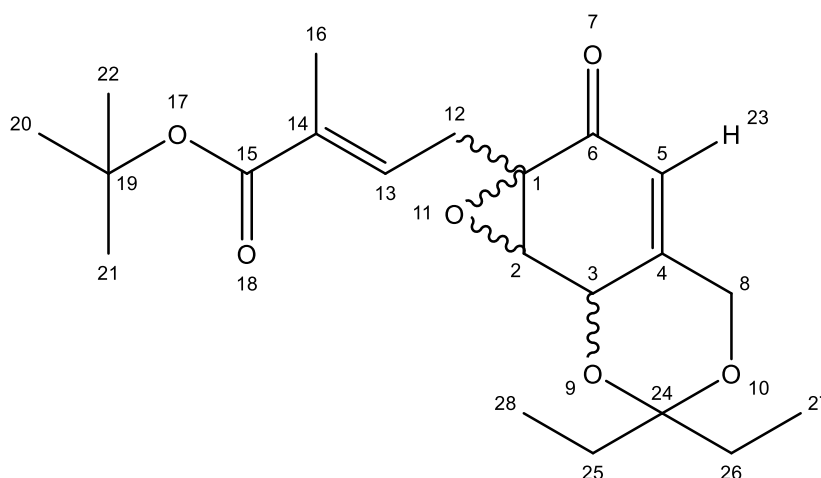
1.74 (26 mg, 0.08 mmol) was dissolved in a solution of *p*-toluene sulphonic acid in pentan-3-one (0.4 mg/ mL, 4 mL) and stirred at 100 ºC overnight with stirring. The reaction was monitored by TLC (hexane/ EtOAc 1:1). Upon completion, the reaction was quenched with the addition of 1 mL of saturated $NaHCO_3$ (aq.) and the mixture was concentrated under reduced pressure. The residue was subsequently re-dissolved in DCM and washed with brine. The organic layers were extracted into DCM (3 × 10 mL), dried with anhydrous $MgSO_4$, filtered and concentrated under reduced pressure. The product was purified by preparatory TLC (hexane/ EtOAc 1:1) yielding a yellow oil (12 mg/ 15%). R_f = 0.80 (hexane/ EtOAc 1:1)**.**MS: *m/z* (+ESI) exact mass calc'd for $C_{21}H_{30}O_6$ $[M + Na]^+$ 401.1935, found 401.1939. ^{1}H NMR (400 MHz, Chloroform-*d*) δ 6.50 (dddd, *J* = 10.0, 5.7, 2.8, 1.0 Hz, 1H, C13-H), 6.00 (q, *J* = 1.5 Hz, 1 H, C5-H), 5.69 (q, *J* = 1.7 Hz, 1 H, C5-H*), 4.83 (dq, *J* = 3.4, 1.7 Hz, 1H, C3-H), 4.75 (dt, *J* = 3.0, 1.3 Hz, 1H, C3-H*), 4.44 (ddt, *J* = 6.3, 3.1, 1.5 Hz, 2H, C8-H), 3.74 (d, *J* = 3.0 Hz, 1H, C2-H), 3.66 (d, *J* = 2.7 Hz, 1H, C2-H*), 2.94 (ddd, *J* = 15.9, 8.3, 2.9 Hz, 1H, C12-H), 2.72 – 2.62 (m, 1H, C12-H), 2.43 (q, *J* = 7.4 Hz, 2H, C25/C26-H), 1.87 – 1.79 (m, 4H, C16/25/26-H), 1.74 (qd, *J* = 7.4, 3.2 Hz, 1H, C25/26-H), 1.48 (s, 9H, *t*-Bu), 1.06 (t, *J* = 7.3 Hz, 3H, C27/28-H), 0.94 (dt, *J* = 18.8, 7.5 Hz, 3H, C27/28-H). ^{13}C NMR (101 MHz, Chloroform-*d*) δ 192.93, 156.83, 133.16, 132.64, 132.46, 120.93, 80.72, 80.64, 66.03, 65.14, 63.20, 61.42, 60.74, 59.34, 56.41, 35.61, 28.24, 27.20, 27.12, 24.78, 12.98, 8.06, 7.84.

* Denotes diastereotopic protons in a 1:1 ratio.

7.2.37. tert-butyl (E)-2-methyl-4-(6'-oxo-4',6',7a',7b'-tetrahydro-6a'H-spiro[cyclohexane-1,2'-oxireno[2',3':5,6]benzo[1,2-d][1,3]dioxin]-6a'-yl)but-2-enoate (Compound 2.74)
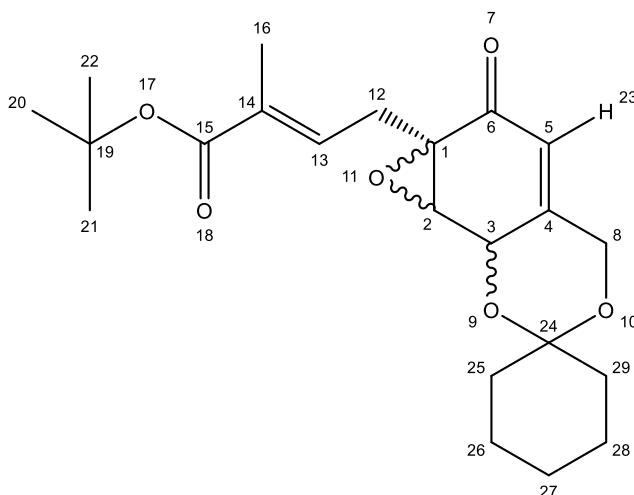
1.74 (16 mg, 0.05 mmol) was dissolved in a solution of *p*-toluene sulphonic acid in 1,1-dimethoxycyclohexane (0.4 mg/ mL in 3 mL) and heated to 60 °C with stirring for 1.5 h. The reaction was monitored by TLC (hexane/ EtOAc 1:1). Upon completion, the reaction was quenched with the addition of 1 mL of saturated $NaHCO_3$ (aq.) and concentrated under reduced pressure. The residue was subsequently re-dissolved in DCM and washed with brine, then organic layers were extracted into DCM (3 × 10 mL), dried with anhydrous $MgSO_4$, filtered and concentrated under reduced pressure. The product was purified by preparatory TLC (hexane/ EtOAc 1:1) yielding the product as a yellow oil (9.2 mg, 0.018 mmol, 36%). $R_f = 0.90$ (hexane/ EtOAc 1:1). MS: *m/z* (+ESI) exact mass calc'd for $C_{22}H_{30}O_6$ [M + Na]$^+$ 413.1935, found 413.1937. ^{1}H NMR (400 MHz, Chloroform-*d*) δ 6.50 (ddq, *J* = 8.6, 7.2, 1.5 Hz, 1H, C13-H), 6-5.99 (m, 0.1H, C5-H*) 5.69 (q, *J* = 1.6 Hz, 1H, C5-H*), 4.85 (dq, *J* = 3.2, 1.7 Hz, 1H, C3-H), 4.75-4.74 (m, 0.1H, C3-H*), 4.53 – 4.36 (m, 2H, C8-H), 3.74-3.73 (m, 0.1H, C2-H*), 3.66 (d, *J* = 2.7 Hz, 1H, C2-H), 2.99 – 2.89 (m, 1H, C12-H), 2.72 – 2.61 (m, 1H, C12-H), 1.95 – 1.85 (m, 1H, cyclohexyl), 1.83 (q, *J* = 1.1 Hz, 3H, C16-H), 1.73 (td, *J* = 7.6, 7.0, 4.5 Hz, 1H, cyclohexyl), 1.61 – 1.50 (m, 3H, cyclohexyl), 1.47 (s, 9H, *t*-Bu), 1.45 – 1.42 (m, 1H, cyclohexyl), 1.21 (s, 1H, cyclohexyl), 1.16 (s, 1H, cyclohexyl), 0.98 – 0.81 (m, 2H, cyclohexyl). ^{13}C NMR (101 MHz, Chloroform-*d*) δ 193.35, 167.08, 153.16, 133.09, 132.65, 117.95, 101.11, 80.63, 64.96, 61.32, 59.70, 56.42, 34.69, 31.56, 28.24, 27.09, 25.46, 22.90, 22.82, 12.97. *Denotes diastereotopic protons in a 9:1 ratio.

Chapter 8. Bibliography

1.   Tong, S. Y. C.; Davis, J. S.; Eichenberger, E.; Holland, T. L.; Fowler, V. G., Jr., *Staphylococcus aureus* infections: epidemiology, pathophysiology, clinical manifestations, and management. *Clin Microbiol Rev.* **2015,** *28* (3), 603-661.

2.   Hobbs, M. R.; Grant, C. C.; Thomas, M. G.; Berry, S.; Morton, S. M. B.; Marks, E.; Ritchie, S. R., *Staphylococcus aureus* colonisation and its relationship with skin and soft tissue infection in New Zealand children. *Eur J Clin Microbiol Infect Dis.* **2018,** *37* (10), 2001-2010.

3.   Kluytmans, J.; van Belkum, A.; Verbrugh, H., Nasal carriage of *Staphylococcus aureus*: epidemiology, underlying mechanisms, and associated risks. *Clin Microbiol Rev.* **1997,** *10* (3), 505.

4.   Ritchie, S. R.; Isdale, E.; Priest, P.; Rainey, P. B.; Thomas, M. G., The turnover of strains in intermittent and persistent nasal carriers of *Staphylococcus aureus*. *J infect.* **2016,** *72* (3), 295-301.

5.   Sollid, J. U.; Furberg, A. S.; Hanssen, A. M.; Johannessen, M., *Staphylococcus aureus*: determinants of human carriage. *Infect. Genet.Evol.***2014,** *21*, 531-41.

6.   Chambers, H. F.; DeLeo, F. R., Waves of resistance: *Staphylococcus aureus* in the antibiotic era. *Nat. Rev. Microbiol* **2009,** *7* (9), 629-641.

7.   Moran, G. J.; Krishnadasan, A.; Gorwitz, R. J.; Fosheim, G. E.; McDougal, L. K.; Carey, R. B.; Talan, D. A., Methicillin-resistant *S. aureus* infections among patients in the emergency department. *N. Engl. J. Med.* **2006,** *355* (7), 666-74.

8.   Lowy, F. D., *Staphylococcus aureus* infections. *N. Engl. J. Med.* **1998,** *339* (8), 520-32.

9.   Solberg, C. O., Spread of *Staphylococcus aureus* in hospitals: causes and prevention. *Scand. J. Infect. Dis.* **2000,** *32* (6), 587-95.

10.   Verhoeven, P. O.; Gagnaire, J.; Botelho-Nevers, E.; Grattard, F.; Carricajo, A.; Lucht, F.; Pozzetto, B.; Berthelot, P., Detection and clinical relevance of *Staphylococcus aureus* nasal carriage: an update. *Expert Rev. Anti Iinfect. Ther.* **2014,** *12* (1), 75-89.

11.   Nouwen, J. L.; Fieren, M. W. J. A.; Snijders, S.; Verbrugh, H. A.; Van Belkum, A., Persistent (not intermittent) nasal carriage of *Staphylococcus aureus* is the determinant of CPD-related infections. *Kidney Int.* **2005,** *67* (3), 1084-1092.

12.   Jenul, C.; Horswill, A. R., Regulation of *Staphylococcus aureus* Virulence. *Microbiol. Spectr.* **2018,** *6* (1), 10.1128/microbiolspec.GPP3-0031-2018.

13.   Boyce, T.; Murray, E.; Holmes, A., What are the drivers of the UK media coverage of meticillin-resistant *Staphylococcus aureus*, the inter-relationships and relative influences? *J. Hosp. Infect.* **2009,** *73* (4), 400-7.

14.   Pereira, L. B., Impetigo - review. *An. Bras. Dermatol* **2014,** *89* (2), 293-299.

15.   Alsterholm, M.; Flytström, I.; Bergbrant, I. M.; Faergemann, J., Fusidic acid-resistant *Staphylococcus aureus* in impetigo contagiosa and secondarily infected atopic dermatitis. *Acta Derm. Venereol.* **2010,** *90* (1), 52-7.

16.   Capdevila, O.; Grau, I.; Vadillo, M.; Cisnal, M.; Pallares, R., Bacteremic pneumococcal cellulitis compared with bacteremic cellulitis caused by *Staphylococcus aureus* and *Streptococcus pyogenes*. *Eur J Clin Microbiol Infect Dis.* **2003,** *22* (6), 337-41.

17.   Fernández Guerrero, M. L.; González López, J. J.; Goyenechea, A.; Fraile, J.; de Górgolas, M., Endocarditis caused by *Staphylococcus aureus*: A reappraisal of the epidemiologic, clinical, and pathologic manifestations with analysis of factors determining outcome. *Medicine* **2009,** *88* (1), 1-22.

18.   Ragle, B. E.; Karginov, V. A.; Bubeck Wardenburg, J., Prevention and treatment of *Staphylococcus aureus* pneumonia with a beta-cyclodextrin derivative. *Antimicrob. Agents Chemother.* **2010,** *54* (1), 298-304.

19.   Olson, M. E.; Horswill, A. R., *Staphylococcus aureus* osteomyelitis: bad to the bone. *Cell Host Microbe* **2013,** *13* (6), 629-631.

20.   Paulsen, J.; Mehl, A.; Askim, Å.; Solligård, E.; Åsvold, B. O.; Damås, J. K., Epidemiology and outcome of *Staphylococcus aureus* bloodstream infection and sepsis in a Norwegian county 1996-2011: an observational study. *BMC Infect. Dis.* **2015,** *15*, 116-116.

21.   Argudín, M. Á.; Mendoza, M. C.; Rodicio, M. R., Food poisoning and *Staphylococcus aureus* enterotoxins. *Toxins* **2010,** *2* (7), 1751-1773.

22.   Mishra, A. K.; Yadav, P.; Mishra, A., A Systemic Review on Staphylococcal Scalded Skin Syndrome (SSSS): A Rare and Critical Disease of Neonates. *Open Microbiol. J.* **2016,** *10*, 150-159.

23.   Proft, T.; Fraser, J. D., Bacterial superantigens. *Clin. Exp. Immunol.* **2003,** *133* (3), 299-306.

24.   Wertheim, H. F.; Vos, M. C.; Ott, A.; van Belkum, A.; Voss, A.; Kluytmans, J. A.; van Keulen, P. H.; Vandenbroucke-Grauls, C. M.; Meester, M. H.; Verbrugh, H. A., Risk and outcome of nosocomial *Staphylococcus aureus* bacteraemia in nasal carriers versus non-carriers. *Lancet* **2004,** *364* (9435), 703-5.

25.   von Eiff, C.; Becker, K.; Machka, K.; Stammer, H.; Peters, G., Nasal carriage as a source of *Staphylococcus aureus* bacteremia. Study Group. *N. Engl. J. Med.* **2001,** *344* (1), 11-6.

26.   Ahmed, E. F.; Gad, G. F.; Abdalla, A. M.; Hasaneen, A. M.; Abdelwahab, S. F., Prevalence of methicillin resistant *Staphylococcus aureus* among Egyptian patients after surgical interventions. *Surg. Infect.* **2014,** *15* (4), 404-11.

27.   Naber, C. K., *Staphylococcus aureus* Bacteremia: epidemiology, pathophysiology, and management strategies. *Clin. Infect. Dis.* **2009,** *48* (Supplement_4), S231-S237.

28.   Miller, L. G.; Perdreau-Remington, F.; Rieg, G.; Mehdi, S.; Perlroth, J.; Bayer, A. S.; Tang, A. W.; Phung, T. O.; Spellberg, B., Necrotizing fasciitis caused by community-associated methicillin-resistant *Staphylococcus aureus* in Los Angeles. *N. Engl. J. Med.* **2005,** *352* (14), 1445-1453.

29.   Rich, J.; Lee, J. C., The Pathogenesis of *Staphylococcus aureus*; Infection in the Diabetic NOD Mouse. *Diabetes* **2005,** *54* (10), 2904.

30.   Cheng, N. C.; Wang, J. T.; Chang, S. C.; Tai, H. C.; Tang, Y. B., Necrotizing fasciitis caused by *Staphylococcus aureus*: the emergence of methicillin-resistant strains. *Ann. Plast. Surg.* **2011,** *67* (6), 632-6.

31.   Schuchat, A.; Broome, C. V., Toxic shock syndrome and tampons. *Epidemiol. Rev.* **1991,** *13*, 99-112.

32.   Klompas, M., Toxic Shock Syndromes. In *Decision Making in Medicine (Third Edition)*, Mushlin, S. B.; Greene, H. L., Eds. Mosby: Philadelphia, 2010; pp 336-337.

33.   Freitas, E. A.; Harris, R. M.; Blake, R. K.; Salgado, C. D., Prevalence of USA300 strain type of methicillin-resistant *Staphylococcus aureus* among patients with nasal colonization identified with active surveillance. *Infect. Control Hosp. Epidemiol.* **2010,** *31* (5), 469-75.

34.   Carrel, M.; Perencevich, E. N.; David, M. Z., USA300 Methicillin-Resistant *Staphylococcus aureus*, United States, 2000-2013. *Emerg. Infect. Dis.* **2015,** *21* (11), 1973-1980.

35.   Kazakova, S. V.; Hageman, J. C.; Matava, M.; Srinivasan, A.; Phelan, L.; Garfinkel, B.; Boo, T.; McAllister, S.; Anderson, J.; Jensen, B.; Dodson, D.; Lonsway, D.; McDougal, L. K.; Arduino, M.; Fraser, V. J.; Killgore, G.; Tenover, F. C.; Cody, S.; Jernigan, D. B., A clone of methicillin-resistant *Staphylococcus aureus* among professional football players. *N. Engl. J. Med.* **2005,** *352* (5), 468-75.

36.   Otto, M., Community-associated MRSA: what makes them special? *Int. J. Med. Microbial.***2013,** *303* (6-7), 324-330.

37.   Laupland, K. B.; Lyytikäinen, O.; Sgaard, M.; Kennedy, K. J.; Knudsen, J. D.; Ostergaard, C.; Galbraith, J. C.; Valiquette, L.; Jacobsson, G.; Collignon, P.; Schnheyder, H. C.; for the International Bacteremia Surveillance, C., The changing epidemiology of *Staphylococcus aureus* bloodstream infection: a multinational population-based surveillance study. *Clin. Microbiol. Inf.* **2013,** *19* (5), 465-471.

38.   Frimodt-Møller, N.; Espersen, F.; Skinhøj, P.; Rosdahl, V. T., Epidemiology of *Staphylococcus aureus* bacteremia in Denmark from 1957 to 1990. *Clin. Microbiol. Infect.* **1997,** *3* (3), 297-305.

39.   Allard, C.; Carignan, A.; Bergevin, M.; Boulais, I.; Tremblay, V.; Robichaud, P.; Duperval, R.; Pepin, J., Secular changes in incidence and mortality associated with *Staphylococcus aureus* bacteraemia in Quebec, Canada, 1991-2005. *Clin. Microbial. Infect.* **2008,** *14* (5), 421-8.

40.   Wyllie, D. H.; Peto, T. E. A.; Crook, D., MRSA bacteraemia in patients on arrival in hospital: a cohort study in Oxfordshire 1997-2003. *BMJ* **2005,** *331* (7523), 992.

41.   El Atrouni, W. I.; Knoll, B. M.; Lahr, B. D.; Eckel-Passow, J. E.; Sia, I. G.; Baddour, L. M., Temporal trends in the incidence of *Staphylococcus aureus* bacteremia in Olmsted County, Minnesota, 1998 to 2005: a population-based study. *Clin. Infect. Dis.* **2009,** *49* (12), e130-e138.

42.   Klevens, R. M.; Morrison, M. A.; Nadle, J.; Petit, S.; Gershman, K.; Ray, S.; Harrison, L. H.; Lynfield, R.; Dumyati, G.; Townes, J. M.; Craig, A. S.; Zell, E. R.; Fosheim, G. E.; McDougal, L. K.; Carey, R. B.; Fridkin, S. K.; Invasive methicillin-resistant *Staphylococcus aureus* infections in the United States. *JAMA* **2007,** *298* (15), 1763-1771.

43.   Tleyjeh, I. M.; Abdel-Latif, A.; Rahbi, H.; Scott, C. G.; Bailey, K. R.; Steckelberg, J. M.; Wilson, W. R.; Baddour, L. M., A systematic review of population-based studies of infective endocarditis. *CHEST* **2007,** *132* (3), 1025-1035.

44.   Chu Vivian, H.; Cabell Christopher, H.; Benjamin Daniel, K.; Kuniholm Erin, F.; Fowler Vance, G.; Engemann, J.; Sexton Daniel, J.; Corey, G. R.; Wang, A., Early predictors of in-hospital death in infective endocarditis. *Circulation* **2004,** *109* (14), 1745-1749.

45.   Calderwood, S. B.; Swinski, L. A.; Waternaux, C. M.; Karchmer, A. W.; Buckley, M. J., Risk factors for the development of prosthetic valve endocarditis. *Circulation* **1985,** *72* (1), 31-37.

46.   DeLeo, F. R.; Otto, M.; Kreiswirth, B. N.; Chambers, H. F., Community-associated meticillin-resistant *Staphylococcus aureus*. *Lancet* **2010,** *375* (9725), 1557-68.

47.   Pallin, D. J.; Egan, D. J.; Pelletier, A. J.; Espinola, J. A.; Hooper, D. C.; Camargo, C. A., Jr., Increased US Emergency Department Visits for Skin and Soft Tissue Infections, and Changes in Antibiotic Choices, During the Emergence of Community-Associated Methicillin-Resistant *Staphylococcus aureus*. *Ann. Emerg. Med.* **2008,** *51* (3), 291-298.

48.   Peng, H.; Liu, D.; Ma, Y.; Gao, W., Comparison of community- and healthcare-associated methicillin-resistant *Staphylococcus aureus* isolates at a Chinese tertiary hospital, 2012–2017. *Sci. Rep* **2018,** *8* (1), 17916.

49.   Hiramatsu, K.; Cui, L.; Kuroda, M.; Ito, T., The emergence and evolution of methicillin-resistant *Staphylococcus aureus*. *Trends Microbiol.* **2001,** *9* (10), 486-493.

50.   Lee, S. M.; Ender, M.; Adhikari, R.; Smith, J. M.; Berger-Bächi, B.; Cook, G. M., Fitness cost of staphylococcal cassette chromosome *mec* in methicillin-resistant *Staphylococcus aureus* by way of continuous culture. *Antimicrob agents chemother.* **2007,** *51* (4), 1497-9.

51.   Cheung, G. Y.; Wang, R.; Khan, B. A.; Sturdevant, D. E.; Otto, M., Role of the accessory gene regulator *agr* in community-associated methicillin-resistant *Staphylococcus aureus* pathogenesis. *Infect Immun* **2011,** *79* (5), 1927-35.

52.	Voyich, J. M.; Braughton, K. R.; Sturdevant, D. E.; Whitney, A. R.; Saïd-Salim, B.; Porcella, S. F.; Long, R. D.; Dorward, D. W.; Gardner, D. J.; Kreiswirth, B. N.; Musser, J. M.; DeLeo, F. R., Insights into mechanisms used by *Staphylococcus aureus* to avoid destruction by human neutrophils. *J Immunol* **2005,** *175* (6), 3907-19.

53.	Seung, K. J.; Keshavjee, S.; Rich, M. L., Multidrug-resistant tuberculosis and extensively drug-resistant tuberculosis. *Cold Spring Harb. Perspect. Med.* **2015,** *5* (9), a017863-a017863.

54.	Johnson, S.; Samore, M. H.; Farrow, K. A.; Killgore, G. E.; Tenover, F. C.; Lyras, D.; Rood, J. I.; DeGirolami, P.; Baltch, A. L.; Rafferty, M. E.; Pear, S. M.; Gerding, D. N., Epidemics of diarrhea caused by a clindamycin-resistant strain of *Clostridium difficile* in four hospitals. *N. Engl. J. Med.***1999,** *341* (22), 1645-51.

55.	World Health, O., *Antimicrobial resistance: global report on surveillance*. World Health Organization: Geneva, 2014.

56.	Renwick, M.; Mossialos, E., What are the economic barriers of antibiotic R&D and how can we overcome them? *Expert Opin. Drug Discov.* **2018,** *13* (10), 889-892.

57.	Payne, D. J.; Miller, L. F.; Findlay, D.; Anderson, J.; Marks, L., Time for a change: addressing R&D and commercialization challenges for antibacterials. *Philos. Trans. R. Soc. Lond. B. Biol. Sci.* **2015,** *370* (1670), 20140086-20140086.

58.	Kong, K.-F.; Schneper, L.; Mathee, K., Beta-lactam antibiotics: from antibiosis to resistance and bacteriology. *APMIS* **2010,** *118* (1), 1-36.

59.	Lloyd, N. C.; Morgan, H. W.; Nicholson, B. K.; Ronimus, R. S., The composition of Ehrlich's salvarsan: resolution of a century-old debate. *Angew. Chem. Int.* **2005,** *44* (6), 941-944.

60.	Miller, E. L., The penicillins: a review and update. *J. Midwifery Women's Health* **2002,** *47* (6), 426-34.

61.   Lobanovska, M.; Pilla, G., Penicillin's discovery and antibiotic resistance: lessons for the future? *Yale J. Biol. Med.* **2017,** *90* (1), 135-145.

62.   Hart, F. D.; Burley, D.; Manley, R.; Brown, G., Penicillin V. *BMJ* **1956,** *1* (4965), 496-497.

63.   Sáez-Llorens, X.; McCracken, G. H., Chapter 37 - Clinical pharmacology of antibacterial agents. In *Infectious Diseases of the Fetus and Newborn Infant (Sixth Edition)*, Remington, J. S.; Klein, J. O.; Wilson, C. B.; Baker, C. J., Eds. W.B. Saunders: Philadelphia, 2006; pp 1223-1267.

64.   Fishovitz, J.; Hermoso, J. A.; Chang, M.; Mobashery, S., Penicillin-binding protein 2a of methicillin-resistant *Staphylococcus aureus*. *IUBMB Life* **2014,** *66* (8), 572-577.

65.   Foster, T. J., Antibiotic resistance in *Staphylococcus aureus*. Current status and future prospects. *FEMS Microbiol. Rev.* **2017,** *41* (3), 430-449.

66.   Kotra, L. P.; Mobashery, S., β-Lactam antibiotics, β-lactamases and bacterial resistance. *Bulletin de l'Institut Pasteur* **1998,** *96* (3), 139-150.

67.   Tipper, D. J.; Strominger, J. L., Mechanism of action of penicillins: a proposal based on their structural similarity to acyl-D-alanyl-D-alanine. *Proc.Natl. Acad. Sci. USA* **1965,** *54* (4), 1133-1141.

68.   Zeng, D.; Debabov, D.; Hartsell, T. L.; Cano, R. J.; Adams, S.; Schuyler, J. A.; McMillan, R.; Pace, J. L., Approved Glycopeptide Antibacterial Drugs: Mechanism of Action and Resistance. *Cold Spring Harb. Perspect. Med.* **2016,** *6* (12).

69.   Arbeit, R. D.; Maki, D.; Tally, F. P.; Campanaro, E.; Eisenstein, B. I., The safety and efficacy of daptomycin for the treatment of complicated skin and skin-structure infections. *Clin. Infect. Dis.* **2004,** *38* (12), 1673-81.

70.   Bayer, A. S.; Schneider, T.; Sahl, H. G., Mechanisms of daptomycin resistance in Staphylococcus aureus: role of the cell membrane and cell wall. *Ann. N. Y. Acad. Sci.* **2013,** *1277* (1), 139-58.

71.   Taylor, S. D.; Palmer, M., The action mechanism of daptomycin. *Bioorg. Med. Chem.* **2016,** *24* (24), 6253-6268.

72.   Chopra, I.; Roberts, M., Tetracycline antibiotics: mode of action, applications, molecular biology, and epidemiology of bacterial resistance. *Microbiol. Mol. Biol. Rev.* **2001,** *65* (2), 232-260.

73.   Wilson, D. N., The A-Z of bacterial translation inhibitors. *Crit. Rev. biochem. Mol. Biol.* **2009,** *44* (6), 393-433.

74.   Nguyen, F.; Starosta, A. L.; Arenz, S.; Sohmen, D.; Dönhöfer, A.; Wilson, D. N., Tetracycline antibiotics and resistance mechanisms. *Biol. Chem.* **2014,** *395* (5), 559-75.

75.   Davis, B. D.; Chen, L. L.; Tai, P. C., Misread protein creates membrane channels: an essential step in the bactericidal action of aminoglycosides. *Proc.Natl. Acad. Sci. USA.* **1986,** *83* (16), 6164-8.

76.   Aubry-Damon, H.; Soussy, C. J.; Courvalin, P., Characterization of mutations in the rpoB gene that confer rifampin resistance in *Staphylococcus aureus*. *Antimicrob. Agents. Chemother.* **1998,** *42* (10), 2590-2594.

77.   Campbell, E. A.; Korzheva, N.; Mustaev, A.; Murakami, K.; Nair, S.; Goldfarb, A.; Darst, S. A., Structural mechanism for rifampicin inhibition of bacterial rna polymerase. *Cell* **2001,** *104* (6), 901-12.

78.   Gade, N. D.; Qazi, M. S., Fluoroquinolone Therapy in *Staphylococcus aureus* infections: where do we stand? *J Lab Physicians* **2013,** *5* (2), 109-112.

79.   Zhanel, G. G.; Walkty, A.; Vercaigne, L.; Karlowsky, J. A.; Embil, J.; Gin, A. S.; Hoban, D. J., The new fluoroquinolones: a critical review. *Can. J. Infect. Dis.* **1999,** *10* (3), 207-238.

80.   Reece, R. J.; Maxwell, A., DNA gyrase: structure and function. *Crit. Rev. biochem. Mol. Biol.* **1991,** *26* (3-4), 335-75.

81.   Aldred, K. J.; Kerns, R. J.; Osheroff, N., Mechanism of quinolone action and resistance. *Biochemistry* **2014,** *53* (10), 1565-1574.

82.   Lowy, F. D., Antimicrobial resistance: the example of *Staphylococcus aureus*. *J. Clin. Invest.* **2003,** *111* (9), 1265-73.

83.   Zhang, H. Z.; Hackbarth, C. J.; Chansky, K. M.; Chambers, H. F., A proteolytic transmembrane signaling pathway and resistance to beta-lactams in staphylococci. *Science* **2001,** *291* (5510), 1962-5.

84.   Gregory, P. D.; Lewis, R. A.; Curnock, S. P.; Dyke, K. G., Studies of the repressor (BlaI) of beta-lactamase synthesis in *Staphylococcus aureus*. *Mol. Microbiol.* **1997,** *24* (5), 1025-37.

85.   Jensen, S. O.; Lyon, B. R., Genetics of antimicrobial resistance in *Staphylococcus aureus*. *Future Microbial.* **2009,** *4* (5), 565-82.

86.   Jevons, M. P., "Celbenin" - resistant Staphylococci. *BMJ* **1961,** *1* (5219), 124-125.

87.   Ito, T.; Kuwahara-Arai, K.; Katayama, Y.; Uehara, Y.; Han, X.; Kondo, Y.; Hiramatsu, K., Staphylococcal cassette chromosome mec (SCCmec) analysis of MRSA. *Methods Mol. Biol.* **2014,** *1085*, 131-48.

88.   Urushibara, N.; Aung, M. S.; Kawaguchiya, M.; Kobayashi, N., Novel staphylococcal cassette chromosome *mec* (SCC*mec*) type XIV (5A) and a truncated SCC*mec* element in SCC composite islands carrying *speG* in ST5 MRSA in Japan. *J. Antimicrob. Chemother.* **2020,** *75* (1), 46-50.

89.   Saudagar, P. S.; Survase, S. A.; Singhal, R. S., Clavulanic acid: a review. *Biotechnol. Adv.* **2008,** *26* (4), 335-351.

90.   Papp-Wallace, K. M.; Endimiani, A.; Taracila, M. A.; Bonomo, R. A., Carbapenems: past, present, and future. *Antimicrob. Agents Chemother.* **2011,** *55* (11), 4943.

91.   Symonds, J.; Geddes, A. M., Cephalosporins in gram-positive infections. *Drugs* **1987,** *34 Suppl 2*, 121-34.

92.   Gardete, S.; Tomasz, A., Mechanisms of vancomycin resistance in *Staphylococcus aureus*. *J. Clin. Invest.* **2014,** *124* (7), 2836-2840.

93.   McGuinness, W. A.; Malachowa, N.; DeLeo, F. R., Vancomycin Resistance in *Staphylococcus aureus*. *Yale J. Biol. Med.* **2017,** *90* (2), 269-281.

94.   Long, K. S.; Poehlsgaard, J.; Kehrenberg, C.; Schwarz, S.; Vester, B., The Cfr rRNA methyltransferase confers resistance to phenicols, lincosamides, oxazolidinones, pleuromutilins, and streptogramin A antibiotics. *Antimicrob. Agents Chemother.* **2006,** *50* (7), 2500-2505.

95.   Powers, M. E.; Wardenburg, J. B., Igniting the fire: *Staphylococcus aureus* virulence factors in the pathogenesis of sepsis. *PLoS Pathog.* **2014,** *10* (2), e1003871.

96.   Cheung, A. L.; Nishina, K. A.; Trotonda, M. P.; Tamber, S., The SarA protein family of *Staphylococcus aureus*. *Int. J. Biochem. Cell Biol.* **2008,** *40* (3), 355-361.

97.   Novick, R. P., Autoinduction and signal transduction in the regulation of staphylococcal virulence. *Mol. Microbiol.* **2003,** *48* (6), 1429-49.

98.   Recsei, P.; Kreiswirth, B.; O'Reilly, M.; Schlievert, P.; Gruss, A.; Novick, R. P., Regulation of exoprotein gene expression in *Staphylococcus aureus* by agar. *Mol. Gen. Genet.* **1986,** *202* (1), 58-61.

99.   Morfeldt, E.; Janzou, L.; Arvidson, S.; Löfdahl, S., Cloning of a chromosomal locus (*exp*) which regulates the expression of several exoprotein genes in *Staphylococcus aureus*. *Mol. Gen. Genet.* **1988,** *211* (3), 435-440.

100.   Peng, H. L.; Novick, R. P.; Kreiswirth, B.; Kornblum, J.; Schlievert, P., Cloning, characterization, and sequencing of an accessory gene regulator (*agr*) in *Staphylococcus aureus*. *J. Bacteriol.* **1988,** *170* (9), 4365-4372.

101.   Cheng, A. G.; McAdow, M.; Kim, H. K.; Bae, T.; Missiakas, D. M.; Schneewind, O., Contribution of Coagulases towards *Staphylococcus aureus* Disease and Protective Immunity. *PLoS Pathog.* **2010,** *6* (8), e1001036.

102.   Adler, A.; Temper, V.; Block, C. S.; Abramson, N.; Moses, A. E., Panton-Valentine leukocidin-producing *Staphylococcus aureus*. *Emerg Infect Dis* **2006,** *12* (11), 1789-1790.

103.   Novick, R. P.; Geisinger, E., Quorum sensing in staphylococci. *Annu. Rev. Genet.* **2008,** *42*, 541-64.

104.   Rutherford, S. T.; Bassler, B. L., Bacterial quorum sensing: its role in virulence and possibilities for its control. *Cold Spring Harb. Perspect. Med..* **2012,** *2* (11).

105.   Side, D. D.; Nassisi, V.; Pennetta, C.; Alifano, P.; Di Salvo, M.; Talà, A.; Chechkin, A.; Seno, F.; Trovato, A., Bacterial bioluminescence onset and quenching: a dynamical model for a quorum sensing-mediated property. *R. Soc. Open. Sci.* **2017,** *4* (12), 171586-171586.

106.   Daniels, R.; Vanderleyden, J.; Michiels, J., Quorum sensing and swarming migration in bacteria. *FEMS Microbiol. Rev.* **2004,** *28* (3), 261-289.

107.   Novick, R. P.; Projan, S. J.; Kornblum, J.; Ross, H. F.; Ji, G.; Kreiswirth, B.; Vandenesch, F.; Moghazeh, S., The *agr* P2 operon: an autocatalytic sensory transduction system in *Staphylococcus aureus*. *Mol. Gen. Genet.* **1995,** *248* (4), 446-58.

108.   Janzon, L.; Löfdahl, S.; Arvidson, S., Identification and nucleotide sequence of the delta-lysin gene, hld, adjacent to the accessory gene regulator (*agr*) of *Staphylococcus aureus*. *Mol. Gen. Genet.* **1989,** *219* (3), 480-5.

109.   Bronner, S.; Stoessel, P.; Gravet, A.; Monteil, H.; Prévost, G., Variable expressions of *Staphylococcus aureus* bicomponent leucotoxins semiquantified by competitive reverse transcription-PCR. *Appl. Environ. Microbiol.* **2000,** *66* (9), 3931-3938.

110.   Tseng, C. W.; Zhang, S.; Stewart, G. C., Accessory gene regulator control of staphyloccoccal enterotoxin D gene expression. *J. Bacteriol.* **2004,** *186* (6), 1793.

111.   Regassa, L. B.; Couch, J. L.; Betley, M. J., Steady-state staphylococcal enterotoxin type C mRNA is affected by a product of the accessory gene regulator (*agr*) and by glucose. *Infect. Immun.* **1991,** *59* (3), 955-62.

112.   Reed, S. B.; Wesson, C. A.; Liou, L. E.; Trumble, W. R.; Schlievert, P. M.; Bohach, G. A.; Bayles, K. W., Molecular characterization of a novel *Staphylococcus aureus* serine protease operon. *Infect. Immun.* **2001,** *69* (3), 1521-1527.

113.   Shaw, L.; Golonka, E.; Potempa, J.; Foster, S. J., The role and regulation of the extracellular proteases of *Staphylococcus aureus*. *Microbiol.* **2004,** *150* (Pt 1), 217-228.

114.   Joo, H.-S.; Chan, J. L.; Cheung, G. Y. C.; Otto, M., Subinhibitory concentrations of protein synthesis-Inhibiting antibiotics promote increased expression of the *agr* virulence regulator and production of phenol-soluble modulin cytolysins in community-associated methicillin-resistant *Staphylococcus aureus*. *Antimicrob. Agents Chemother.* **2010,** *54* (11), 4942.

115.   Rooijakkers, S. H.; Ruyken, M.; van Roon, J.; van Kessel, K. P.; van Strijp, J. A.; van Wamel, W. J., Early expression of SCIN and CHIPS drives instant immune evasion by *Staphylococcus aureus*. *Cell. Microbial.* **2006,** *8* (8), 1282-93.

116.   Saravia-Otten, P.; Müller, H. P.; Arvidson, S., Transcription of *Staphylococcus aureus* fibronectin binding protein genes is negatively regulated by *agr* and an *agr*-independent mechanism. *J. Bacteriol.* **1997,** *179* (17), 5259.

117.   Wolz, C.; McDevitt, D.; Foster, T. J.; Cheung, A. L., Influence of *agr* on fibrinogen binding in *Staphylococcus aureus* Newman. *Infect. Immun.* **1996,** *64* (8), 3142-3147.

118.   Boisset, S.; Geissmann, T.; Huntzinger, E.; Fechter, P.; Bendridi, N.; Possedko, M.; Chevalier, C.; Helfer, A. C.; Benito, Y.; Jacquier, A.; Gaspin, C.; Vandenesch, F.; Romby, P., *Staphylococcus aureus* RNAIII coordinately represses the synthesis of virulence factors and the transcription regulator Rot by an antisense mechanism. *Genes Dev* **2007,** *21* (11), 1353-1366.

119.   Novick, R. P.; Ross, H. F.; Projan, S. J.; Kornblum, J.; Kreiswirth, B.; Moghazeh, S., Synthesis of staphylococcal virulence factors is controlled by a regulatory RNA molecule. *Embo. J.* **1993,** *12* (10), 3967-75.

120.   Qiu, R.; Pei, W.; Zhang, L.; Lin, J.; Ji, G., Identification of the putative staphylococcal AgrB catalytic residues involving the proteolytic cleavage of AgrD to generate autoinducing peptide. *J. Biol. Chem.* **2005,** *280* (17), 16695-704.

121.   Jensen, R. O.; Winzer, K.; Clarke, S. R.; Chan, W. C.; Williams, P., Differential recognition of *Staphylococcus aureus* quorum-sensing signals depends on both extracellular loops 1 and 2 of the transmembrane sensor AgrC. *J. Mol. Biol.* **2008,** *381* (2), 300-9.

122.   Wang, B.; Zhao, A.; Novick, R. P.; Muir, T. W., Key driving forces in the biosynthesis of autoinducing peptides required for staphylococcal virulence. *Proc. Natl. Acad. Sci. U. S. A.* **2015,** *112* (34), 10679-84.

123.   Mayville, P.; Ji, G.; Beavis, R.; Yang, H.; Goger, M.; Novick, R. P.; Muir, T. W., Structure-activity analysis of synthetic autoinducing thiolactone peptides from *Staphylococcus aureus* responsible for virulence. *Proc. Natl. Acad. Sci. U. S. A.* **1999,** *96* (4), 1218-23.

124.   Cosgriff, C. J.; White, C. R.; Teoh, W. P.; Grayczyk, J. P.; Alonzo, F., 3rd, Control of *Staphylococcus aureus* quorum sensing by a membrane-embedded peptidase. *Infect Immun* **2019,** *87* (5).

125.   George Cisar, E. A.; Geisinger, E.; Muir, T. W.; Novick, R. P., Symmetric signalling within asymmetric dimers of the *Staphylococcus aureus* receptor histidine kinase AgrC. *Mol. Microbiol.* **2009,** *74* (1), 44-57.

126.   Reynolds, J.; Wigneshweraraj, S., Molecular insights into the control of transcription initiation at the *Staphylococcus aureus agr* operon. *J. Mol. Biol.* **2011,** *412* (5), 862-81.

127.   Gupta, R. K.; Luong, T. T.; Lee, C. Y., RNAIII of the *Staphylococcus aureus agr* system activates global regulator MgrA by stabilizing mRNA. *Proc. Natl. Acad. Sci. U. S. A.* **2015,** *112* (45), 14036-14041.

128.   Geisinger, E.; Muir, T. W.; Novick, R. P.; Bassler, B. L., Agr receptor mutants reveal distinct modes of inhibition by staphylococcal autoinducing peptides. *Proc. Natl. Acad. Sci. U. S. A.* **2009,** *106* (4), 1216-1221.

129.   Wright, J. S., 3rd; Jin, R.; Novick, R. P., Transient interference with staphylococcal quorum sensing blocks abscess formation. *Proc. Natl. Acad. Sci. U. S. A.* **2005,** *102* (5), 1691-1696.

130.   Dufour, P.; Jarraud, S.; Vandenesch, F.; Greenland, T.; Novick, R. P.; Bes, M.; Etienne, J.; Lina, G., High genetic variability of the *agr* locus in *Staphylococcus* species. *J. Bacteriol.* **2002,** *184* (4), 1180-6.

131.   Olson, M. E.; Todd, D. A.; Schaeffer, C. R.; Paharik, A. E.; Van Dyke, M. J.; Büttner, H.; Dunman, P. M.; Rohde, H.; Cech, N. B.; Fey, P. D.; Horswill, A. R., *Staphylococcus epidermidis agr* quorum-sensing system: signal identification, cross talk, and importance in colonization. *J. Bacteriol.* **2014,** *196* (19), 3482-3493.

132.   Rowe, S. E.; Mahon, V.; Smith, S. G.; O'Gara, J. P., A novel role for SarX in *Staphylococcus epidermidis* biofilm regulation. *Microbiology* **2011,** *157* (Pt 4), 1042-1049.

133.   Wang, N.; Neilan, A. M.; Klompas, M., Staphylococcus intermedius infections: case report and literature review. *Infect Dis Rep* **2013,** *5* (1), e3-e3.

134.   Hatch, S.; Sree, A.; Tirrell, S.; Torres, B.; Rothman, A. L., Metastatic complications from *Staphylococcus intermedius*, a zoonotic pathogen. *J Clin Microbiol* **2012,** *50* (3), 1099-1101.

135.   Ji, G.; Pei, W.; Zhang, L.; Qiu, R.; Lin, J.; Benito, Y.; Lina, G.; Novick, R. P., *Staphylococcus intermedius* produces a functional *agr* autoinducing peptide containing a cyclic lactone. *J. Bacteriol.* **2005,** *187* (9), 3139-3150.

136.   Pinkston, K. L.; Gao, P.; Diaz-Garcia, D.; Sillanpää, J.; Nallapareddy, S. R.; Murray, B. E.; Harvey, B. R., The Fsr quorum-sensing system of *Enterococcus faecalis* modulates surface display of the collagen-binding MSCRAMM Ace through regulation of gelE. *J. Bacteriol.* **2011,** *193* (17), 4317-4325.

137   Hancock, L. E.; Perego, M., The *Enterococcus faecalis fsr* two-component system controls biofilm development through production of gelatinase. *J. Bacteriol.* **2004,** *186* (17), 5629-5639.

138.   Nakayama, J.; Chen, S.; Oyama, N.; Nishiguchi, K.; Azab, E. A.; Tanaka, E.; Kariyama, R.; Sonomoto, K., Revised model for *Enterococcus faecalis fsr* quorum-sensing system: the small open reading frame *fsrD* encodes the gelatinase biosynthesis-activating pheromone propeptide corresponding to staphylococcal agrd. *J. Bacteriol.* **2006,** *188* (23), 8321-6.

139.   Ali, L.; Goraya, M. U.; Arafat, Y.; Ajmal, M.; Chen, J.-L.; Yu, D., Molecular mechanism of quorum-sensing in *Enterococcus faecalis*: its role in virulence and therapeutic approaches. *Int. J. Mol. Sci.* **2017,** *18* (5), 960.

140.   Darkoh, C.; Asiedu, G. A., Quorum sensing systems in Clostridia. In *quorum sensing vs quorum quenching: a battle with no end in sight*, Kalia, V. C., Ed. Springer India: New Delhi, 2015; pp 133-154.

141. Darkoh, C.; DuPont, H. L.; Norris, S. J.; Kaplan, H. B., Toxin synthesis by *Clostridium difficile* is regulated through quorum signaling. *mBio* **2015,** *6*.

142. Foletti, D.; Strop, P.; Shaughnessy, L.; Hasa-Moreno, A.; Casas, M. G.; Russell, M.; Bee, C.; Wu, S.; Pham, A.; Zeng, Z.; Pons, J.; Rajpal, A.; Shelton, D., Mechanism of action and *in vivo* efficacy of a human-derived antibody against *Staphylococcus aureus* α-haemolysin. *J. Mol. Biol.* **2013,** *425* (10), 1641-1654.

143. Gordon, C. P.; Williams, P.; Chan, W. C., Attenuating *Staphylococcus aureus* virulence gene regulation: a medicinal chemistry perspective. *J. Med. Chem.* **2013,** *56* (4), 1389-404.

144. P, M. D.; Affas, Z.; Reynolds, C.; Holden, M. T.; Wood, S. J.; Saint, S.; Cockayne, A.; Hill, P. J.; Dodd, C. E.; Bycroft, B. W.; Chan, W. C.; Williams, P., Structure, activity and evolution of the group I thiolactone peptide quorum-sensing system of *Staphylococcus aureus*. *Mol. Microbiol.* **2001,** *41* (2), 503-12.

145. Ji, G.; Beavis, R.; Novick, R. P., Bacterial interference caused by autoinducing peptide variants. *Science* **1997,** *276* (5321), 2027-30.

146. Mansson, M.; Nielsen, A.; Kjærulff, L.; Gotfredsen, C. H.; Wietz, M.; Ingmer, H.; Gram, L.; Larsen, T. O., Inhibition of virulence gene expression in *Staphylococcus aureus* by novel depsipeptides from a marine photobacterium. *Mar. Drugs* **2011,** *9* (12), 2537-2552.

147. Nielsen, A.; Månsson, M.; Bojer, M. S.; Gram, L.; Larsen, T. O.; Novick, R. P.; Frees, D.; Frøkiær, H.; Ingmer, H., Solonamide B inhibits quorum sensing and reduces *Staphylococcus aureus* mediated killing of human neutrophils. *PloS one* **2014,** *9* (1), e84992.

148. Murray, E. J.; Crowley, R. C.; Truman, A.; Clarke, S. R.; Cottam, J. A.; Jadhav, G. P.; Steele, V. R.; O'Shea, P.; Lindholm, C.; Cockayne, A.; Chhabra, S. R.; Chan, W. C.; Williams, P., Targeting *Staphylococcus aureus* quorum sensing with nonpeptidic small molecule inhibitors. *J. Med. Chem.* **2014,** *57* (6), 2813-9.

149. Papenfort, K.; Bassler, B. L., Quorum sensing signal-response systems in Gram-negative bacteria. *Nat. Rev. Microbiol.* **2016,** *14* (9), 576-588.

150.   Qazi, S.; Middleton, B.; Muharram, S. H.; Cockayne, A.; Hill, P.; O'Shea, P.; Chhabra, S. R.; Cámara, M.; Williams, P., N-acylhomoserine lactones antagonize virulence gene expression and quorum sensing in *Staphylococcus aureus*. *Infect Immun* **2006,** *74* (2), 910-919.

151.   Sully, E. K.; Malachowa, N.; Elmore, B. O.; Alexander, S. M.; Femling, J. K.; Gray, B. M.; DeLeo, F. R.; Otto, M.; Cheung, A. L.; Edwards, B. S.; Sklar, L. A.; Horswill, A. R.; Hall, P. R.; Gresham, H. D., Selective chemical inhibition of *agr* quorum sensing in *Staphylococcus aureus* promotes host defense with minimal impact on resistance. *PLoS Pathog.* **2014,** *10* (6), e1004174.

152.   Zhang, L.; Gray, L.; Novick, R. P.; Ji, G., Transmembrane topology of AgrB, the protein involved in the post-translational modification of AgrD in *Staphylococcus aureus*. *J. Biol. Chem.* **2002,** *277* (38), 34736-42.

153.   Nakayama, J.; Uemura, Y.; Nishiguchi, K.; Yoshimura, N.; Igarashi, Y.; Sonomoto, K., Ambuic acid inhibits the biosynthesis of cyclic peptide quormones in gram-positive bacteria. *Antimicrob. Agents Chemother.* **2009,** *53* (2), 580-6.

154.   Li, J. Y.; Harper, J. K.; Grant, D. M.; Tombe, B. O.; Bashyal, B.; Hess, W. M.; Strobel, G. A., Ambuic acid, a highly functionalized cyclohexenone with antifungal activity from *Pestalotiopsis spp*. and *Monochaetia sp*. *Phytochemistry* **2001,** *56* (5), 463-8.

155.   Todd, D. A.; Parlet, C. P.; Crosby, H. A.; Malone, C. L.; Heilmann, K. P.; Horswill, A. R.; Cech, N. B., Signal Biosynthesis Inhibition with Ambuic Acid as a Strategy To Target Antibiotic-Resistant Infections. *Antimicrob. Agents Chemother.* **2017,** *61* (8), e00263-17.

156.   Qi, Q. Y.; Li, E. W.; Han, J. J.; Pei, Y. F.; Ma, K.; Bao, L.; Huang, Y.; Zhao, F.; Liu, H. W., New ambuic acid derivatives from the solid culture of *Pestalotiopsis neglecta* and their nitric oxide inhibitory activity. *Sci. Rep.* **2015,** *5*, 9958.

157.   Li, C. S.; Yang, B. J.; Turkson, J.; Cao, S., Anti-proliferative ambuic acid derivatives from Hawaiian endophytic fungus *Pestalotiopsis sp*. FT172. *Phytochemistry* **2017,** *140*, 77-82.

158.   Ding, G.; Li, Y.; Fu, S.; Liu, S.; Wei, J.; Che, Y., Ambuic acid and torreyanic acid derivatives from the endolichenic fungus *Pestalotiopsis sp*. *J. Nat. Prod.* **2009,** *72* (1), 182-6.

159.   Siklos, M.; BenAissa, M.; Thatcher, G. R., Cysteine proteases as therapeutic targets: does selectivity matter? A systematic review of calpain and cathepsin inhibitors. *Acta. Pharm. Sin. B* **2015,** *5* (6), 506-19.

160.   Buttle, D. J.; Mort, J. S., Cysteine Proteases. In *Encyclopedia of Biological Chemistry (Second Edition)*, Lennarz, W. J.; Lane, M. D., Eds. Academic Press: Waltham, 2013; pp 589-592.

161.   Hofer, F.; Kraml, J.; Kahler, U.; Kamenik, A. S.; Liedl, K. R., Catalytic site pKa values of aspartic, cysteine, and serine proteases: constant pH MD simulations. *J. Chem. Inf. Model.* **2020,** *60* (6), 3030-3042.

162.   Powers, J. C.; Asgian, J. L.; Ekici, O. D.; James, K. E., Irreversible inhibitors of serine, cysteine, and threonine proteases. *Chem. Rev.* **2002,** *102* (12), 4639-750.

163.   Jung, S. H.; Hwang, G. S.; Lee, S. I.; Ryu, D. H., Total synthsis of (+)-ambuic acid: alpha-bromination with 1,2-dibromotetrachloroethane. *J. Org. Chem.* **2012,** *77* (5), 2513-8.

165.   Mehta, G.; Pan, S. C., Total synthesis of the novel, biologically active epoxyquinone dimer (±)-torreyanic acid: a biomimetic approach. *Org. Lett.* **2004,** *6* (22), 3985-3988.

165.   Corey, E. J.; Chaykovsky, M., Dimethyloxosulfonium methylide ((CH3)2SOCH2) and dimethylsulfonium methylide ((CH3)2SCH2). Formation and application to organic synthesis. *J. Am. Chem. Soc.* **1965,** *87* (6), 1353-1364.

166.   Corey, E. J.; Chaykovsky, M., Dimethylsulfonium methylide, a reagent for selective oxirane synthesis from aldehydes and ketones. *J. Am. Chem. Soc.* **1962,** *84* (19), 3782-3783.

167.   Li, C.; Johnson, R. P.; Porco, J. A., Total synthesis of the quinone epoxide dimer (+)-torreyanic acid: application of a biomimetic oxidation/electrocyclization/Diels−Alder dimerization ascade. *J. Am. Chem. Soc.* **2003,** *125* (17), 5095-5106.

168.   Mehta, G.; Pan, S. C., A total synthesis of the epoxyquinone based antifungal natural product (±)-ambuic acid. *Tetrahedron Lett.* **2005,** *46* (17), 3045-3048.

169.   Corey, E. J.; Shibata, T.; Lee, T. W., Asymmetric Diels−Alder reactions catalyzed by a triflic acid activated chiral oxazaborolidine. *J. Am. Chem. Soc.* **2002,** *124* (15), 3808-3809.

170.   Corey, E. J., Enantioselective catalysis based on cationic oxazaborolidines. *Angew. Chem. Int. Ed. Engl.* **2009,** *48* (12), 2100-17.

171.   Sim, J. Y.; Hwang, G.-S.; Kim, K. H.; Ko, E. M.; Ryu, D. H., Asymmetric synthesis of (+)-cis-nemorensic acid from a chiral Diels-Alder adduct of 2,5-dimethylfuran. *Chem. commun.* **2007,** (47), 5064-5065.

172.   Farina, V. K., Venkat; Scott, William J, The Stille reaction. In *Organic Reactions*, 1997; Vol. 50.

173.   K. Stille, J., *The Palladium-Catalyzed Cross-Coupling Reactions of Organotin Reagents with Organic Electrophiles[New Synthetic Methods(58)]*. 1986; Vol. 25, p 508-524.

174.   Cordovilla, C.; Bartolomé, C.; Martínez-Ilarduya, J. M.; Espinet, P., The Stille reaction, 38 years later. *ACS Catal.* **2015,** *5* (5), 3040-3053.

175.   Juliá, S.; Masana, J.; Vega, J. C., "Synthetic enzymes". Highly stereoselective epoxidation of chalcone in a triphasic toluene-water-poly[(*S*)-alanine] system. *Angew. Chem. Int.* **1980,** *19* (11), 929-931.

176.   Juliá-Colonna asymmetric epoxidation. In *Comprehensive Organic Name Reactions and Reagents*, pp 1583-1587.

177.   Kelly, D. R.; Roberts, S. M., The mechanism of polyleucine catalysed asymmetric epoxidation. *ChemComm.* **2004,** (18), 2018-2020.

178. Berkessel, A.; Gasch, N.; Glaubitz, K.; Koch, C., Highly enantioselective enone epoxidation catalyzed by short solid phase-bound peptides: dominant role of peptide helicity. *Org. Lett.* **2001,** *3* (24), 3839-3842.

179. Mehta, G.; Pan, S. C., Total synthesis of the novel antifungal agent (±)-jesterone. *Org. Lett.* **2004,** *6* (5), 811-813.

180. Mehta, G.; Pan, S. C., First total synthesis of yanuthones: novel farnesylated epoxycyclohexenoid marine natural products. *Tetrahedron Lett.* **2005,** *46* (31), 5219-5223.

181. Patschinski, P.; Zhang, C.; Zipse, H., The Lewis base-catalyzed silylation of alcohols—a mechanistic analysis. *J. Org. Chem.* **2014,** *79* (17), 8348-8357.

182. Corey, E. J.; Venkateswarlu, A., Protection of hydroxyl groups as tert-butyldimethylsilyl derivatives. *J. Am. Chem. Soc.* **1972,** *94* (17), 6190-6191.

183. Harries, C., Über die einwirkung des ozons auf organische verbindungen. *Justus Liebigs Ann. Chem.* **1905,** *343* (2-3), 311-344.

184. Criegee, R., Mechanism of Ozonolysis. *Angew. Chem. Int.* **1975,** *14* (11), 745-752.

185. Geletneky, C.; Berger, S., The Mechanism of ozonolysis revisited by ^{17}O-NMR spectroscopy. *Eur. J. Org. Chem.* **1998,** *1998* (8), 1625-1627.

186. Criegee mechanism of ozonolysis. In *Name Reactions: A Collection of Detailed Reaction Mechanisms*, Li, J. J., Ed. Springer Berlin Heidelberg: Berlin, Heidelberg, **2006**; pp 173-174.

187. Rieche, A.; Meister, R.; Sauthoff, H., Über ozonide und ihre spaltung. *Justus Liebigs Ann. Chem.* **1942,** *553* (1), 187-249.

188. Robiette, R.; Richardson, J.; Aggarwal, V. K.; Harvey, J. N., Reactivity and selectivity in the Wittig reaction: a computational study. *J. Am. Chem. Soc.* **2006,** *128* (7), 2394-409.

189.   Williamson, A., XLV. Theory of ætherification. *Lond. Edinb. Dubl. Phil. Mag. and Journal of Science* **1850,** *37* (251), 350-356.

190.   Liang, Q.; Sun, Y.; Yu, B.; She, X.; Pan, X., First Total Syntheses and Spectral Data Corrections of 11-α-Methoxycurvularin and 11-β-Methoxycurvularin. *J. Org. Chem.* **2007,** *72* (25), 9846-9849.

191.   Aspinall, H. C.; Greeves, N.; Lee, W.-M.; McIver, E. G.; Smith, P. M., An improved Williamson etherification of hindered alcohols promoted by 15-crown-5 and sodium hydride. *Tetrahedron Lett.* **1997,** *38* (26), 4679-4682.

192.   Moon, B.; Park, Y. C.; McClintock, J. B.; Baker, B. J., Structure and bioactivity of erebusinone, a pigment from the antarctic sponge *Isodictya erinacea*. *Tetrahedron* **2000,** *56* (46), 9057-9062.

193.   Appel, R., Tertiary phosphane/tetrachloromethane, a versatile reagent for Chlorination, dehydration, and P-N Linkage. *Angew. Chem. Int.***1975,** *14* (12), 801-811.

194.   Appel Reaction. In *Comprehensive Organic Name Reactions and Reagents*, pp 95-99.

195   Nieves, I.; Abad, J.-L.; Montes, L. R.; Goñi, F. M.; Delgado, A., Approaches to polyunsaturated sphingolipids: new conformationally restrained analogs with minimal structural modifications. *Tetrahedron* **2016,** *72* (5), 605-612.

196.   Mills, J. S.; Showell, G. A., Exploitation of silicon medicinal chemistry in drug discovery. *Expert Opin. Investig. Drugs* **2004,** *13* (9), 1149-1157.

197.   Barraza, S. J.; Denmark, S. E., Synthesis, reactivity, functionalization, and ADMET properties of silicon-containing nitrogen heterocycles. *J. Am.n Chem. Soc.* **2018,** *140* (21), 6668-6684.

198.   Franz, A. K.; Wilson, S. O., Organosilicon molecules with medicinal applications. *J. Med. Chem.* **2013,** *56* (2), 388-405.

199.   Lukevics, E.; Ignatovich, L., Comparative study of the biological activity of organosilicon and organogermanium compounds. *Appl. Organomet. Chem.* **1992,** *6* (2), 113-126.

200.   Perestelo, N. R.; Llanos, G. G.; Reyes, C. P.; Amesty, A.; Sooda, K.; Afshinjavid, S.; Jiménez, I. A.; Javid, F.; Bazzocchi, I. L., Expanding the chemical space of withaferin A by incorporating silicon to improve its clinical potential on human ovarian carcinoma cells. *J. Med. Chem.***2019,** *62* (9), 4571-4585.

201.   Loose, D. S.; Kan, P. B.; Hirst, M. A.; Marcus, R. A.; Feldman, D., Ketoconazole blocks adrenal steroidogenesis by inhibiting cytochrome P450-dependent enzymes. *J. Clin. Investig.* **1983,** *71* (5), 1495-1499.

202.   Heel, R. C.; Brogden, R. N.; Carmine, A.; Morley, P. A.; Speight, T. M.; Avery, G. S., Ketoconazole: a review of its therapeutic efficacy in superficial and systemic fungal infections. *Drugs* **1982,** *23* (1), 1-36.

203.   Nobile, C. J.; Johnson, A. D., *Candida albicans* biofilms and human disease. *Annu. Rev. Microbiol.* **2015,** *69*, 71-92.

204.   Faught, E., Topiramate in the treatment of partial and generalized epilepsy. *Neuropsychiatr. Dis. Treat.* **2007,** *3* (6), 811-821.

205.   Naegel, S.; Obermann, M., Topiramate in the prevention and treatment of migraine: efficacy, safety and patient preference. *Neuropsychiatr. Dis. Treat.* **2010,** *6*, 17-28.

206.   Dodgson, S. J.; Shank, R. P.; Maryanoff, B. E., Topiramate as an inhibitor of carbonic anhydrase isoenzymes. *Epilepsia* **2000,** *41* (S1), 35-9.

207.   White, H. S.; Brown, S. D.; Woodhead, J. H.; Skeen, G. A.; Wolf, H. H., Topiramate enhances GABA-mediated chloride flux and GABA-evoked chloride currents in murine brain neurons and increases seizure threshold. *Epilepsy Res.* **1997,** *28* (3), 167-79.

208.   Maryanoff, B. E., Phenotypic assessment and the discovery of topiramate. *ACS Med. Chem. Lett.* **2016,** *7* (7), 662-665.

209.   Jin, Y.; Yeh, C.-H.; Kuttruff, C. A.; Jørgensen, L.; Dünstl, G.; Felding, J.; Natarajan, S. R.; Baran, P. S., C-H oxidation of ingenanes enables potent and selective protein kinase C isoform ictivation. *Angew. Chem. Int.* **2015,** *54* (47), 14044-14048.

210.   Moore, J. A.; Anet, F. A. L., 5.19 - Eight-membered rings. In *Comprehensive Heterocyclic Chemistry*, Katritzky, A. R.; Rees, C. W., Eds. Pergamon: Oxford, 1984; pp 653-707.

211.   Lorette, N. B.; Howard, W. L., Preparation of ketals from 2,2-dimethoxypropane. *J. Org. Chem.* **1960,** *25* (4), 521-525.

212.   Thoendel, M.; Horswill, A. R., Identification of *Staphylococcus aureus* AgrD residues required for autoinducing peptide biosynthesis. *J. Biol. Chem.* **2009,** *284* (33), 21828-38.

213.   McKerrow, J. H., The diverse roles of cysteine proteases in parasites and their suitability as drug targets. *PLoS Negl. Trop.Dis.* **2018,** *12* (8), e0005639.

214.   Rosenthal, P. J., Cysteine proteases of malaria parasites. *Int. J. Parasitol.* **2004,** *34* (13-14), 1489-99.

215.   McKerrow, J. H.; Engel, J. C.; Caffrey, C. R., Cysteine protease inhibitors as chemotherapy for parasitic infections. *Bioorg. Med. Chem.* **1999,** *7* (4), 639-44.

216.   Engel, J. C.; Doyle, P. S.; Hsieh, I.; McKerrow, J. H., Cysteine protease inhibitors cure an experimental *Trypanosoma cruzi* infection. *J. Exp. Med.* **1998,** *188* (4), 725-734.

217.   Liu, C.-L.; Guo, J.; Zhang, X.; Sukhova, G. K.; Libby, P.; Shi, G.-P., Cysteine protease cathepsins in cardiovascular disease: from basic research to clinical trials. *Nat. Rev. Cardiol.* **2018,** *15* (6), 351-370.

218. Magrath, J.; Abeles, R. H., Cysteine protease inhibition by azapeptide esters. *J. Med. Chem.* **1992,** *35* (23), 4279-4283.

219. Proulx, C.; Sabatino, D.; Hopewell, R.; Spiegel, J.; García Ramos, Y.; Lubell, W. D., Azapeptides and their therapeutic potential. *Future Med. Chem.* **2011,** *3* (9), 1139-1164.

220. Bacha, U.; Barrila, J.; Gabelli, S. B.; Kiso, Y.; Mario Amzel, L.; Freire, E., Development of broad-spectrum halomethyl ketone inhibitors against coronavirus main protease 3CL(pro). *Chem Biol Drug Des* **2008,** *72* (1), 34-49.

221. Schiefer, I. T.; Tapadar, S.; Litosh, V.; Siklos, M.; Scism, R.; Wijewickrama, G. T.; Chandrasena, E. P.; Sinha, V.; Tavassoli, E.; Brunsteiner, M.; Fa, M.; Arancio, O.; Petukhov, P.; Thatcher, G. R. J., Design, synthesis, and optimization of novel epoxide incorporating peptidomimetics as selective calpain inhibitors. *J. Med. Chem.* **2013,** *56* (15), 6054-6068.

222. Donaldson, W. A., Synthesis of cyclopropane containing natural products. *Tetrahedron* **2001,** *57* (41), 8589-8627.

223. Simmons, H. E.; Smith, R. D., A new synthesis of cyclopropanes from olefins. *J. Am. Chem. Soc.* **1958,** *80* (19), 5323-5324.

224. Simmons, H. E.; Smith, R. D., A New Synthesis of cyclopropanes. *J. Am. Chem. Soc.***1959,** *81* (16), 4256-4264.

225. Nakamura, M.; Hirai, A.; Nakamura, E., Reaction pathways of the Simmons−Smith reaction. *J. Am. Chem. Soc.***2003,** *125* (8), 2341-2350.

226. Danishefsky, S. J.; Masters, J. J.; Young, W. B.; Link, J. T.; Snyder, L. B.; Magee, T. V.; Jung, D. K.; Isaacs, R. C. A.; Bornmann, W. G.; Alaimo, C. A.; Coburn, C. A.; Di Grandi, M. J., Total synthesis of baccatin III and taxol. *J. Am. Chem. Soc.***1996,** *118* (12), 2843-2859.

227. Kuehne, M. E.; Xu, F., Total synthesis of strychnan and aspidospermatan alkaloids. 3. The total synthesis of (.+-.)-strychnine. *J. Org. Chem.* **1993,** *58* (26), 7490-7497.

228.   Johnson, C. R.; Haake, M.; Schroeck, C. W., Chemistry of sulfoxides and related compounds. XXVI. Preparation and synthetic applications of (dimethylamino)phenyloxosulfonium methylide. *J. Am. Chem. Soc.* **1970,** *92* (22), 6594-6598.

229.   Gololobov, Y. G.; Nesmeyanov, A. N.; lysenko, V. P.; Boldeskul, I. E., Twenty-five years of dimethylsulfoxonium ethylide (Corey's reagent). *Tetrahedron* **1987,** *43* (12), 2609-2651.

230.   Xiang, Y.; Fan, X.; Cai, P.-J.; Yu, Z.-X., Understanding regioselectivities of Corey–Chaykovsky reactions of dimethylsulfoxonium methylide (DMSOM) and dimethylsulfonium methylide (DMSM) toward enones: a DFT Study. *Eur. J. Org.Chem.* **2019,** *2019* (2-3), 582-590.

231.   Lee, A., Chiral amine-catalyzed α-benzylation of α-branched aldehydes. *Bull. Korean Chem. Soc.* **2015,** *36* (11), 2585-2586.

232.   Ng, J. S., Epoxide formation from aldehydes and ketones- a modified method for preparing the Corey-Chaykovsky reagents. *Synth. Commun.* **1990,** *20* (8), 1193-1202.

233.   Dimethylsulfonium Methylide. In *Encyclopedia of Reagents for Organic Synthesis*.

234.   Thompson, S. K.; Heathcock, C. H., Total synthesis of some marasmane and lactarane sesquiterpenes. *J. Org. Chem.* **1992,** *57* (22), 5979-5989.

235.   Gawande, M. B.; Shelke, S. N.; Zboril, R.; Varma, R. S., Microwave-assisted chemistry: synthetic applications for rapid assembly of nanomaterials and organics. *Acc. Chem. Res.* **2014,** *47* (4), 1338-1348.

236.   Nekkaa, I.; Palkó, M.; Mándity, I. M.; Fülöp, F., Continuous-flow retro-Diels–Alder reaction: an efficient method for the preparation of pyrimidinone derivatives. *Beilstein J. Org.Chem.***2018,** *14*, 318-324.

237.   Close, D.; Xu, T.; Smartt, A.; Rogers, A.; Crossley, R.; Price, S.; Ripp, S.; Sayler, G., The evolution of the bacterial luciferase gene cassette (*lux*) as a real-time bioreporter. *Sensors* **2012,** *12* (1), 732-752.

238.   Qazi, S. N.; Counil, E.; Morrissey, J.; Rees, C. E.; Cockayne, A.; Winzer, K.; Chan, W. C.; Williams, P.; Hill, P. J., *agr* expression precedes escape of internalized *Staphylococcus aureus* from the host endosome. *Infect Immun* **2001,** *69* (11), 7074-82.

239.   Du, X.-L.; Zhang, H.-S.; Guo, X.-F.; Deng, Y.-H.; Wang, H., 6-Oxy-(acetyl piperazine) fluorescein as a new fluorescent labeling reagent for free fatty acids in serum using high-performance liquid chromatography. *J. Chromatogr. A* **2007,** *1169* (1), 77-85.

240.   Thomas, T. C.; McNamee, M. G., Purification of membrane proteins. *Meth. Enzymol.* **1990,** *182*, 499-520.